The Coevolutionary Dynamics of the *Ralstonia solanacearum* and its bacteriophages – implications for biocontrol of bacterial wilt

Sophie Alice James

PhD

University of York

Biology

November 2023

Abstract

The *Ralstonia solanacearum* species complex (RSSC) is a destructive closely related bacterial plant pathogen that cause immense economic and agricultural damage worldwide. RSSC consists of three species *Ralstonia pseudosolanacearum, Ralstonia solanacearum* and *Ralstonia syzygii*. Due to their remarkable similarities, both genetically and phenotypically, the boundaries to define each species of RSSC as completely separate from each other becomes unclear and instead are grouped together in a species complex. Control of RSSC is extremely difficult as a result of geographical distribution, broad host range, virulence, persistence in natural reservoirs and now climate change. Several strategies have been proposed to control RSSC including, interplanting, resistant cultivars and biocontrols. However, many remain insufficient. Lytic bacteriophage (phages) are viruses which can infect and kill bacteria; they have often been purposed as a potential biocontrol for RSSC. Numerous studies have found that phages are effective at suppressing RSSC and even providing plant protection in greenhouse and field experiments. However, infectivity level, infectivity range and phage resistance evolution are major obstacles in developing phages as effective biocontrols.

RSSC and its phage engage in antagonistic coevolutionary dynamics, the reciprocal adaptation and counter-adaptation between interacting host and parasite populations. This thesis aims to exploit the coevolutionary trajectories of phages and RSSC to develop highly effective biocontrols through experimental evolution. We first pre-adapted ("trained") phages against three genotypes of *Ralstonia solanacearum* in mono- or combination cultures (Chapter 2) with one-sided experimental evolution, with the aim of improving infectivity and infectivity range of phages. We found that multiple genotype trained phages were much more effective at suppressing two genotypes of *R. solanacearum* compared to their single genotype trained phages. Unfortunately, phage resistance evolved rapidly against trained phages. Next, coevolution experiments on four phages against one genotype of *R. solanacearum* was tested to see if evolving interacting populations would result in increased infectivity levels (Chapter 3). However, rapid evolution of resistance in *R. solanacearum* drove phages to extinction, suggesting coevolutionary dynamics were highly asymmetrical. Finally, combination experiments were conducted to see if having multiple phages in combination would suppress *R. solanacearum* resistance evolution and characterise highly effective phages in our collection (Chapter 4).

Overall, this thesis provides insights and predictions into asymmetrical evolution and resistance in *R. solanacearum* but also highlights the potential of bacteriophages to control *R. solanacearum*.

List of Contents

List of Tables

List of Figures

List of Supplementary Figures

Acknowledgements

As has been said – “it takes a village to raise a child” – this project has been my child for the last 3 years and I’m so grateful to my village. Firstly, I’d like to thank my supervisors Ville Friman and Paul Fogg for all the support, advice, direction and enthusiasm. I thought Ville’s move to Helsinki might be a problem, but at no time did I ever feel the distance was an issue. Also, thanks to Andrea Harper for her excellent comments, therapy and support and for keeping me on track. I would also like to thank my lab teams at the University of York, in particular Sara and Bryden for their generosity and kindness and for keeping me sane in trying times. My family for their love and support, particularly Emma, my twin. Also, I really need to thank my friends for their kindness and humour even though most of them don’t understand what I’ve been researching. My dogs - Poppy (RIP), Hettie and Izzy for the walks to clear my head and the contributions to meetings and excellent work when standing on my keyboard. Finally, I’d like to thank my Granny for proof-reading every piece of work I’ve written, including this thesis, since GCSE’s. Dyslexia is not a barrier!

Declaration by Author

I declare that this thesis is a presentation of original work, and I am the sole author. This work has not previously been presented for an award at this, or any other, university. All sources are acknowledged as References.

Chapter 1

General Introduction

1.1 The *Ralstonia solanacearum* Species Complex

The *Ralstonia solanacearum* Species Complex (RSSC) describes a group of globally diverse but closely related plant pathogens (species) that are the causative agent of bacterial wilt in nearly 200 plant species across several plant families (Castillo and Greenberg, 2007). For example, important agricultural crops such as tomato (*Solanum Lycoersicon*), potato (*S. tuberosum*), banana (*Musa* genus), ginger (*Zingiber officinale*) and cashew (*Anacardium occidentale*) are plant hosts to RSSC (Choudhary et al., 2018). RSSC is highly destructive and causes extensive agricultural and economic damage. Low and middle-income countries are more reliant on their agricultural sectors in their economies. For example, in Uganda and Ethiopia their agricultural sectors support 25% and 47% of their economies respectively (Bank, 2021, Group, 2016). In 2020, Uganda and Ethiopia crop losses were over 90% due to RSSC outbreaks (Ahmed et al., 2022). With its global distribution, climate change and lack of effective control measures, RSSC is and will remain a problematic plant pathogen globally with its burden likely to increase in the near future.

1.1.1 Classification and Diversity

Historically, RSSC has been renamed and regrouped several times over (due to genetic and phenotypic diversity). Originally, RSSC was divided and characterised into races (based on host range) and biovar system of *Ralstonia solanacearum* (Fegan and Prior, 2005). In RSSC, biovars were based on their ability to utilise and oxidise three disaccharides, trehalose, maltose and cellobiose. Also, hexose alcohols, mannitol, sorbitol and dulcitol (Huang et al., 2012). From the 2000s until the mid-2010s, RSSC was divided into four phylotypes of *Ralstonia solanacearum* (I, II, III and IV). Similar to the newest classification, it was based on geographical origin (Figure 1.1) (Fegan and Prior, 2005).

Now, RSSC stands as a species complex. RSSC comprises of three different species *Ralstonia pseudosolanacearum*, *Ralstonia solanacearum* and *Ralstonia syzygii* (Figure 1.1) (Safni et al., 2014). All three species share similarity in their infection cycles and the symptoms that they cause (Lowe-Power et al., 2018). Genetic analysis also shows remarkable similarities despite

divergent lifestyles between species. *R. solanacearum* and *R. syzygii*, for example, have different lifestyles. *R. syzygii* is transmitted by insects, whereas *R. solanacearum* is soilborne. Nevertheless, genetic analysis (DNA-DNA hybridisation) revealed that these two species are very closely related and form one genomic species (Remenant et al., 2011). Strains with average pairwise nucleotide identity (ANI) at 95% or above can have vastly different hosts and ranges. Whereas phylogenetically distinct strains, where ANI is below 95% can have similarity in their hosts and ranges (Sharma et al., 2022). Genetic exchange events (recombination) between the three species are prevalent. Horizontal gene transfer also played a significant role in diversifying RSSC into three species as well as pathogenicity and adaptation of RSSC (Geng et al., 2022). Taken together and along with its global disruption, this has made classification of RSSC tricky and a continuing challenge (Remenant et al., 2010). The current classification is based on genomic analysis and reflects their geographical origin and evolutionary lineages (Safni et al., 2014). However, as this is a fairly recent classification it is important to mention the previous classifications as they are still in use.

1.1.1.1 *Ralstonia solanacearum*

The main focus of this thesis is *Ralstonia solanacearum*, which has been divided further into two phylotypes IIA and IIB based on genetic diversity (Figure 1.1) (Genin and Denny, 2012, Cellier et al., 2012, Mahbou Somo Toukam et al., 2009). *R. solanacearum* can infect a number of plants from across a range including *Solanaceae* (the nightshade plants), *Anthurium* (family of flowering plants), *Heliconia* (genus of tropical flowering plants) and *Musa* (genus that includes bananas and plantain). The strains of *R. solanacearum* are known for their adaptation to temperate climates (Elphinstone et al., 1996a). Originally, thought to be a tropical plant pathogen, *R. solanacearum* (cold-tolerant IIB-1) was the causative agent of a series of outbreaks of brown rot disease in potatoes across Europe since the 1970s (Huet, 2014, Bragard et al., 2019).

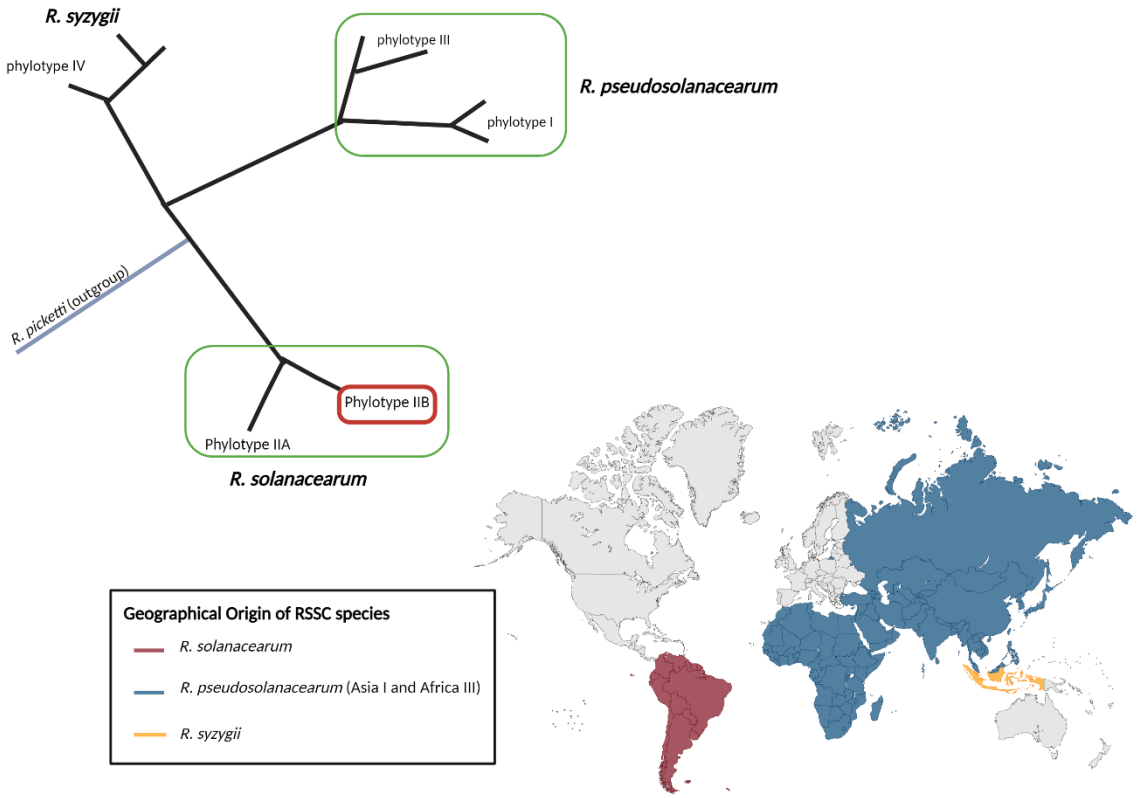

Figure 1.1 – A root phylogenetic tree of the *Ralstonia solanacearum* Species Complex (representative strains), adapted from Lowe-Power et al (Lowe-Power et al., 2018). Originally, constructed using whole-genome average nucleotide identity (ANI). The tree shows the relatedness of each species in RSSC, as well as the historical phylotypes. Phylotypes within a green box show ANI >96%, highlighting closely related phylotypes. Phylotype IIB (red box) are cold-tolerant strains of *R. solanacearum*, strains relevant to Europe and the UK. These phylotypes were used throughout this thesis. The classification of RSSC currently reflects geographical origin and evolutionary lineages. The map highlights the geographical origins of each species within RSSC. For *R. solanacearum* this is Latin America; *Ralstonia pseudosolanacearum* Asia (phylotype I) and Africa (phylotype III) and finally, for *R. syzygii* Indonesia. Created in Biorender.com.

1.1.2 Infection cycle

RSSC can be found in several environments, soil, water and even insects (Remenant et al., 2011, Caruso et al., 2005) RSSC infection cycle begins with entry into their host (Figure 1.1). Through sensing and chemotaxis, RSSC moves using flagellar motility to their host's roots (Genin and Denny, 2012). RSSC uses type IV pili to attach themselves to the root surface (reversible or irreversible) and forms microcolonies (Lowe-Power et al., 2018). Through natural openings or wounds in the root, RSSC migrates, or rather invades, the vascular system rapidly and travels to the xylem (Caldwell et al., 2017, Lowe-Power et al., 2018). To aid invasion of the plant, RSSC might be able to manipulate root development. Although, the mechanism is unclear, morphological alterations to the roots have been observed from plants infected with RSSC (Xue et al., 2020). Morphological alterations include cell death, inhibition of primary root growth and disruption of activity in roots (Xue et al., 2020). RSSC then moves up through the xylem and infection spreads systemically in the plant. Rapid replication in RSSC (exceeding 10^8 CFU/g) and production of exopolysaccharides (ESP) occurs (Lowe-Power et al., 2018). Other virulent factors are activated to mitigate the host's immunity and aid with colonisation, quorum sensing coordinates this, triggered by cell density (Lowe-Power et al., 2018, Hikichi et al., 2017). The type II (T2SS) and type III secretion system (T3SS) is an important virulence factor in RSSC, responsible for inducing effector proteins leading to rapid and successful colonisation of the xylem (Coll and Valls, 2013, Poueymiro and Genin, 2009). Both secretion systems are essential for pathogenicity (Poueymiro and Genin, 2009). Eventually, xylem vessels are obstructed, sap flow is reduced, and wilting symptoms appear due to impaired water conductance (Hikichi et al., 2017, Lowe-Power et al., 2018, Xue et al., 2020). The plant eventually dies and RSSC is returned to the environment. RSSC will then persist in the environment until it can reinfect another vulnerable plant, restarting the cycle (Figure 1.1).

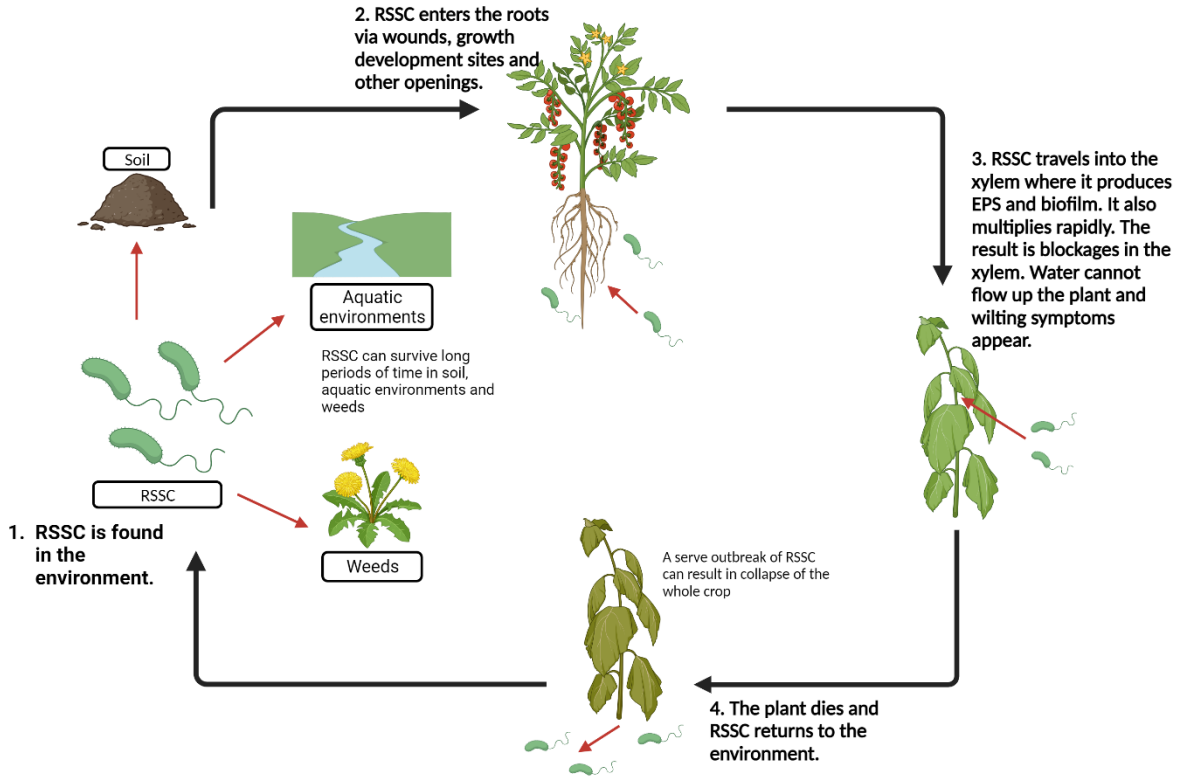

Figure 1.2 - Overview of the infection cycle of RSSC. 1) RSSC is found in the environment and persists within aquatic environments and non-hosts. 2) RSSC enters the roots of a susceptible host through wounds and natural openings. 3) RSSC travels up the xylem where multiplication, EPS production and biofilm production rapidly occurs, creating blockages in the xylem and wilting symptoms appear. 4) The plant dies and RSSC is returned to the environment. Adapted from (Ahmed et al., 2022). Created in Biorender.com.

1.1.2.1 The role of extracellular polymeric substances and biofilms in RSSC.

Biofilms are a complex matrix of microbial communities and polymeric material which is attached to a surface, including living tissues (López et al., 2010). Biofilms and extracellular polymeric substances (EPS) are closely intertwined, EPS forms the structure of biofilms (Flemming et al., 2007). EPS consists of polysaccharides, proteins, extracellular DNA (eDNA) and lipids which form a matrix (Di Martino, 2018). Biofilms and EPS plays significant roles in bacteria interactions and functions (Flemming, 2016). These interactions and functions can range from protection and communication to aggregation and carbon storage (Costa et al., 2018). EPS is a main virulence factor and plays an important role in the colonisation of plants during infection (Saile et al., 1997). EPS synthesis is regulated by quorum sensing (PhcA, quorum-sensing-dependent-regulatory protein) and when cells reach high densities, the quorum sensing triggers the mass production of EPS (Genin and Boucher, 2002, Peyraud et al., 2016). The EPS produced, blocks the flow of water through the xylem, resulting in wilting symptoms and eventually plant death (McGarvey et al., 1999). EPS can also help protect RSSC from plant defences, it prevents recognition of RSSC from the plant host. Plant defence genes are upregulated in the presence of mutant-defective EPS strains of *R. solanacearum* (Milling et al., 2011). EPS is likely to play a significant role in biofilm formation in RSSC where biofilms have been shown to form in xylem vessels of the plant (Minh Tran et al., 2016). Biofilms in RSSC may play significant roles in virulence and systematic spread through the plant. *R. solanacearum* mutants with defects in their biofilm production are less virulent (Mori et al., 2016, López et al., 2010).

1.1.3 The difficulty in controlling RSSC.

Control of RSSC is notoriously difficult. There are several factors that make control of RSSC difficult, including and not limited to geographical distribution, broad host range, virulence, persistence in natural reservoirs and now climate change.

As mentioned above, RSSC consists of three species (Figure 1.1). Multiple strains of RSSC and even different species of RSSC can co-exist together (Vogelaar et al., 2023, Santiago et al., 2017). This contributes to the difficulty of controlling RSSC as not one control strategy will work for all species and strains (Bragard et al., 2019). This means that multiple control measures will need to be implemented, which is costly and time consuming, with no guarantee of success (Sundin et al., 2016).

The RSSC host range is vast, which creates problems for control when hosts remain unknown, making it difficult to determine plants which are likely to harbour or succumb to RSSC (Morris and Moury, 2019, Bragard et al., 2019). Presently, over 200 plant species have been identified as hosts for RSSC from several different botanical families (Genin, 2010). RSSC can also easily adapt and expand its host range readily through various mechanisms, creating opportunities to evade control measures (Genin, 2010). For example, strains UW163 and IBSBF 1502 are closely related but IBSBF 1502 gained the ability to infect members of the *Curcurbitaceae* family, because ofdifferences in transcriptomic profiles (genes remain unclear) (Ailloud et al., 2015). Another advantage to having a vast host range is that it provides more opportunity for transmission and survival. It is also important to remember that RSSC can become asymptomatic in it's host as well, again creating problems for control measures, as this increases survival and persistence (Elphinstone et al., 1996a). Detection methods are often not sensitive enough and do not detect low numbers of the target pathogen.

RSSC has consistently been reported as one of the most destructive plant pathogens to agricultural crops (Mansfield et al., 2012). RSSC is highly virulent with the ability to cause wide-spread disease and possible rapid population collapse. *Solanum lycopersicum* (tomato) and *Solanum tuberosum* (potato) plants inoculated with *R. solanacearum* showed wilting symptoms in 5-7 days and 80% were dead by 21 days (Siri et al., 2011). A similar situation was observed with *R. pseudosolanacearum,* wilting symptoms were observed in 7 days. What contributes to RSSC aggression is a diverse collection of virulence mechanisms increasing its level of pathogenicity (see review by Vailleau and Genin 2023 on virulence strategies from RSSC) (Vailleau and Genin, 2023). It is important to point out that virulence can vary between strains of RSSC (Wang et al., 2018, Siri et al., 2011, Lebeau et al., 2011). Nevertheless, highly aggressive strains are problematic when controlling RSSC, especially as they are able to overcome "resistant" cultivars. The resistant tomato cultivar "Hawaii 9996" is resistant to *R. pseudosolanacearum* but the cultivar is not resistant to strains of *R. solanacearum* (Lewis Ivey et al., 2021).

RSSC can survive without their hosts for long periods (even years) in a range of environments such as soil, water and plants (asymptomatically). However, RSSC persistence is heavily determined by abiotic and biotic conditions (Álvarez et al., 2010). In soil, RSSC can survive in soil for a time but how long is debated. Some have suggested that RSSC can be detected 1-2 years after host removal, others have suggested 4 years and higher (van Elsas et al., 2000). RSSC survival in soil is heavily determined by soil conditions. *R. solanacearum* phylotype II was found in fields in the Netherlands a year after an outbreak. Further assessment (soil microcosms) from these isolated strains suggested that soil temperature and moisture had significant impacts on RSSC persistence. Lower temperature and drought-like conditions dramatically reduced its abundance (van Elsas et al., 2000). In the environment, droughts and temperature fluctuations are likely to have significant impacts on the survival of RSSC. Seasonal variation on their abundance is possible. Warmer waters in spring and summer can increase the presence of RSSC while cooler temperatures in autumn and spring decreases RSSC. RSSC can remain virulent and viable after a period of cold temperatures (Álvarez et al., 2022). In Europe, bittersweet nightshade (*Solanum dulcamara*) a common weed that resides on riverbanks helps RSSC to persist in the environment by harbouring RSSC in its roots and releasing it back into the environment (Álvarez et al., 2010).

Researchers expect that climate change will increase the prevalence of plant diseases, including bacterial wilt caused by RSSC (Delgado-Baquerizo et al., 2020). Plant pathogens tend to cause disease outbreaks when conditions (the environment) are favourable to them (Singh et al., 2023, Chaloner et al., 2021). Species and phylotypes of RSSC that are strongly associated with tropical regions may begin to move into newer regions as the climate warms (Chaloner et al., 2021). In Northern Europe, the dominant RSSC species and strains are cold-tolerant *R. solanacearum* (IIB), but this may soon change (Bragard et al., 2019). The Netherlands has recently reported that *R. pseudosolanacearum* is present within their aquatic environments and wild bittersweet nightshade (Vogelaar et al., 2023).Posing a considerable risk to food security in Europe (Bragard et al., 2019).

1.1.4 Strategies for controlling RSSC.

A number of strategies have been investigated to control RSSC, but most have remained insufficient for the reasons described above. Strategies to control RSSC include changing farming practices, breeding plant resistant crops, chemical control and biological controls (Nion and Toyota, 2015). To mitigate RSSC, changing farming practices have been suggested. For example, interplanting with non-susceptible plants has reduced disease incidence as susceptible plants are protected by non-susceptible plants (Lai et al., 2011, Li et al., 2020). Field experiments in China have shown that garlic (*Allium sativum* L.) interplanted with tobacco plants (*Nicotiana tabacum*) can significantly reduce the abundance of RSSC within the field, compared to monoculture fields. Incidence of disease was lower in fields with interplanting of garlic (Lai et al., 2011). In a similar field experiment, marigolds (*Tagetes erecta* L.) also effectively reduced the abundance of RSSC (*R. pseudosolanacearum* phylotype I) and disease incidence (Li et al., 2020). However, intercropping can reduce crop yield and increase the complications of crop management (Huss et al., 2022).

Given the challenges that come with controlling RSSC, many suggest that an effective method is through resistant cultivars. Developing resistant plants is extremely challenging (Huet, 2014). Partly due to RSSC itself but also plant traits. No one cultivar will be resistant to all strains of RSSC. *S. lycopersicum* "Hawaii 9996" is resistant to *R. pseudosolanacearum* but not all strains of *R. solanacearum* (Wang et al., 2018, Lewis Ivey et al., 2021). Similarly, *Capsicum annum* (pepper) and aubergine were resistant to strains within the three species of RSSC but not all (Lebeau et al., 2011, Lewis Ivey et al., 2021). With its global distribution and high genetic diversity, it is likely that a resistant plant will eventually become susceptible to a strain. Breeding resistance in plants can have detrimental impacts on the growth, development and yield of agricultural crops (Hammond-Kosack and Parker, 2003).

Chemical control such as pesticides are often used for control of plant diseases and have been used to control RSSC outbreaks (Nion and Toyota, 2015). Chemicals such as methyl bromide can significantly reduce bacterial wilt (Santos et al., 2006). However, methyl bromide is currently banned under international law (Montreal Protocol) for ozone depletion properties and has been phased out internationally (Martin, 2003, Velders et al., 2007).An alternative to methyl bromide such as methyl iodide to control plant pathogens has been suggested (Martin, 2003). Field trials with ginger (*Zingiber officinale*) in China have

suggested that methyl iodide is effective at suppressing *R. solanacearum* (Li et al., 2014b). Other chemicals like calcium cyanamide, ammonia water and a mixture of ammonium bicarbonate and lime have also been evaluated for their ability to suppress *R. solanacearum.* However, success was limited, often requiring high concentrations of the chemicals and the level of suppression was low (Liu et al., 2016). Another challenge with using chemicals is they are often damaging to both the environment and human health, with countries often restricting and even banning their use (Wang et al., 2023c). This has led to a desire to look for sustainable alternatives to control plant pathogens, such as biocontrols (Lahlali et al., 2022). Biocontrols have consistently provided potential for control of RSSC. Utilising plant-derived compounds, bacteria and viruses (for viruses, see below) have all been proposed as promising biocontrol methods against RSSC (Ahmed et al., 2022, Vailleau and Genin, 2023). Plant-derived compounds such as hydroxycoumarins can significantly inhibit the growth of RSSC (Yang et al., 2016). *Bacillus amyloliquefaciens* has successfully reduced the abundance of RSSC and successfully protected tobacco plants against bacterial wilt through niche exclusion (Wu et al., 2016). *Streptomyces* sp. NEAU-HV9 isolated from fields in China showed antimicrobial activity (actinomycin D) against *R. solanacearum* (Ling et al., 2020). *Pseudomonas* strains have also been effective at suppressing *R. solanacearum* through secondary metabolites with antimicrobial activity (Clough et al., 2022).

1.2 Bacteriophages as biocontrol agents

Bacteriophages (known as phages) are viruses that infect bacteria and archaea. Phages are the most diverse and abundant entities on Earth with estimates suggesting that there is an impressive 10^{31} in the biosphere (Dion et al., 2020). Phages have been purposed as a biocontrol of RSSC and other plant pathogens (Ahmed et al., 2022). There are at least three different lifecycles that phages utilise to carry out their replication: lytic, chronic and lysogenic (Figure 1.3). All three lifecycles begin with phage entry into the host, via absorption (Chevallereau et al., 2022). Through interactions between binding proteins on the phage and cell receptors on the surface of their hosts, initial contact can be made (Salmond and Fineran, 2015). Initial contact is thought to be random, only if the right collision between a phage and it's host is made will absorption begin (Leprince and Mahillon, 2023). There is an extensive range of receptors that phages utilise for entry into the host (Stone et al., 2019). Receptors are also thought to be a major determinant of host range and specificity (Bertozzi Silva et al., 2016). After absorption, the phage's genetic material is injected into the host's cytoplasm. After entry, the three cycles diverge and use various means of virion production and release modes.

Phage receptors are a critical component of all three phage lifecycles, where the initial steps of infection begin. As mentioned above, phages have an extensive range of receptors that they can utilise (Stone et al., 2019). Receptors are cell surface exposed molecules. Receptors include proteins, lipopolysaccharides (LPS), teichoic acids, pili and flagella (Dowah and Clokie, 2018). In *R. solanacearum* the membrane-spanning protein secretion system, Type II secretion system (T2SS), used to transfer proteins from the periplasm across the outer membrane, is a phage receptor of the phage phiAP1 (Xavier et al., 2022, Korotkov et al., 2012). LPS is a common phage receptor of gram-negative bacteria. LPS consists of lipid A, the core polysaccharide and the O-polysaccharide (also known as the O-antigen) (Bertozzi Silva et al., 2016). Phages can bind to any one of these three components of LPS (Bertozzi Silva et al., 2016). For example, the phage JG004 of *P. aeruginosa* it is the core polysaccharide receptor. Mutants of *P. aeruginosa* which lacked *algc* gene were resistant to JG004, the gene encodes an enzyme which is required for the biosynthesis of the core polysaccharide of LPS (Garbe et al., 2011). Whereas the O-antigen of LPS was a receptor for *Podoviridae* phages of *Salmonella enterica* (Shin et al., 2012). LPS is also a possible receptor

of *R. solanacearum* phages as well. It is suspected that LPS is the receptor for the phage ϕRSA1 (Fujiwara et al., 2008). For gram-positive bacteria, teichoic acids can act as receptor for phages (Dowah and Clokie, 2018). Teichoic acids are highly diverse polysaccharides that cover the cell surface and play essential roles in metabolism and even pathogenesis of gram-positive bacteria (Brown et al., 2013). Due to the high complexity of cell walls of gram-positive bacteria, only a few receptors have been identified in gram-positive bacteria (Bertozzi Silva et al., 2016, Dowah and Clokie, 2018). Phages A118 of *Listeria monocytogenes* utilises teichoic acid as a receptor (Wendlinger et al., 1996). Pili are appendages on the cell surface of bacteria that play important roles in movement and adherence and for pathogenic bacteria like *R. solanacearum* are important virulence factors. Pili can also be receptors for phages. The type IV pili is an important virulence factor for *R. solanacearum* and is a receptor for the phage ϕRSM (Askora et al., 2009). Finally, flagella, vital for motility of bacteria has been identified as a receptor for phages (Nakamura and Minamino, 2019). Interestingly, flagella are often used as form of translocation for phages, moving them from the flagella to the cell surface where they interact with another surface receptor (secondary receptor) (Nakamura and Minamino, 2019). The phage 7-7-1 that infects *Agrobacterium* sp. H13-3 uses the flagellum for attachment and translocation to the cell before using LPS as a secondary receptor (Gonzalez et al., 2018). Although, RSSC has flagella it is unclear if phages use this as a receptor (Corral et al., 2020). This will require further isolation and characterisation of RSSC phages.

The lytic cycle of virulent and temperate phages (Figure 1.3). After entry into their host, virion particles are produced through exploitation of the bacteria, using their machinery for virion production (Williamson et al., 2017). Host-metabolism shut-down and degradation of macromolecules occur, allowing uptake of resources (Warwick-Dugdale et al., 2019). Auxiliary metabolic genes from the phage are expressed. Energy and resources are redirected from the host to phage assembly and production due to expression of these genes (Crummett et al., 2016). Phages that infect cyanobacteria photosynthetic genes (*psbA* and *hli* genes) are expressed during infection and co-transcribed with phage capsid genes. This increases the yield of D1 protein which maintains photosynthesis and energy within the host, necessary for phage replication (Lindell et al., 2005, Crummett et al., 2016). Once their progeny is created, they are released via lysis resulting in the death of the host cell

(Williamson et al., 2017). Phages can cause lysis with numerous strategies and often depend on cell-wall composition (Cahill and Young, 2019). Phages can inhibit the bacterial cell wall peptidoglycan biosynthesis, rupturing the cell wall. Or they can employ holin and endolysin proteins that induce the formation of pores and cleave the cell wall peptidoglycan (Catalão et al., 2013). These phages then move on to infect other cells, restarting the cycle (Williamson et al., 2017).

Lytic phages isolated from endemic areas of Spain showed biocontrol potential against *R. solanacearum* (phylotype II) in tomato plants. Lytic activity from these phages were also present against *R. pseudosolanacearum* to some extent (Álvarez et al., 2019). Lytic phages ψRSA1, ψRSB1 and ψRSL1 were able to decrease the cell density of *R. solanacearum* in mono- or in combination. ψRLS1 was particularly effective at protecting tomato plants from *R. solanacearum* (Fujiwara et al., 2011). With no-wilting symptoms or latent infection in tomato plants with the lytic phage RsPod1EGY, as well as inhibiting formation of EPS (Elhalag et al., 2018)

Filamentous phages are often associated with the chronic lifecycle of phages (Figure 1.3). The main characteristic of a chronic lifecycle is that the cycle does not end in lysis. Instead, assembled virions (using host machinery) are released from the host via secretion through the host envelope (Hay and Lithgow, 2019, Loh et al., 2019). The chronic infection caused by filamentous phages ϕRSM1 and ϕRSM3 resulted in a loss of virulence in *R. solanacearum* (Addy et al., 2012b). Several virulence factors were significantly reduced including, cell motility and EPS production (Addy et al., 2012b). On the other hand, the filamentous phage ϕRSS1 enhanced twitching motility through inducing *phcA* (global virulence regulator) which resulted in increased virulence in *R. solanacearum* (Addy et al., 2012a).

The lysogenic cycle involves the integration of the phage's genome into their hosts or exists as a plasmid to form prophages (Williamson et al., 2017). Prophages are then passed through the bacteria population, one generation after the other, through bacteria cell replication (Williamson et al., 2017). Prophages have significant impacts on their hosts, especially on fitness and virulence (pathogenic bacteria) (Fortier and Sekulovic, 2013). In RSSC, prophages are diverse and widespread with potential impacts on fitness and virulence, as auxiliary genes have been identified that are linked to metabolism and virulence (Greenrod et al., 2022). Type III effectors (T3Es) have been identified in prophages integrated into RSSC, an important virulence factoras well as nickel and cobalt resistance protein CnrB, believed to help with niche-adaptation (Gonçalves et al., 2021).

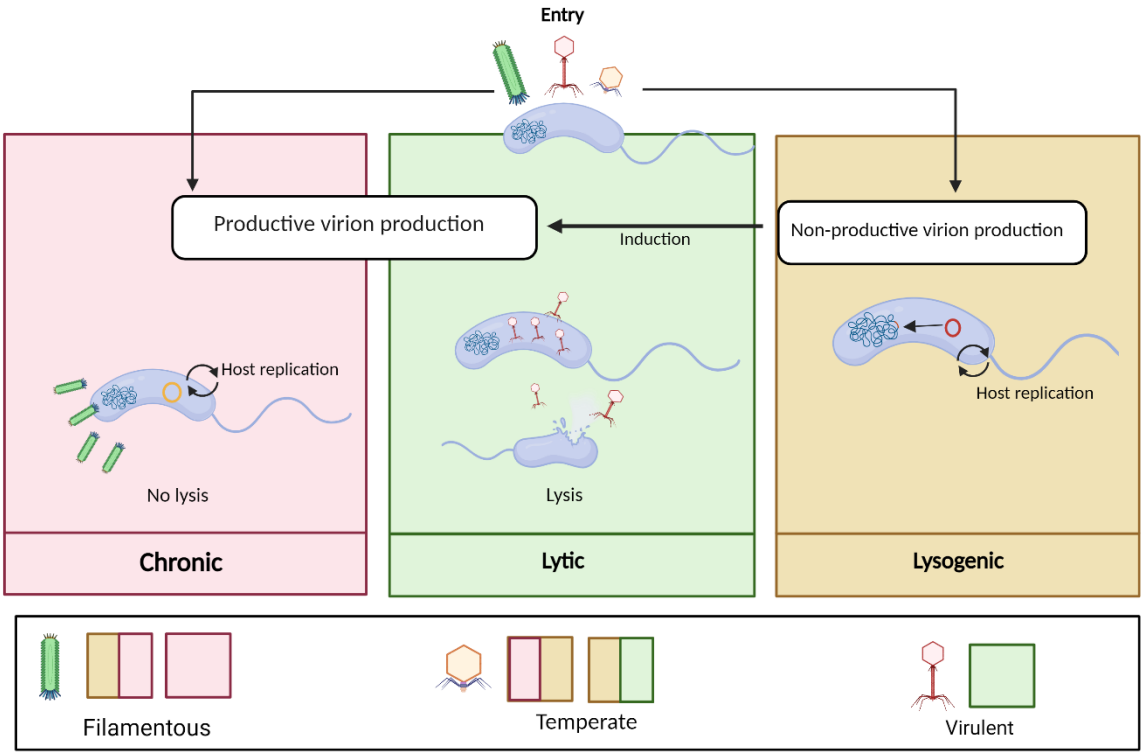

Figure 1.3 – A diagram of the three lifecycles of phages, chronic, lytic and lysogenic. Filamentous phages are often associated with chronic lifecycles (red box), these viruses are assembled in their host but released via secretion and no lysis occurs. Phages can also replicate as the host replicates. The lytic cycle (green box) results in the death of their host. Phages are assembled in their host and released via lysis. Virulent phages follow the lytic cycle exclusively. The lysogenic cycle (yellow box), phages incorporate their genome into their host and replicate when the host replicates. Temperate and filamentous phages can follow the lysogenic cycle. However, certain conditions can cause temperate phages to switch to the lytic cycle. Created in Biorender.com. Adapted from (Chevallereau et al., 2022).

1.2.1 The advantages and challenges of using phages in agriculture and for biocontrol of RSSC.

As mentioned above various phage types have the ability to control and suppress RSSC, highlighting their potential as biocontrol in agriculture. They offer an environmentally friendly alternative to chemicals with low risks to animal and human health. However, it is not without challenges (Garvey, 2022).

Phages are highly specific often only infecting one species of bacteria, or even a few strains within a species (Sieiro et al., 2020). The advantage of their specificity is that the phage biocontrol only targets the chosen plant pathogen (Vikram et al., 2021). In turn, this could protect the rhizosphere where a diverse rhizosphere is critical in maintaining healthy plants; promoting growth and protecting plants from environmental stresses (Mukhtar et al., 2019, Alawiye and Babalola, 2019). However, the specificity can become a challenge when considering the diversity and global distribution of RSSC (Figure 1.1), phages would need to have broad host ranges (Abdurahman et al., 2019, Hyman, 2019). To achieve this it would require knowledge of phage specificity to RSSC and knowledge of species and strains of RSSC, which could be time-consuming and costly (Holtappels et al., 2021). Phages with broad host ranges have been isolated and characterised with the potential to be good candidates for phage biocontrol (Ross et al., 2016). For example, the lytic phage ϕD5 is capable of infecting five *Dickeya* species, the causative agent of soft rot and blackleg disease in potatoes (Czajkowski et al., 2014). Also, experimental evolution, phage cocktails and/or genetic recombination could mitigate this challenge overcoming RSSC diversity through host range expansion (Baliyan et al., 2022).A 5 phage cocktail of *Escherichia coli* phages could infect over 90% of strains whereas with individual phages this was ~70% of strains (Kim et al., 2021). T4-like phage WG01 host-determinant gene 37 was replaced with the QL01 gene 37. This resulted in an expanded host range in recombinant-WG01 progeny. Expanding the host range to 63 strains (out of 113) of *E. coli* from 41 including 8 previously resistant strains to both wild-type WG01 and QL01 (Chen et al., 2017). However it could result in a much larger and more complicated level of production which could be expensive (Garvey, 2022).

Phages can be reduced from abiotic factors such as temperature and pH. Again, experimental evolution could mitigate the challenge of abiotic factors (Baliyan et al., 2022). Improving phage stability might help reduce the need for reapplication. Experimental evolution on the *E. coli* phage T3 resulted in higher heat tolerance relative to their wild type (Favor et al., 2020). If phages can be adapted to tolerant abiotic factors like temperature and pH, stability and efficiency could be maintained.

Biofilms are matrix of EPS produced by microbes themselves that adhere to surfaces and play significant roles in survival and pathogenesis of bacteria (Flemming et al., 2016). Biofilms can make it difficult for control measures to be effective against plant pathogens, with chemical control measures, biofilms can slow the rate of diffusion of the chemical, reducing toxicity (Azeredo et al., 2021, Sundin et al., 2016). Biofilms also play an important role in bacterial defence against phages. From trapping phages within the biofilm matrix to prevent receptor-binding and subsequent infection, to producing phage-inactivating enzymes (Ferriol-González and Domingo-Calap, 2020). However, phages have evolved the ability to breakdown this defence. Phages can encode enzymes such as endolysins and virion-associated peptidoglycan hydrolases that can disrupt biofilms (Azeredo et al., 2021). The phage ψ15 was able to degrade the biofilm of *Pseudomonas putida,* it was suspected that enzymes found on the tail-spike was responsible (Cornelissen et al., 2011).

Bacteria can readily evolve resistance to phages rapidly and has often been a criticism of phage biocontrol (Azam and Tanji, 2019). However, mutations that evolve resistance can often incur trade-offs (see below) which can have significant impacts on virulence (Burmeister and Turner, 2020, Ferenci, 2016). Mutations related to LPS synthesis conferred phage resistance but at the cost to biofilm and virulence ability in plant pathogens. Phage resistance in the plant pathogen *Xanthomanos oryzae* pv. oryzae, causative agent of leaf blight disease of rice had mutations in glycosyltransferase. An enzyme related to LPS synthesis. Phage resistance mutants could not form lesions on rice leaves compared to their ancestor, suggesting a reduction in virulence (Zhang et al., 2022). Phages and bacteria engaged in various types of antagonistic coevolution (see below), often resulting in phages adapting to overcome this resistance (Azam and Tanji, 2019).

1.3 Phage Resistance Mechanisms in Bacteria

Due to the intense coevolutionary dynamics between phages and bacteria, bacteria are under a near constant selection pressure to evolve various defence mechanisms against phages (Hampton et al., 2020, Labrie et al., 2010, Georjon and Bernheim, 2023). There is immense diversity of defence mechanisms each with unique characteristics and capabilities (Bernheim and Sorek, 2020, Labrie et al., 2010). Systems can be divided into 'innate' and 'adaptive' immunity for a prokaryote. Some even have evolved to protect the population rather than the individual (Bernheim and Sorek, 2020). Prokaryotic defence systems are often clustered together in the genome on 'defence islands' with many studies exploiting this to identify and characterise defence mechanisms within bacteria (Doron et al., 2018). However, many still remain obscure and are yet to be discovered (Barrangou and van der Oost, 2018). RSSC has a diverse range of defence mechanisms, the defence mechanisms mentioned below have all be identified within RSSC, including the strains of *R. solanacearum* used in this thesis (Castillo et al., 2020, Payne et al., 2022). Unfortunately, there is limited understanding how the defences mechanisms function mechanistically within RSSC, instead the examples given are there to provide insights into how these defence mechanisms might function within RSSC.

1.3.1 Receptor Modification

Bacteria often protect themselves from phage infection through surface modification, changing or masking the phage receptors on their surfaces (Bertozzi Silva et al., 2016). For example, *Vibrio cholerae* mutates its ompU receptor to prevent absorption from the vibrio-phage ICP2 (Hampton et al., 2020, Seed et al., 2014). In *Yersinia pestis*, resistance was achieved through defects on lipopolysaccharides (LPS) receptors due to mutations in enzymes involved in LPS biosynthesis (Filippov et al., 2011). In *Staphylococcus* point mutations or deletions in the enzyme undecaprenyl-phosphate N-acetylglucosaminyl 1-phosphate transferase conferred phage resistance. The transferase is necessary for wall teichoic acid formation, a receptor for phages (Jurado et al., 2022). Depletion of wall teichoic acid leads to phage resistance (Xia et al., 2011, Jurado et al., 2022). In *R. solanacearum*, phage resistance was the possible result of evaluated phospholipid production from mutations in the *mla* cluster which in turn masked the receptor O-antigen from RSψP29 and prevented phage absorption (Hong et al., 2014). In coevolution experiments between phage

and bacteria, surface modification is a frequent adaptation from bacteria to overcome phage infection (Buckling and Rainey, 2002, Brockhurst et al., 2007). However, it is up for debate whether surface modification is a key strategy for bacteria in ecosystems. Losing or attenuation of the functioning of a receptor in a complex and dynamic ecosystem such as the rhizosphere could be very costly (Fortuna et al., 2019). Phage receptors are lipopolysaccharide, teichoic acids, proteins or capsules on the cell surface. They perform important roles as membrane porins, chemical receptors, adhesions, pilins and more (Hyman and Abedon, 2010). Essential, for survival and functionality of bacteria (Hyman and Abedon, 2010). Phage resistant bacteria that have evolved from receptor loss or change are vulnerable to other factors (biotic and abiotic). Surface modification often coincides with evolutionary trade-offs (Fortuna et al., 2019).

1.3.2 Restriction modification and related defences

Restriction modification (RM) and related defences focus their efforts on phage DNA after injection. The following RM and related defence mechanisms have all been identified in RSSC and are described below (Castillo et al., 2020, Aoun et al., 2023). These are restriction modification, Defence Island Associated with Restriction-Modification (DISARM) and Bacteriophage Exclusion (BREX) (Payne et al., 2022). These defences recognise non-self-DNA and destroy it. Restriction modification defences are diverse and ubiquitous (Vasu and Nagaraja, 2013). In general, restriction modification consists of a methyltransferase and a restriction endonuclease. The methyltransferase methylates the bacterial genome, providing protection. Restriction endonuclease then cleaves the non-methylated DNA (Labrie et al., 2010). A functional restriction modification system introduced in *Streptococcus thermophilus* provided phage resistance (Dupuis et al., 2013).

There are several other related defence mechanisms to restriction modification, highlighting a complex and diverse class of defence mechanisms. Defence Island Associated with Restriction-Modification (DISARM) is an elegant example of a restriction-modification related defence mechanism (Hampton et al., 2020, de Jonge et al., 2019, Ofir et al., 2018). DISARM consists of three core genes (*drmA, drmB* and *drmC*) and two viable ones, depending on the class. For class I, *drmD* and *drmMI* and for class II, *drmABC* and *drmMII* (Ofir et al., 2018). When cloned into *Bacillus paralichenformis* 9954a, DISARM was able to provide protection against a mixture of lytic and lysogenic phages, as the culture failed to collapse. There were

also no significant differences in the rate of absorption between bacteria lacking DISAM and those with (Ofir et al., 2018). This provided an indication that DISARM engaged in internal defence. Illumina sequencing also showed that phage DNA did not replicate and degraded over time (Ofir et al., 2018).

A final example of restriction modification related defences is Bacteriophage Exclusion (BREX). Found widespread across bacterial genomes (10%), BREX is a six gene cassette consisting of methyltransferase, RNA-binding anti-termination protein, ATP-binding protein, a protease and a protein with unknown function (Goldfarb et al., 2015, Nunes-Alves, 2015). Cloning a functional BREX system into the BREX-lacking *Bacillus subtilis*, Goldfarb et al found that it provided resistance against lytic and lysogenic phages by blocking phage replication (Goldfarb et al., 2015). BREX uses methylation of a specific motif (short, recurring pattern in DNA) to recognise self-DNA, interestingly this motif is different between *B. subtilis* (TAGGAG) and *E. coli* (GGTAAG) (Goldfarb et al., 2015, Gordeeva et al., 2018). Unfortunately, the defensive mechanism remains unknown (Goldfarb et al., 2015).

1.3.3 Abortive-infection systems

Abortive-infection systems protect the population of bacteria from phage infection, often a last resort if other lines of defence have failed (Labrie et al., 2010, Hampton et al., 2020, Lopatina et al., 2020). Similar to other defence mechanisms, abortive-infection systems are complex and diverse. However, all have the same characteristics; sensing phage infection and triggering the infected cell to commit suicide. Cell death occurs before phages can complete their replication cycle, preventing the spread of infection among the population (Lopatina et al., 2020). Within RSSC, five abortive-infection systems have been identified (Castillo et al., 2020).

Cyclic oligonucleotide-based antiphage signalling system (CBASS) is a widespread abortive-infection system comprising of four major classes (Millman et al., 2020b). Overall, CBASS works by sensing phage infection with specific proteins, producing a secondary messenger molecule which activates a cell-killing effector protein (Duncan-Lowey and Kranzusch, 2022, Lopatina et al., 2020). Cohen et al, first demonstrated that CBASS provided protection against phage infection. Cohen et al, cloned the CBASS system of *Vibrio cholerae* serovar O1 biovar El Tor (*V. cholerae* El Tor) and the system from *Escherichia coli* TW11681 into *Escherichia coli* MG1655 (CBASS-lacking). This *E. coli* MG1655 with CBASS provided protection against an array of diverse phages (Cohen et al., 2019). Despite its widespread and diversity, much of the mechanistical side of CBASS remains unknown. CBASS was identified in strains of *R. solanacearum* (Tesson et al., 2022, Payne et al., 2022).

1.3.4 CRISPR-Cas systems

Clustered regularly interspaced short palindromic repeats regions and associated genes systems (CRISPR-Cas systems) are a form of adaptive immunity against phages (Hampton et al., 2020, Koskella and Taylor, 2018). CRISPR-Cas systems work through a series of stages adaptation, expression and interference. Adaptation describes the process of corporation of foreign DNA, i.e., phage DNA, is incorporated into the CRISPR loci as a 'spacer'. During, expression, this spacer is transcribed and processed into small interfering CRISPR RNAs (crRNAs). The final stage, interference, involves these crRNAs guiding endonucleases to the target DNA (in some cases RNA) sequences which is subsequently cleaved and degraded. The target sequence are complementary to the 'spacer' (Barrangou, 2015). The CRISPR-Cas system I, provided immunity to a wild-type and susceptible strain of *Streptococcus thermophilus*. When exposed to two virulent phages, the CRISPR-Cas system require new 'spacers' which matched the sequences in these two phages and provided resistance to *S. thermophilu*s (Barrangou et al., 2007). CRISPR-Cas systems have remarkable diversity, can be found in abundance across both bacteria and archaea lineages. Currently, there are two classes each with several types. These systems differ in their composition, effector complexes and targets (Koonin et al., 2017). Also, bacteria are known to harbour more than one system. This means that CRISPR-Cas can provide adaptive immunity against a diverse range of phages. In *S. thermophilus* strain DGCC7710, Carte et al found through deep sequencing of crRNAs, that four CRISPR-Cas systems were present and functionally independent of one another (Carte et al., 2014). CRISPR-CAS systems have been identified in RSSC, Type I-E CRISPR-Cas system was prevalent in RSSC but it may be inactivate as it did not provide resistance to phage phiAP1 in *R. solanacearum* (strains CFBP2957 and K60^{T}) (Castillo et al., 2020, da Silva Xavier et al., 2019).

1.3.5 Prophages

Prophages are also known to provide defence for their host against other phages (superinfection exclusion). They do this because they themselves are vulnerable to phage predation. If their hosts die, their genome cannot be passed to the next generation. To prevent this, prophages express and provide phage defence mechanisms to their hosts to protect themselves (Hampton et al., 2020). Prophages can express defence mechanisms that protect the individual and/or the population. The prophage BTP1 found in *Salmonella enterica* encodes multiple systems that provide *S. enterica* with phage resistance. One defence mechanism was an operon that modifies the cellular lipopolysaccharides (LSP) which is a phage receptor for, the phage P22 (Kintz et al., 2015). Interestingly, deletion of this operon did not restore complete susceptibility to P22. This result suggested another defence mechanism was in play. Another gene *BstA* found in BTP1 seemed to provide resistance, as its own deletion increased susceptibility to P22. For further validation, *BstA* was cloned into *Salmonella typhimurium* where it provided resistance to phages. BstA proteins provide a population-level from a resistance by triggering an abortive effect preventing the spread of phage infection (Owen et al., 2021). Likewise, *Entercoccus faecalis* prophage 6 provided resistance to phage Idefix through a novel abortive mechanism known as abiα. Although, it remains relatively unclear how abiα works, it was observed that lysis of the cell was premature when infected with Idefix. It should be noted that the abiα is widespread among various phages (Lossouarn et al., 2019). Prophages are widespread across RSSC and could possibly confer phage resistance (Greenrod et al., 2022).

1.4 Counter Resistance Mechanisms in Phage

Like bacteria, phages themselves have also evolved a number of mechanisms to counteract the rise of resistance in their hosts (Samson et al., 2013). It has also been suggested that these anti-resistant mechanisms cluster together in the genome which could suggest the possibility that "anti-defence islands" exist (Chevallereau et al., 2022). The discovery of novel defence systems in bacteria has also led to an increase interest in finding counteract measures in phages. Although, many novel defences remain uncharacterised. Researchers have identified a few proteins that allow phages to evade these unknown defence mechanisms (Gao and Feng, 2023). Unfortunately, understanding of phage counter resistance mechanisms against RSSC is very limited but as phages and RSSC engaged in coevolutionary dynamics, it is highly possible that it could engage in the following counteracts (Wang et al., 2017).

1.4.1 Counteract: Preventing Absorption

Bacteria are known to alter (or mask) their receptors to prevent phage absorption. However, it is possible for phages to counter this. Point mutations can give the phage the ability to access the new altered receptor. The most extensively studied example is phage λ. Phage λ whose target receptor is LamB on *Escherichia coli*, gained the ability to target OmpF and a mutated LamB, when resistant *E. coli* mutated the original LamB receptor to prevent absorption. Mutations were found on the tail fibre (Burmeister et al., 2021). A similar situation, appeared for phage SPO1 through mutations on its baseplate and tail fibre, it gained the ability to access new receptors on phage resistant *B. subtilis* (Hampton et al., 2020). If a receptor is masked, phages countermeasure this by degrading the structures around the receptor. Capsules and exopolysaccharide (EPS) for example, can help mask a receptor (Samson et al., 2013, Hong et al., 2014). *Erwinia amylovora* phage L1 encodes a depolymerase enzyme that can breakdown amylovoran (a component of EPS) in the plant pathogen *E. amylovora*. Amylovoran is a major virulence factor but also helps mask phage receptors. This enzyme was able to breakdown amylovoran and increase *E. amylovora* susceptibility to phage L1 (Born et al., 2014).

Increasing absorption rates is a classic example of phages adapting to overcome phage resistance in bacteria. Increased absorption rates are adapted in response to lower expression (densities) of phage receptors (Burmeister et al., 2016). Phage U136B increases its absorption rates in response to phage resistance in *E. coli.* Evolved U136B had increased absorption rates to the receptor TolC compared to their ancestor. Mutations found in a putative tail fibre protein which might be responsible for host recognition function (Burmeister et al., 2023).

1.4.2 Counteract: Restriction Modification and other related defences.

Phages can have various mechanisms to protect themselves from restriction modification and other related defence mechanisms (Hampton et al., 2020). Methylation of their own DNA is one example. *E. coli* phages methylated the same motif in their genome which is also found in *E. coli* to protect themselves from BREX (Gordeeva et al., 2018). T3 phage that infect *E. coli* are able to overcome the BREX system. It is suggested T3 phage encodes an enzyme (SAMase) that results in the cleavage of S-adenosyl-L-methionine (SAM). SAM is a key component for target modification and target cleavage in these systems, including BREX, acts as a donor for methylation. Reduction in SAM is a key strategy to inhibit BREX (Andriianov et al., 2023). Direct inactivation of restriction endonucleases is also possible. Restriction protein (Ocr) of T7 can mimic DNA and bind tightly to EcoK1 restriction endonucleases (Gao and Feng, 2023). Phages can also escape DISARM but mechanisms remain unknown (Ofir et al., 2018).

1.4.3 Counteract: Abortive infection system

CBASS is an abortive infection system. Phages can inhibit this mechanism through anti-CBASS proteins (Gao and Feng, 2023). Protein Abc1 can counteract this defence. The protein degrades the cyclic nucleotide signals that activates this system. When *Yersinia aleksiciae* CBASS system was integrated into *E. coli* and challenged with T4 phages carrying Abc1 (wild type) or not (engineered),growth of the non-Abc1 T4 phages suffered as a result of not being able to evade CBASS (Hobbs et al., 2022).

1.4.4 Counteract: CRISPR-Cas Systems

Anti-CRISPR mechanisms are diverse and widespread, reflecting the diversity and abundance of CRISPR-Cas in bacteria. The systems reflect a complex and ancient arms race between phages and bacteria (Borges et al., 2017).

Mutations in target protospacers or PAM can prevent recognition and spacer acquisition. Spacer acquisition in CRISPR-1 in *S. thermophilus* was a key defence mechanism to phage challenge which in turn increased resistance. However, phages with mutations (single nucleotide and deletions) were found, believed to confer a response to phage resistance (Deveau et al., 2008).

Anti-CRISPR proteins (Acrs) perform various and complex activities to prevent CRISPR-Cas immunity (Gao and Feng, 2023). Some prevent CRISPR-Cas recognising and binding of the phage's DNA. AcrVIA1 directly binds to Cas13 of CRISPR-Cas system VI-A. This prevents recognition and binding of the target site, required for activation (Meeske et al., 2020). AcrF1 and AcrF2 interact with Cascade. A Cascade is a Cas protein and crRNA complex that surveys sequences looking for sequences complementary to the crRNA. When a match is found, nucleases are recruited to cleave the target sequence. AcrF1 and AcrF2 interact with the Cas proteins of this cascade, inhibiting binding (Pawluk et al., 2018). While others prevent recruitment of the proteins involved (Gao and Feng, 2023). AcrF3 binds to Cas3 helicase-nuclease effector which prevents its recruitment by Cascade (Bondy-Denomy et al., 2015, Pawluk et al., 2018). Finally, others can inactivate CRISPR-Cas (Gao and Feng, 2023). Anti-CRISPR protein AcrF6 was able to inhibit both type I-E and I-F systems. Plasmids coding AcrF6 were expressed in *P. aeruginosa* and challenged against phages (targeted for type I-E or I-F). This led to an increase in sensitivity to the phages, suggesting that the systems were inactivate. AcrF6 was found in prophages of various species such as *Oceanimonas smirnovii* and *Methylophaga frappieri* suggesting that this protein is widespread (Pawluk et al., 2016).

1.5 Bacteria and bacteriophage coevolution

Bacteria and the evolution of bacteriophages are closely intertwined. Both exert extreme selection pressures on each other. Bacteria and bacteriophages engaged in evolutionary mechanism known as “coevolution” where their interactions with each other drive each other’s evolutionary paths (Koskella et al., 2022). The term “coevolution” is a broad term often used to describe different categories and even processes of evolution. In general, it refers to reciprocal evolutionary change between interacting populations over time (Medina et al., 2022).

Overall, coevolution is complex as a result of a web of various different types of interactions (Hembry et al., 2014). A key interaction is antagonism, an interaction that bacteriophage and bacteria themselves experience together. Antagonistic coevolution refers to the reciprocal adaptation and counter-adaptation between interacting host and parasite populations (Gómez and Buckling, 2011). For host it involves the evolution of resistant mechanisms to reduce the burden of phage infection. Phages then counter-act this through mechanisms that increase their infectivity or host range (Koskella et al., 2022). Understanding of coevolutionary dynamics with RSSC and bacteriophages remain limited, especially in areas surrounding RSSC’s ability to evolve resistance to phages and their arsenal of defence mechanisms (Vailleau and Genin, 2023, Holtappels et al., 2021).

There are two types of antagonistic coevolution: arms race dynamics and fluctuating selection dynamics. Both are used to describe the evolutionary changes that occur between interacting phages and bacteria (de Jonge et al., 2019).

1.5.1 Arms Race Dynamics

Arms Race Dynamics (ARD) describes the escalation of adaptation and counter-adaptation between two antagonistic interacting populations (Figure 1.4) (Granato et al., 2019). Focusing on, bacteria and phages, ARD is defined by the evolution of phage resistance in bacteria with the phages counteracting this resistance. Ecologically speaking, ARD is an important factor that allows coexistence between antagonistic interacting populations. ARD can prevent phages from decimating their hosts, preventing them from driving their host and themselves to extinction (Avrani et al., 2012). However, if the dynamic is asymmetrical it can drive the extinction of one of the interacting populations (Wright et al., 2016). ARD is often driven by directional selection (the movement of allele frequency is in one direction). Within bacteria and phage ARD, bacterial hosts become resistant to a wide variety of phage isolates and phages becomes infective to a wide range of genotypes.

This dynamic was observed between *Pseudomonas fluorescens* and phage SBW25ϕ2. *P. fluorescens* increased its resistance to SBW25ϕ2 while SBW25ϕ2 increased its infectivity to *P. fluorescens* (Buckling and Rainey, 2002). Again, ARD was observed with the same species in a different experiment. Time-shift assays, where bacteria and phages isolated from various points across time are tested against each other, showed an escalation of infectivity for the phage and resistance in bacteria. Interestingly, when *P. fluorescens* was coevolved with two different genotypes of SBW25ϕ2, resistance rapidly evolved but reached a limit, while the phages continued to evolve. *P. fluorescens* became less resistant to contemporary phages through time (Castledine et al., 2022b). This suggests that resistance became costly to *P. fluorescens* when multiple genotypes are involved which could imply that ARD is limited. Arms race was also observed in between *E. coli* and the phage λ, *E. coli* evolved resistance to ancestral λ through mutations in maltose transport proteins preventing λ being able to inject DNA into the cytoplasm. The phage quickly counters this through evolving the ability to use other proteins such as outer-membrane protein (OmpF) as a receptor (Burmeister et al., 2021). Likewise, *Synechococcus* sp. WH7803 evolved resistance to its phage RIM8 in ARD-like manner. *Synechococcus* isolated in the future were more resistant then isolates from the past (Marston et al., 2012).

1.5.2 Fluctuating Selection Dynamics

Fluctuation Selection Dynamics (FSD) is described as fluctuations of directional selection of a given genotype/phenotype through evolutionary time (Figure 1.4)(Ford et al., 2017). The fluctuation selection dynamics between bacteria and phage is often characterised by temporal changes in resistance for the bacteria and infectivity for the phages (Chevallereau et al., 2022). It is an important driver of diversity within populations as it prevents a genotype/phenotype becoming dominant in the population (Burdon et al., 2013). Characteristic of FSD is that phages will become infective to the most common genotype within their host population. Negative-frequency dependent selection is often the driver of FSD as this common genotype is also the least fit in the population so will be selected against while rare fitter genotypes are selected for (Braga et al., 2018).

P. fluorescens and SBW25ϕ2 was used to observe FSD in sterilised soil microcosms. Here, *P. fluorescens* highest resistance was to phages that were contemporary (most common) rather than from the past or future, a characteristic of FSD (Gómez and Buckling, 2011). *P. fluorescens* and SBW25ϕ2 are model species, used to study extensively to study, *in vitro*, coevolutionary dynamics. Frequently, ARD is observed (Brockhurst et al., 2007, Buckling and Rainey, 2002, Castledine et al., 2022b). However, in this system, where soil microcosms were to used to reflect a more natural and complex setting FSD was observed instead. This questions how common and intense ARD is in natural communities. The presence of multiple abiotic and biotic selection pressures could alter coevolutionary dynamics between phages and their hosts (Bell, 2010). Fluctuating selection dynamics have been observed between *Vibrio crassostreae* and phages in a natural setting (oyster farm), infectivity from phages were highest to contemporary *V. crassostreae* and infectivity declined to *V. crassostreae* isolated from the past or future (Piel et al., 2022).

1.5.3 ARD and FSD are not mutually exclusive.

ARDs and FSDs are not separate coevolutionary mechanisms, it is possible that they switch between the two dynamics. For example, *P. fluorescens* SBW25 and its phage SBW25ϕ2 when coevolved together suggested that the system changes its dynamics over time (Hall et al., 2011). The system showed that ARD gave way to FSD over time. On the population level in a short period of time, phenotypes with higher infectivity (phage) or resistance (bacteria) quickly replaced other phenotypes in the populations, consistent with ARD. However, over longer periods of time, phenotypes began to oscillate, a common feature of FSD. Also, over time, the mean infectivity and resistance fluctuated as well, another feature of FSD (Hall et al., 2011). This was similar with *Salmonella anatum* and its phage JNwz02, ARD was observed at the beginning of the experiment but transitioned into FSD overtime due to increased fitness costs (competitiveness) associated with ARD. Mutation frequency rates in *S. anatum* while under ARD indicating an escalation of phage resistance but slowed over time likely as result of rising fitness costs allowing FSD to take over (Zhao et al., 2024). Three replicate communities of the same bacteria, *Pseudomonas aeruginosa* and the same phage OMKO1, also showed that ARD and FSD are not mutually exclusive of each other. One of the communities showed typical ARD while the other two showed FSD. Through time-shift assays, two communities of *P. aeruginosa* showed characteristic FSD, *P. aeruginosa* from these communities had higher resistance to contemporary phages. Whereas, the other community showed an escalation of resistance through time, with the most susceptible bacteria isolated from the past (Kortright et al., 2022a). The dynamics of ARD and FSD are not fixed, escalating costs that are associated with increasing infectivity and resistance can constraint ARD, suggesting there is a limit (Hall et al., 2011). Coevolution dynamics between *Prochlorococcus* and T7-like cyanophages suggested that ARD and FSD were not mutually exclusive. ARD was observed as highly resistant *Prochlorococcus* was isolated and evolved phages with the ability to overcome this resistance. However, mutations that allowing resistance and infectivity to evolve appeared to be fluctuating suggesting FSD (Schwartz and Lindell, 2017).

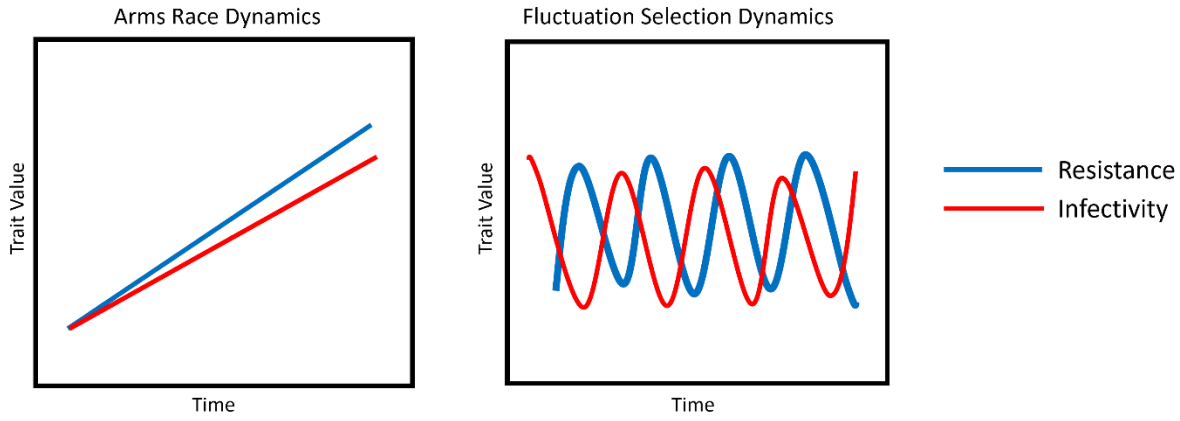

Figure 1.4 – Two modes of coevolutionary dynamics: Arms Race Dynamics (ARD) and Fluctuation Selection Dynamics (FSD). ARD describes the escalation of traits between two interacting species over time, e.g., phage infectivity and bacteria resistance. FSD describes the fluctuation of a phenotype from a given trait overtime. Driven by directional selection, at any given time, a phenotype might be advantageous, i.e., confer high resistance. Increasing fitness and reproductive success. The phenotype becomes common in the population. However, circumstances can change, phages adapt to this phenotype. Fitness decreases, reproduction is less successful. The phenotype abundance decreases and becomes rare until circumstances change again.

1.5.4 Asymmetrical Evolution

There is evidence that coevolutionary interactions between bacteria and phage can be asymmetrical with this asymmetry tipped in favour of bacteria (Figure 1.5) (Lenski and Levin, 1985). In other words, bacteria have an evolutionary advantage over phages. They can easily overcome phage infection and rapidly evolve resistance which the phages are not be able to overcome. Asymmetrical evolution was observed when exploring the coevolutionary dynamics between bacteria and phage collected from chestnut trees in the UK, over a three-year period (2011-2014). Bacteria appeared to be highly resistant to phages from their past, no matter how recent the phage was isolated (Dewald-Wang et al., 2022). Asymmetrical dynamics were also observed within *Salmonella* Enteritidis and its phage ϕSan2. Resistance within *S.* Enteritidis evolved rapidly and remained stable throughout the experiment, phages could not counteract it. (Holguín et al., 2019). Phage extinction events indicate that asymmetrical coevolution resistance within bacteria evolves, phages cannot overcome it and are driven to extinction. *Streptococcus thermophilus* and phage 2972 also showed evidence of asymmetry. A number of phage lines went extinct as resistance in the host increased (Common et al., 2019). A similar situation occurred with *E. coli* and phage U136B, a number of phage lines also went extinct as well (Burmeister et al., 2023).

Asymmetry may arise between bacteria and phage because resistant mutations in bacteria are easier to come by. Whereas, phages may experience genetic constraints, limiting their ability to counteract. Receptor modification, for example, can be achieved through multiple types of mutations, whereas for the phage, adaptation to another receptor (or the modified) is much more specific contributing to a greater mutation constraint and limiting their evolutionary ability (Avrani et al., 2012, Koskella and Brockhurst, 2014). Resistance in *S.* Enteritidis to ϕSan23 was caused by receptor changes to the BtuB receptor. It appeared that the phage failed to adapt to a new receptor (Holguín et al., 2019). Coevolutionary interactions between *Prochlorococcus* and T7-like podoviruses showed that phages were able to overcome resistant *Prochlorococcus* genotypes through host range expansion. However, host range expansion did not overcome every single resistant genotype. This suggests that asymmetry within this system was present. Genetic analysis of phages showed mutations in genes near the tail fibre, possibly dictating their host range. Genetic constraints

within phages prevented re-infectivity to all resistant genotypes (Schwartz and Lindell, 2017).

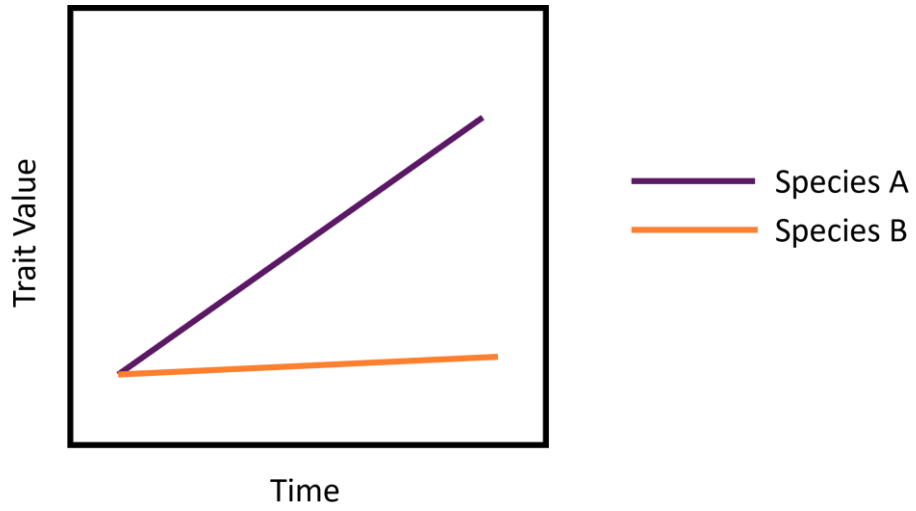

Figure 1.5 – Asymmetrical Evolution. One species evolves rapidly, leaving the other coevolving species behind. For example, bacteria can evolve resistance to phages and phages cannot adapt.

1.6 Evolutionary Trade-offs and Trade-ups

Evolutionary trade-offs are situations where an increase in fitness for one trait is detrimental to another (Mauro and Ghalambor, 2020, Burmeister and Turner, 2020). Microbes within the same environment can select for different traits which, in turn, leads to them experiencing different trade-offs. Between two traits (growth and resistance), microbes of the same species will select for one or the other. Consequence of this, is that the extreme population will have microbes with high growth rates and low resistance while others will have low growth rates and high resistance. Others will fall in between these two extremes, diversifying the population (Figure 1.6) (Ferenci, 2016).

Both bacteria and phages experience evolutionary trade-offs along their evolutionary trajectories due to their coevolutionary interactions. For instance, when bacteria evolve phage resistance, trade-offs can be evident in several traits such as biofilm formation, metabolism, motility, virulence and other types of resistance (antibiotics and environmental stresses) (Ferenci, 2016). Whereas phages can encounter trade-offs between host range, infectivity, multiplication, survival outside the host and transmission (de Jonge et al., 2019, De Paepe and Taddei, 2006).

A classic example of evolutionary trade-offs is between antibiotic resistance and phage resistance. Antibiotic resistance is often associated with cellular proteins such as efflux pumps. Efflux pumps remove toxic substances, including antibiotics out of the cell (Soto, 2013). Often or not, these proteins are receptor targets for phages. Phages can exert a strong selection pressure (due to mortality), that causes the bacteria to mask or even alter their proteins to prevent phage infection (absorption) (Bertozzi Silva et al., 2016). This can lead to impairment of these proteins, affecting their ability to resist antibiotics (Burmeister et al., 2020). In phage resistant *Salmonella typhimurium* the efflux pump-associated *TolC* was suppressed, which in-turn, made *S. typhimurium* susceptible to antibiotics (ampicillin and ciprofloxacin) (Laure and Ahn, 2022). Several strains of *P. aeruginosa* that evolved resistance to the phage OMKO1 became sensitive to several classes of antibiotics. The outer membrane porin M of the multidrug efflux systems MexAB and MexXY (Mex systems) are the receptor-binding sites of OMKO1. The presence of OMKO1 caused *P. aeruginosa* to select for phage resistance, resulting in alterations to the Mex systems. Phage resistant *P. aeruginosa* strains (both clinical and environmental) were sensitive to antibiotics (Chan et

al., 2016). In RSSC, phage resistance made the plant pathogen more vulnerable to antibiotics produced by *Bacillus amyloiquefaciens* (Wang et al., 2017).

Evolutionary trade-offs can have detrimental effects on bacteria, sometimes, making them vulnerable to competition. For instance, competition assays found that *P. fluorescens* with increased resistance to SBW25ϕ2 had lower fitness compared to susceptible *P. fluorescens* (Hall et al., 2011). Another *P. fluorescens* system with phage ϕ2 also highlighted fitness costs. Resistant *P. fluorescens* has reduced competitive ability (Brockhurst et al., 2007). In *R. solanacearum* phage resistance. *Bacillus amyloiquefaciens* is a competitor of *R. solanacearum*, phage resistant *R. solanacearum* was considerably more vulnerable to the antimicrobials produced by *B. amyloiquefaciens* (Wang et al., 2017).

Virulence is a trait of pathogenic bacteria that can be subjected to evolutionary trade-offs with phage resistance. *Shigella flexneri* that became resistant to a phage known as A1-1 suggested trade-offs with virulence. A1-1 targets the surface receptor OmpA which is known to be required for virulence in *S. flexneri*. Phage resistant *S. flexneri* were found to be lacking in the OmpA receptor which impacted their ability to spread intracellularly (Kortright et al., 2022b). *R. solanacearum* experienced trade-offs with volaille organic compounds (VOC). Resistance to VOC resulted in complete loss of pathogenicity. Mutations in genes encoding lipopolysaccharide O-antigen and type pilus biosynthesis might have contributed to this, as both are linked to virulence (Wang et al., 2023a). Receptor modification within the T2SS in *R. solanacearum,* conferred phage resistance but at a cost to virulence. Multiple virulence factors are secreted via the T2SS system, mutations to T2SS conferred phage resistance but it lost it functionality. Virulence to tomato plants was significantly reduced (Xavier et al., 2022). Evolutionary trade-offs involving virulence is a particular interest of researchers as it can be exploited for biocontrol application.

Phages themselves also experience trade-offs in a number of traits along their evolutionary paths (Goldhill and Turner, 2014, de Jonge et al., 2019). Although, understanding around RSSC phage trade-offs remain unclear.

Increasing host range is often associated with reduced infectivity. Phage isolates that coevolved with *P. fluorescens* had increased host range but their ability to reduce bacterial growth was lowered. This indicated an evolutionary trade-off (Poullain et al., 2008). Phages that were able to overcome resistance in *Prochlorococcus* had significantly lower fitness compared to their ancestor (Schwartz and Lindell, 2017).

An example of a trade-off within phages is between mortality and multiplication. In other words, how long a phage can survive outside the host (stability) and the number of progenies produced within a host. Using 16 well characterised coliphages of *E. coli,* De Paepe et al, found evidence of this trade-off. Phages with high multiplication rates often had high mortality rates and verse-versa. They suspect it was mediated by changes in the capsid structure (De Paepe and Taddei, 2006).

Phages also experienced trade-offs between environmental stress and several other traits (Goldhill and Turner, 2014). An RNA phage, phage ϕ6, experienced a trade-off between thermal stability and reproduction. Selecting for thermal stability and structure in the enzyme (lysin protein P5, lytic transglycosylase) lead to trade-offs. Evolved phage ϕ6 could survive in higher temperatures compared to the wild type. However, a fitness disadvantage was evident. Reproductive fitness of the evolved phage was lower than its wild-type at 25^{o}C but extracellular survival at higher temperatures was increased (Dessau et al., 2012). T7 phages were adapted to high concentrations of urea which resulted in a trade-off with growth. Urea adapted phages had a lower rate of decay in urea compared to the wild-type but a lower growth rate (Heineman and Brown, 2012). Interestingly, this trade-off was not as profound, with only a slight reduction in growth. The results here, raise questions about the constraints and impacts of the trade-offs. Nevertheless, both examples, here highlight that adaptation to environmental stresses can lead to evolutionary trade-offs.

However, it is possible that adaptations within bacteria and phages can lead to evolutionary trade-ups rather an evolutionary trade-off. Evolutionary trade-ups describe a phenomenon where selection for one trait increases not only its own fitness but also another trait. In some cases, there is little to no effect on other traits (Heineman and Brown, 2012). Through, novel experimental evolutionary regimes (a rotation of coevolving and one-sided evolution), a small percentage of phages were able to overcome a common evolutionary trade-off, growth rate and infectivity. These phages had high growth rates as well as high infectivity and were even capable of driving their hosts to extinction (Zhang et al., 2021). Evidence of a trade-up was found in adapting *E. coli* to low temperatures (20^{o}C). When testing the fitness of these evolutionary lineages at 40^{o}C, only 15 out of 24 lineages showed a significant trade-off. Even one showed an increase in fitness, perhaps, an evolutionary trade-up (Bennett and Lenski, 2007).

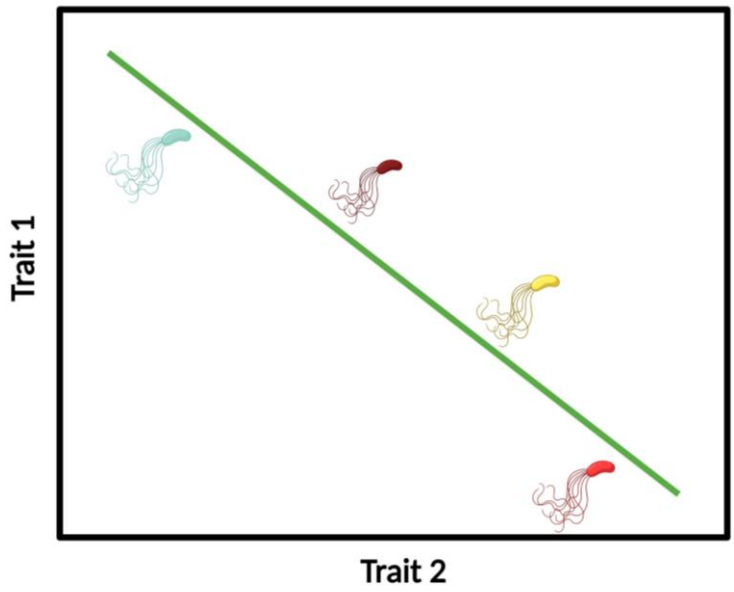

Figure 1.6 – Evolutionary Trade-offs. An increase in fitness to one trait could be detrimental to another. Over time, evolutionary trade-offs can lead to speciation. At the extreme, two species with high fitness for either trait. Intermediates along the trajectory of a trade-offs are likely to form. Created in Biorender.com.

Thesis Outline

Over the course of this project, I aim to use the phages to develop effective biocontrols against the *Ralstonia solanacearum* Species Complex (RSSC) through exploitation of their coevolutionary trajectories. Within this project, I aim to answer the following questions:

1. **Can we increase infectivity levels of phages through coevolution?**

I investigated a selection of phages to see if we can increase phages infectivity levels by evolving phages. I first kept the evolution one-sided (training), forcing only phages to evolve (Chapter 2) and then with RSSC and phages together (Chapter 3).

2. **What are the dynamics of their coevolution?**

I aimed to understand the modes of coevolutionary phages and RSSC were engaging in, through coevolution experiments *in vitro* (Chapter 3).

3. **Can I suppress phage resistance evolution in RSSC?**

Through the use of phage training (Chapter 2) and phage combinations (Chapter 3) I aimed to see if phage resistance evolution in RSSC could be suppressed.

4. **What are the genetic mechanisms underlying increased infectivity levels and phage resistance in RSSC?**

With whole-genome sequencing of phages (Chapter 2) and resistant clones of RSSC (Chapter 3 and Chapter 4), I investigated what genetic mechanisms are behind increased infectivity for phages (Chapter 2) and phage resistance (Chapter 3 and Chapter 4).

5. **What are the costs of phage resistance in RSSC?**

Several assays were performed (Chapter 3 and Chapter 4) to understand the costs of phage resistance and its conseqeunces to RSSC. I focused on three traits, fitness (growth), biofilm formation and exracellular polysaccharde (EPS), all closelly linked with its virulence and success as a plant pathogen.

To answer the questions presented here, this thesis containis the following chapters presented in the style of research manuiscripts:

Chapter 2: Exposing bacteriophages to multiple genotypes can improve outcome of phage training with phylopathogenic *Ralstonia solanacearum* bacterium.

For chapter 2, I use phage training to increase phage infectivity and delay potential phage resistance through the process of "phage training". Through experimental evolution, I aim to pre-adapt one phage against three genotypes of *R. solanacearum* (ancestral) in pairwise or multi-bacterial co-cultures. Finally, with whole-genome sequencing, I aim to understand the genetic mechanisms behind increased infectivity in phages. I found that multi-bacterial co-cultures were much more effective at suppressing the growth of two genotypes of *R. solanacearum*. However, in some cases we found little to no improvement from phages and phage resistance in *R. solanacearum* still rapidly evolved despite the training.

Chapter 3: Evidence of asymmetrical evolution between *Ralstonia solanacearum* and bacteriophages.

Following results from chapter 2, I decided to investigate whether coevolutionary phages and *R. solanacearum* together would increase the effectivness of phages. I performed a coevolution experiment with four phages against one genotype of *R. solanacearum*. I found evidence of asymmetrical evolution. Phage resistance rapidly evovled in resistance and drove phages to extinction. However, this came at a cost to *R. solanacearum* as I found evidence of evolutionary trade-offs in fitness and biofilm production.

Chapter 4: Conflicts between bacteriophages within bacteriophage combinations and resistance evolution can reduce effiacy of phages.

Since phage resistance evolved rapidly in *R. solanacearum* in previous chapters, I aimed to suppress phage resistance evolution through the use of phage combinations. By selecting 8 phages from our collection. I created various combinations (up to 3 phages max) and challenged the phages against *R. solanacearum* UW551. However, I found that conflicts between bacteriohages were emerging and phage resistance still evovled. Again, I found evidence of evolutoinary trade-offs in fitness and EPS production.

Chapter 2

Exposing bacteriophage to multiple genotypes can improve outcome of phage training with phytopathogenic *Ralstonia solanacearum* bacterium.

2.1 Abstract

The *Ralstonia solanacearum* species complex (RSSC) is a destructive plant pathogen that causes bacterial wilt in over 200 plant species, including important agricultural crops. A potential control method against RSSC is the use of bacteriophages (phages). Phages are viruses that infect bacteria and if virulent can even kill their host. They offer an environmentally friendly alternative to synthetic chemicals. However, there are several challenges when developing phages as biocontrols including infectivity level, infectivity range and resistance evolution. To mitigate these challenges phage training has been purposed, the process of pre-adapting phages to their bacterial host using experimental evolution. Here, we used phage training to pre-adapt one phage against three genotypes of *R. solanacearum* in either pairwise or multi-bacterial co-cultures. We hypothesised that we would see an increase in phage infectivity and a potential delay in phage resistance. Overall, we found that phages trained against multiple *R. solanacearum* genotypes had an advantage over phages trained against single genotypes in terms of suppressing ancestral bacterial growth. Interestingly, we found that phage training provided little to no improvement in some treatments. Even, one training treatment lost its infectivity. We identified mutations in sugar binding protein and tail fibres which are possibly associated with receptor binding. Furthermore, *R. solanacearum* could easily involve resistance against trained phages. From our results, we suggest that there are benefits to using multiple genotypes in phage training and offer an alternative training regime. This also highlights a complicated and dynamic interaction between *R. solanacearum* and phages.

2.2 Introduction

The *Ralstonia solanacearum* species complex (RSSC) is an extremely destructive plant pathogen that causes bacterial wilt in a wide range of plants (Castillo et al., 2020, Genin and Denny, 2012). Included in this list are the world's most important agricultural crops, such as tomatoes, potatoes, and bananas (Mansfield et al., 2012). RSSC causes bacterial wilt disease through rapid formation of biofilms, production of exopolysaccharides (EPS) and high bacterial densities within the xylem of a susceptible plant host. The result of this is blockage and reduction in sap flow which leads to the death of the plant (Lowe-Power et al., 2018, Hikichi et al., 2017). Currently, RSSC is comprised of three species: *Ralstonia pseudosolanacearum, Ralstonia solanacearum* and *Ralstonia syzygii* (Safni et al., 2014).

A potential strategy for controlling RSSC and other plant pathogens is the use of bacteriophages (phages) (Buttimer et al., 2017). Phages offer an environmentally-friendly alternative to synthetic chemicals (Yamada, 2012). They are known to have little to negligible impact on the surrounding rhizosphere (Yang et al., 2023). Two lytic phages were effective at protecting two-month-old banana plants from moko disease caused by RSSC infections (Ramírez et al., 2020). Phages ψRSA1, ψRSB1 and ψRSL1 caused rapid decreases in RSSC abundance either alone or in combination (Fujiwara et al., 2011). Lytic bacteriophage PE204 also successfully protected plants from *R. solanacearum*. No wilting symptoms were observed in tomato plants, highlighting the biocontrol of phages (Bae et al., 2012).

Although there are many advantages to phage biocontrols, there are a few disadvantages. Specificity for phages can be described as a double-edge sword, on one hand specificity protects the surrounding rhizosphere but on the other, phages might fail to provide enough coverage (Buttimer et al., 2017). RSSC consists of different species, each with their own unique phylotypes and strains. They can be found in close geographical proximity to each other (Vogelaar et al., 2023, Abdurahman et al., 2019). In Uganda, a molecular epidemiology study on RSSC, found a diverse set of RSSC strains in close geographical proximity to each other, consisting of different phylotypes and even different species of RSSC (Abdurahman et al., 2019). Phages would need to be able to infect multiple genotypes to be used as a biocontrol as they would need to provide enough coverage (Abdelsattar et al., 2021).

The evolution of phage resistance is a concern when developing phage biocontrols. Resistance is evident in a number of bacteria and phage systems (Buttimer et al., 2017). In

the plant pathogen *Pseudomonas syringae* pv*. aesculin* (causative agent of horse chestnut bleeding canker disease), the proportion of resistance to phages never falls below 66% (James et al., 2020). In RSSC, resistance to phages evolved rapidly, within 30 hours (Fujiwara et al., 2011). Both rapid evolution and high levels of resistance are problematic when considering phages for biocontrols. For a phage to be successful as a biocontrol, resistance to the phages must be suppressed. However, because phages engage in coevolutionary dynamics with their hosts, it is possible that phages can counteract this resistance (Hampton et al., 2020).

Phage cocktails have been shown to reduce the evolution of resistance in bacteria and increase the efficacy of phages (Mateus et al., 2014). However, competition between phages can reduce for the same hosts the efficacy of the cocktail and resistance is still possible (Costa et al., 2019, Culot et al., 2019).A phage cocktail of three phages against *Salmonella* Typhimurium showed no increase in efficacy compared to their single counterparts (Pereira et al., 2016). The rate of phage resistant mutants appearing in *Escherichia coli* was similar in the cocktail (phSE-5 and ELY-1) as it was to the single phSE-5. ELY-1 had the lowest rate of resistant mutant emergence (Costa et al., 2019). Phage cocktails still present some challenges when developing biocontrols.

Phage training may help to mitigate some of the challenges of using phages as biocontrols. Phage training is the process of using phages own evolutionary path to pre-adapt them to their bacterial hosts (Rohde et al., 2018). This increases their infectivity creating highly virulent phages (Borges, 2021). The training process also allows phages to experience how their hosts evolve resistance and adapt to this. These phages from the “future” will be capable of rapid counter-attack to the rise of phage resistance in their ancestral host (Borges, 2021, Borin et al., 2021). Resistance that arises as a result of selection pressures from trained phages could also be costly and insufficient (Borges, 2021).

Zhang et al were able to train phages to have a high infectivity and to be able to suppress phage resistance evolution against *Pseudomonas fluorescens* SBW25 (Zhang et al., 2021). Also, Borin et al observed that trained phages were able to suppress resistance evolution in *Escherichia coli* (Borin et al., 2021). The evolution of phage resistance in *E. coli* evolved quicker for untrained phages than trained. 100% of all replicates evolved complete resistance to the untrained phages but only 1 completely resistance replicate was isolated

from the trained phages treatment (Borin et al., 2021). Borin et al, highlight the potential of using phage training to overcome the evolution of resistance in bacteria (Borin et al., 2021). A similar situation was observed with ten *Pseudomonas aeruginosa* strains and four phages (14/1, phiKZ, PNM and PT7). Resistance levels were higher in strains of *P. aeruginosa* against ancestor phages rather than trained ones (Friman et al., 2016). PaoP5 was trained against *P. aeruginosa* PAOw-1. This bacteria strain is resistant to PaoP5 due to alterations found on the phage receptor O-antigen. Through phage training, PaoP5 was able to overcome this resistance. Mutations allowed PaoP5 to recognise the altered O-antigen (Yang et al., 2020).

Often phage training focuses on one genotype/strain of bacteria, *E. coli* B strain REL606 or *P. fluorescens* SBW25, for example (Borin et al., 2021, Zhang et al., 2021). Rarely, does phage training focus on using multiple different genotypes of the same species of bacteria simultaneously. Results from evolution experiments have shown that evolving phages with multiple genotypes often leads to host range expansion (Sant et al., 2021). Is it possible that by using multiple genotypes of the same bacterial species (*R. solanacearum*) we can train a phage, with an increase in infectivity and infectivity range?

Here we trained a single phage (PY015) against three different genotypes of *R. solanacearum.* We planned to train the phages in both mono- and combination cultures to assess whether multiple genotype phage training has an impact on outcomes of infectivity level and infectivity range. We hypothesised that monoculture training treatments would lead to the phages becoming more specialised with a high level of infectivity for one genotype but low level for another (Howard-Varona et al., 2018). While we expect that phages in combination training treatments would lead to the phages becoming generalists, with a high level of infectivity for more than one genotype. We also assess the impact trained phages have on the evolution of phage resistance against *R. solanacearum*. We hypothesised that trained phages would prevent (or delay) the emergence of phage resistance.

We have found that phages trained with multiple genotypes of *R. solanacearum* have an advantage over single genotype trained phages. Multiple genotype trained phages were more capable of suppressing bacterial growth than their single genotype counterparts. Interestingly, in some cases we found little or no improvement from the phage training with the ancestral phage outperforming the trained. We also found that *R. solanacearum* can

evolve resistance rapidly against trained phages. These results could have potential repercussions on the use of trained phages in agricultural applications. Their inability to prevent phage resistance is less than ideal. Moreover, these results highlight an extremely complicated evolutionary dynamic between phages and *R. solanacearum*.

2.3 Materials and Methods

2.3.1 Strains and Phage Isolates

We selected at random three phages (PY043, PY015 and PY017) that could infect *R. solanacearum* to find a suitable candidate for the training with a phage infectivity assay. As well as three genotypes of *R. solanacearum* that the phage could be trained against. Within a 96-well plate, 180µl of casamino acid-peptone-glucose (CPG, 1g casamino acid, 10g peptone, 5g glucose per litre) plate which were incubated at +28^{o}C for 72 hours, 10µl of *R. solanacearum* (5 genotypes selected at random) and 10µl of phage (or water for the control) was added and incubated at +28^{o}C (Kelman, 1954). Optical density reads (600nm) were measured every 24 hours for three days (Figure 2.1). The data concluded that ideal candidate was PY015 due to the different levels of infectivity it had on different *R. solanacearum* genotypes (Figure 2.1). On 2088 infectivity levels were high but with further training infectivity levels could be maintained for longer and prevent phage resistance in 2088 evolving (Figure 2.1A). On K60, PY015 had low levels of infectivity which could be improved through training (Figure 2.1B). Finally, PY015 had variable degree of infectivity to UW551, training PY015 here could prevent this variability and give PY015 high infectivity against UW551 (Figure 2.1C). The other two genotypes of *R. solanacearum* tested had similar outcomes to 2088 and K60 (Figure 2.1 A-B) but K60 is a model genotype of *R. solanacearum* and well characterised so was chosen over 081. 2088 was chosen over due to authenticity it is recognised by NCPPB as a genotype of *R. solanacearum* while 385 is yet to be authenticated. Before the training, abundance and volume of PY015 was increased, see "2.3.5 Phage Enrichment". PY015 was stored at +4^{o}C. The phage isolate PY015 was isolated in the River Thames, UK in 2019. PY015 belongs to the *Podoviridae* family. Three genotypes 2088, K60 and UW551 were chosen for training and further assessment of the trained phages. All three genotypes belonged to the phylotype IIB but varied in their origins, isolation year and host (Table 2.1). First, an isogenic stock of each genotype was created for the experiments. Each genotype was collected from cryo-stock and streaked onto CPG plates (15g Agar) which were incubated at +28^{o}C for 48 hours. Next, a single colony was picked and placed into 25ml of CPG media, which was incubated, shaking at 100rpm in the same conditions as mentioned before. Each strain was then standardised to an OD of 0.3 (Tecan sunrise). Once standardised each genotype was cryopreserved by adding 600µl of sample to 400µl glycerol (20%) and the Colony Forming Unit/ml (CFU/ml) was calculated (see 2.3.4

Quantification of Bacteria Densities for the method). At 0.3 OD, 2088 had a CFU/ml count of $5.2x10^8$, K60 $9.7x10^8$ and UW551 $1.37x10^9$.

Table 2.1 – Overview of the three strains of *R. solanacearum* used throughout this experiment. All three strains belong to phylotype IIB known for its ability to adapt to the cold. This phylotype is important for Europe and the UK.

Genotype	National Collection of Plant Pathogenic Bacteria (NCPPB)	Country of Origin	Year of Isolation	Host
2088	2088	Nigeria	1968	*Solanum tuberosum* (potato)
K60	325	United States	1953	*Solanum lycopersicum* (tomato)
UW551	4362	Kenya	2003 in the USA	*Pelargonium hortorum* (garden geranium)

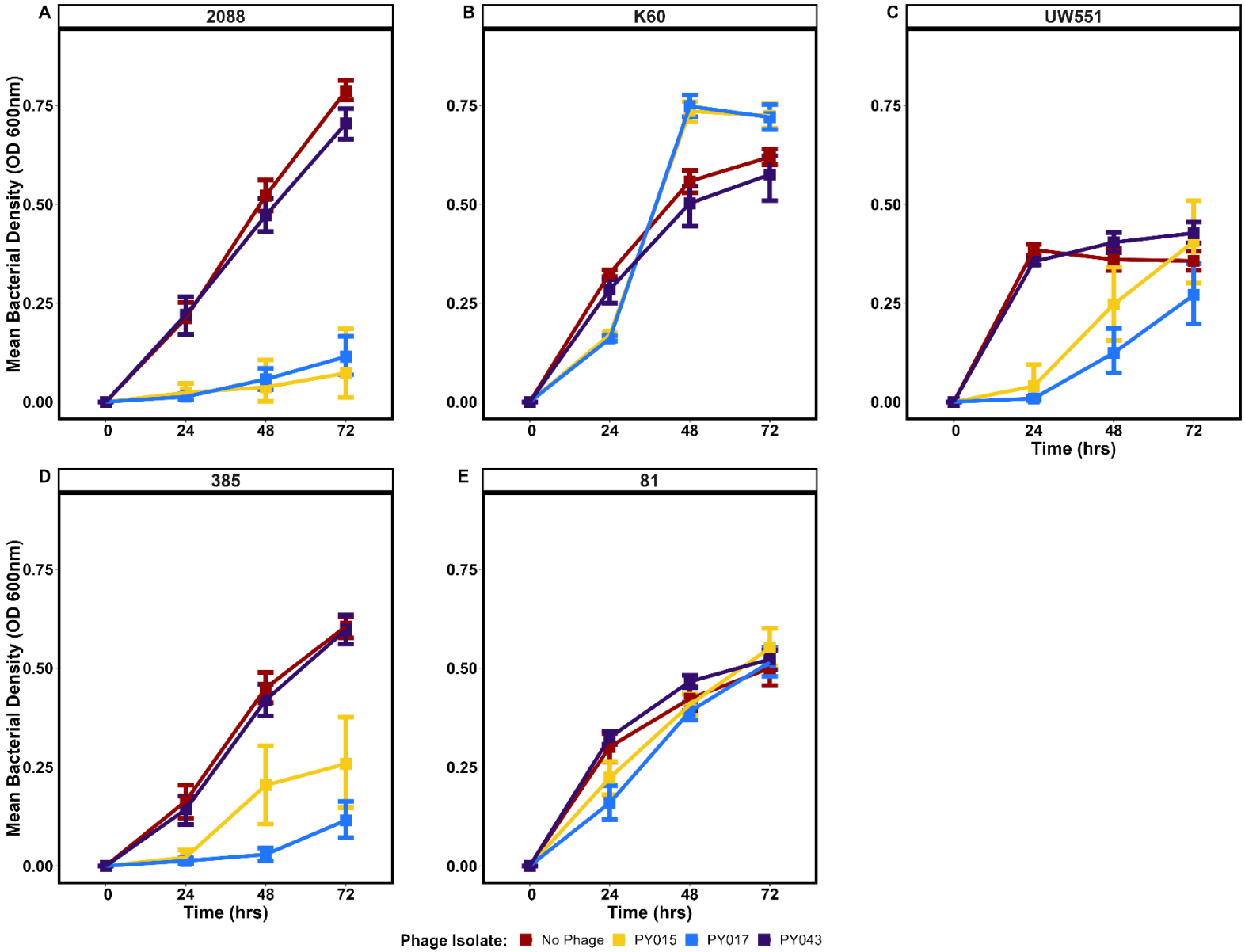
A
2088
B
K60
C
UW551
D
385
E
81
Mean Bacterial Density (OD 600nm)
0.00
0.25
0.50
0.75
0
24
48
72
Time (hrs)
Phage Isolate:
No Phage
PY015
PY017
PY043

Figure 2.1 – Phage Infectivity assays. Phage infectivity assays were carried out to determine ideal candidates of R. solanacearum genotypes and phages for phage training. Five strains of R. solanacearum were grown in the presence of three different phages (PY015, PY017 and PY043) for 72 hours to determine infectivity levels of each phage to each strain. Each panel is a different genotype of R. solanacearum, A) 2088, B) K60, C) UW551, D) 385 and E) 81. For the phage, PY015 (yellow) was chosen due to different level of infectivity (low-high) on various genotype of R. solanacearum. 2088, K60 and UW551 were chosen as the genotypes for PY015 to be trained again due to different levels of infectivity PY015 had against these genotypes. All three genotypes are authenticated by the NCPPB and other authorities. UW551 and K60 are model strains of R. solanacearum that are well characterised, aiding with research.

2.3.2 Phage Training

The phage isolate PY015 was exposed to three different genotypes of *R. solanacearum* for 27 days or nine training cycles. PY015 was trained under seven treatments which comprised of mono- and combination culture of these three genotypes (Figure 2.1). Alongside 2ml of CPG media, 12µl of phage (initial: 108 PFU/ml) and 12µl (in total) of *R. solanacearum* was added to a 24-well plate with six replicates and incubated at 28^{o}C for three days. For the monoculture training treatments, a total of 12µl of one genotype was added (10^8 CFU/ml), two combination training treatment 6µl of each genotype (10^8 CFU/ml for both) was added for a total of 12µl and for three combination training treatment 4µl of each genotype (10^8 CFU for all) was added for a total of 12µl.

At the end of the three days, the phages and population were isolated and optical density (600nm) reads were taken as well. The population was cryopreserved at -80^{o}C by adding 400µl of 50% glycerol to 600µl of sample. The trained phages were isolated by adding 900µl of sample to 100µl of chloroform. This was vortexed for 30 seconds and then centrifuged at 13000 rpm for 5 minutes. The supernatant was removed, filtered (0.2µm) and stored at +4^{o}C. After this was completed, 12µl of isolated trained phages was added back to their corresponding training treatment with the exact same conditions as before. The cycle was then repeated nine times (27 days). For each cycle we used the same ancestral strains of *R. solanacearum* to keep the training one-sided, only the phages evolved.

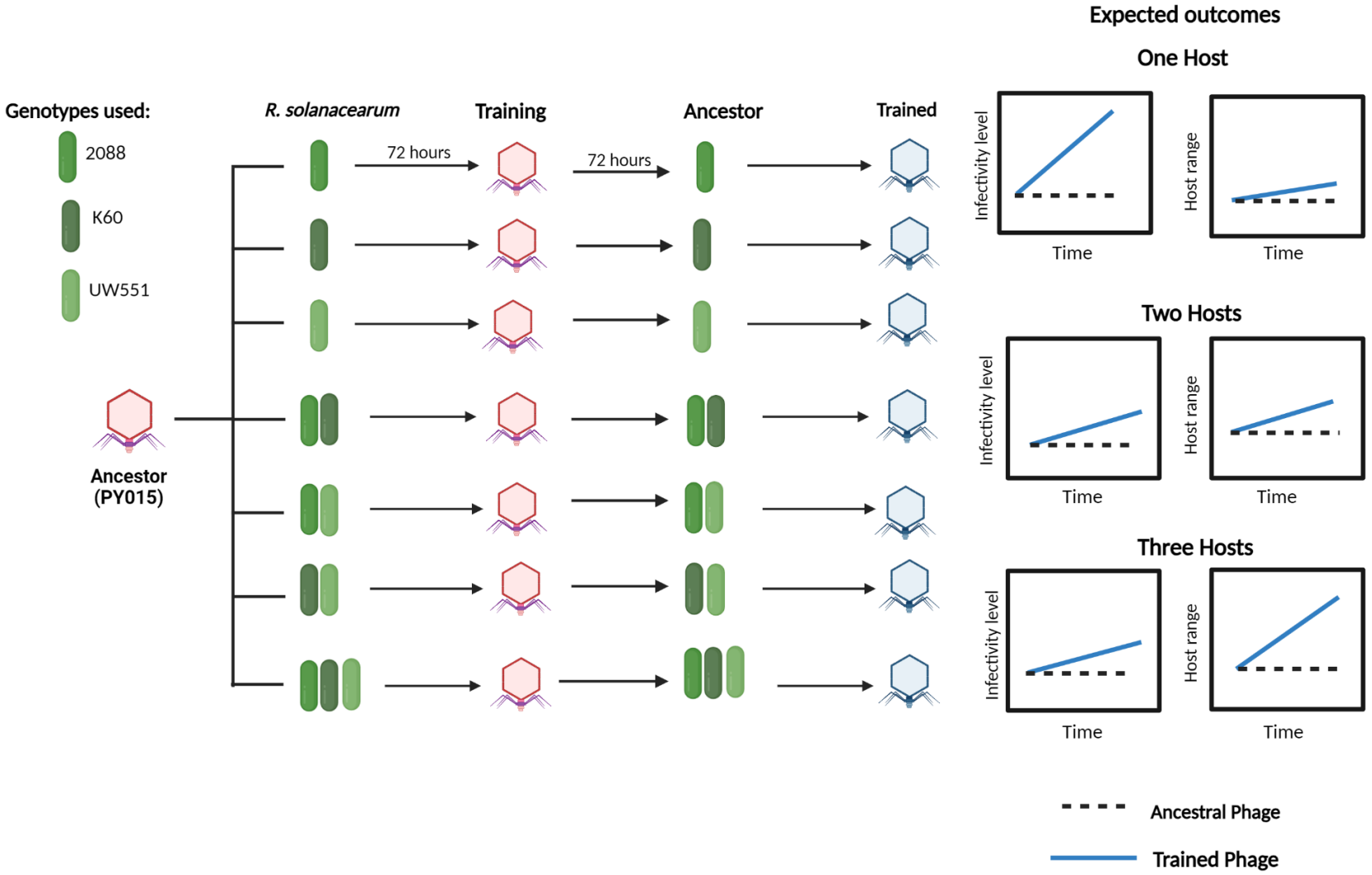
Genotypes used:
2088
K60
UW551
Ancestor
(PY015)
R. solanacearum
72 hours
Training
72 hours
Ancestor
Trained
Expected outcomes
One Host
Infectivity level
Time
Host range
Time
Two Hosts
Infectivity level
Time
Host range
Time
Three Hosts
Infectivity level
Time
Host range
Time
Ancestral Phage
Trained Phage

Figure 2.2 – A schematic view of the phage training experiment and its treatments. Ancestral phage (PY015) was exposed to mono and combination cultures of three different genotypes of *R. solanacearum* for 72 hours (2088, K60 and UW551). After the 72 hours, phages were isolated, and the population cryopreserved. The isolated phages were again exposed to their corresponding treatment and the training continued for 27 days (or nine cycles). The panels show our expected outcomes when training phages with one, two or three hosts (genotypes of *R. solanacearum*). We expected that infectivity will increase with training but to what extent differ between training treatments. With one host training treatments, over time infectivity will become high tagainsttheir training host. With multiple hosts in the training treatment, infectivity would increase but also host range would increase as the phage adapts to more than one genotype. Created in Biorender.com.

2.3.3 Quantification of Phage Densities

Phage densities were recorded as the Plaque-Forming Unit (PFU/ml). A square plate was divided among the replicates (six in total) and a serial dilution was created using the isolated phages (10^{-1} to 10^{-8}). To this end, 300µl of overnight culture of 2088 (a susceptible host) was added to 10ml of soft CPG agar, poured onto a square CPG agar plate and left to solidify. 10µl of each dilution was added onto the plate and was incubated at +28°C for 24 hours. The PFU/ml was calculated from these plates with the following equation:

PFU/ml = number of plaques formed/ [dilution factor x volume of phage]

In some cases, we used circular plates where each plate was a serial dilution and a replicate. 5ml of soft CPG agar was used instead of 10ml.

2.3.4 Quantification of Bacteria Densities

Bacterial densities for each strain were recorded as the colony forming unit (CFU/ml). A serial dilution (10^{1} to 10^{8}) was created. 10µl of each dilution was added to a circular CPG plate and spread. The CPG plates were left to incubate from 48-72 to hours at 28°C. The CFU/ml was calculated from the following equation:

CFU/ml = [number of colonies x dilution factor] / volume of culture plate

2.3.5 Phage Enrichment

To further assess the trained phages, they had to be enriched to increase their abundance and their volume. 10µl of phage was added to 100µl of 2088 (grown in 25ml of CPG for 48 hours before phage inoculation) along with 35ml of fresh CPG media. This was then incubated for 48 hours at +28°C, shaking at 100rpm. Next, 10ml was removed and 1ml of chloroform was added. This was mixed, and then centrifuged. Once centrifuged, the supernatant was removed and stored at +4°C. The phage abundance was determined also, following the method as described above. Phage enrichment was conducted as little as possible to avoid further selection on the phages. Phage enrichment was only conducted for the initial ancestral PY015 stock and the DNA isolation.

2.3.6 Phage Infectivity Assays

To investigate if trained phages where more infective than their ancestor, we performed phage infectivity assays. We looked at their ability to suppress bacterial growth over 72 hours. To perform these assays, a 96-well plate was divided between the trained phages and ancestor (six replicates). To each well 180µl of CPG media, 10µl of *R. solanacearum* (2088, K60 or UW551) and 10µl of phage was added. Water (diH_2O) was added to the outermost wells to prevent evaporation. The optical density (OD 600nm) was then recorded every 15 minutes for 72 hours (Tecan Sunrise). The MOI was set to 1 (10^3 cells of bacteria and 10^3 viral particles of phage).

2.3.7 Fluctuation Tests

We performed fluctuation tests on the ancestral and on the final trained phages with ancestral *R. solanacearum*. This was conducted to determine the effects these phages have on phage resistance evolution in *R. solanacearum*. We wanted to see if trained phages could suppress resistance evolution that could potentially arise in ancestral *R.* solanacearum. We used a similar approach to Borin et al (Borin et al., 2021). First, overnight culture of ancestral *R. solanacearum* (of each genotype) was diluted (1:100) and inoculated into a 96-well plate, to create independent isogenic cultures. This plate was grown for 48 hours at +28°C. Next, 10µl of bacteria was inoculated into another 96-well plate along with 20µl of phage (diH_2O for the control) and 150µl of CPG media. OD 600nm point reads were taken, and the plate was grown for 48 hours at +28°C. Point reads were taken at 0and 48 hours (Tecan Sunrise).

To determine whether a well was resistant to phage we used the same approach that Borin et al used, we used their OD reads at 0 and 48 hours (Borin et al., 2021). A population was considered resistant if their OD at 48 hours was above the average OD value at 0 hours for each host (2088, K60 and UW551). We also had to take into consideration that potential for evolutionary trade-offs which could be related to growth. Trade-offs between phage and fitness (growth) is common which could lower the OD despite the presence of phage resistant bacteria (Burmeister and Turner, 2020). A well could look susceptible but is resistant due to lower fitness of the phage resistant bacteria. Being above this value indicated bacterial growth and potential phage resistance so the well was deemed resistant.

We also calculated the mutant frequencies using the P_0 method. First, we performed CFU counts on the wells at the start and at the end of the experiment to calculate the number of cells in each well (on average). At the end of the experiment, we calculated the proportion of wells that remained sensitive to each treatment. Using the following equation from Borin et al, we calculated the mutation frequencies (Borin et al., 2021).

$$\mu r = \frac{\ln P0}{(N - N0)}$$

Where P0 is the proportion of wells sensitive, N is the number of cells in each well, N0 is the number of cells at the start of each culture and μr is the mutation frequency.

2.3.8 Ancestral and Coevolved Hosts Phage Infectivity Assays

Another type of phage infectivity assay was conducted in order to look at the effects of ancestral and coevolve on ancestral and trained phages. We took ancestral *R. solanacearum* genotype 2088 and the two coevolved hosts from "2088 Only" and "2088 + K60 + UW551" training treatments. The coevolved host from "2088 Only" training treatment was chosen was because it was the only training treatment from the single genotype training treatments left with both trained phages and coevolved hosts. The K60 training treatment, phages were unrecoverable and possibly extinct and the UW551 training treatment bacteria were unrecoverable. The multiple genotype training "2088 + K60 + UW551" was the most effective training treatment so chosen based on its effectiveness. The coevolved hosts chosen for this experiment were bacteria isolated from the final three days of the training from where the final phages were isolated (24-27 days). Coevolved hosts were isolated from cryo-stocks of isolated populations from the training. The population was streaked onto a CPG plate and left to incubate for 48-72 hrs until colonies formed at +28^{o}C. A single colony was taken and re-streaked and grown again. This was repeated twice to remove phage from the bacteria. On the final plate, a single colony was placed into 25ml of CPG and left to grow at 28^{o}C, shaking100 rpm until an optical density (OD 600nm) of 0.3 OD was reached. Once the desired OD was reached, the bacteria was cryo-preserved until needed and CFU counts were taken (see above for methods).

For this phage infectivity assay, we took three 96-well plates which contained each host type (ancestral or coevolved). We divided the plate between the ancestor, "2088 Only" and "2088+YO373+UW551" phages. Each well contained 180µl of CPG, 10µl of *R. solanacearum* (ancestral or coevolved) and 10µl phage. We also included "Bacteria Only" controls, where 10µl of diH_2O was used instead of phage. For 62 hours, the optical density (OD 600nm) was recorded every 15 minutes (SPECTROstar Nano). The MOI was set to 1 (10^6 cells of bacteria and 10^6 viral particles of phage).

2.3.9 Phage Genomics

In order to understand the genetic changes that have occurred in the trained phages we sent a representative of each training treatment for whole genome sequencing at MicrobesNG. Obtaining high enough DNA quantities was extremely difficult, especially from the trained phages. To obtain enough DNA, we aimed to increase the titre of phages to above 10^8 PFU/ml. We first enriched the phages and calculated the titre on circular CPG plates (described above). From these plates we scraped six plates of each treatment into 50ml falcon tubes along with equal amounts of CPG media. The falcon tubes were incubated at +4^{o}C for 1 hour, rolling. After 1 hour, falcon tubes were centrifuged at maximum speed for 10 minutes and the supernatant was removed and filtered (0.2µm) and stored at +4^{o}C. The titration was recalculated. Once we reached our target, we proceeded with the DNA extraction.

Seven training treatments ("K60 Only" was not included due to extinction) and ancestral PY015 DNA was isolated using Phage DNA Isolation Kit from NORGEN BIOTEK CORPORATION. We followed the protocols provided but we made some modifications (modifications were provided by Dr Bryden Fields). For lysate preparation, two modifications were conducted. For the first, an optional step which was DNase Treatment, we used 15µl instead of 10µl of Norgen's RNase-Free DNase I and incubated at room temperature for 30 minutes instead of 15 minutes. This optional step was carried out to remove host genomic DNA. The second, was for the optional step of adding Proteinase K (20mg/ml) to increase DNA yields. 10µl of Proteinase K was added instead of 4µl, incubated at +55^{o}C for 1 hour instead of 30 minutes. Then at +65^{o}C for 30 minutes instead of 15 minutes, inverting the tubes every 5 minutes. At DNA elution steps, we used 75µl nuclease free water heated to +65^{o}C instead of Elution Buffer B. This was incubated at room temperature for 5 minutes before centrifuging. Qubit^{TM} High Sensitivity dsDNA kit was used to check the yield and make sure the DNA quantity met the threshold for MicrobesNG.

Variant calling pipeline was provided by Dr Bryden Fields (Community, 2022). First, we evaluated the quality of the reads with FASTAQC reports (Andrews, 2010). We used the PY015 ancestor genome raw read as a reference genome. Reference genome was assembled using SPAdes followed by annotation of the reference genome with Prokka (Prjibelski et al., 2020). SNIPPY was used for the variant calling (Seemann, 2014). Raw reads of the trained phages were mapped against the ancestor (reference genome). Quality of SNIPPY output was evaluated with samtool flagstat (Li et al., 2009). Genes of interest, i.e., genes which saw variation from the ancestor, were analysed to identify the proteins and understand their functions with BLAST (Altschul et al., 1997). We first used HHpred (default settings) to identify the proteins where variation was found, using the ancestral protein sequence. Next, protein sequences (focussed down onto genes with variance found in them) from the ancestor and trained phages were aligned through clustalΩ (Sievers et al., 2011). Swiss-model was also used for analysis of the proteins, modelling the ancestral and trained phage proteins to gain understanding in their structures and to see if genetic variation has caused changes in the proteins (Bertoni et al., 2017, Bienert et al., 2017, Guex et al., 2009, Studer et al., 2020, Waterhouse et al., 2018).

2.3.10 Statistical Analysis

Statistical analysis and data visualisation was performed using R statistical software, version 4.2.3 (Team, 2023). Figures were produced using the ggplot2 package (Wickham, 2016). For statistical analysis on the bacterial densities and phage abundance, focusing on the effects of time and treatment during the training, we used two-way repeated ANOVA with Bonferroni as post hoc analysis. The packages 'nlme' and 'car' were used to conduct the two-way repeated ANOVA (Pinheiro J, 2023, Weisberg, 2019). From the 'rcompanion' package we conducted post hoc analysis with Bonferroni on this two-way repeated ANOVA (Mangiafico, 2022). For all phage infectivity assays, we normalised the data against the 0-hour timepoint. This was done so we would only be looking at growth. The area under the curve (AUC) for all phage infectivity assays was calculated using the 'Growthcurver' package (Sprouffske, 2020). For Statistical analysis on AUC, we used Kruskal-Wallis Tests followed by pairwise Wilcoxon tests with Benjamini Hochberg (BH) p value adjustment, using functions from stats R package (Team, 2023). Finally, for the fluctuation tests, we calculated the proportion of resistance within the populations (Team, 2023). This was followed by chi-squared for association for statistical analysis, using the MASS package (Ripley, 2002).

2.4 Results

2.4.1 Bacterial densities decrease during the phage training.

We monitored the bacterial densities over time (as culture optical density, OD 600nm) to see if infectivity was increasing with each training cycle. A reduction in the bacterial densities should indicate an increase in infectivity. The bacterial densities for each training treatment decrease over each training cycle (Figure 2.2A-B). This suggests that phages were becoming more infective during their training. Statistical analysis appears to confirm that time had a significant effect on culture optical density and possibly infectivity (ANOVA Time: $F_{1,6} = 134.84$, $p < 0.01$). Training phages requires time as it wasn't until timepoint 6 that we saw significant changes in bacterial densities. Post Hoc analyses (Bonferroni's post-hoc analyses) shows that there were only significant differences between training cycles after six training cycles. There are no significant differences between training cycles 1 to 6 ($p < 0.05$). It should be noted that this reduction in bacterial densities over time was not gradual. Between timepoint 6 and 7, there was a significant decrease in bacterial density for five of the training treatments (Figure 2.2A-B). Phage training treatment "2088 Only" had a significant drop, to equivalent bacterial density of "UW551 Only" (Figure 2.2A, $p < 0.01$). After timepoint 6, all treatments except "UW551 Only" saw decreases in their bacterial density (Figure 2.2A). The "UW551 Only" training treatment saw complete suppression of bacteria throughout the training treatment, perhaps, PY015 was too virulent, completely wiping out the bacterial population or the abortive phage defence mechanism CBASS was triggering a culture collapse. The bacterial population from "UW551 Only" training treatment was unrecoverable.

Two-way repeated measures ANOVA statistical analysis further suggested that the interaction between both time and training treatments was significant (Figure 2.2A-B, (Treatment: $F_{1,6} = 645.64$, $p < 0.01$). Statistical analysis confirmed that training treatment groups differed significantly in bacterial densities. In the mono-culture training treatments in particular in "2088 Only" and "K60 Only" treatments, there were reductions over time in bacterial growth. However, for the monoculture training treatment "UW551 Only", we observed that the bacterial growth was suppressed throughout the training (Figure 2.2A). For the combination culture training treatments, we observed a similar pattern,

bacterial densities were reduced but this reduction is similar to that of either “2088 Only” or “K60 Only” monoculture treatments, depending on which genotypes were present (Figure 2.2B). For example, combination training treatments containing genotype K60 were similar to the “K60 Only” monoculture training treatment (Figure 2.2A-B). This similarity suggests that the most unaffected strains within the training treatment dictate the outcome of training treatment and bacterial densities in multi-bacteria treatments. Post -hoc analyses (Bonferroni’s post-hoc analyses) show there were significant differences in training treatments when certain genotypes were present in training treatment. For example, there was significant difference between training treatments “2088 + UW551” and “K60 Only” ($p < 0.001$) but no significant difference between training treatments “2088 + UW551” and “2088 Only” ($p > 0.05$).

Overall, we found that both time (training cycles) and phage training treatments had significant effects on bacterial densities, suggesting that phage infectivity evolution is also affected by these two factors.

2.4.2 Phage abundance stayed unchanged during training.

We expected the phage abundance would increase over time as the phages are trained to become more infective. Interestingly, phage abundances hardly changed throughout training of the seven training treatments (Figure 2C-D). Despite the lack of change in phage abundance for the other six treatments, Two-way ANOVA has shown that there was a significant difference between training treatments ($F_{6,1} = 920.037$, $p < 0.01$). Post hoc analysis (Bonferroni’s post-hoc test) showed that this interaction was driven by the loss of phage in “K60 Only”, while no significant differences between other training treatments were found. In this treatment, the phage became unrecoverable despite numerous adaptations to the phage isolation protocols involved. Therefore, it was not possible to determine PFU/ml of “K60 Only” phages throughout the training (Figure 2.2C). It is possible that these phages were driven to extinction. However, since we observed a decrease in bacterial density overtime in this treatment. It is likely that a phage is present but in small relative abundance (Figure 2.2A). This decrease in bacterial density overtime is also the reason we continued to transfer the treatment beyond transfer 3, it indicated the possibility that a phage could be present and could possibly be extracted at other transfers. Unfortunately, we failed to do so.

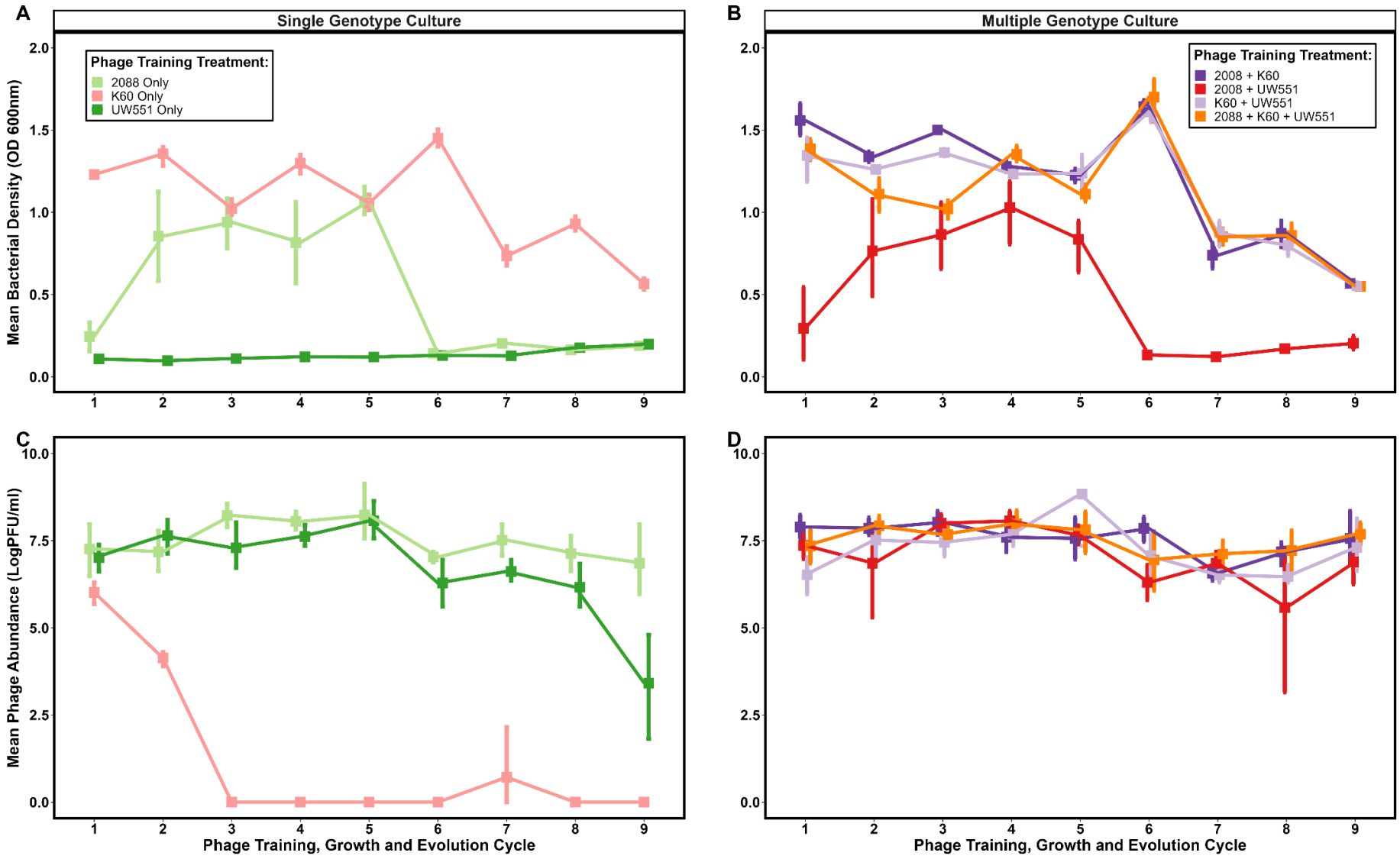
A
Single Genotype Culture
Phage Training Treatment:
2088 Only
K60 Only
UW551 Only
Mean Bacterial Density (OD 600nm)
B
Multiple Genotype Culture
Phage Training Treatment:
2008 + K60
2008 + UW551
K60 + UW551
2088 + K60 + UW551
C
Mean Phage Abundance (LogPFU/ml)
Phage Training, Growth and Evolution Cycle
D
Phage Training, Growth and Evolution Cycle

Figure 2.3 – The bacterial densities (optical density 600nm) and phage abundance (PFU/ml) of each training treatment throughout the experiment. Measurements were taken at the end of each cycle (3 days). A and C, show the bacterial densities and phage abundance for single (or mono) genotype training treatments. B and D, show the bacterial densities and phage abundance for multiple genotype training treatments. A-B, single genotype training treatments. C-D, multiple genotype training treatments. Each data point consists of six independent replicates and shows the mean ±SEM/SD. CFU/ml was not calculated during the training treatment; it would have been very difficult to differentiate between genotypes due to their morphological similarities.

2.4.3 Phage Infectivity assays suggest multiple genotype trained phages were more effective than single genotype trained phages.

To directly test if trained phage populations had become more infective, we compared their ability to suppress the growth of the ancestral *R. solanacearum* strains compared to their ancestral phages. We hypothesised that trained phages would be more infective than their ancestors, but we expect to see variation between the phage training treatments. As single genotype trained phages evolved to become more specialised, we expected that they would have higher suppression for the genotype they were trained with, while less effective suppression for genotypes they were not trained with, should be observed. For the multiple genotypes trained phages we expected to see increased bacterial suppression across all three genotypes as they become more generalised regarding their infectivity and increased host range.

Overall, we saw variation between phage training treatments (Figure 2.4). For genotype 2088, there were significant differences between the phage treatments (Figure 2.4A-B, Kruskal-Wallis: $X^2_{28.823}$, $p < 0.001$). Surprisingly, no improvement between "2088 Only" and the ancestral PY015 was observed, with a few replicates performing worse than the ancestral phage (pairwise Wilcoxon test with BH adjusted for p values, $p = 0.619$). The ancestor also failed to suppress 2088 (Figure 2.4A-B). This suggests that phage training did not improve phage infectivity on 2088 strain. The situation was similar for "UW551 Only" and "2088 + K60" trained phages, no signs of improvement was found and there was no significant difference between ancestral PY015 and "2088 + K60" (Figure 2.4B, pairwise Wilcoxon Test with BH adjusted for p values, $p = 0.784$). We did find a significant difference between "UW551 Only" and the PY015 ancestor, indicating decrease in infectivity after phage training (Figure 2.4B, pairwise Wilcoxon Test with BH adjusted for p values, $p = 0.026$). Moreover, genotype 2088 grew better in the presence of "UW551 Only" suggesting a loss of trained phage infectivity on this genotype. The remaining three multiple genotype trained phages "2088 + K60", "K60 + UW551" and "2088 + K60 + UW551" showed considerable bacterial suppression and an increase in infectivity (Figure 2.4A-B).

Although, its single genotype training treatment was driven to extinction, it was important to assess the remaining trained phages against this genotype, especially the phages trained in multiple combinations with K60 to ascertain whether they had evolved the ability to

suppress K60. For genotype K60 we found a significant difference between treatments (Figure 2.4C-D) (Kruskal-Wallis: $X^2_{20.52}$, p = 0.005). However, post hoc analysis (pairwise Wilcoxon Test with BH adjusted for p values) suggested that differences were between the control and all other treatments, no significant differences between the treatments themselves and the ancestor PY015 ancestor (Figure 2.4C). Towards the end of the growth curve, there is a slight increase of bacterial density for the control (no phage) treatment while the other treatments remained the same which could explain the difference (Figure 2.4C). Overall, there was no real suppression from any trained phages against K60. It should be noted that the growth of K60 was poor, with a rapid increase followed by plateau for the remainder of the growth curve (Figure 2.4C-D).

For genotype UW551, we found that treatments varied very strongly (Kruskal-Wallis: $X^2_{34.393}$, p < 0.001). Both ancestral and trained phage treatment where capable of suppressing the growth of ancestral UW551 and there were differences between the training treatments (Figure 2.4E-F). Surprisingly, the ancestor phage was the most successful phage treatment and completely suppressed UW551 for 72 hours (Figure 2.4E-F). The only treatments that were on a par with the ancestor phage were the multiple genotype trained phages, especially “2088 + K60”, “K60 + UW551” and “2088 + K60 + UW551” (Figure 2.4F, pairwise Wilcoxon Test with BH adjusted for p values, p = 0.6, p = 0.968 and p = 0.440, respectively). Although this means there was no significant difference, it suggests that these three training treatments did not lead to loss in phage infectivity. There was a slight difference between the ancestor and “2088 + UW551” likely as the result of a slight increase in bacterial density over time (pairwise Wilcoxon Test with BH adjusted for p values, p = 0.034). Again, it is the single genotype trained phages that perform the worst and although, both were capable of bacteria suppression, it was not to the extent of the ancestor phage (Figure 2.4E-F).

Overall, it appears that phages trained with multiple genotypes were more effective, especially against 2088 and UW551 (Figure 2.4A-B and 2.4E-F). In certain cases, single genotype trained phages performed worse than the ancestral phage, (Figure 2.4). Specifically, we expected the “UW551 Only” trained phages to be highly infective against UW551, indicating a move towards specialism. However, it performed much worse than the ancestral phage and other trained phage types (Figure 2.4E-F). No phages were able to suppress the growth of genotype K60, whether they were ancestral or trained phages due to high levels of resistance (Figure 2.4B-C). It is also important to note that resistance emerges in ancestral bacteria (except for UW551) a common theme in this chapter. Perhaps, this reflects an asymmetrical coevolutionary dynamic between *R. solanacearum* and PY015.

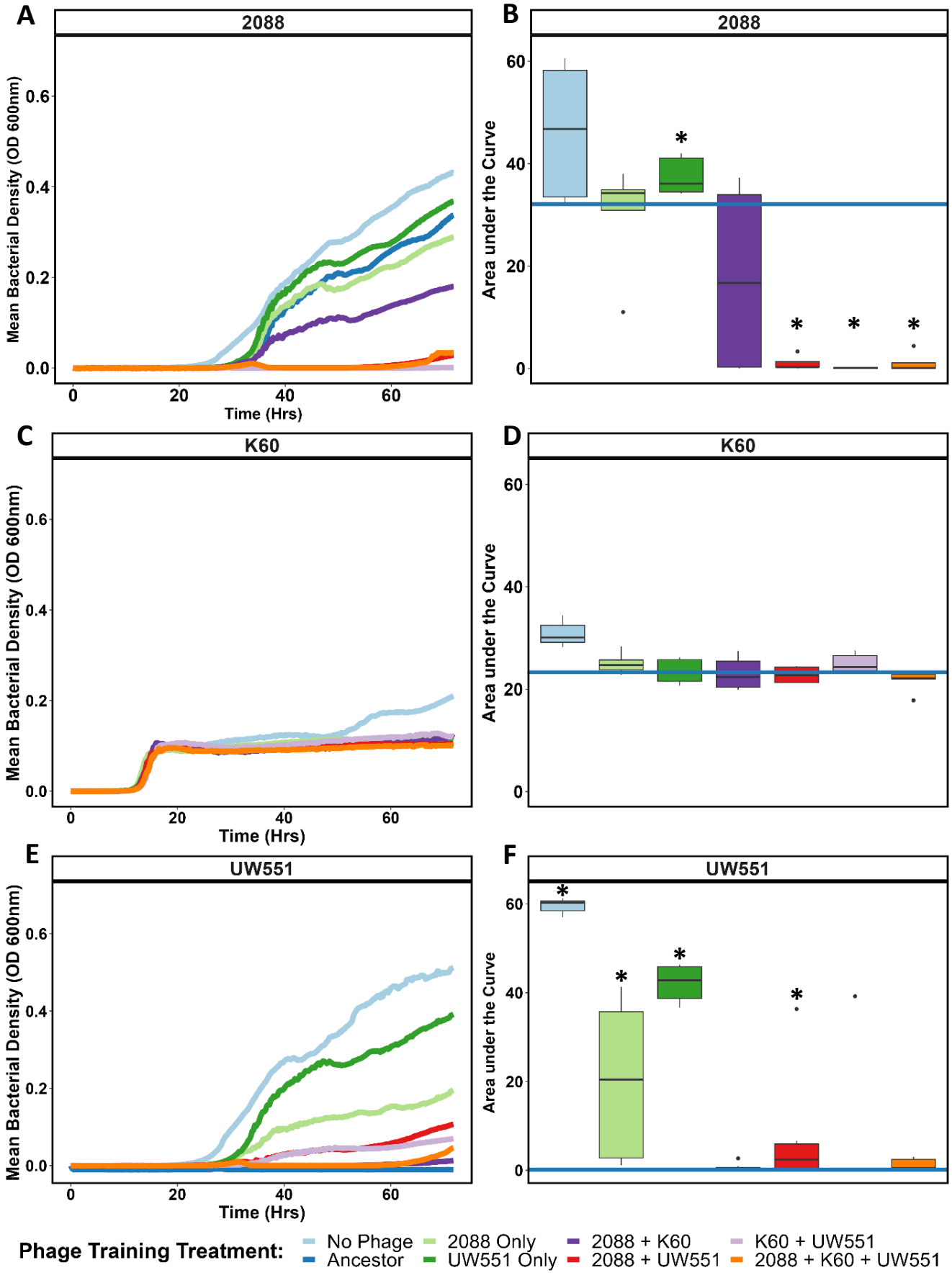
A
2088
Mean Bacterial Density (OD 600nm)
0.0
0.2
0.4
0.6
0
20
40
60
Time (Hrs)
B
2088
Area under the Curve
0
20
40
60
C
K60
Mean Bacterial Density (OD 600nm)
Time (Hrs)
D
K60
Area under the Curve
E
UW551
Mean Bacterial Density (OD 600nm)
Time (Hrs)
F
UW551
Area under the Curve
Phage Training Treatment:
No Phage
Ancestor
2088 Only
UW551 Only
2088 + K60
2088 + UW551
K60 + UW551
2088 + K60 + UW551

Figure 2.4 – Phage Infectivity Assays used to quantify phage infectivity evolution from the training in terms of pathogen suppression. Ancestral and trained phages were inoculated with each genotype of ancestral *R. solanacearum*, and the growth of each genotype was monitored, measuring the optical density (OD 600nm) every 15 minutes for 72 hours. A-B) The phage infectivity assay for genotype 2088. C-D) The phage infectivity assay for genotype K60. E-F) The phage infectivity assay for genotype UW551. The mean growth of *R. solanacearum* over time is shown in panels A, C and E for each genotype. The area under the curve is shown in panels B, D and F, with the dark blue representing the mean area under the curve of the ancestral phage, PY015. For genotypes K60 and UW551, N = 6 for each phage treatment. For genotype 2088, ancestor N=5, "2088 Only" N=5, "UW551 Only" N =5 and the remaining phage treatments N = 6. The phages from "K60 Only" treatments are not assessed due to their extinction in the training. Phage Treatments with * symbols are significantly different to the ancestor phage based on pairwise Wilcoxon tests with Benjamini Hochberg p value adjustment post hoc tests (* $p < 0.05$, ** $p < 0.01$, *** $p < 0.001$).

2.4.4 *R. solanacearum* rapidly evolves resistance to trained phages.

We used fluctuation tests to determine the effects trained phages have on resistance evolution in *R. solanacearum*. For our fluctuation tests, we challenged populations of each *R. solanacearum* genotype to a high volume and titre of each phage treatment (ancestor and trained) and determined the percentage (or proportion) of the population that is resistant to phages. From here, we can determine the effects that phage treatments have on phage resistance evolution but also, we can calculate mutant frequencies. We expected that trained phages would be able to suppress phage resistance evolution for longer. However, resistance evolved in all three *R. solanacearum* genotypes to all phage types, and this was very rapid, taking place within 48 hours. We also found there was variation among the phage treatments and overall, we found that multiple genotype trained phages were more effective than single genotype trained phages (Figure 2.5). There are also contrasts with the phage infectivity assays (Figure 2.4), this remains unclear but perhaps it was to do with bacteria actively growing in this experiment, but this would require further exploration to determine this effect on phage and *R. solanacearum* interactions. Another possible explanation for these contrasts, is that phages here were exerting a greater selection pressure to evolution resistance due to a higher volume being added, again this would require further exploration.

When using 2088 as a host, we found that the evolution of resistance was dependent on phage treatment ($X^2(6) = 828.42$, $p > 0.001$) and the single genotype trained phages were performing the worst. Multiple genotype trained phages performed better especially, “2088 + K60 + UW551” trained phages. The proportion of resistance in the population was below 50% of the population. What was surprising was that it was the ancestral PY015 that performed the best and only 8 out of 288 populations evolved resistance to the ancestor (Figure 2.4A). Taken together, we observed that multiple genotype trained phages are better at suppressing resistance evolution but not to the extent of the ancestor phage (Figure 2.5A).

K60 evolved highly resistant to all phage treatments (Figure 2.5B). This was unsurprising given that we saw similar dynamics in the phage infectivity assays and as its own training treatment “K60 only” was driven to extinction during phage training experiment. Surprisingly, we found that there was an association between phage treatments ($X^2(6)$ = 159,98, $p > 0.001$) and a few susceptible populations in “2088 + K60” treatment was observed. However, resistance remains above 75% of the population (Figure 2.5B).

With UW551, we again observed resistance evolution, while proportion of resistance in populations was dependent on phage treatment ($X^2(6) = 354.74$, $p < 0.001$). Like genotype 2088, the multiple genotype trained phages and the ancestor phages performed most effectively in terms of least observed resistance (Figure 2.5C). All replicate populations evolved resistant to “UW551 Only” phage training treatment suggesting an ineffective phage and potential loss of infectivity. Over 50% had become resistant to “2088 Only”. All this within 48 hours. However, the multiple genotype trained phages and the ancestral all had similar proportions of resistance in the population (around 45%) (Figure 2.5C). Like with phage infectivity assays, there might be little improvement in the trained phages. What was surprising was that in the three-genotype trained phage, 58% of the population was resistant compared to other phages such as the ancestor (42%) or “2088 + K60” (38%) phage treatments (Figure 2.5C).

We also calculated the mutant frequencies based on the fluctuation test results (see methods and materials). We found that mutant frequencies did differ between training treatments and the genotype of *R. solanacearum* (Table 2.2 and Figure 2.5). We had expected that frequency of mutants would be lower when challenged with trained phages compared to the ancestral PY015 phages (Borin et al., 2021).

For 2088, we saw that the ancestor phage was able to suppress resistance in 2088 better than the trained phages (Figure 2.5A). This was reflected in the lower frequency of phage resistant mutants (Table 2.2). The ancestral phage had a mutant frequency of $3.38x10^{-13}$, the lowest of all phage treatments. It was closely followed by "K60 + UW551" and "2088 + K60 + UW551" at $8.63x10^{-12}$ and $4.79x10^{-12}$, respectively. However, "2088 Only", "2088 + K60" and "2088 + UW551" all had similar mutant frequencies ~10^{-11}. 91% were resistant to "2088 Only" whereas only 62% were resistant to "2088 + UW551". We were unable to calculate the mutant frequencies for "UW551 Only" trained phages, as all wells were resistant, suggesting that this phage treatment was ineffective.

For K60, it was possible to estimate mutant frequencies only in 4 out of the 7 treatments as other populations were completely resistant (Table 2.2). Of the three treatments, we were unable to calculate for, the population was resistant. We did not find this surprising, as with the phage infectivity assays, K60 remained a highly resistant genotype. The three that we were able to calculate had similar phage resistance mutant frequencies (~10^{-9}) which were also much higher for K60 than the other *R. solanacearum* genotypes (Table 2.2). The results here highlight that K60 is a highly resistant genotype of *R. solanacearum*.

For UW551, mutant frequencies again were all very similar at around 10^{-11} (Table 2.2). Again, amplifying the possibility that there was no improvement in trained phages for this genotype. Only "2088 Only" had a higher mutation rate at $1.45x10^{-10}$. Reflecting that 73% of the population was resistant to this phage treatment (Figure 2.4C). Like 2088 and K60, UW551 was resistant to "UW551 Only" training treatment, we could not calculate the mutant frequency (Table 2.2). Taken together, the mutant frequencies from genotype UW551 suggest that single genotype trained phages are ineffective while multiple genotype trained phages showed similar or little improvement compared to the ancestor phage.

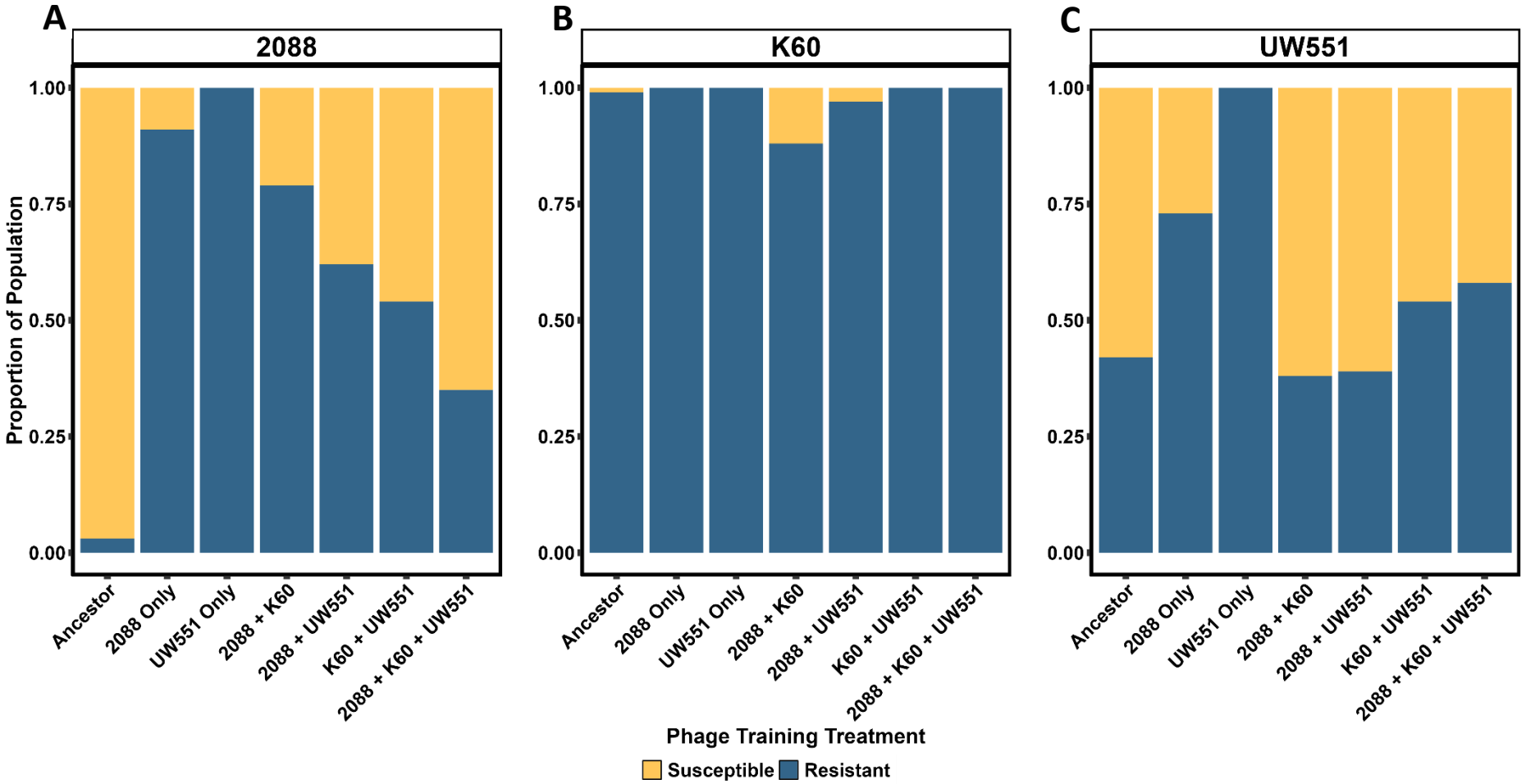

Figure 2.5 – The proportion of *R. solanacearum* that is susceptible (yellow) or resistant (blue) to phage treatments at a population level. Isogenic population of each genotype was created and incubated at +28°C for 48 hours, along with untrained and trained phages. After the 48 hours, the optical density (600nm) was measured for each population and it was determined which populations were resistant or susceptible to each phage treatment. Populations were deemed resistant if the optical density was above the average optical density that was taken at 0 hours. Above this value indicated growth and potential resistance. A) The population of genotype 2088, B) The population of K60 and C) The population of UW551.

Table 2.2 – The mutant frequencies from each phage treatment against each of the three genotypes of *R. solanacearum.* Mutant frequencies using the P_0 method where calculated following Borin et al equation (Borin et al., 2021).

Genotype	Training Treatment	Mutation Rate	Note
2088	Ancestor	$3.38x10^{-13}$	
2088	2088 Only	$2.68x10^{-11}$	
2088	UW551 Only	NA	No sensitive wells, all were resistant.
2088	2088 + K60	$1.73x10^{-11}$	
2088	2088 + UW551	$1.08x10^{-11}$	
2088	K60 + UW551	$8.63x10^{-12}$	
2088	2088 + K60 + UW551	$4.79x10^{-12}$	
K60	Ancestor	$5.12x10^{-09}$	
K60	2088 Only	NA	No sensitive wells, all were resistant.
K60	UW551 Only	NA	No sensitive wells, all were resistant.
K60	2088 + K60	$2.36x10^{-09}$	
K60	2088 + UW551	$3.90x10^{-09}$	
K60	K60 + UW551	NA	No sensitive wells, all were resistant.
K60	2088 + K60 + UW551	NA	No sensitive wells, all were resistant.
UW551	Ancestor	$6.05x10^{-11}$	
UW551	2088 Only	$1.45x10^{-10}$	
UW551	UW551 Only	NA	No sensitive wells, all were resistant.
UW551	2088 + K60	$5.31x10^{-11}$	
UW551	2088 + UW551	$5.49x10^{-11}$	
UW551	K60 + UW551	$8.63x10^{-11}$	
UW551	2088 + K60 + UW551	$9.64x10^{-11}$	

2.4.5 Trained Phages are more effective at suppressing their ancestral host than their coevolved host.

We conducted another phage infectivity assay to test the level of infectivity of trained and untrained phages have on ancestral and coevolved hosts of *R. solanacearum*. Overall, we found that both ancestor and trained phages were highly effective at suppressing the growth of ancestral 2088 but not their coevolved hosts (Figure 2.6A-B).

For the ancestral 2088 genotype, all phages untrained and trained completely suppressed the growth of the pathogen (Figure 2.6A-B). As expected, "2088 + K60 + UW551" trained phages were successful at suppressing the ancestral host, reflecting what we saw in the other phage infectivity assay (Figure 2.4A-B). However, what was unexpected was that "2088 Only" and the ancestor completely suppressed this genotype unlike in the previous phage infectivity assays (Figure 2.4A-B and 2.6A-B). As a result, we found no significant differences between ancestral and trained phages (Kruskal-Wallis: $X^2_{13.463}$, $p = 0.004$, pairwise Wilcoxon test with BH adjusted for p values, $p > 0.05$). The only significant difference was between "No Phage" treatment and the other phages (Figure 6.B). It is unclear why this contrasts with the other phage infectivity assay and brings into question how effective "2088 +K60 + UW551" was. If the ancestral phage highly infective to genotype 2088 of *R. solanacearum* and caused complete suppression of *R. solanacearum*, it is unlikely any training occurred.

Unlike the ancestral host, all phage treatments failed to completely suppress the growth of the two coevolved hosts. (Figure 2.6B-C). We found no significant differences between phage treatments for the single genotype coevolved host and the multiple genotype coevolved host (Kruskal-Wallis: $X^2_{0.753}$, $p = 0.861$ and Kruskal-Wallis: $X^2_{0.56}$, $p = 0.906$, respectively). Both results suggest that once resistance sets in, phages cannot overcome it.

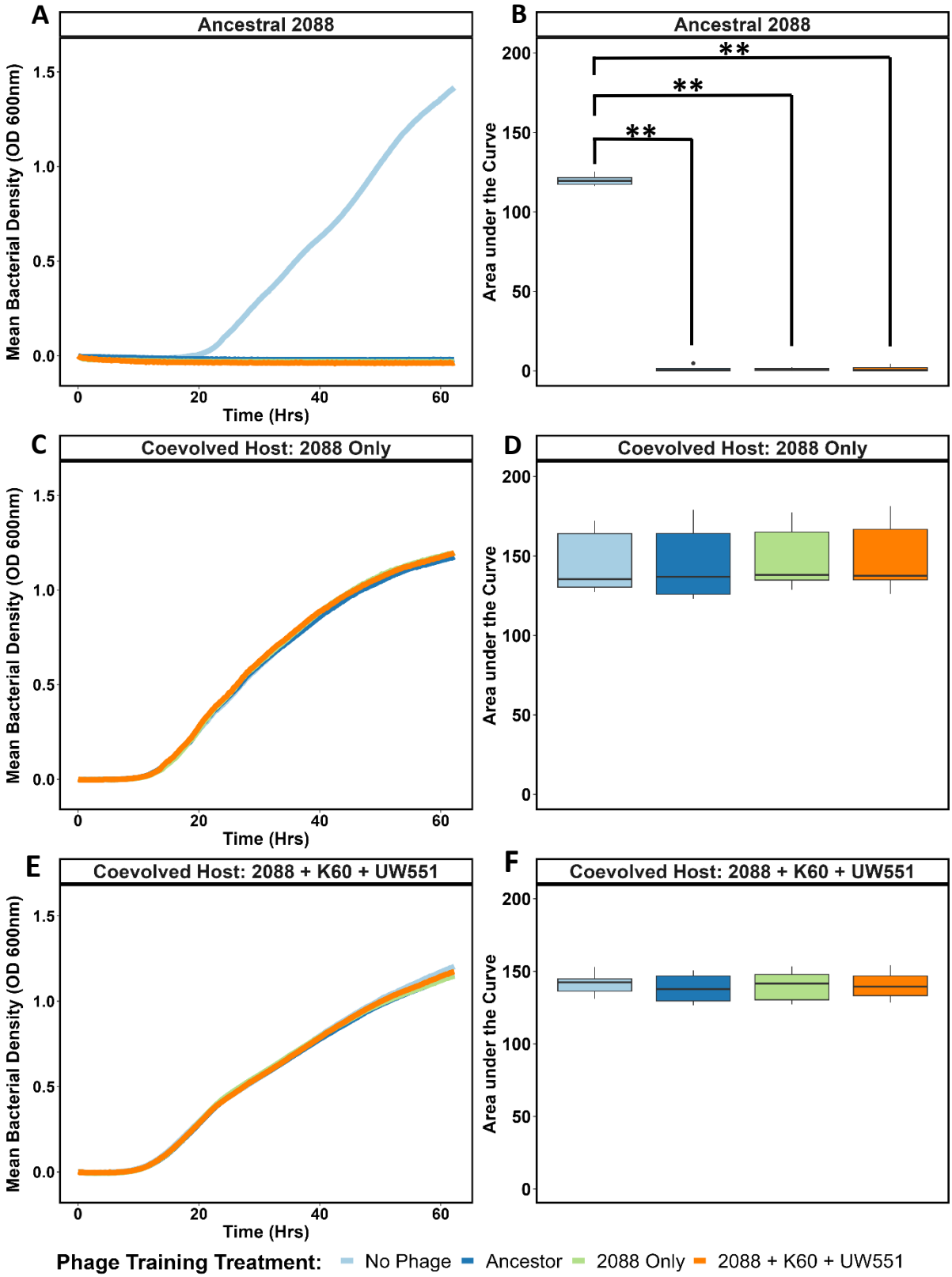
A
Ancestral 2088
Mean Bacterial Density (OD 600nm)
Time (Hrs)
B
Ancestral 2088
Area under the Curve
**
**
**
C
Coevolved Host: 2088 Only
Mean Bacterial Density (OD 600nm)
Time (Hrs)
D
Coevolved Host: 2088 Only
Area under the Curve
E
Coevolved Host: 2088 + K60 + UW551
Mean Bacterial Density (OD 600nm)
Time (Hrs)
F
Coevolved Host: 2088 + K60 + UW551
Area under the Curve
Phage Training Treatment:
No Phage
Ancestor
2088 Only
2088 + K60 + UW551

Figure 2.6 – Phage Infectivity assays to understand the effects ancestral and coevolved hosts have on untrained and trained phages and provide insights into the coevolutionary dynamics between phages and hosts during training**.** The coevolved hosts were isolated from the final training cycle, where the trained phages were originally isolated from. Ancestral 2088 genotype of *R. solanacearum* and two coevolved hosts were grown in the presence of three phages, ancestral PY015, trained "2088 Only" phages and trained "2088 + K60 + UW551" and incubated for 62 hours at +28^{o}C. Their optical density (600nm) was recorded every 15 minutes. A-B) Ancestral host, C-D) Coevolved host, "2088 Only" and E-F) Coevolved host, "2088 + K60 + UW551. The panels A, C and E shows the mean growth of each host over time. Panels B, D and F shows the area under the curve. The * symbols are significant differences between treatments based on pairwise Wilcoxon tests with Benjamini Hochberg p value adjustment post hoc tests (* $p < 0.05$, ** $p < 0.01$, *** $p < 0.001$).

2.2.6 Genetic variation found in two training treatments affecting two different proteins.

We aimed to find any nucleotide and potential protein changes that might have evolved in the phages as result of the training (Table 2.3). Out of the seven phage training treatments sequenced, only two had evidence of nucleotide sequence changes in terms of single nucleotide polymorphism (SNPs). “UW551 Only” trained phages that a single SNP in nucleotide position 71, changing the nucleotide sequence from A to G (Table 2.3). This SNP was nonsynonymous changing the amino acid sequence from aspartic acid to glycine (Figure 7A). Analysis on this amino acid sequence on BLAST identified the protein to be a hypothetical protein of *Ralstonia* phage vRsoP-WF2. Further analysis on HHpred identified the protein to be related to the sugar binding protein of *Acinetobacter nosocomialis* (Figure 7C). Structural modelling of both the ancestral PY015 protein and the trained phage protein revealed that structural changes to the protein had occurred (Figure 7B-C). The trained “UW551 Only" phages appeared to have lost their infectivity (Figure 2.4), the structural changes to the protein here could have been detrimental to the phages. However, it is clear that further analysis and exploration around this protein is needed to understand its function in PY015.

The “2088 + UW551” phages had genetic variation in a potential tail fibre (or spike) protein, identified through BLAST and HHpred (Table 2.3 and Figure 2.8). This protein had 3 SNPs, all nonsynonymous (Table 2.3). The amino acid sequence was altered from threonine to adenine at nucleotide position 718, valine to guanine at nucleotide position 2495 and asparagine to aspartic acid at 2572 (Table 2.3 and Figure 2.8A). The SNPs here have seemed to have significantly altered the structure of the protein, with “2088 + UW551” there was evidence of improvement in infectivity level, particularly against *R. solanacearum* genotype 2088 (Figure 2.4A and Figure 2.8B-C). Perhaps, changes in their tail fibres have led to changes in their infectivity.

It is doubtful that only two training treatments had mutations, especially considering the changes in infectivity in other training treatments. The 3 genotype trained phages were highly effective, but no mutations were identified. With more purification and sequencing more replicates, mutations would have been identified.

Table 2.3 – Single nucleotide polymorphism (SNPS) identified in the phage training treatments and the changes to the amino acid sequence that occurred. Proteins with amino acid changes have also been identified through BLAST and HHpred. Ancestral PY015 was sent to sequencing and used as a reference for the variant calling. Nucleotide position is the position of the variant counting from 1. Only 1 replicate from each training treatment was sent to sequencing in part due to difficulty in isolating DNA for sequencing.

Training Treatment	Nucleotide Position	The Variant Type	Nucleotide Change	Amino Acid Change	Protein of Interest identified with BLAST	Protein of Interest identified with HHpred
2088 Only						
UW551 Only	71	SNP (nonsynonymous)	A → G	Aspartic acid → Glycine	Hypothetical Protein of *Ralstonia* phage vRsoP-WF2	Sugar binding Protein of *A. nosocomialis* (related)
2088 + K60						
2088 + UW551	718	SNP (nonsynonymous)	A → G	Threonine → Adenine	Tail Fibre Protein of *Ralstonia* phage vRsoP-WF2	*Acinetobacter baumannii* phage ϕAB6 tailspike protein (related)
	2495	SNP (nonsynonymous)	T → G	Valine → Guanine		
	2572	SNP (nonsynonymous)	A → G	Asparagine → Aspartic acid		
K60 + UW551						
2088 + K60 + UW551						

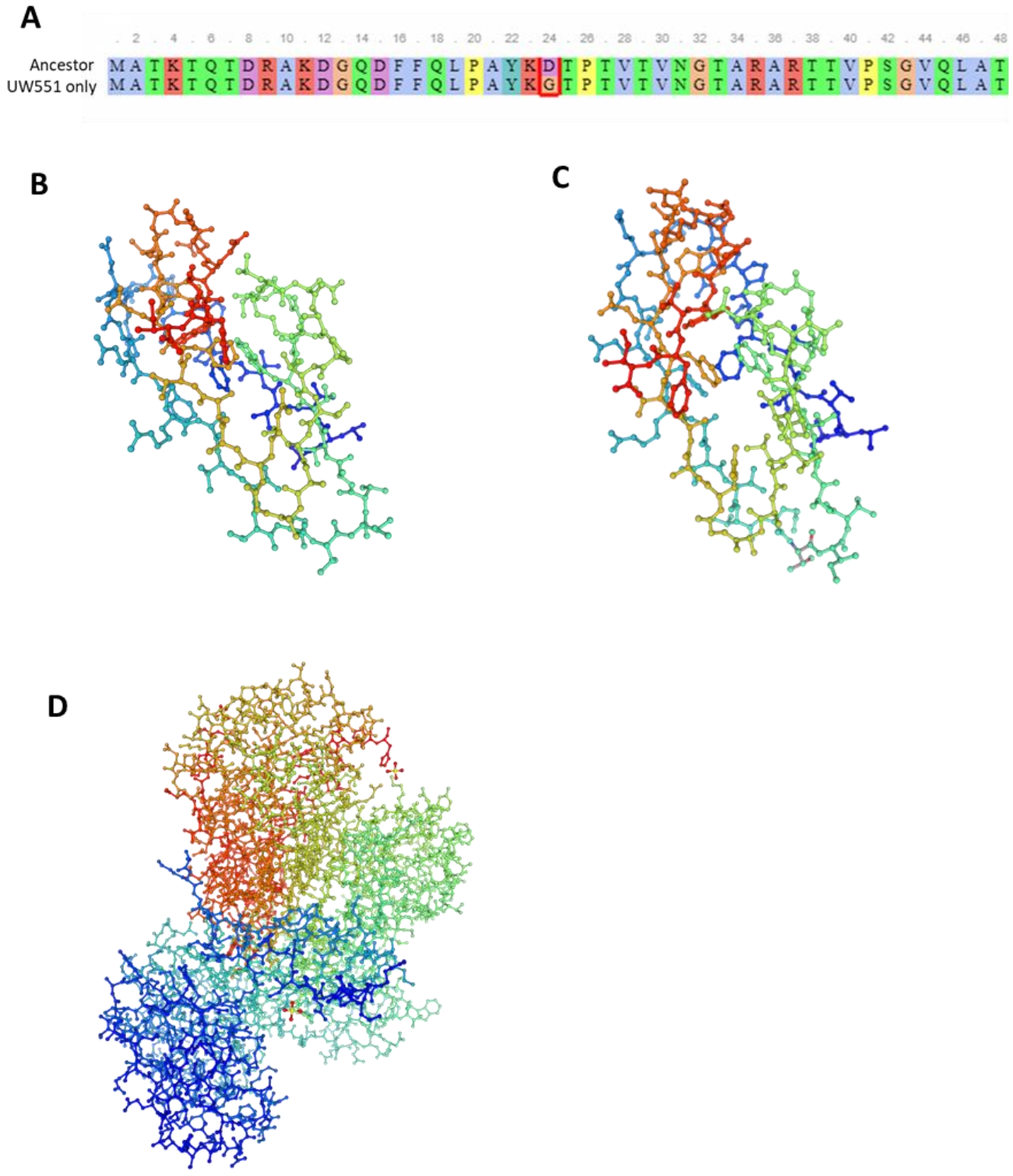
A
2 4 6 8 10 12 14 16 18 20 22 24 26 28 30 32 34 36 38 40 42 44 46 48
Ancestor M A T K T Q T D R A K D G Q D F F Q L P A Y K D T P T V T V N G T A R A R T T V P S G V Q L A T
UW551 only M A T K T Q T D R A K D G Q D F F Q L P A Y K G T P T V T V N G T A R A R T T V P S G V Q L A T
B
C
D

Figure 2.7 – The amino acid sequence and protein structures from trained phages “UW551 Only”. A) The amino acid sequences of both ancestral PY015 and trained phages aligned in clusteralΩ to highlight the nonsynonymous SNP that resulted in change of an amino acid from aspartic acid to glycine at amino acid sequence position 24 (highlighted in red). B-C protein models built in the Swiss-model with the aim to understand the structure of the protein, BLAST identified this as a hypothetical protein while HHpred identified to a sugar binding protein. B) The ancestral protein, the amino acid sequence of the protein was used from ancestral PY015 to build the model. C) The protein model built from the amino acid sequence of the trained phages used to identify if any structural changes have occurred as result of the SNP. D) The sugar binding protein of *A. nosocomialis*, a related protein to the hypothetical protein identified, is possible that the phage protein could form similar functions, protein model was extracted from Swiss-model (Urusova et al., 2019).

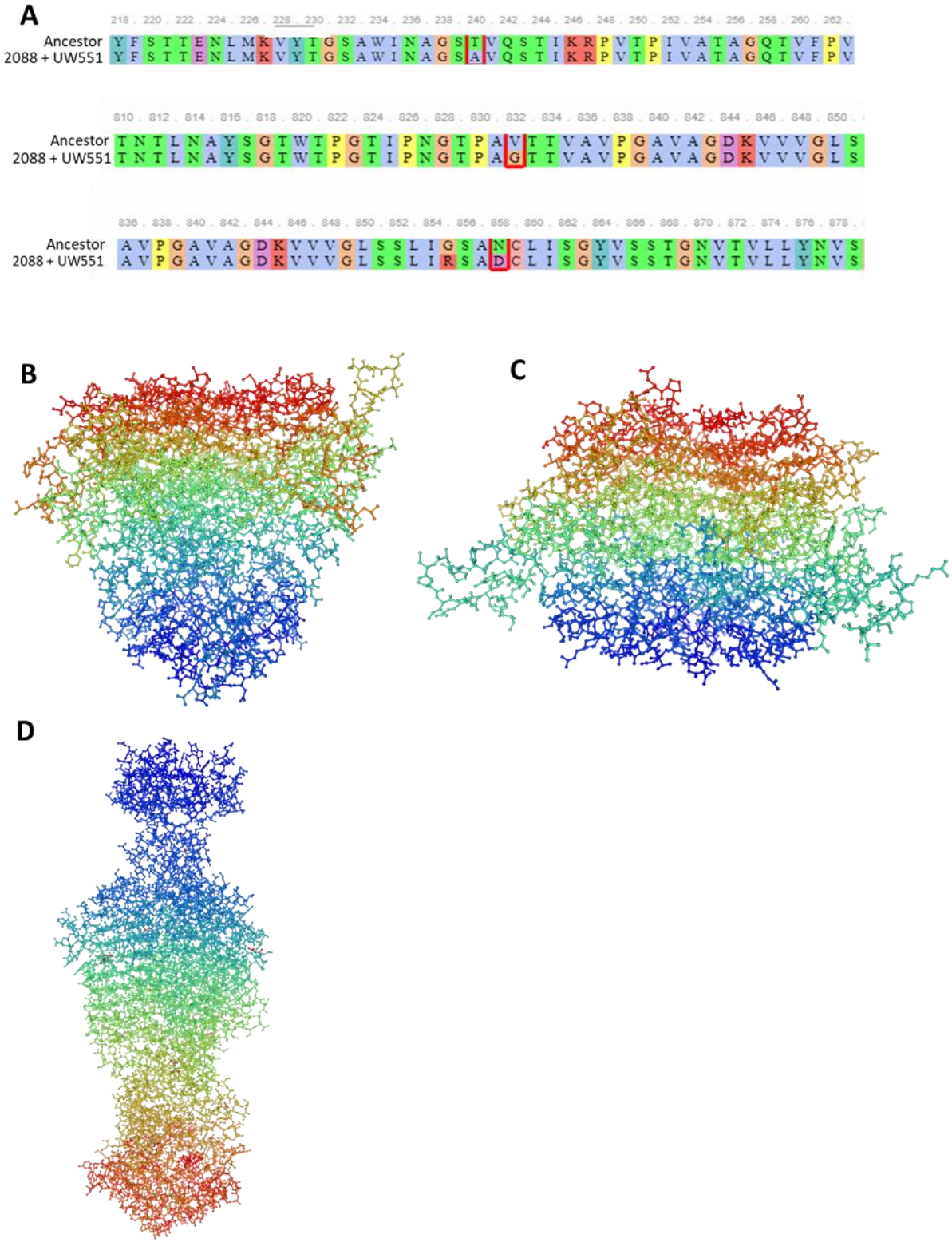
A
Ancestor
2088 + UW551
B
C
D

Figure 2.8 - The amino acid sequence and protein structures from trained phages “2088 + UW551”. A) The amino acid sequences of both ancestral PY015 and trained phages aligned in clusteralΩ to highlight the nonsynonymous SNPs that resulted in change of an amino acid from threonine to adenine at nucleotide position 718, valine to guanine at nucleotide position 2495 and asparagine to aspartic acid at nucleotide position 2572. B-C protein models built in the Swiss-model in the proteins with the aim to understand the structure of the protein, BLAST identified this as a protein tail fibre protein of *Ralstonia* phage vRsoP-WF2 while HHpred identified the protein to be related to the tail-spike protein of *A. baumannii* phage ϕAB6. B) The ancestral protein, the amino acid sequence of the protein from ancestral PY015 was used to build the model. C) The protein model built from the amino acid sequence of the trained phages used to identify if any structural changes have occurred as result of the SNPs. D) The tail-spike protein of *A. baumanii*, a related protein to the protein identified, it is possible that the phage protein could form similar functions, protein model was extracted from Swiss-model (Lee et al., 2017).

2.5 Discussion

Here we studied whether we could increase infectivity in one phage PY015 with single or multi-bacterial cultures of three genotypes of *R.* solanacearum (2088, K60 and UW551). Overall, our results suggest that training phages with multiple genotypes of *R. solanacearum* creates more infective phages than with only one genotype. Evidenced by the phage infectivity assays of 2088 and UW551 (Figure 2.3). On the other hand, there is also evidence that there was no improvement in infectivity from the training. Particularly, "UW551 Only" trained phages which in some cases, appeared to lose its infectivity. Our results also suggest that *R. solanacearum* itself can rapidly evolve resistance to both the ancestral and trained phages even within one training cycle (Figure 2.4 and Figure 2.5). Finally, we observed profound variation between the genotypes of *R. solanacearum* and the phage treatments. Together, this suggests training treatments involving multiple genotypes of *R. solanacearum* are better than single genotype training treatments but *R. solanacearum* can still rapidly evolve resistance to trained phages.

The bacterial population density results from the training showed promise. Bacterial density was decreasing over time indicating an increase in infectivity. Interestingly, the appearance of those similar patterns between mono and combination training treatments on bacterial densities suggest that the most resistant genotype within the combination training treatment plays a key role. As observed when making comparisons between the "K60 Only" training treatment and the combination training treatments that contain this genotype, K60 (Figure 2.2). There might be a benefit to including resistant genotype in the training treatment. Perhaps, this genotype is forcing the phages to select for increased virulence on the other susceptible genotypes within the training treatment. The genotype UW551 contains a defence mechanism known as CBASS (Table 2.3) (Millman et al., 2020a). CBASS is an abortive-infection system that triggers cell death in the presence of phage infected cells which protects the population (Cohen et al., 2019). When the phage was inoculated alongside with UW551, it is possible CBASS was triggered causing the culture to collapse, reducing the host availability. Cohen et al observed a culture collapsed at high phage abundances. This culture collapse was triggered by CBASS (Cohen et al., 2019). Conducting experiments similar to Cohen et al could help determine if CBASS was triggering a culture collapse.

A surprising result was that phage abundance remained unchanged throughout the training. We hypothesised that phage abundance would increase over time because infectivity should have increased. Trade-offs between infectivity and phage stability are possible. Increased infectivity might result in decreased stability (Goldhill and Turner, 2014). Trained phages might have lost their stability which could explain the lack of increase in their abundance. It is possible that abundance was increasing during the training due to higher infectivity levels but because phage particles might be unstable, phages degraded quickly after, causing a drop in abundance. We questioned whether this drop was due to this instability? This was observed in mutants of the phage vB_BthS_BMBphi which had increased instability. This mutation on their phage tails allowed them to interact with resistant host mutants but at cost to their stability (Yuan et al., 2019). If there was a trade-off between stability and infectivity this could be problematic for developing biocontrols. Stability is important for processing and long-term storage of phages (Malik et al., 2017). Unfortunately, the "K60 Only" treatment was lost, we could not recover a PFU/ml count for this treatment. Even spot testing could not isolate the phage. It remains unclear, why this training treatment was lost. K60 has nine phage defence systems in its genome, and it is possible that PY015 could not overcome these defence mechanisms (Table 2.3) (Payne et al., 2022). A number of coevolutionary experiments have reported phage extinctions due to high levels of resistance in their hosts and partly this also suggests that phages were just unable to adapt to the bacteria.

Phage infectivity assays showed evidence that phages trained with multiple genotypes of *R. solanacearum* were more infective than the phages trained with only one genotype. Moreover, we observed that phages trained with one genotype lost their infectivity, even to the genotype they were trained with. We expected that one genotype trained phages would specialise becoming highly infective against their selected host but not to an alternative host (Howard-Varona et al., 2018). This was not the case. It appears that high infectivity was selected against. This loss of infectivity was observed in phages against *Vibrio* sp. CV_1 (Barbosa et al., 2013). Mono-treatments of three phages V_1G, V_1P_1 and V_1P_2 all lost infectivity in both non-evolving and evolving hosts (Barbosa et al., 2013). Perhaps, single genotype training treatments result in infectivity being selected against. Phages could

reduce their infectivity as survival tactics such as phage persistence. For example it has previously been shown that mutants of the phage vB_BthS_BMBphi infectivity was significantly decreased allowing long-term phage persistence (Yuan et al., 2019).

Training with multiple genotypes was expected to select for phages that would become generalists with increased infectivity range (Sant et al., 2021). However, as phages evolve to become more generalist, there can be a trade-off between infectivity level and infectivity range (de Jonge et al., 2019). Surprisingly, we did not see this trade-off. The phages trained with three genotypes of *R. solanacearum* had the highest infectivity levels and highest infectivity range. High infectivity levels in this treatment could have been selected for because of the increased host availability, reducing the chance of lower infectivity being selected for (Leggett et al., 2013). It is unclear why infectivity was lost in some phage training treatments even though bacterial densities decreased during the training experiment. Further experiments will be required to understand this.

We did identify SNPs in only two of the training treatments. This was surprising as we saw considerable variation in their abilities compared to their ancestor. So, we expected to identify more SNPs across more training treatments. In particular, we did expect that all multiple trained phages would have genetic changes as these treatments seemed to improve in their infectivity in some cases. The only training treatments identified with SNPs were “UW551 Only” and “2088 + UW551”. The single genotype “UW551 Only” was the worst performing trained phage and even lost its infectivity. It could be possible that genetic changes might have contributed to this. HHpred identified the protein as a sugar binding protein (Greenfield et al., 2020). A diverse array of sugar binding proteins are present in phages, to help facilitate their binding to receptors on bacteria such as lipopolysaccharides (LPS) (Simpson et al., 2015). Changes to the sugar binding protein could improve binding and virulence of the phage. However, what we saw was detrimental to the phage. Unclear why this change would be selected for.

Changes in the tail protein can change the infectivity of phages (Zhang et al., 2021). The SNPs identified in “2088 + UW551” was in the tail fibre protein. Tail fibre proteins mediate the binding to receptors on their hosts (Taslem Mourosi et al., 2022). Changes to the tail fibre proteins have been linked to changed infectivity and appear to be under strong selection (Scanlan et al., 2011). Tail fibre changes in phage ϕ were observed during

coevolution experiments with its host *Pseudomonas fluorescens* SBW25, the changes were linked to adaptative change in absorption efficiency (Paterson et al., 2010). It is likely that "2088 + UW551" was under similar selection pressures, resulting in changes to the tail fibre protein and its infectivity. One clear limitation of this is that we were only able to send a representative of each training treatment for whole genomic sequencing. Perhaps, if more representatives were sent, we would be able to identify SNPs in other training treatments.

Further assessment of these trained phages revealed a more dynamic and complex interaction. Fluctuation tests have indicated that *R. solanacearum* can rapidly evolve resistance to phages. This observation has been seen before. RSSC has evolved resistance to phages in as a little as 30 hours (Fujiwara et al., 2011). With training, we aimed to delay this but trained phages ultimately failed (Borges, 2021). Our observations with trained phages was opposite to what Borin et al observed with phages and *E. coli* (Borin et al., 2021). It was more surprising that both the more susceptible genotypes 2088 and UW551 rapidly evolved resistance to the trained phages. Perhaps, the lost receptors on these genotypes were enough to prevent infection from all phage treatments. Coevolutionary studies have shown that receptor changes on bacteria is a rapid and quick response to phage infection. Additionally, phage training of PaoP5 allowed the phage to recognise an altered O-antigen on *P. aeruginosa* PAOw-1. However, training failed if *P. aeruginosa* PAOw-1 lost its receptor (Yang et al., 2020). It could be possible the trained phages could recognise an altered receptor on *R. solanacearum,* but total loss of the receptor made the trained phages insufficient. Genomic analysis of the resistant *R. solanacearum,* isolates might reveal more.

High mutant frequencies allow bacteria to adapt in response to abiotic and biotic factors in their environment (Denamur and Matic, 2006). We hypothesised that trained phages would lower the mutation rate and in doing so would lower the chances of resistant mutants arising. There would be less mutations available against trained phages and the frequency of phage resistant mutants would be lower. However, instead we found that mutant frequencies did not differ between the ancestor phage and trained phage (Table 2.2). The effects that phages have on mutant frequencies remain unclear (Chevallereau et al., 2022). However, in the presence of phages, mutations can be elevated (Pal et al., 2007). Increasing the chance of mutations conferring resistance to arise (Chevallereau et al., 2022, Pal et al., 2007). We did not observe this.

Focusing on genotypes 2088 and UW551, there was clear variation between the phage types (trained or ancestral) used in the fluctuation tests. It appears that it is harder for *R. solanacearum* to evolve resistance against combination trained phages. Combination trained phages are likely to have a broader infectivity range and exploit a wider range of infectivity mechanisms. For *R. solanacearum* to evolve resistance, more mutations will be required (Wang et al., 2019, Liu et al., 2020). Surprisingly, for genotype 2088, the ancestor outperforms all other phage types. Preliminary data and the results observed here, indicates that the ancestral was already highly virulent against 2088.

Although, *R. solanacearum* evolved resistance to phages rapidly, we cannot determine how problematic this could potentially be for biocontrol application. Often resistance to phages comes with evolutionary trade-offs (Burmeister and Turner, 2020). It might be worth exploring evolutionary trade-offs in *R. solanacearum*. Trade-offs in other pathogenic bacteria can affect virulence. Numerous studies have shown that there is a trade-off between phage resistance and virulence in hosts (Wei et al., 2010, Yun et al., 2018). In *Vibrio cholerae* O1 and the bacteriophage JSF4, resistant mutants were less motile than their non-resistant ancestor. The less motile resistant mutants were less virulent (Wei et al., 2010). *Pseudomonas tolasii* 6264, causative agent of brown blotch disease, was non-virulent when they acquired resistance to phages (Yun et al., 2018). Like these examples, it is possible that in *R. solanacearum* virulence could be impacted by the evolution of phage resistance, but we have yet to explore it. Genomic sequencing, competition assays comparing non-resistant and resistant hosts of the same genotype and plant models could help to determine if resistance is costly to *R. solanacearum*.

Despite us isolating phages every three days for the duration of the training, we only focused on the final timepoint. In the future, it would be worth exploring other timepoints, especially time point 6. Observations from bacterial densities during the training suggest that infectivity within phages significantly increases at this time point (Figure 2.2). It is possible that these phages are more virulent but later disappear for some reason.

For this phage training we kept the evolution one-sided, focusing on the phages evolution. This approach is different from Borin et al, who looked at coevolving bacteria together which appeared to be more effective (Borin et al., 2021). Perhaps, coevolving PY015 with the three genotypes might have been more effective if bacteria had been left to evolve as well. However, if coevolution was highly asymmetrical, phage-bacteria coevolution could lead to phage extinction rather than "training" it. Asymmetrical evolution has been shown to tip coevolutionary dynamics in the favour of the bacteria, where phages are unable to overcome evolution of resistance (Lenski and Levin, 1985). Once resistance arises, phages cannot adapt to overcome it. In experiments looking at the coevolutionary dynamics of *Streptococcus thermophilus* and phage 2972, a number of phage lines went extinct once resistance evolved (Common et al., 2019). If a similar situation was occurring in our training treatment, this could have explained the absence of infectivity evolution in our training treatment. We did see evidence of this type of asymmetry when comparing ancestral and trained phage infectivity on coevolved bacterial hosts (Figure 2.5), neither of the phage treatments were able to suppress the growth of the coevolved hosts that were completely resistant, which suggest that once resistance was established, phage could not overcome it.

Conclusion

Overall, there is promise that phage training could mitigate some of the challenges of using phages as biocontrols. In some cases, we were able to increase infectivity and infectivity range, two challenges for phage biocontrol. We also provide recommendations for phage training regimes. Mostly, phage training involves the use of a single susceptible genotype. However, we have observed potential benefits of including more genotypes within a training regime and put forward a case for including resistant genotypes. From our observations, the phages with the most potential were the phages trained with three genotypes with resistant K60 in the treatment.

However, we also need to express some concern with phage training. In other cases, we saw little to no improvement from the trained phages and even a loss of infectivity. We also saw that *R. solanacearum* can rapidly evolve resistance to phages, including trained ones. This raises questions on how effective training is and whether it is a valid strategy with *R. solanacearum*. However, we have yet to explore the potential evolutionary trade-offs with phage resistance in *R. solanacearum*, and we should also explore using these phages *in*

planta experiments, where the dynamics and outcomes could change dramatically, especially around resistance evolution.

Table 2.4 – The Phage defence mechanisms found in all three genotypes of *R. solanacearum* used in this experiment. Defence mechanisms were identified through PADLOC (Payne et al., 2022). Defence mechanisms are likely to play a significant role in the resistance of certain genotypes, K60 was highly resistant to PY015, likely due its defence mechanisms.

Genotype	Defence Mechanism	Function
2088	Restriction Modification, Type I	Degradation of nucleic acids
	Restriction Modification, Type II	Degradation of nucleic acids
	Restriction Modification, Type IIG	Degradation of nucleic acids
	CBASS	Abortive infection
	PARIS	Abortive infection
K60	Restriction Modification, Type I	Degradation of foreign DNA
	Zorya	Unknown
	Abi2	Abortive infection
	CRISPR-CAS, Type IE (2 in total)	Degradation of foreign DNA
	Wadjet	Unknown
	Druantia	Unknown
	Lit	Abortive infection
	Lamassu	Unknown
UW551	Restriction Modification, Type I	Degradation of nucleic acids
	Restriction Modification, Type II	Degradation of nucleic acids
	Restriction Modification, Type IIG	Degradation of nucleic acids
	CBASS	Abortive Infection
	PARIS	Abortive Infection

Chapter 3

Evidence of Asymmetrical Evolution between *Ralstonia solanacearum* and Bacteriophages

3.1 Abstract

Understanding coevolutionary dynamics between pathogenic bacteria and bacteriophages is critical when developing biocontrols, especially the evolution of phage resistance. Phage resistance can evolve rapidly due to receptor modification and a repertoire of phage defence systems that bacteria can quickly acquire. However, phages themselves can counteract resistance through changes in their infectivity levels and ranges. Through exploitation of these coevolutionary dynamics, we could isolate phages with increased infectivity levels and ranges to be used in biocontrol applications. Here, we study the coevolutionary dynamics of *Ralstonia solanacearum* a destructive plant pathogen and four phages (individually). With the aim of understanding their coevolutionary dynamics but to also isolate highly effective phages for potential biocontrol applications. We observed that coevolutionary dynamics between *R. solanacearum* are highly asymmetrical, with *R. solanacearum* rapidly evolving resistance to all four phages. We find evidence of parallel evolutionary mutations in two proteins in resistance *R. solanacearum* from different phage treatments. The two proteins found with genetic variation are related to biosynthesis of lipopolysaccharides and antibiotics. Phage resistance is often costly leading to evolutionary trade-offs with a number of traits, some critical to the virulence and pathogenicity of *R. solanacearum*. We observed evolutionary trade-offs in two traits in *R. solanacearum* fitness (growth) and biofilm production.

3.2 Introduction

Antagonistic coevolution is the process of reciprocal adaptation and counter-adaptation between ecologically interacting species (Koskella, 2014). Bacteria and bacteriophages (phages) engage often in antagonistic coevolution (Ebert and Fields, 2020, Hall et al., 2020). The coevolution between bacteria and phages results in host adaptations (resistance) that reduce the burden of phage infection, while the phage can counter adapt to increase its infectivity (de Jonge et al., 2019, Hall et al., 2020). Here, we studied the coevolutionary dynamics between *R. solanacearum* bacterium and phages in a short-term laboratory experiment. *R. solanacearum* is a destructive plant phytopathogen that causes bacterial wilt in a range of plants, including important agricultural crops (Álvarez et al., 2019). With recent interest using phages as biocontrol agents to control this pathogen, we here studied if *R. solanacearum* engages in coevolution, resulting in more resistant bacteria and more infective phages, or if coevolutionary outcomes could be asymmetric, where the evolution of one partner dominates.

Bacteria employ various mechanisms to mitigate phage infection such as receptor modifications (Georjon and Bernheim, 2023, Hampton et al., 2020). Receptor modification prevents phage adsorption, protecting themselves from the first phase of a phage infection cycle. In *R. solanacearum* the type II secretion system (T2SS) and type IV pili are important receptor sites for phages, and modification of these structures has resulted in phage resistance (Xavier et al., 2022, Narulita et al., 2016). However, phages can counteract this through mutations in their tail fibres. Mutations found in tail fibres of ϕ2 phage were correlated with increased infectivity range to genotypes of *Pseudomonas fluorescens* SBW35. Tail fibres were shortening which was a possible adaptation to increased absorption efficiency (Paterson et al., 2010).

Bacteria and phages can engage in two types of antagonistic coevolution: Arms Race Dynamics or Fluctuating Selection Dynamics (Ebert and Fields, 2020, Hall et al., 2020, de Jonge et al., 2019). Arms Race Dynamics (ARD) is often characterised by trait escalation, where an increase in resistance and/or infectivity range through time by directional selection for more resistant bacteria and more infective phages (Figure 3.1) (Hall et al., 2020). *Escherichia coli* and its phage Qβ showed ARD when coevolved together. *E. coli* first evolved resistance to infection while Qβ countered this with improved efficiency release and a

change in host range (Kashiwagi and Yomo, 2011). Genetic analysis of both *E. coli* and Qβ also showed increased rates of the mutations, especially in genes associated with infection and cell lysis for Qβ and for *E. coli* within genes associated with the F pilus (receptor for Qβ) (Kashiwagi and Yomo, 2011). Another *E. coli* phage PP01, also showed ARD with *E. coli* in the absence of bile salts. ARD with PP01 and *E. coli* was characterised by increasing resistance in *E. coli* and increasing infectivity ranges in PP01 (Scanlan et al., 2019). In natural environments, *Flavobacterium columnare* showed ARD with phages with changes to its type VI-B CRISPR system. Here, resistance-infectivity coevolution was triggered by intracellular phage defence systems, where changes in *F. columnare* CRISPR spacer content correlated with increased infectivity ranges of phages through the years (Laanto et al., 2017).

Fluctuating Selection Dynamics (FSD) is different from ARD where bacterium and phage genotypes fluctuate periodically instead of direct trait escalation over time. Here, a genotype that is resistant to a phage becomes dominant in the population, which causes the phage to evolve counter-resistance to it since it has become common (Brockhurst and Koskella, 2013). Being a rare genotype is often advantageous, providing selective benefit (Ford et al., 2017). This often leads to cycles of different genotypes over time driven by negative-frequent selection (Brockhurst and Koskella, 2013). Coevolution of *Staphylococcus aureus* (pathogen) and *Enterococcus faecalis* (defence microbe) was driven by FSD (Ford et al., 2017). Similar genotypes fluctuated through time, with various genotypes becoming dominant multiple times during the experiment. It also appeared that *S. aureus* was responsible for the cycling of adaptation with *E. faecalis*, responding to the new adaptations that appeared over time (Ford et al., 2017). *Pseudomonas fluorescens*-phage coevolutionary dynamics in soil was also driven by FSD, where *P. fluorescens* was evolving highest levels of resistance to its contemporary phage (Gómez and Buckling, 2011).

ARD and FSD are not exclusive modes of antagonistic coevolution. Coevolving populations can switch and shift between the two modes (Hall et al., 2011). For example, coevolutionary dynamics between *P. fluroescens* SBW25 and phage SBW25ϕ2 shifted from ARD to FSD over time, likely due to the increasing costs of infectivity and resistance adaptation (Hall et al., 2011). Coevolutionary outcomes also vary between replicate selection lines. In another study, two out of three replicate communities consisting of *Pseudomonas aeruginosa* and its phage OMKO1 showed FSD while one engaged in ARD (Kortright et al., 2022a).

However, it is possible that the dynamics between phages and bacteria can be asymmetrical. For example, phage resistance could evolve in the bacteria, without concomitant infectivity evolution by phages (Lenski and Levin, 1985). Resistance in bacteria to phages can easily be achieved through receptor modification and loss by various mutations, whereas phages evolve specific binding to the changed receptor, which is likely to experience greater mutational constraint (Koskella and Brockhurst, 2014). Numerous coevolution studies have observed phages going extinct after bacteria evolve resistance. In *Pseudomonas fluorescens* SBW25 and lytic phage SBW25ϕ2 extinction events occurred due to high levels of resistance in *P. fluorescens* populations (Wright et al., 2016). Phage extinction of HP1c1 was also observed when phage resistant sub-populations of *Haemophilus influenzae* exceeded 34%, indicating that high levels of resistance can drive phages to extinction (Turkington et al., 2019).

Resistance to phage often coincides with evolutionary trade-offs (Mauro and Ghalambor, 2020). Traits such as virulence can be severely impacted by phage resistance, resulting in reduction of pathogenicity. The Type II Secretion System (T2SS) plays a critical role in phage infection of phiAP1 to *R. solanacearum*. Changes to the T2SS, also a result of phage resistance, resulted in a significant reduction in virulence on tomato plants because multiple virulence factors are secreted via the T2SS system (Xavier et al., 2022). Similarly, the type IV pilus is an important virulence factor for biofilm production (Narulita et al., 2016). Evolution of phage resistance might not limit the use of phages as biocontrol agents to *R. solanacearum*. Phages are increasingly developed as potential biocontrol strategies against *R. solanacearum* outbreaks and an extensive diversity of phages is available (Castillo et al., 2020, Genin and Denny, 2012, Trotereau et al., 2021). Numerous studies have highlighted the potential for using phages against *R. solanacearum*, where phages have been reported to reduce the abundance and disease severity of *R. solanacearum* (Elhalag et al., 2018, Ramírez et al., 2020, Álvarez et al., 2019, Fujiwara et al., 2011). However, like other pathogenic bacteria, resistance to phages is a concern when developing phage biocontrols (Rohde et al., 2018). Moreover, knowledge around resistance evolution in *R. solanacearum* remains limited (Vailleau and Genin, 2023).

To study this, we conducted a 30-day coevolution experiment with one genotype of *R. solanacearum* and four different phages isolated from the UK and China. We aimed to

understand whether 1) *R. solanacearum* and phages engage in coevolution 2) Determine if the coevolution follows ARD or FSD or shifts between both dynamics 3) If coevolution leads to trade-offs in resistant *R. solanacearum* 4) Understand the genetic mechanisms behind evolved resistance. We find that the interactions between *R. solanacearum* and phages is highly asymmetrical leading to phage extinctions due to a rapid evolution of phage resistance in *R. solanacearum*. Cross-resistance was also common. We found evidence of evolutionary trade-offs between resistance and two other traits, critical to *R. solanacearum's* success as a highly destructive plant pathogen, growth and biofilm formation. Genomic analyses of phage resistant *R. solanacearum* showed genetic variation in two proteins; Undecaprenyl-phosphate alpha-N-acetylglucosaminyl 1-phosphate transferase and Tyrocidine synthase 3, involved in lipopolysaccharide (LPS) and antibiotic synthesis respectively.

3.3 Materials and Methods

3.3.1 Strains and Phage Isolates.

One genotype of *Ralstonia solanacearum* (the model genotype UW551, NCPPB 4362) belonging to phylotype IIB (cold-tolerant strain) was chosen for this coevolution experiment. This genotype was isolated in the USA in 2003 from *Pelargonium hortorum* (also known as garden geranium). First, an isogenic stock of UW551 was created see 2.3.1 Strains and Phage Isolates for the protocol. The culture was standardised to 0.4 optical density (OD 600nm, SPECTROstar nano). Once standardised UW551 was cryopreserved (see 2.3.1 Strains and Phage Isolates) The Colony Forming Unit/ml (CFU/ml) was calculated (see 2.3.4 Quantification of Bacteria Densities). At a 0.4OD, UW551 had a CFU/ml of $3x10^9$.

Based on preliminary data (unavailable), we then chose four different phage isolates for coevolution experiment (Table 1). Preliminary data from these phages showed variation in infectivity to UW551 and we also saw a recovery in OD which could be indicative of phage resistance in UW551. This gave us an indication that coevolution dynamics were occurring with these phages, making them good candidates for a long-term coevolution experiment. Before the coevolution experiment, 10µl of each phage (Table 3.1) was enriched with 100µl of overnight culture of UW551 in 35ml of fresh CPG media (see below for the method). The phages were then isolated and stored at +4°C until required. Plaque Forming Unit/ml (PFU/ml) was calculated for phages (see 3.3.4 Quantification of Phage Densities]). Initial phage stocks had a PFU/ml count of $4x10^7$ (PY045),$1x10^9$ (PY059),$1x10^9$ (PY04) and $4x10^9$ (PY065).

Table 3.1 – Overview of the phage isolates used in this coevolution experiment.

Isolate	Year of Isolation	Location of Isolation	TEM Morphology
PY045	2018	Nanjing, China	Podoviridae
PY059	2021	River Foss, York, UK	Unknown
PY04	2019	River Thames, UK	Podoviridae
PY065	2021	River Jubilee, UK	Podoviridae

3.3.2 Coevolution Experiment

To start the coevolution experiment (Figure 3.1), UW551 was grown in 25ml of CPG media to an optical density reading of 0.4 (OD 600nm). This culture was diluted from ~10^9 CFU/ml to ~10^7 CFU/ml before 10µl of UW551 was added to five 24-well plates, each with six replicates (wells). Alongside UW551, 2ml of CPG media was added and 10µl of phage. Four of the five wells contained one of the chosen phage isolates (Table 1) and the final fifth plate contained bacteria only (Control). The Multiplicity of Infection (MOI) was set to 1 (10^7 viral particles to 10^7 bacterial cells). Each plate was packed into mini grip bags with a wet towel to prevent desiccation and incubated at +28°C for 72 hours. At the end of the 72 hours, optical density reads (OD 600nm) were taken, followed by isolation of the populations of phages and bacteria. 200µl of the samples were also transferred into a new well alongside 1.8ml of fresh CPG. 200µl was used so we could transfer large population sizes of bacteria and phages and help reduce the risk of genetic bottlenecking (see 3.5 Discussion). Evolved populations were isolated by removing 600µl of sample and added to 400µl of glycerol (at 20% of final glycerol concentration) and stored at -80°C. Moreover, 900µl of samples were used to isolate the phages (see 3.3.3 Isolation of Phages). The remaining sample was used to calculate bacterial cell densities and isolate resistant clones (see 3.3.4 Quantification of Bacteria Densities and 3.3.6 Isolation of *Ralstonia solanacearum* clones). This serial transfer process was repeated for 10 cycles, totalling 30 days.

Coevolution Experiment

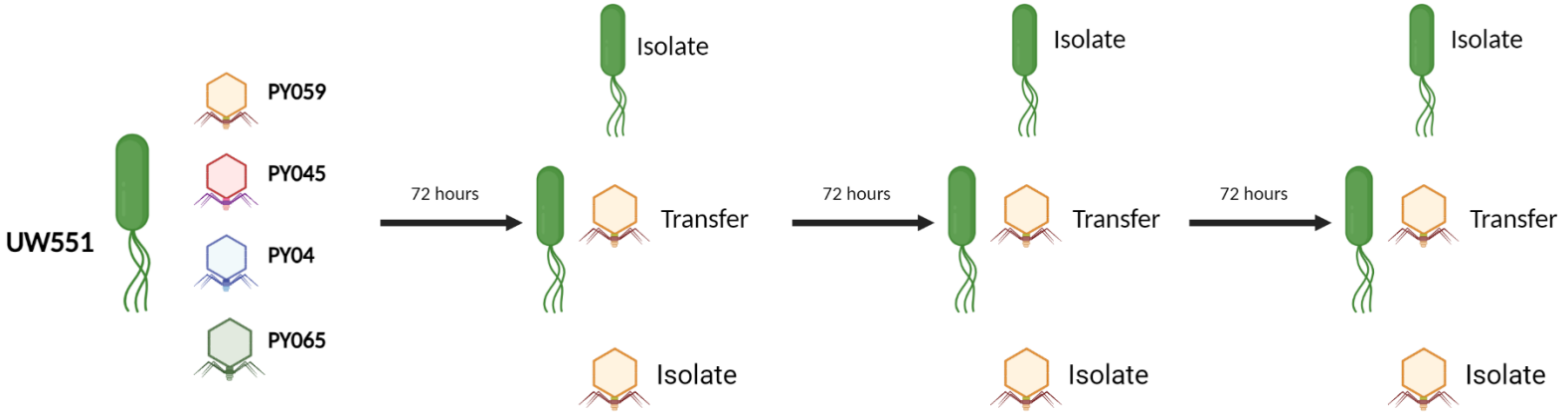

Possible Outcomes:

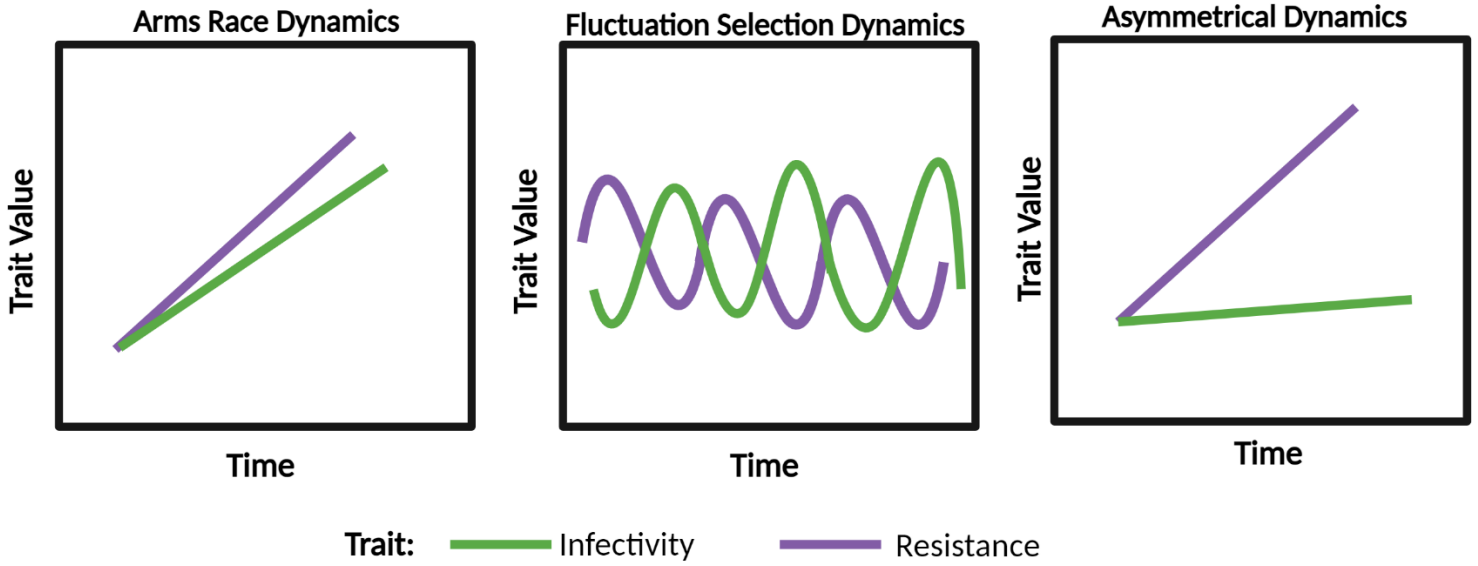

Figure 3.1 – Experimental design for the coevolution experiment. *R. solanacearum* UW551 was coevolved with four different phages, PY059, PY045, PY04 and PY065. Every 72 hours, optical density reads (OD 600nm) were taken, followed by isolation of the population, phages and bacteria. This was repeated for a total of ten times (30 Days). Three possible outcomes of this coevolution were, arms race dynamics, fluctuation selection dynamics and asymmetrical dynamics. Arms race dynamics, the escalation of infectivity and resistance over time. Fluctuation Selection Dynamics, fluctuation in infectivity and resistance over time. Asymmetrical dynamics, the escalation of one trait in only one of the coevolving populations. Created in Biorender.com

3.3.3 Isolation of Phages

At the end of each transfer, phages were isolated see 2.3.2 Phage Training for the protocol.

3.3.4 Quantification of Phage Densities

Throughout the coevolution experiment phage densities were monitored and recorded as the Plaque-Forming Unit (PFU/ml) (See 2.3.3 Quantification of Phage Densities). Here, UW551 was used for the overnight culture and the soft agar . was supplemented with 10mM of $CaCl_2$ and 10mM of $MgCl_2$ Supplementing the agar helps phages bind to receptors making it easier for them to form plaques on the soft agar (Ács et al., 2020, Tan et al., 2009). Adaptations were made to the media here in order to confirm that phages had gone extinct. Spot assays were also performed in a comparable manner, this was done to confirm the presence of phage, if titres were too low. Instead, using a serial dilution, 10-20µl of phage lysate was directly added to the plate.

3.3.5 Quantification of Bacteria Densities

As well as phage densities, bacterial densities were also monitored throughout the coevolution experiment as Colony Forming Unit/ml. A serial dilution (10^{-1} to 10^{-8}) was performed using a 96-well plate (10µl of sample to 90µl of CPG) with each column representing a replicate. The 96-well plate was divided into two with the first half representing one phage treatment and the second half representing another phage treatment. A CPG or Tripheny tetrazolium chloride (TTC) agar plate (Casamino acid 1g, Peptone 10g, Glucose 5g, 15g Agar, 5ml of 1% stock solution of 2,3, 5-tripheny tetrazolium chloride per litre) was divided up between the six replicates of one phage isolate (Kelman, 1954). TTC plates were used to monitor the production of non-virulent colonies and virulent colonies. On TTC plate virulent colonies appear white with pinkish centres while non-virulent colonies appear dark red (Kelman, 1954). Using a multi-channel pipette, 5µl of each dilution was spotted into the plate. The plates were than incubated at +28^{o}C for 48 hours for a CPG plate and up to 96 hours for a TTC plate. The CFU/ml was calculated from the following equation:

$$\text{CFU/ml} = [\text{number of colonies} \times \text{dilution factor}] / \text{volume of culture plate}$$

3.3.6 Isolation of *Ralstonia solanacearum* clones

From the plates used to monitor bacterial densities we also isolated individual *R. solanacearum* colonies (clones). Once the number of colonies had been recorded, we took 12 individual colonies from each replicate of each treatment (including the control) and added them to 96-well plates with 120µl of CPG. Clones were incubated at +28^{o}C for 48 hours after 60µl of glycerol was added (20% final concentration), plates were wrapped up and stored at -80^{o}C until required. Colonies were isolated from TTC plates which included a mixture of potentially non-virulent and virulent colonies based on colony morphology.

Due to problems with contamination (*Staphylococcus*) within populations from time-point 4 on (Figure 3.2, see results and discussion), we had to reisolate clones. From the 96-well plates that were used to store the clones originally, 5µl of each clone was spotted onto modified SMSA plates (TTC medium, using 5ml of glycerol instead of 5g of glucose) to confirm if clones were *R. solanacearum*. Modified SMSA medium contains the following antibiotics: Crystal violet 5mg, Polymyxin β sulphate, Bacitracin 25mg, Chloromycetin 5mg, Penicillin 0.5mg and Cycloheximide (Elphinstone et al., 1996b). Through using modified SMSA we able to remove *Staphylococcus* out of the samples as it is a selective media for RSSC (Elphinstone et al., 1996b). Once spotted, we grew up the clones at +28^{o}C until colonies appeared. Individual colonies were then re-streaked onto both circular CPG and SMSA plates and again grown at +28^{o}C until colonies appeared again. Individual colonies were then picked and grown in 25ml of CPG for 72 hours. This was then re-streaked onto CPG and SMSA plates with the process being repeated again. After the 72 hours, 600µl of sample was removed and placed into eppendorfs with 400µl of glycerol (20%). We used PCR and sequencing to confirm we had re-isolated UW551 (see 3.3.11 Sequencing). CFU counts were also performed (see3.3.5 Quantification of Bacteria Densities). The re-isolated clones were then used to check phage resistance, fitness trade-offs, cross-resistance and biofilm formation. It is possible that the antibiotics and re-streaking impact the clones' growth, however, SMSA media is a selective media for *R. solanacearum* and our priority was removing the contaminant which required the use of antibiotics as we could not use CPG and morphological differences for re-isolation (Figure 3.2). Once clones were re-isolated, they were moved back on CPG media to allow recovery.

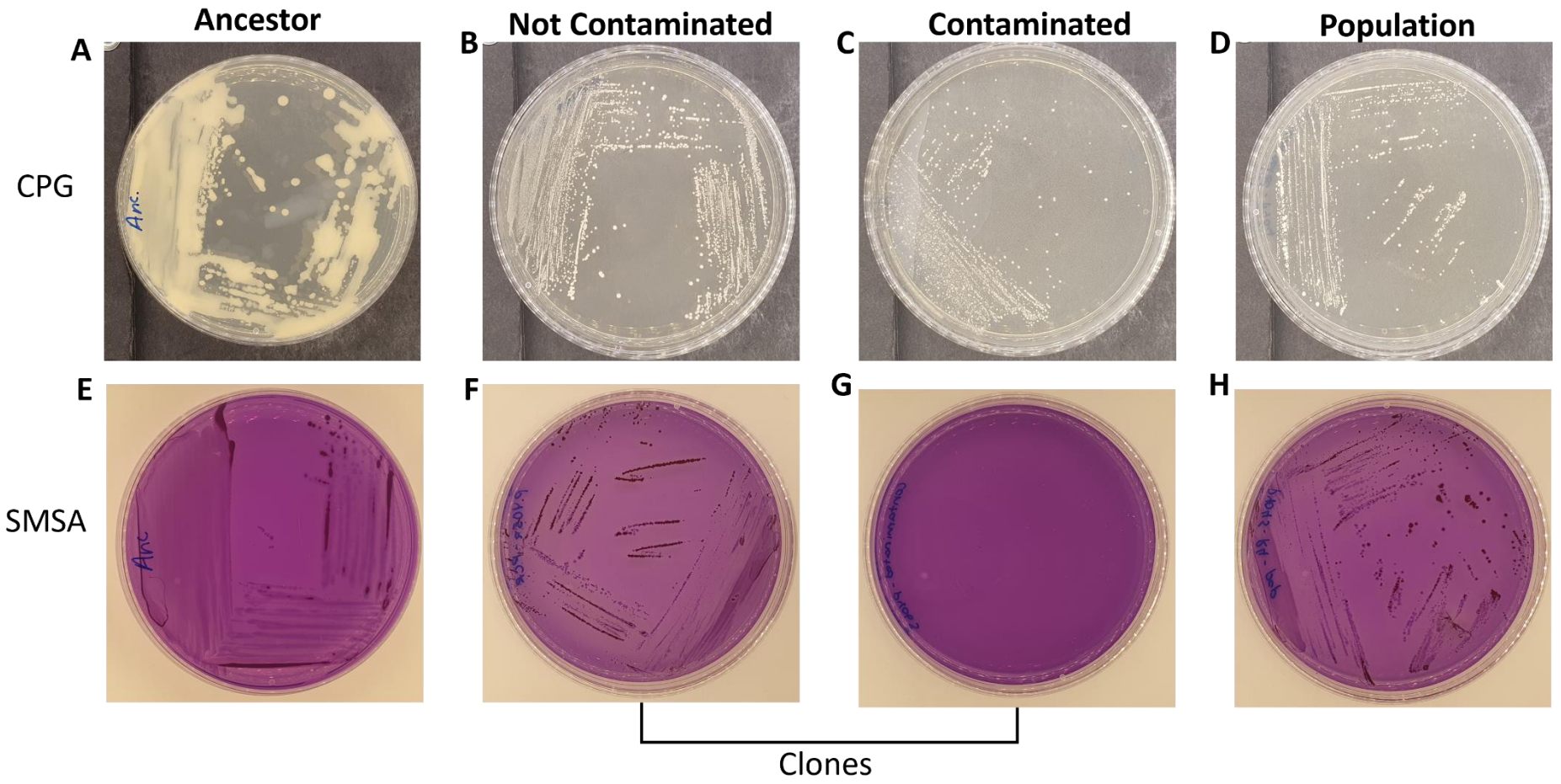
Ancestor
Not Contaminated
Contaminated
Population
A
B
C
D
CPG
E
F
G
H
SMSA
Clones

Figure 3.2 - Photographs of plates to highlight the morphological similarities between contaminated and noncontaminated plates. A-D) *R. solanacearum* and contaminate grown on CPG plates. E-H) *R. solanacearum* and contaminate grown on SMSA, selective media for *R. solanacearum*. A and E, Ancestral UW551. B and F, *R. solanacearum* colonies from a clone that was confirmed to be *R. solanacearum* by PCR and whole-genome sequencing. C and G, the contaminate where whole-genome sequencing identified as *Staphylococcus* sp, previously thought to be a clone of *R. solanacearum*. D and H, the population of *R. solanacearum* and phages that clones were isolated from. The population is from transfer 4 where phages were declared extinct. On CPG plates (photos B-D) the plates look indistinguishable, so it is impossible to re-isolate *R. solanacearum* on CPG. We cannot even establish a timeline of where the contamination occurred which is why it was difficult to determine if it was just in the clones isolated from the coevolution experiment or whether it was the populations during the coevolution experiment. During the coevolution experiment morphological changes to *R. solanacearum* has occurred making it look morphologically different to its ancestor (A), adding to the difficulty of using CPG for re-isolation purposes. On SMSA, the contaminate failed to grow on SMSA media (G) while *R. solanacearum* clones were able to (F), this allowed us to re-isolate *R. solanacearum* for further experiments. The population was also grown on SMSA to confirm the presence of *R. solanacearum* at transfer 4, phage extinction. From these plates and further experiments, we have concluded that R. *solanacearum* was present at transfer 4 of the coevolution experiment and was highly resistant to all four phages.

3.3.7 Phage Enrichment

In order to create a stock of ancestral phages =, phage enrichment was used to increase the abundance of phages and their volume following 2.3.5 Phage Enrichment protocol, 100µl of overnight culture of UW551 was used instead. Also, see 3.3.4 Quantification of Phage Densities to determine the phage abundance. .

3.3.8 Phage Infectivity Assays

Phage Infectivity assays were conducted to see if phages and UW551 were engaging in coevolutionary dynamics before the phage extinction events occurred (before timepoint 4). We chose all successfully isolated coevolved phages from all four phage treatments. From PY045 and PY059 we used coevolved phages from timepoints 1, 2 and 3. For PY04 and PY065 we selected coevolved phages from timepoints 1 and 2. Due to high levels of resistance (and potential contamination) we only used ancestral UW551 for phage infectivity assays instead of coevolved *R. solanacearum* clones. To a 96-well plate, 100µl of CPG and 5µl of ancestral UW551 was added and grown for 24 hours at +28^{o}C. After 24 hours, 2µl of bacteria and 5µl of phage was added to a new 96-well plate with 100µl of CPG (5µl of sterilised diH_2O for the control) and incubated at +28^{o}C for 48 hours. Optical density (OD 600nm) reads were taken at 0 hours, 24 hours and 48 hours.

3.3.9 Phage Infectivity and Cross-Resistance Assays

All further assessment of resistant UW551 was conducted on clones isolated at timepoint 4. At timepoint 4, all phages were confirmed extinct and also sequencing confirmed that these clones were *R. solanacearum* UW551 and not the contaminant.

Re-isolated clones at timepoint 4 were re-evaluated for their resistance and cross-resistance. Prior to infectivity assays, we re-grew the clones from cryo-stock for 72 hours in 25ml of CPG. To set up assays, 10µl of pre-grown UW551 and 10µl of phage was added to a 96-well along with 180µl of CPG at the multiplicity of infection (MOI) of 1 (10^4 cells to 10^4 viral particles). Optical density (OD 600nm) reads were taken at 0 hours, 24 hours, 48 hours and 72 hours. To assess if cross-resistance had occurred, we inoculated all clones, plus ancestral UW551, with all ancestral phages PY059, PY045, PY04 and PY065. In case of cross-resistance, bacteria exposed to one phage during the coevolution experiment were expected to be able to grow in the presence of other phages they had not been exposed previously.

3.3.10 Fitness Assays

We also assessed the fitness of the clones with growth assays in the absence of phages to determine if evolutionary trade-offs were present. Fitness assays were conducted in the same way as the phage infectivity and cross-resistance assays as described above. However, no phage was added, and 10µl of sterilised diH_2O was added instead.

3.3.11 Biofilm Assays

Biofilms are important for virulence in RSSC (Mori et al., 2016). Often phage resistance is traded with virulence (Scanlan et al., 2015) We decided to look at biofilm production to see if any trade-offs might be present in the resistant clones and whether this trade-off was linked to virulence. To assess if resistance to our phages resulted in trade-offs between biofilm production in UW551, we performed biofilm assays on the re-isolated clones and ancestor. Prior, to the biofilm assays, clones and ancestral UW551 were grown in 25ml of CPG for 72 hours at +28^{o}C. To a 96-well 20µl of *R. solanacearum* (~10^4 cells) was added to 180µl of CPG and regrown at +28^{o}C for 72 hours. After 72 hours, the culture was tipped out into Virkon and plates rinsed with deionised water. Plates were then left to dry for 15 minutes. 200µl of 0.1% crystal violet was then added to all wells (and a control plate) and left for 20 minutes. The crystal violet was then removed, and the plates rinsed gently with deionised water and again, left to dry for 15 minutes. 220µl of ethanol was then added to solubilise the crystal violet for 15 minutes. The optical density (600nm) was recorded with the control plate as the blank.

3.3.12 Sequencing

Whole genome sequencing was conducted on ancestral and coevolved (transfer 4) UW551 isolates at MicrobesNG (Birmingham, UK). DNA was extracted using the Qiagen DNeasy Blood and Tissue Kit (modifications to the protocol were provided by Dr Evelyn Farnham and Dr Martina Stoycheva) (Farnham, 2022, Stoycheva, 2022) . Buffers provided by the kit were prep according to manufacturer's protocol.

First, bacterial pellet preparation, ancestral and coevolved UW551 from cryo-stocks were streaked onto both modified SMSA and CPG plates. CPG plates were also included as some clones struggled to grow on modified SMSA plates. Phage resistant *R. solanacearum* can become sensitive to antibiotics, including polymyxin B which is an antibiotic used in modified SMSA (Elphinstone et al., 1996b, Hong et al., 2014). Colonies from the plates were removed and placed into eppendorfs with 200µl of distilled water (sterilised). Eppendorfs were then centrifuged at maximum speed for 5 minutes, the supernatant was removed, and the pellet was frozen at -80^{o}C for 30 minutes. Cell lysis 180µl of Buffer ATL was used to resuspend the pellet (ATL precipitate needs to be dissolved beforehand on a hot block at 37^{o}C). 20µl of proteinase K (40 mAU/mg protein) was then added, mixed by vortexing and incubated at 56^{o}C for 2 hours. DNA purification, 2µl of RNase A (50mg/ml) was added, mixed by vortexing and incubated for 15 minutes at room temperature. Vortexed again for 15 seconds, then 200µl of Buffer AL was added and vortexed again. 200µl of ethanol was added, mixed by vortexing and pulsed spin 3 times. Samples were transferred to a DNeasy Mini spin column and incubated at room temperature for 5 minutes. Samples were centrifuged at 13000rpm for 3 minutes, the flow-through collected in the spin column was discarded, and another centrifuge at 13rpm for 1 minute. Washing steps, 500µl of buffer AW1 was added, incubated at room temperature for 5 minutes. The samples were then centrifuged at 13000rpm for 3 minutes, flow-through discarded and centrifuge again for 1 minute. The same process with buffer AW1 was applied to buffer AW2 but repeated twice. The DNeasy Mini spin column was placed into a new 2ml collection tube and incubated at room temperature for 15 minutes with lids open to dry the membrane and prevent residual ethanol interfering with subsequent reactions. For the fifth and final step, elution, 50µl of nuclease-free water was added and left at room temperature for 3 minutes and centrifuge at

13000 rpm for 1 minute. This step was repeated 3 times. Finally, eluted liquid was placed into eppendorfs with 20µl for quantification and PCR.

Due to the problems, we had with contamination, we wanted to make sure that we had successfully re-isolated *R. solanacearum* and also successfully extracted their DNA. We conducted polymerase chain reaction (PCR) and gel electrophoresis to confirm this. For the PCR, we created a master mix of Promega GoTaq® Master Mixes (GoTaq®), nuclease-free water and forward and reverse primers. Primers used were *R. solanacearum* specific, RSF (5' GTGCCTGCCTCCAAAACGACT 3') and RSR (5' GACGCCACCCGCATCCCTC 3') (Chen et al., 2010). To the PCR tube we added 15µl of the master mix and 5µl of DNA. Each sample should have 10µl of GoTaq®, 3µl of water, 1µl of forward primer, 1µl of reverse primer and 5µl pf DNA. Two controls were also included 5µl of RSSC strain GMi1000 as a positive control and another of 5µl of H_2O as a negative control. PCR was based on guidelines provided by the manufacture of GoTaq®. The following steps were carried out:

1) 4 minutes and 30 seconds at +95^{o}C
2) 30 seconds at +95^{o}C
3) 30 seconds at +55^{o}C
4) 1 minute at +72^{o}C
5) 10 minutes at +72^{o}C
6) Cooled to +4^{o}C.

Steps 2-4 were repeated 40 times.

Once PCR was completed, we conducted gel electrophoresis. 0.8% Agarose gels were prepared in 1xTBE with ethidium bromide added. The gel was submerged into 1xTBE. To the samples 1x Quick-Load® Purple 1 kb DNA Ladder was added (New England Biolabs). 10µl of samples were added to the gel and was left to run for 30 minutes at 80V, gel was then imaged under UV. Using the positive control (GMI1000), we determined which isolates were *R. solanacearum* UW551 (Supplementary Figure 3.1).

Qubit™ High Sensitivity dsDNA kit (Invitrogen) was used to check the yield and make sure the DNA quantity met the threshold for MicrobesNG. Isolates, that successfully matched the band of the positive control and met the threshold of DNA quantity for microbesNG, were sent away for whole genome sequencing. See 2.3.9 Phage Genomics for the variant calling pipeline used to analyse the sequences. For reference genome, the ancestral UW551 was used.

3.3.13 Statistical Analysis

Statistical analysis and data visualisation was performed using R statistical software, version 4.2.3 (Team, 2023). Figures were produced using the ggplot2 package (Wickham, 2016). Statistical analysis of the population dynamics of both phage and *R. solanacearum* UW551 (mean PFU/ml and mean CFU/ml counts respectively), we used Kruskal-Wallis Tests followed by Pairwise Wilcoxon test with Benjamini Hochberg (BH) p value adjustment, using functions from stats R package (Team, 2023). For statistical analysis of phage infectivity assays, we used Kruskal-Wallis Tests followed by pairwise Wilcoxon test with BH p value adjustment, using functions from stats R package as well, focusing on the 48 hour timepoint (Team, 2023). For the phage infectivity and cross-resistance assays, we normalised the data against the 0-hour timepoint. This was done so we would only be looking at growth without background optical density. Scheirer-Ray-Hare statistical test was used to look at the effects of phages and all *R. solanacearum* isolates on cross resistance, using functions from stats R package (Team, 2023). One-way ANOVA was conducted to compare differences in growth rate and biofilm production between bacterial isolates, using functions from stats R package (Team, 2023). For biofilm production, data was normalised to a blank media control.

3.4 Results

3.4.1 Population Dynamics of *R. solanacearum* and Bacteriophages

During the coevolution experiment we monitored the population dynamics of bacteria and phages as CFU/ml and PFU/ml (Figure 3.3). Both CFU/ml and PFU/ml (their abundance) would help give an indication whether the phages and bacteria were engaging in coevolution and if there is any asymmetry when one of the species might be dominating the other. Overall, there was evidence of a coexistence between phages and *R. solanacearum* for the first three transfers (9 days). However, this coexistence soon ceased to exist due to the extinction of phages and possibly contamination (see 3.4.3 Contamination was found in clones at timepoint 4).

For PY059, significant differences between the initial population and other transfers were observed (Figure 3.3B, Kruskal-Wallis:$X^2_{63.421}$, $p < 0.001$). From the initial phage abundance to transfer 1, we found that phage abundance was increasing (Wilcoxon test with BH adjusted for p values, $p = 0.003$). However, no significant differences were found between the initial population and transfers 2 and 3, as phage abundance began to decline (Wilcoxon test with BH adjusted for p values, $p > 0.05$, $p > 0.05$, respectively).

We found a similar pattern between PY059 and PY045 (Figure 3.3C). For PY045, significant differences between the initial phage population and coevolutionary transfers were observed (Figure 3.3C, Kruskal-Wallis:$X^2_{62.448}$, $p < 0.001$). From the initial phage abundance to transfer 1, we found that phage abundance did increase (Wilcoxon test with BH adjusted for p values, $p = 0.003$). However, no significant differences were found between the initial population and transfers 2 and 3, as phage abundance began to decline (Wilcoxon test with BH for adjusted for p values, $p > 0.05$, $p > 0.05$, respectively). Phages went extinct at transfer 4.

For PY04, we found a significant difference between the initial phage population and transfer 1 due to increase in phage abundance (Figure 3.3D Kruskal-Wallis:$X^2_{61.472}$, $p < 0.001$, Wilcoxon test with BH adjusted for p values, $p = 0.004$). However, the significant difference between the initial phage population and transfer 3 was due to a significant decrease in phage abundance (Wilcoxon test with BH adjusted for p values, $p = 0.004$). (Figure 3.3D). This was a similar situation for PY065 (Figure 3.3E, Kruskal-Wallis:$X^2_{61.472}$, $p < 0.001$, Wilcoxon test with BH adjusted for p values, $p = 0.0129$). After transfer 4, phages had gone extinct in both coevolution treatments (Figure 3.3 D-E).

From transfer 4 (12 days), we were unable to detect phages from any of the treatments (Figure 3.2). From here, we attempted spot testing to confirm if any phages were present. Only a handful of replicates survived to transfer 4 and only one replicate from PY045 survived to transfer 5 (15 days). Phage extinctions were seen in all replicates and all treatments by transfer 6 (18 days).

Looking at the population dynamics of UW551, we observed that abundance of UW551 for the first three days (transfer 0 to 1) remained high for UW551 in phage treatments PY059 and PY045 (Figure 3.3B-C) but undetectable for PY04 and PY065 (Figure 3.3D-E). For PY059, we did find significant differences between bacterial abundance (Kruskal-Wallis:$X^2_{56.521}$, $p < 0.001$). Since, bacterial abundance was increasing throughout the experiment, it was unlikely that the fluctuations were caused by the presence of phages (Figure 3.3B). Post hoc analysis showed that significant differences were found between the initial bacteria abundance and transfer 3 but as the abundance was higher at transfer 3 it suggested that resistance was established (Figure 3.3B, Wilcoxon test with BH adjusted for p values, $p = 0.009$). Phages were extinct by transfer 4. For PY045 we did find significant differences between bacteria abundance (Figure 3.3C, Kruskal-Wallis: $X^2_{46.879}$, $p < 0.001$). However, it was unlikely that drives were causing these fluctuations in bacterial abundance. Post hoc analysis revealed that the significant differences were found between the initial bacteria abundance at the start of the experiment and transfers after phage extinction.

We found significant differences between bacteria abundance in PY04 treatment (Kruskal-Wallis: $X^2_{50.507}$, $p < 0.001$). There was a significant decrease in bacteria abundance from the initial start of the experiment to the 2nd transfer (Figure 3.3D, Pairwise Wilcoxon test with BH adjusted for p values, $p = 0.007$). However, at the 3rd transfer we found no significant difference between the initial start of the experiment and transfer 3, suggesting that *R. solanacearum* had recovered and resistance was established in the population (Figure 3.3D, Wilcoxon test with BH adjusted for p values, $p > 0.05$). It was a similar pattern for PY065 (Figure 3.3E), we found significant differences between bacteria abundance in PY065 treatment (Kruskal-Wallis: $X^2_{51.1}$, $p < 0.001$). Bacteria abundance decreased significantly from the initial start of the experiment to transfer 2 (Figure 3.3E, Wilcoxon test with BH adjusted for p values, $p = 0.007$). At the 3rd transfer, we found no significant difference compared with the initial start of the experiment (Wilcoxon test with BH adjusted for p values, $p > 0.05$). At transfer 4 onwards (12 days), all UW551 populations recovered or retained high densities (Figure 3.3E).

Overall, we found that rather than ARD or FSD, the coevolutionary dynamics with UW551 and all four phages was highly asymmetrical. The decline of phage abundance and the recovery for UW551 (particular for PY04 and PY065) suggest that phage resistance evolved rapidly, and phages could not adapt, resulting in their decline and eventual extinction in all four treatments (Figure 3.3)

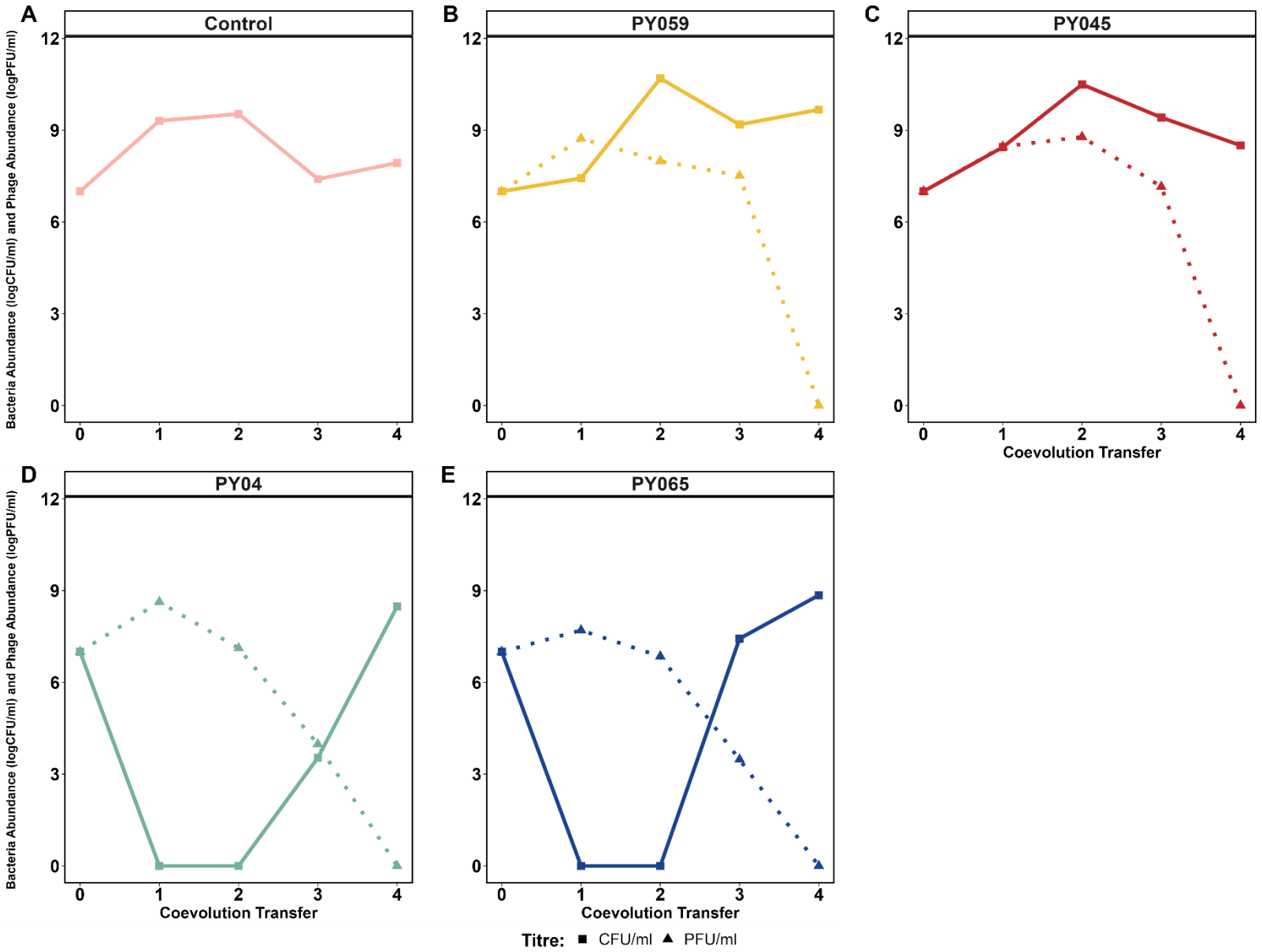
A
Control
B
PY059
C
PY045
D
PY04
E
PY065
Bacteria Abundance (logCFU/ml) and Phage Abundance (logPFU/ml)
Coevolution Transfer
Titre: ■ CFU/ml ▲ PFU/ml

Figure 3.3 – The population dynamics of *R. solanacearum* UW551 (CFU/ml) and phages (measured as PFU/ml) during the coevolution experiment. UW551 was grown in the presence of one phage for 30 days, with the population being transferred into fresh CPG media every 3 days. The populations were measured every 3 days as well. A) The control, UW551 only and no phages, B) UW551 and PY059, C) UW551 and PY045, D) UW551 and PY04 and E) UW551 and PY065. Only the first four transfers are shown this is due to phage extinction at transfer 4.

3.4.2 Phage Infectivity Assays suggest possible coevolutionary dynamics occurred.

We challenged all available isolated phages from the coevolution experiment against ancestral UW551 to see if any coevolutionary dynamics had occurred before transfer 4, where phages were declared extinct.). If coevolution had occurred before the extinction event, we would have seen evidence of changes in infectivity from the phages. If ARD were occurring, we would expect to see increased infectivity levels from phages that were isolated at later transfers. Whereas if FSD was occurring during the coevolution experiment, we would expect to see fluctuations in infectivity from phages through time.

For ancestral and coevolved PY059 we found that were significant differences between phage treatments (Figure 3.4 A-B, Kruskal Wallis: $X^2_{234.61}$, $p < 0.001$). All phage treatments were able to suppress ancestral UW551 but differences between the phages themselves did arise (Figure 3.4 A-B). We found that only transfer 1 and 3 had significant differences between the ancestral PY015 suggesting that infectivity changes occurred which could indicate coevolutionary dynamics occurring before phage extinction (Figure 3.4B, Wilicoxon test with adjusted BH for p values, $p < 0.001$ and $p < 0.001$, respectively). Compared to the ancestor, there is a slight rise in the OD which could suggest a decrease of infectivity at these transfers but between transfer 1 and transfer 2 there is a potential increase in infectivity as the OD drops again (Figure 3.4 A-B, Wilicoxon test with adjusted BH for p values, $p < 0.001$). However, there is no significant difference between the ancestor and transfer 2 so infectivity does not increase higher than the ancestor PY015 (Figure 3.4 A-B, Wilicoxon with adjusted BH for p values, $p > 0.05$). Again, the OD slightly increases between transfer 2 and transfer 3 phages, suggesting that there was another decrease in infectivity between timepoints (Figure 3.4B, Wilicoxon with adjusted BH for p values, $p < 0.001$). Taken together, the results could indicate FSD was due the subtle fluctuations in infectivity over time.

For coevolved PY045 it was a similar situation, overall, we saw subtle fluctuations in infectivity over time which could indicate FSD before the phage extinction. There were significant differences between phage treatments (Kruskal-Wallis:$X^2_{237.44}$, $p < 0.001$). Again, all phages were able to suppress ancestral UW551 effectively, but we did find differences between each coevolved phage, suggesting changes in infectivity over time. We found no significant difference between ancestor and coevolved phages from transfer 1 suggesting

that there was no significant change in infectivity (Figure 3.4 C-D, Wilicoxon test with adjusted BH for p values, $p < 0.01$). However, there is potential infectivity between transfer 1 and transfer 2, it appears that infectivity increased slightly (Figure 3.4 C-D, Wilicoxon test with adjusted BH for p values, $p < 0.01$). Interestingly, between the ancestor and transfer 2 there was a slight increase in infectivity (Figure 3.4 C-D, Wilicoxon test with adjusted BH for p values, $p < 0.01$). However, it appears that infectivity has decreased at transfer 3, the OD is highest with phages from transfer 3 (Figure 3.4 C-D). Overall, PY045 infectivity levels fluctuate as they coevolve with UW551.

For PY04 it is difficult to determine what infectivity changes have occurred during the coevolution experiment (Figure 3.4 E-F). Statistical analysis has suggested that coevolutionary dynamics were occurring, highlighting that there were significant differences between PY04 treatments (Figure 3.4 E-F, Kruskal-Wallis: $X^2_{171.68}$, $p < 0.001$). All phage treatments are highly effective at suppressing the growth of ancestral UW551, regardless of isolation time (Figure 3.4 E-F). There is a significant difference between ancestor PY04 and transfer 1 PY04 suggesting a change infectivity but whether this is an increase or decrease in infectivity is difficult to determine (Figure 3.4 E-F, Wilicoxon test with adjusted BH for p values, $p < 0.001$). The situation is the same between transfer 1 and transfer 2 PY04 phages, there is change to infectivity but it difficult to determine the direction it changes (Figure 3.4 E-F, Wilicoxon test with adjusted BH for p values, $p < 0.001$). Interestingly, we found no significant differences between ancestor PY04 and transfer 2 (Figure 3.4 E-F, Wilicoxon test with adjusted BH for p values, $p > 0.05$). Overall, evidence suggests that coevolutionary dynamics were occurring with infectivity changes to PY04 over time, but it is very difficult to determine whether this was ARD or FSD.

A similar situation to PY04 was found in PY065, we found that there were infectivity changes occurring over time suggesting that coevolution was happening but it is difficult to determine the dynamic (Figure 3.4 G-H, Kruskal-Wallis:$X^2_{142.87}$, $p < 0.001$). There were changes in infectivity level over time with only the ancestral PY065 being significantly different to transfer 2 phages (Figure 3.4 G-H, Wilicoxon test with adjusted BH for p values, $p = 0.032$). We, however, cannot tell whether there was an increase or decrease in infectivity over time (Figure 3.4 G-H). Nevertheless, PY065 phages remain highly effective at suppressing ancestral UW551 (Figure 3.4 G-H).

Overall, the phage infectivity assay here does point towards coevolutionary dynamics happening as we see subtle changes in infectivity levels over time. The fluctuations of infectivity in coevolved phages could suggest FSD. However, due to the contamination it is difficult to determine if FSD was playing a role due to a lack of contemporary coevolved UW551. The extinction event at transfer 4 highlights that even though FSD could play a role, the coevolution was ultimately asymmetrical, the phage resistance in *R. solanacearum* evolved and phages could not adapt resulting in extinction.

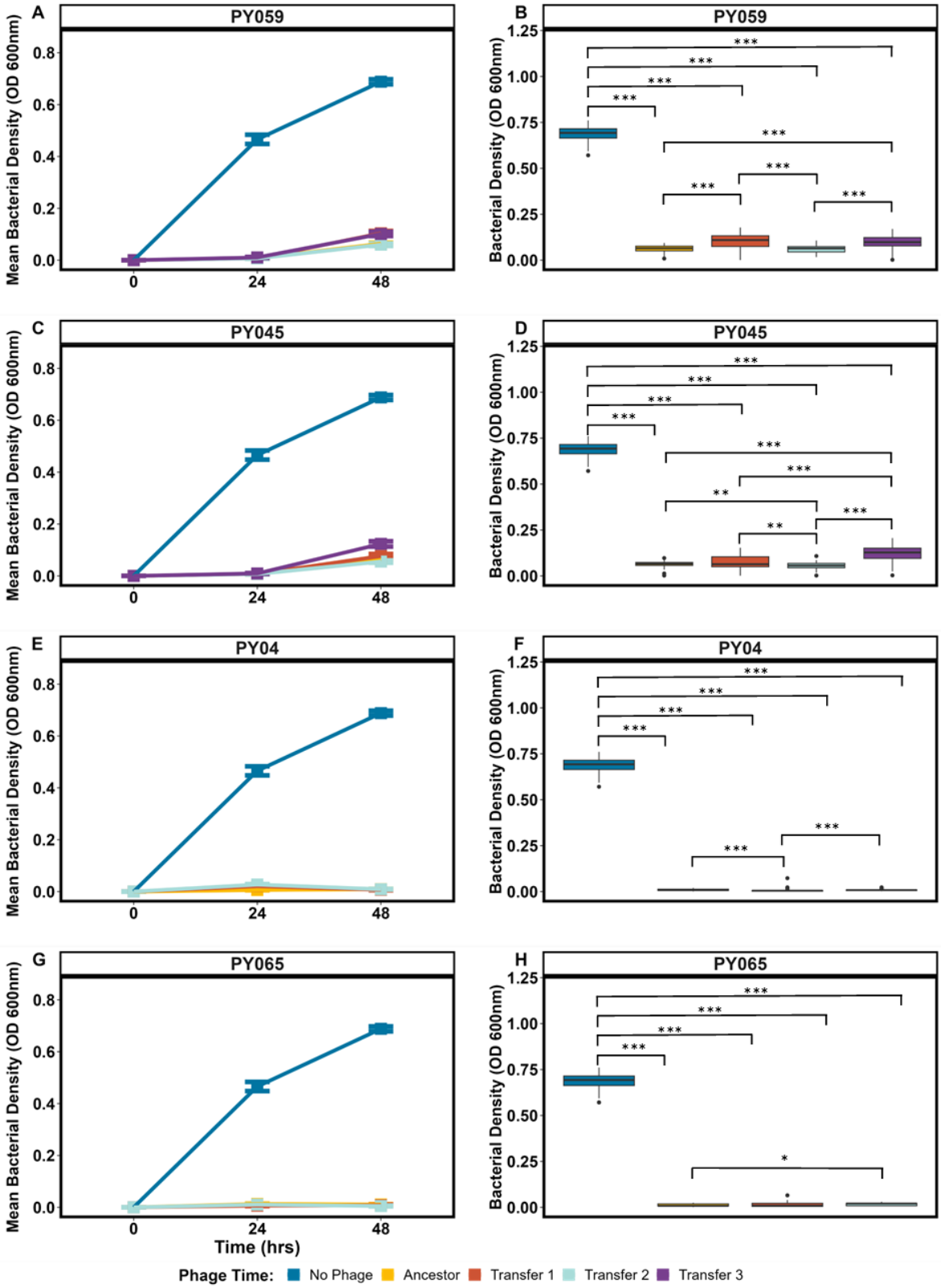
A
PY059
Mean Bacterial Density (OD 600nm)
0.0
0.2
0.4
0.6
0.8
0
24
48
B
PY059
Bacterial Density (OD 600nm)
0.00
0.25
0.50
0.75
1.00
1.25
***
C
PY045
D
PY045
**
E
PY04
F
PY04
G
PY065
H
PY065
*
Time (hrs)
Phage Time:
No Phage
Ancestor
Transfer 1
Transfer 2
Transfer 3

Figure 3.4 – Phage infectivity assays to determine if coevolution was happening and if it was FSD or ARD. All successfully isolated coevolved phages (transfer 1 to transfer 3) and the ancestors were challenged to ancestral UW551 to determine if infectivity levels within the phages had changed over time. Incubated at +28^{o}C for 48 hours, taking OD (600nm) every 24 hours. Panels A, C, E and G shows the growth curve based on mean bacterial density over the 48 hours. Panels B, D, F and H show the bacterial density at the final OD read at 48 hours. A-B) Ancestral PY059 and coevolved PY059 (transfer 1-3) challenged with ancestral UW551. C-D) Ancestral PY045 and coevolved PY045 (transfer 1-3) challenged with ancestral UW5551. E-F) Ancestral PY04 (transfer 1-2) challenged with ancestral UW551. G-H) Ancestral PY065 and coevolved PY065 (transfer 1-2) challenged with ancestral UW551. The * symbols are significant differences between treatments based on pairwise Wilcoxon tests with Benjamini Hochberg p value adjustment post hoc tests (* $p < 0.05$, ** $p < 0.01$, *** $p < 0.001$).

3.4.3 Contamination was found in clones at timepoint 4.

The first round of sequencing confirmed that contamination was present in timepoint 4 clones. We were unaware of the contamination until the sequencing came back, this is one of the reasons why the coevolution experiment continued until transfer 10. We also continued with the hope that the phages were present and could be isolated at a later point. Unfortunately, this did not happen. Due to extinction of phages at timepoint 4, we focused our research here, still unaware of the contamination. Once the sequencing came back and confirmed contamination, we checked clones from timepoints 1, 2, 3 and 10 as well and the evolved populations for contamination (same timepoints). For the clones, 5µl was spotted onto CPG and SMSA plates while for the evolved populations we streaked onto circular CPG and SMSA plates. All were incubated at +28^{o}C until colonies appeared. With comparisons from plates from confirmed *R. solanacearum* re-isolated clones, photos of *Staphylococcus* and photos of *R. solanacearum*. We made judgements on whether contamination was present. Due to morphological similarities, we cannot pinpoint exactly where the contamination occurred (Figure 3.2). Due to time and money constraints we had to go with what we knew, that *R. solanacearum* was present at timepoint 4 in both populations and clones (not all). We carefully re-isolated *R. solanacearum* clones to make sure the contaminate was removed.

These clones were later confirmed to be *R. solanacearum* with PCR (Supplementary Figure 1) and whole-genome sequencing. For us to use other transfers and clones, they would all have to be sent to sequencing for confirmation that they were contaminate free which would require time and money that we did not have (Figure 3.2).

3.4.4 Phage Infectivity and Cross-Resistance

From the re-isolated clones at transfer 4, we re-evaluated their resistance to ancestral phages and determined if cross resistance could be observed. The ancestor and evolved clones were challenged against all four phages, regardless which phages they had coevolved with, including the control from the coevolution experiment. This control was included to see, that adaptations to phage resistance are the result of phages and no other factors like media adaptation. Overall, we found that resistance was present in all re-isolated clones suggesting that resistance evolved in *R. solanacearum* before the phage extinction (Figure 3.5). Cross-resistance was common as we found no significant differences between phage treatments and bacterial isolates (Schierer-Hare-Ray Test, $p > 0.05$). It appears that once *R. solanacearum* evolves resistance, none of the four phages can overcome it, suggesting asymmetrical evolution. As the control is also resistant to phages which could suggest phage resistance evolved in parallel with media adaption. However, within phage coevolving populations, it is likely that phage resistant bacteria are in a much higher frequency (Wang et al., 2023b). Interestingly, in all but PY059, the ancestor UW551 contrasts with the phage infectivity assay used to evaluate whether coevolutionary changes within coevolved phages had occurred (see 3.4.2, Figure 3.4). The ancestor UW551 was completely suppressed to all ancestral and coevolved phages but here, the ancestor was resistant to three of the four phages. This contrast is perhaps due to different population ratios of phages to bacteria. Here, 10µl of both phage and bacteria were added but in the phage infectivity in 3.4.2, 5µl of the phage was added and 2µl of ancestor UW551 was added. A higher volume of phage to bacteria could explain the contrasts, more phages added could mean more infections which resulted in higher suppression.

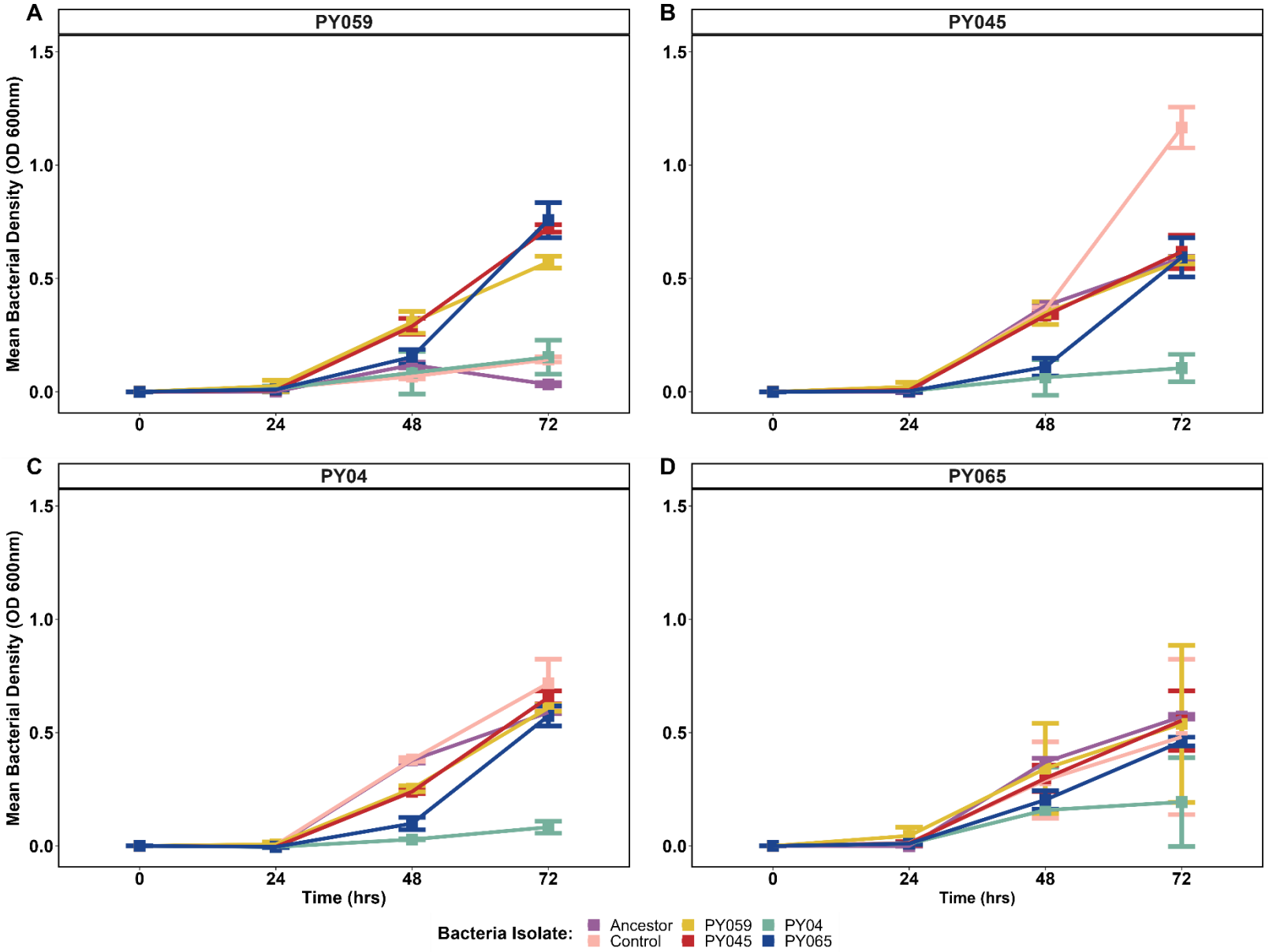
A
PY059
B
PY045
C
PY04
D
PY065
Mean Bacterial Density (OD 600nm)
1.5
1.0
0.5
0.0
0
24
48
72
Time (hrs)
Bacteria Isolate:
Ancestor
Control
PY059
PY045
PY04
PY065

Figure 3.5 – Phage infectivity and cross-resistance Assays. After successful re-isolation of *R. solanacearum* from timepoint 4 (12 days) of the coevolution experiment, the phage resistance of these isolates was reassessed. Isolates from across all phage treatments were challenged against the four ancestral phages to determine their resistance. A) Bacteria isolates challenged against PY059. B) Bacteria isolates challenged against PY045. C) Bacteria isolates challenged against PY04. D) Bacteria isolates challenged against PY065. The bacteria isolate "Ancestor" (purple) is ancestral *R. solanacearum* UW551 which coevolved UW551 originated from. The bacteria isolate "Control" (pink) is the control from the coevolution experiment, where UW551 was evolved alone, not in the presence of phages. This is included in the analysis to determine if phages were responsible for evolutionary adapations and no other factors.

3.4.5 Evidence of evolutionary trade-offs: competitive fitness and biofilm production

Evolutionary trade-offs are often associated with phage resistance, so we investigated to see if this occurred in the re-isolated *R. solanacearum*. We looked at two traits which could be traded-off with resistance, competitive fitness (growth) and biofilm production. We found that only one genotype appeared to experience costs in terms of competitive fitness (Figure 3.6). *R. solanacearum* that was isolated from the PY04 coevolution experiment had a significant reduction in growth compared to the ancestor and other genotypes (Figure 3.6B, One-way ANOVA$_{5,12}$, $F = 10.99$, $p < 0.001$, TUKEY: $p < 0.001$). The other phage resistant UW551 isolates had no competitive fitness costs suggesting that phage resistance incurred no evolutionary trade-offs in this trait (TUKEY: $p > 0.05$).

Biofilm production is an important virulence factor for *R. solanacearum* (Mori et al., 2016). Phage resistance can have significant impacts on biofilm production (Hosseinidoust et al., 2013, Wannasrichan et al., 2022). We found a significant difference in biofilm production between ancestral *R. solanacearum* and coevolved phage resistant UW551 (Figure 3.7, Krustal-Wallis: 15.225, $p = 0.009$). Overall, we found that biofilm production was significantly lower in phage resistant UW551 (Figure 3.7). Only one phage resistant UW551 PY059, had no significant difference compared with ancestral UW551, suggesting biofilm production was not associated with phage resistance here. There was also no significant difference between the control isolate (coevolved without phages) and the ancestor suggesting that detrimental impacts to biofilm production could be associated with phage resistance and a potential evolutionary trade-off. (Figure 3.7).

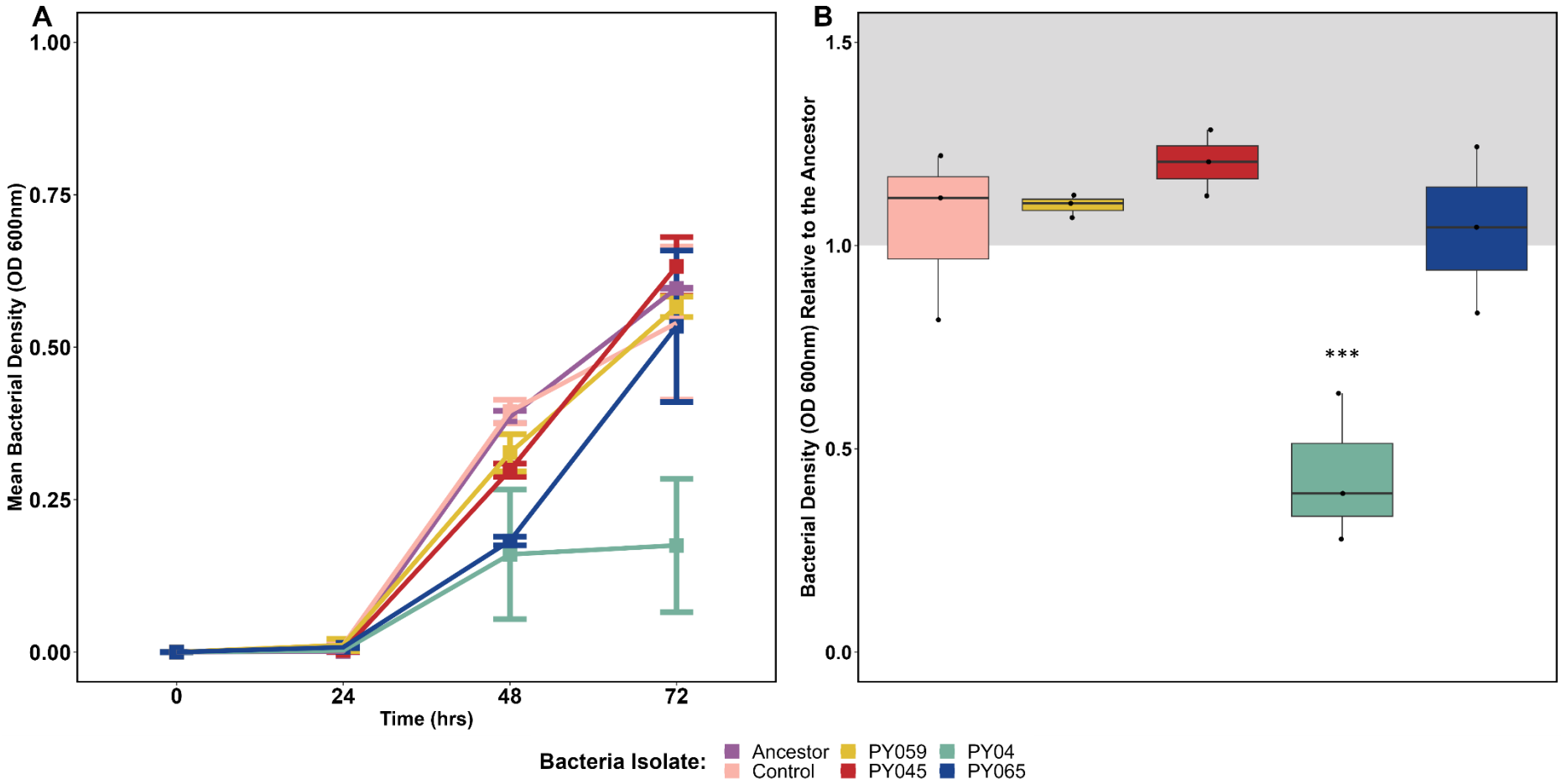

Figure 3.6 – Fitness Assay. Re-isolated *R. solanacearum* was assessed for their competitive fitness (growth). Each R. *solanacearum* isolate was grown alone without phages for 72 hours, taking point reads every 24 hours. A) Growth Curve, measured with OD reading (600nm) every 24 hours for 72 hours with standard deviation B) The bacterial density (OD 600nm) at 72 hours relative to the ancestor, maximum carrying capacity. The bacteria isolate "Control" (pink) is the control from the coevolution experiment, where UW551 was evolved alone, not in the presence of phages. This is included in the analysis to determine if phages were responsible for evolutionary adaptations and not other abiotic factors. One-Way ANOVA and post-hoc TUKEY was used to

determine the statistically significant differences bacteria isolates had on each other in terms of growth, focusing on the 72-hour timepoint (* $p < 0.05$, ** $p < 0.01$ and *** $p < 0.001$).

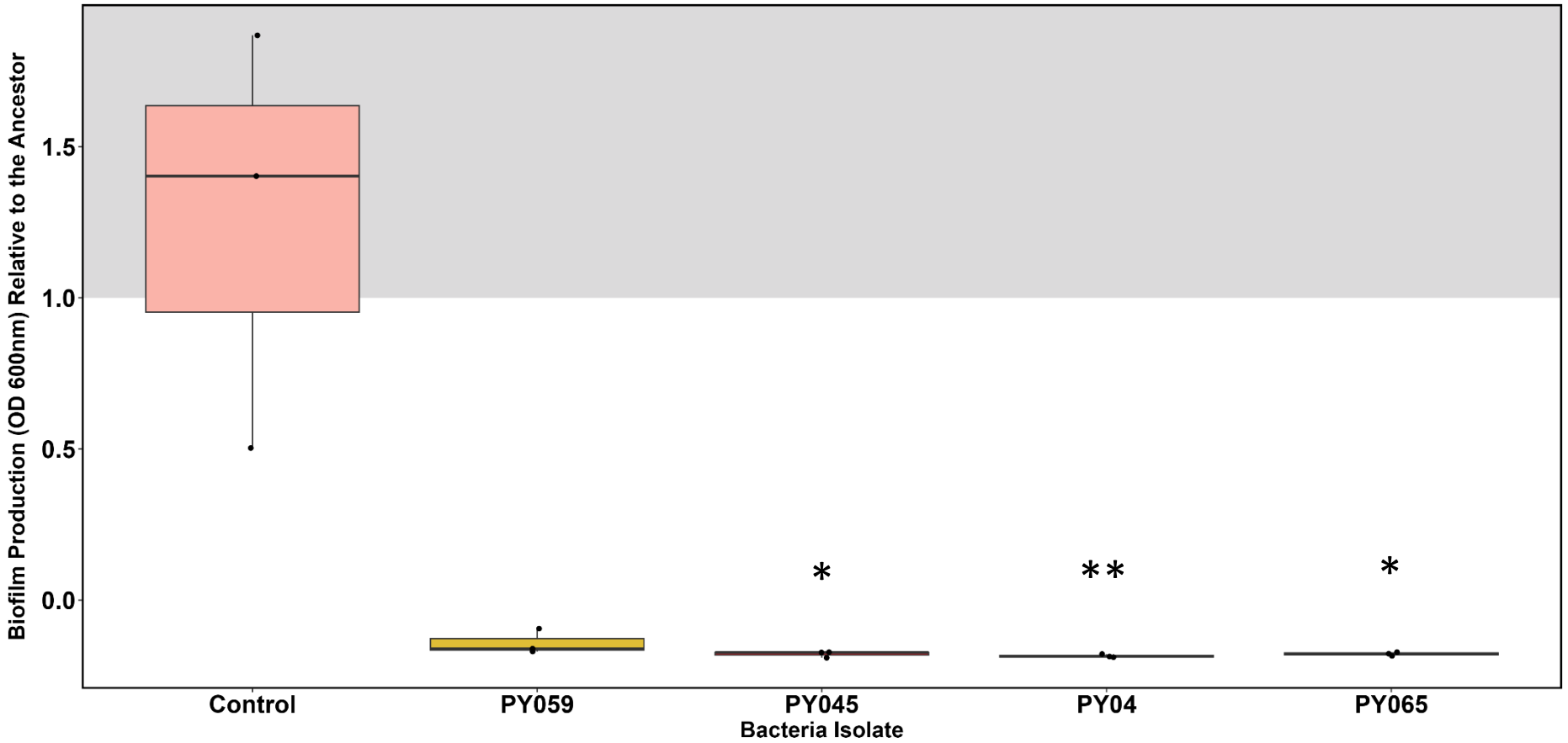
Biofilm Production (OD 600nm) Relative to the Ancestor
1.5
1.0
0.5
0.0
*
**
*
Control
PY059
PY045
PY04
PY065
Bacteria Isolate

Figure 3.7 – Biofilm production relative to the ancestor. Re-isolated coevolved *R. solanacearum* from each of the five coevolution experiment phage treatments was assessed for their ability to produce biofilm, a key virulence factor. Ancestor UW551 and coevolved UW551 were grown for 72 hours before their biofilm production was quantified. The bacteria isolate "Control" (pink) is the control from the coevolution experiment, where UW551 was evolved alone, not in the presence of phages. This is included in the analysis to determine if phages were responsible for evolutionary adaptations and not other abiotic factors. The Kruskal-Wallis test and the post hoc Dunn's test was used to confirm signficiant differences between treatments. The * symbol is used to highlight which treatments are significantly different to the ancestral *R. solanacearum* UW551 (* $p < 0.05$, ** $p < 0.01$, *** $p < 0.001$)

3.4.6 Genetic variation found in phage resistance *R. solanacearum*.

Due to the contamination, we only managed to send one clone from one replication from each coevolved treatment (from transfer 4, phage extinction) plus a control and ancestral UW551 for sequencing. All coevolved clones sent to sequencing were resistant to all phages. Through sequence analysis we found two proteins that had undergone genetic variation to the ancestor (Table 3.2). The first, was a protein identified as a glycosyltransferase where a nonsynonymous single nucleotide polymorphism (SNP) that resulted in the amino acid sequence changing from aspartic acid to alanine at amino acid position 276 (Table 3.2 and Figure 3.8 A-C). Interestingly, this SNP in this protein was found in three of the four coevolved UW551 treatments which could suggest that parallel evolution was occurring during the coevolution experiment. Analysis of the protein structure on SWISS-model has suggested that the structure of glycosyltransferase had changed very little as a result of the amino acid change (Figure 3.8 D-G). Further analysis with proteomics might help to understand how this amino acid change might affect the activity and function glycotransferase, especially if there was a subtle change within the active site of the protein. The second protein identified with genetic variation to the ancestral UW551 was non-ribosomal peptide synthase (Table 3.2). Again, there was evidence of parallel evolution where three of the four coevolved UW551 had the same SNP occurring in the same nucleotide position, 856 (Table 3.2). Interestingly, coevolved UW551 with PY065 had two more variant types within this protein (Table 3.2) A SNP at nucleotide position 825 and a "Complex" variation at 825 which is a combination of SNP and MNP (multiple nucleotide position). However, further analysis on the amino acid sequence revealed that all variant types found here were synonymous, resulting in no changes to the protein (Table 3.2).

Table 3.2 – Single nucleotide polymorphism (SNPS) or Multiple Nucleotide Polymorphism (MNP) identified in coevolved UW551 and the changes to the amino acid sequence that occurred. Proteins with amino acid changes have also been identified through BLAST and HHpred. Ancestral UW551 was sent to sequencing, used as a reference for the variant calling. Nucleotide position is the position of the variant counting from 1. Only 1 replicate from each coevolved treatment was sent to sequencing in part due to the contamination found in clones isolated from transfer 4. The variant type "complex" means a combination of SNP and MNP has occurred.

Coevolution Treatment	Nucleotide Position	The Variant Type	Nucleotide Change	Amino Acid Change	Protein of Interest identified with BLAST	Protein of Interest identified with HHpred
Control						
PY059	827	SNP (nonsynonymous)	A → C	Aspartic acid → Alanine	Glycosyltransferase [*Ralstonia solanacearum* species complex]	Transferase
	858	G → A (synonymous)			Non-ribosomal peptide synthetase [*Ralstonia solanacearum* species complex]	Non-ribosomal peptide synthetase
PY045	827	SNP (nonsynonymous)	A → C	Aspartic acid → Alanine	Glycosyltransferase [*Ralstonia solanacearum* species complex]	Transferase
	858	SNP (synonymous)	G → A		Non-ribosomal peptide synthetase [*Ralstonia solanacearum* species complex]	Non-ribosomal peptide synthetase

PY04	827	SNP (nonsynonymous)	A → C	Aspartic acid → Alanine	Glycosyltransferase [*Ralstonia solanacearum* species complex]	Transferase
PY065	817 825 858	SNP (synonymous) Complex (synonymous) SNP (synonymous)	A → G GGCC → CGCT G → A		Non-ribosomal peptide synthetase [*Ralstonia solanacearum* species complex]	Non-ribosomal peptide synthetase

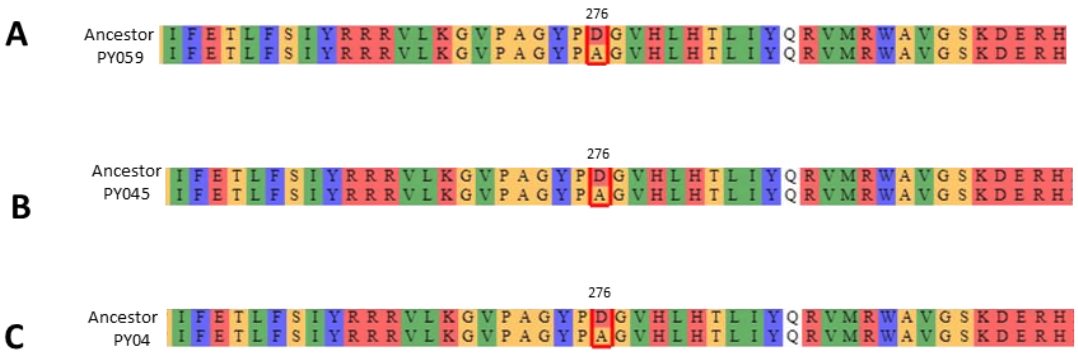
A
Ancestor
PY059
276
B
Ancestor
PY045
276
C
Ancestor
PY04
276

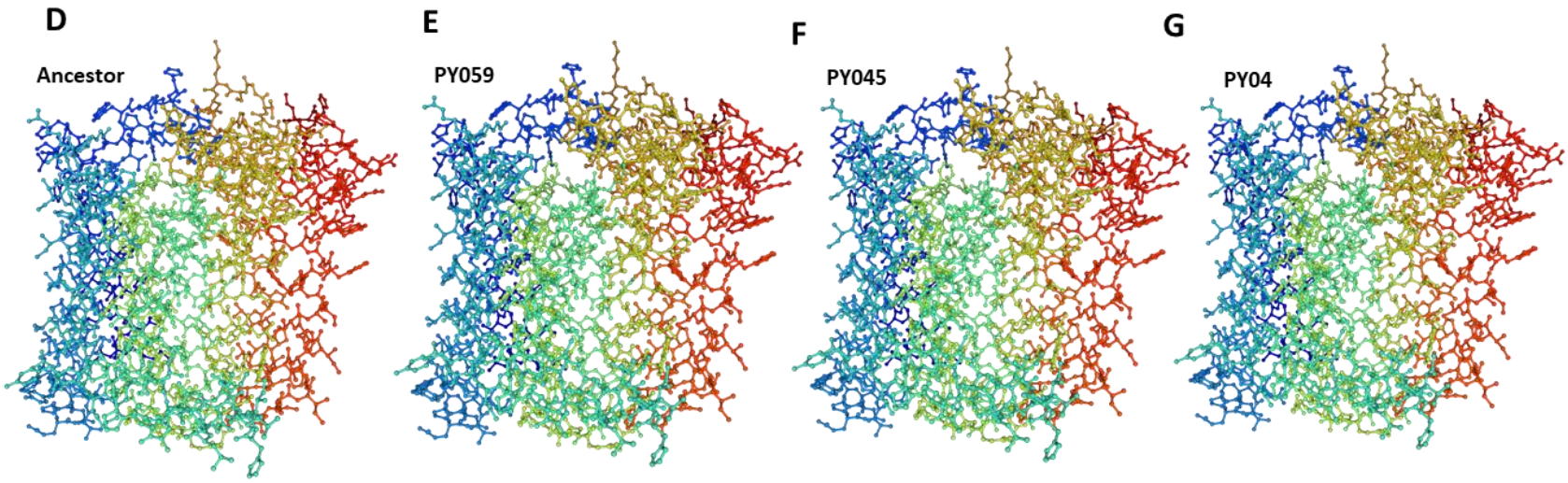
D
Ancestor
E
PY059
F
PY045
G
PY04

Figure 3.8 – The partial amino acid sequence and protein structure of a glycosyltransferase where genetic variation was identified in phage resistant *R. solanacearum* from two different phage treatments. A-C) The amino acid sequence of glycosyltransferase from both ancestral UW551 and coevolved UW551 aligned in clusteralΩ to highlight the nonsynonymous SNP that resulted in change of an amino acid from aspartic acid to glycine at amino acid sequence position 276 of the amino acid sequence (highlighted in red). A) Amino acid sequences of ancestral UW551 and coevolved UW551 with PY059. B) Amino acid sequences of ancestral UW551 and coevolved UW551 with PY045. C) Amino acid sequences of ancestral UW551 and coevolved UW551 with PY04. D-G protein models built in the Swiss-model with the aim to understand the structure of the protein, identified as glycosyltransferase of *Ralstonia solanacearum* species complex. D) The ancestral protein, the amino acid sequence of the protein was used from ancestral UW551 to build the model. E) The protein model built from the amino acid sequence of coevolved UW551 with PY059 used to identify if any structural changes have occurred as result of the SNP. F) The protein model built from the amino acid sequence of coevolved UW551 with PY045 used to identify if any structural changes have occurred as result of the SNP. G) The protein model built from the amino acid sequence of coevolved UW551 with PY04 used to identify if any structural changes have occurred as result of the SNP.

3.5 Discussion

We conducted a coevolution experiment to understand the coevolutionary dynamics between phages and *R. solanacearum* and to determine if arms race dynamics or fluctuating selection dynamics or both is observed. We also wanted to determine if any trade-offs in resistant *R. solanacearum* existed and understand the genetic mechanisms behind evolved resistance. We find that the interactions between *R. solanacearum* and phages is highly asymmetrical leading to phage extinctions due to a rapid evolution of phage resistance in *R. solanacearum*. We also observed this asymmetry in Chapter 2. Cross-resistance was also observed. We found evidence of evolutionary trade-offs between resistance and growth as well as biofilm formation. Genomic analyses of phage resistant *R. solanacearum* showed genetic variation in two proteins; Undecaprenyl-phosphate alpha-N-acetylglucosaminyl 1-phosphate transferase and Tyrocidine synthase 3, involved in lipopolysaccharide (LPS) and antibiotic synthesis respectively, supporting a strong case for parallel evolution.

The population dynamics of both phage and *R. solanacearum* UW551 suggested that asymmetrical evolution was occurring. For the phages, we were unable to detect phages from any of the treatments after 4 transfers suggesting an extinction event. While for the population dynamics of *R. solanacearum*, we observed high abundance for *R. solanacearum* in treatments with PY059 or PY045 but which remained undetectable for treatments with PY04 and PY065 in the first few transfers. From transfer 4, populations recovered, or retained high densities, following similar dynamics to the control (no phage) treatment (Supplementary Figure 3.2). The extinction event of phages and the return to high abundances of *R. solanacearum* was likely driven by the rapid evolution of resistance in *R. solanacearum*. Numerous coevolution experiments have often reported that the system is in favour of the bacteria where bacteria evolve resistance rapidly (Burmeister et al., 2023, Brockhurst et al., 2005, Moulton-Brown and Friman, 2018). Interestingly, phage extinction events were observed with *Pseudomonas fluorescens* (isolate SBW25) and its phage ϕ2 due to genetic bottlenecks. Bottlenecks in their coevolution experiments resulted in the loss of phage sensitive bacteria (Hesse and Buckling, 2016). It is possible that our transfers could

have had bottlenecks in the bacteria population, resulting in loss of sensitive bacteria and driving our phages to extinction.

Bacteria use an arsenal of strategies to acquire resistance to phages (Hampton et al., 2020). Receptor modification is often observed in coevolution experiments, where resistance has rapidly evolved (Jurado et al., 2022, Filippov et al., 2011). In *R. solanacearum* phage resistance to RSψP29 was a result of receptor modification. The O-antigen (receptor) was masked due increased phospholipid production (Hong et al., 2014). Genetic constraints on protein properties in phages can make it difficult for them to adapt to modified or new receptors (Koskella and Brockhurst, 2014, Hall et al., 2013). Due to the rapid evolution of phage resistance in *R. solanacearum* UW551 and phage extinction event in our coevolution. We first decided to check that if there was any evidence of coevolution between phages and *R. solanacearum* before the extinction of phages. We found little evidence, only PY065 had a slightly increased infectivity before the extinction. This rapid rise in resistance and extinction of phages indicates that asymmetrical evolution was occurring (Koskella and Brockhurst, 2014). Phages failed to adapt, perhaps due to receptor modification (Koskella and Brockhurst, 2014)

We identified genetic variation in two proteins: The genotypic changes that occurred in these two proteins were found in all four of the coevolved phage treatments, there is an indication that parallel evolution was occurring (Hall et al., 2013).

The protein belonging to the superfamily of glycosyltransferase is associated with LPS synthesis (Amer and Valvano, 2001). LPS play critical roles in pathogenicity of *R. solanacearum* and are known to be receptors for phages (Kutschera and Ranf, 2019). Defects in the protein involved in the synthesis of LPS, could change the composition and abundance of LSP, resulting in phage resistance, as receptor sites are reduced or modified. Phage resistant *R. solanacearum* resulted in LPS defects which failed to cause disease in tobacco plants (Li et al., 2014a). Also, mutations in other LPS-related proteins can lead to defects in biofilm formation. This could also be applied to the mutation found in our glycosyltransferase, as we also saw a significant decrease in biofilm production (Yang et al., 2013). Interestingly, three of the four coevolved UW551 had SNP in the same position which conferred the exact same nucleotide and amino acid sequence changes. This suggests that parallel evolution is involved, independent populations of *R. solanacearum* evolving the

same phenotypic and genotypic traits in response to phage predation (Hall et al., 2013). Only PY04 appeared to have experienced a fitness cost in competitive fitness . (Lenski, 1988).

Surprisingly, we found genetic variation on non-ribosomal peptide synthetase which is involved in the biosynthesis of the antibiotics , a secondary metabolite (Kleinkauf and von Dohren, 1990) . Changes to the biosynthetic pathways of secondary metabolites could be in response to phage selection pressures, especially if production of antibiotics is increased. Secondary metabolites can confer phage resistance by providing chemical protection (Kronheim et al., 2018). However, further experiments such as whether antibiotics can protect *R. solanacearum* from phage infection would be required, it would be critical to identify the antibiotic produced. Analysis on the amino acid sequence on this non-ribosomal peptide synthetase suggested that the nucleotide sequence changes are synonymous. However, there is increasing evidence that synonymous nucleotide changes can affect the protein but further work would be required to understand the effects of synonymous nucleotide changes in *R. solanacearum* (Shen et al., 2022).

We decided to explore the possibility that phage resistance could be costly (evolutionary trade-offs) to the re-isolated phage resistant genotypes of UW551. Trade-offs between volatile organic compounds and virulence was present in *R. solanacearum*, resulting in significant reductions in pathogenicity *in planta* (Wang et al., 2023a). It is possible that phages could have similar effects. Previously studies observed that trade-offs with phage resistance in *R. solanacearum*, resulted in increased sensitivity to antimicrobials produced by its competitor *Bacillus amyloiquefaciens* (Wang et al., 2017). We explored two traits that could be impacted by phage resistance, growth rates and biofilm production (Burmeister and Turner, 2020). If trade-offs are present in these traits, there could be advantages for using phages as biocontrols. Overall, we found evidence of evolutionary trade-offs in phage resistant *R. solanacearum* but further experiments *in planta* could help us to understand the effects these evolutionary trade-offs have on pathogenicity.

Only one isolate appeared to have an evolutionary trade-off with growth rate, PY04. UW551 coevolved with PY04 growth rate was significantly reduced. For *R. solanacearum*, significantly reduced growth rates are associated with reduced pathogenicity in tomato plants (Macho et al., 2010). Other phage resistant genotypes did not experience this trade-off. Biofilms are critical to pathogenicity, protecting plant pathogenic bacteria abiotic and biotic stresses within their environment and host (Mina et al., 2019). In *R. solanacearum*, biofilms are formed during infection, in the xylem, contributing to spread and virulence (Minh Tran et al., 2016, Lowe-Power et al., 2018). We saw a significant reduction in biofilm production in all phages resistant genotypes of *R. solanacearum* UW551. This could have significant repercussions for pathogenicity in *R. solanacearum*. Abnormalities in biofilms in *R. solanacearum* caused reduced virulence in tomato plants (Minh Tran et al., 2016). Reduction in biofilm can make *R. solanacearum* and other plant pathogenic bacteria vulnerable to other controls, such as antibiotics (Burmeister and Turner, 2020). However, further experiments will need to be conducted to understand their vulnerability to other controls.

The contamination added complications to the experiments. Although, we checked the populations, we could never be certain that contamination was not present, despite streaking of the populations onto the plate. To be certain we would have to do PCR and sequencing, using *Staphylococcus* specific primers (Martineau et al., 2001). The presence of *Staphylococcus* creates an unknown variable in the experiments. What we do know is that *R. solanacearum* was present at the time of phage extinction and was highly resistant.

Conclusion

Despite complications due to contamination, we were still able to recover phage resistant *R. solanacearum*. This coincided with the lack of infectivity changes with phages, suggesting an asymmetrical coevolution, with the bacteria winning. Evolved UW551 was highly resistant to all phages. We also found common mutations in the same proteins, suggesting parallel evolution. Taken together both suggest that phages are utilising similar mechanisms. Did we find evidence of evolutionary trade-offs which could have profound implications for virulence and pathogenicity in *R. solanacearum*. In the development of biocontrols, asymmetrical evolution could potentially be an area of concern considering how fast resistance to phages evolved. However, despite evidence of evolutionary trade-offs in virulence, phages still remain a promising biocontrol against *R. solanacearum*.

3.6 Supplementary Tables and Figures

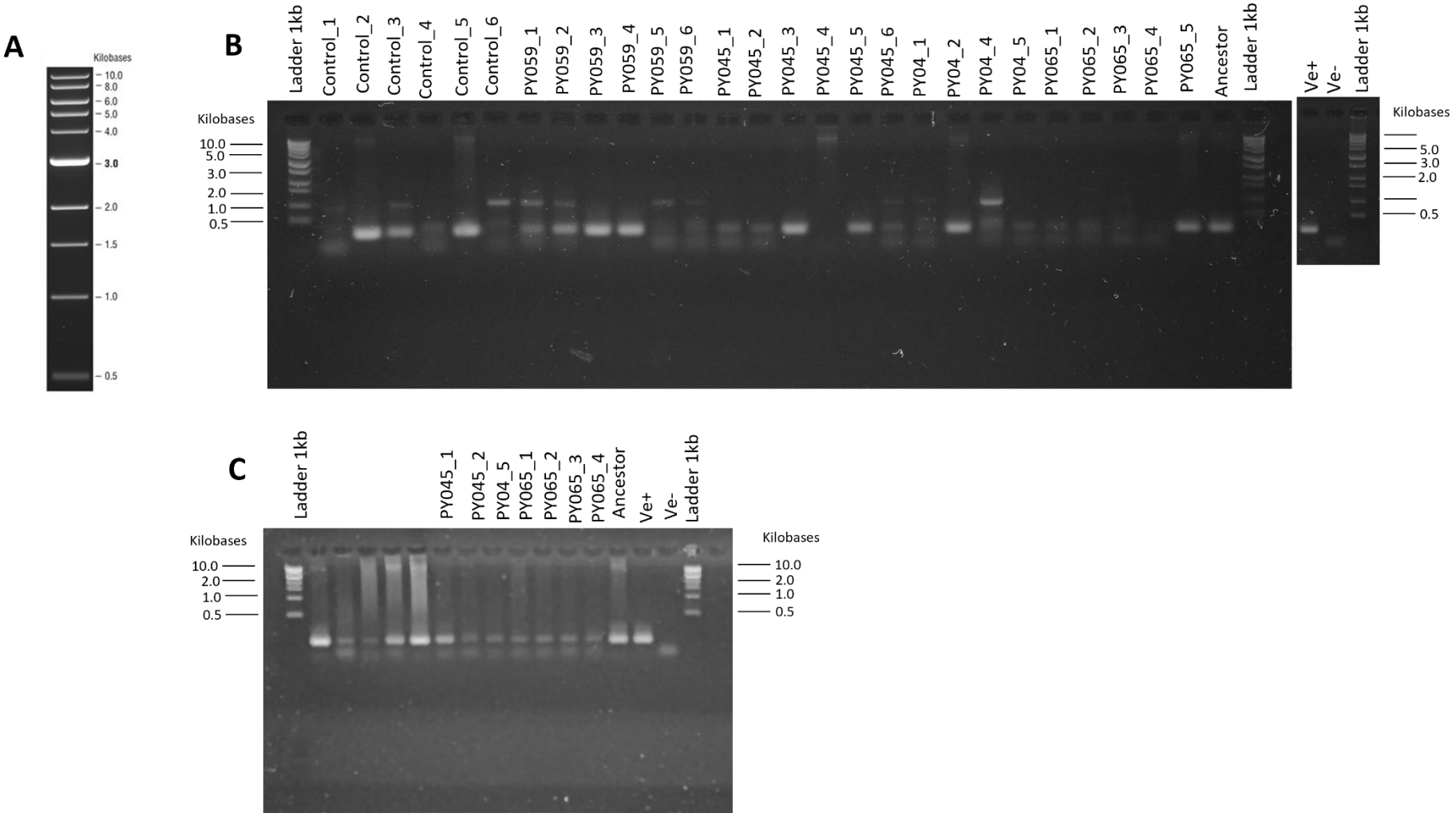

Supplementary Figure 3.1 - Gel images of ancestor and coevolved *R. solanacearum* UW551, used to determine if we had successfully re-isolated coevolved UW551 and successfully extracted its DNA. Isolates were from timepoint 4 where phages were confirmed extinct. We used the positive control (ve+), GMI1000, to determine if we were successful in re-isolating *R. solanacearum* UW551. Bands that aligned with GMI1000, were sent for sequencing and used in further experiments. Ones that did not were discarded. A) Additional guide to the 10kb ladder, available at https://www.neb.com/en-gb/products/n0552-quick-load-purple-1-kb-dna-ladder#Product%20Inproduction. B) The first gel, all isolates from the coevolved experiment, "_1" represents a replicate. C) The second gel isolates we thought were UW551 but did not reach the threshold for MicrobesNG, DNA was reextracted and we tested again.

Chapter 4

Competition between phages within phage combinations and resistance evolution can reduce efficacy of phages.

4.1 Abstract

Rapid evolution of bacteriophage (phage) resistance in bacteria is a potential obstacle for biocontrols as it could potentially reduce the efficacy of the phage in use. Resistance to a phage can be rapid and in some cases without much cost to bacteria. To mitigate this, using multiple phages in combination has often been purposed. Phage combinations often suppress bacteria to greater extents and reduce the risk of resistance evolution. Even if resistance was to evolve, it is often more costly, resulting in evolutionary trade-offs in numerous traits. For pathogenic bacteria, this could be traits related to virulence, severely impacting its pathogenicity. Here, we use eight phages in up to three phage combinations to test whether we can suppress resistance evolution in the destructive plant pathogen *Ralstonia solanacearum*. Overall, we identified a number of highly effective phages but saw little to no significant improvement in combinations, with possible explanations being competition between phages or evolutionary effects in *R. solanacearum*. We found evidence of parallel evolution as we found within different coevolved *R. solanacearum* with the same mutations, as well as potential hypermutators. Evolutionary trade-offs were also observed in competitive fitness (growth) and EPS production.

4.2 Introduction

The constant selection pressure of phages has led bacteria to evolve an immense diversity of strategies to prevent bacteriophage (phage) infection (Georjon and Bernheim, 2023, Labrie et al., 2010). Receptor (surface) modification and rapid acquisition of phage defence mechanisms is how bacteria protect themselves against phages (Hampton et al., 2020). Phage resistance is a potential obstacle for phage biocontrol and phage therapies because it can render the phage useless/inefficient (Oechslin, 2018). Although, phages themselves can coevolve and overcome phage resistance by evolving to be more infective, sometimes, it is not enough, resulting in phage extinctions (Burmeister et al., 2023). To mitigate the challenges of phage resistance in bacteria, use of phage cocktails or combinations have often been purposed (Chan et al., 2013).

Utilising more than one phage can increase the infectivity range of the phage biocontrol, while different characteristics of phages, such as receptor specificity, can be synergised in phage combinations, often resulting in a wider range of activities (Loc-Carrillo and Abedon, 2011). For example, three phages (Va1, Va2 and Va3) that use three different infection strategies could be used to create an effective combination that greatly suppresses phage resistance in *Vibrio alginolyticus* (Li et al., 2022).

However, use of phages in combinations can be complicated and can result in reduced efficacy. Phage-phage interactions are complex and have the potential to become detrimental if competition should arise (Trinh et al., 2017, Molina et al., 2022). Although poorly understood, competition between phages have been reported with consequences of reduced efficacy within the combination rather than the individual (Niu et al., 2021).

Ralstonia solanacearum species complex (RSSC), a plant pathogen that is the causative agent of bacterial wilt in over 200 plant species, responsible for extensive agricultural and economic damage (Castillo and Greenberg, 2007, Mansfield et al., 2012, Bragard et al., 2019). Phages have been purposed as potential biocontrol against RSSC (Ahmed et al., 2022). Numerous studies have highlighted the potential phages have for biocontrol against *R. solanacearum*. In Spain, lytic phages showed great potential, as they suppressed the growth of *R. solanacearum* (Álvarez et al., 2019). Phage combinations have shown potential as disease incidence was reduced by up to 80% in greenhouse experiments with *R. solanacearum* and phage combinations (Wang et al., 2019).

R. solanacearum is no different from other bacteria, it can readily and easily evolve resistance to phages and has a diverse range of anti-phage defence mechanisms that can hinder single phage use as a biocontrol (Holtappels et al., 2021, Castillo et al., 2020). Within this thesis, phage resistance in *R. solanacearum* has often been rapid, resulting in extinctions of phages (Chapter 3). Even pre-adapted phages ("trained", Chapter 2) have struggled to overcome resistance when exposed to *R. solanacearum*. Likewise, resistance to phages within *R. solanacearum* was also evident in less than two days (Fujiwara et al., 2011).

To study whether phage combinations can suppress phage resistance evolution, we conducted a 15-day combination experiment with mono- and combination cultures of eight phages from our collection against *R. solanacearum* UW551, using phages from the UK (Table 4.1). Alongside, phage resistance prevention, we also wanted to determine the morphological changes and genetic mechanisms behind phage resistance through microscopy and whole-genome sequencing, respectively, as well as to understand the evolutionary trade-offs within phage resistance *R. solanacearum* UW551 and how costly it is. We hypothesised that resistance would evolve to higher levels and more readily in monocultures rather than combination cultures. We also hypothesised that resistance within combination cultures would come at a higher cost to fitness with *R. solanacearum*.

Surprisingly, we found that individual phage cultures were much more effective at suppressing *R. solanacearum* than in combination, suggesting possible competition within phage combinations. Again, it was found that *R. solanacearum* could rapidly evolve resistance to phages and cross-resistance was commonly observed. However, we found evidence of evolutionary trade-offs between resistance and two other traits: competitive fitness (growth) and extracellular polysaccharide (EPS) production, which is an important trait for causing infection inside the plants (Denny and Baek, 1991). The underlying molecular mechanisms of phage resistance with *R. solanacearum* were variable. We found genetic variation in four genes encoding the following proteins: glucose-1-phosphate thymidylyltransferase, non-ribosomal peptide synthase, putative TorF family porin and LysR family transcriptional regulator. We also found that hypermutators evolved in the overall presence of phages.

4.3 Methods and Materials

4.3.1 Strains and Phage Isolates.

Strain UW551 (NCPPB 4662) belonging to the species *Ralstonia solanacearum* was chosen for this experiment. It was originally isolated in the USA in 2003 from garden geranium (*Pelargonium hortorum*). See 2.3.1 Strains and Phage Isolates for the protocol. The Colony Forming Unit/ml (CFU/ml) was calculated at a 0.4OD, UW551 had a CFU/ml of $3x10^9$ (SPECTROstar Nano).

We picked 8 phages from our collection known to infect UW551 for the phage combination experiment (Table 4.1). We picked these phages based on year of isolation, geographical location and phylogenetic data (provided by Dr Bryden Fields and unavailable) with the aim of having a diverse collection of phages. Chinese phages, PY038 and PY047 were isolated in different years from tomato fields in Nanjing, China. While UK phages were isolated in different years and different rivers in the UK. Two UK phages, PY022 and PY023, although isolated from the same river, New Bedford River, PY023 was isolated on the confluence of the New Bedford River and Great Ouse in Cambridgeshire approximately 32km away from PY022. Phages had varying morphologies, including viruses that could be characterised as Podoviridae and Myoviridae. Before the combination experiment, each phage was enriched and their abundance calculated as PFU/ml, see 2.3.5 Phage Enrichment and 2.3.3 Quantification of Phage Densities.

Table 4.1 – The collection of phage isolates used in the combination experiment.

Isolate	Year of Isolation	Location	Morphology	Initial Titration
PY038	2020	China	Podoviridae	$3x10^7$
PY047	2018	China	Unknown	$1x10^{10}$
PY022	2020	New Bedford River, UK	Podoviridae	$1x10^9$
PY019	2019	River Thames, UK	Podoviridae	$1x10^9$
PY063	2021	River Trent, UK	Myoviridae	$2x10^6$
PY021	2020	River Avon, UK	Podoviridae	$1x10^8$
PY023	2020	New Bedford River, UK	Podoviridae	$4x10^9$
PY066	2021	River Jubilee, UK	Podoviridae	$2x10^9$

4.3.2 Quantification of Bacteria Densities.

Bacterial densities were calculated as Colony Forming Unit/ml (CFU/ml) see 3.3.5 Quantification of Bacteria Densities.

4.3.3 Phage Combination Experiment

A maximum of 3 phages were used in combination for this experiment (Table 4.2). Into a 96-well plate we added 176µl of CPG followed by 12µl of UW551 and 12µl of phage (in triplicate). Volumes of phages were adjusted depending on the number of phages in the combination; 12µl for one phage treatment, 6µl of each for two phage treatments and 4µl of each for three phage treatments. For the control, we added 12µl of sterilised deionised water in place of phages. Plates were then incubated at +28^{o}C for 72 hours (Figure 4.1). After the 72 hours, optical density reads (OD 600nm) were taken (Tecan sunrise) and 24µl of culture was transferred into another plate with 176µl of CPG media. This was repeated 5 times (for 15 days). At the end of the 5 transfers, final OD reads were taken and resistant UW551 was isolated (see below). The multiplicity of infection (MOI) was set to 1 at the beginning of this experiment (~10^6 cells to ~10^6 viral particles)

Table 4.2 – All phage combinations used in this experiment. We used 8 different phage isolates and built various combinations with these phage isolates, a maximum of 3 phages were used in the most complex combination. Combinations highlighted in red denote successfully isolated coevolved *R. solanacearum* UW551 at the end of the combination experiment. Any that are not highlighted in red, no coevolved UW551 was isolated from.

Phage Combinations	
UW551 alone	PY038 + PY022 + PY066
PY038 alone	PY038 + PY019 + PY021
PY047 alone	PY038 + PY019 + PY023
PY022 alone	PY038 + PY019 + PY066
PY019 alone	PY038 + PY063 + PY021
PY063 alone	PY038 + PY063 + PY023
PY021 alone	PY038 + PY063 + PY066
PY023 alone	PY038 + PY021 + PY063
PY066 alone	PY038 + PY021 + PY066
PY038 + PY047	PY038 + PY023 + PY066
PY038 + PY022	PY047 + PY022 + PY019
PY038 + PY019	PY047 + PY022 + PY063
PY038 + PY021	PY047 + PY022 + PY021
PY038 + PY063	PY047 + PY022 + PY023
PY038 + PY023	PY047 + PY022 + PY066
PY038 + PY066	PY047 + PY019 + PY063
PY047 + PY022	PY047 + PY019 + PY021
PY047 + PY019	PY047 + PY019 + PY023
PY047 + PY063	PY047 + PY019 + PY066
PY047 + PY021	PY047 + PY063 + PY021
PY047 + PY023	PY047 + PY063 + PY023

Table 4.2 – Continued from preceding page

PY047 + PY066	PY047 + PY063 + PY066
PY022 + PY019	PY047 + PY021 + PY023
PY022 + PY063	PY047 + PY021 + PY066
PY022 + PY021	PY047 + PY023 + PY066
PY022 + PY023	PY022 + PY019 + PY063
PY022 + PY066	PY022 + PY019 + PY021
PY019 + PY063	PY022 + PY019 + PY023
PY019 + PY021	PY022 + PY019 + PY066
PY019 + PY023	PY022 + PY063 + PY021
PY019 + PY066	PY022 + PY063 + PY023
PY063 + PY021	PY022 + PY063 + PY066
PY063 + PY023	PY022 + PY021 + PY023
PY063 + PY066	PY022 + PY021 + PY066
PY021 + PY023	PY022 + PY023 + PY066
PY021 + PY066	PY019 + PY063 + PY021
PY023 + PY066	PY019 + PY063 + PY023
PY038 + PY047 + PY022	PY019 + PY063 + PY066
PY038 + PY047 + PY019	PY019 + PY021 + PY023
PY038 + PY047 + PY063	PY019 + PY021 + PY066
PY038 + PY047 + PY021	PY019 + PY023 + PY066
PY038 + PY047 + PY023	PY063 + PY021 + PY023
PY038 + PY047 + PY066	PY063 + PY021 + PY066
PY038 + PY022 + PY019	PY063 + PY023 + PY066
PY038 + PY022 + PY063	

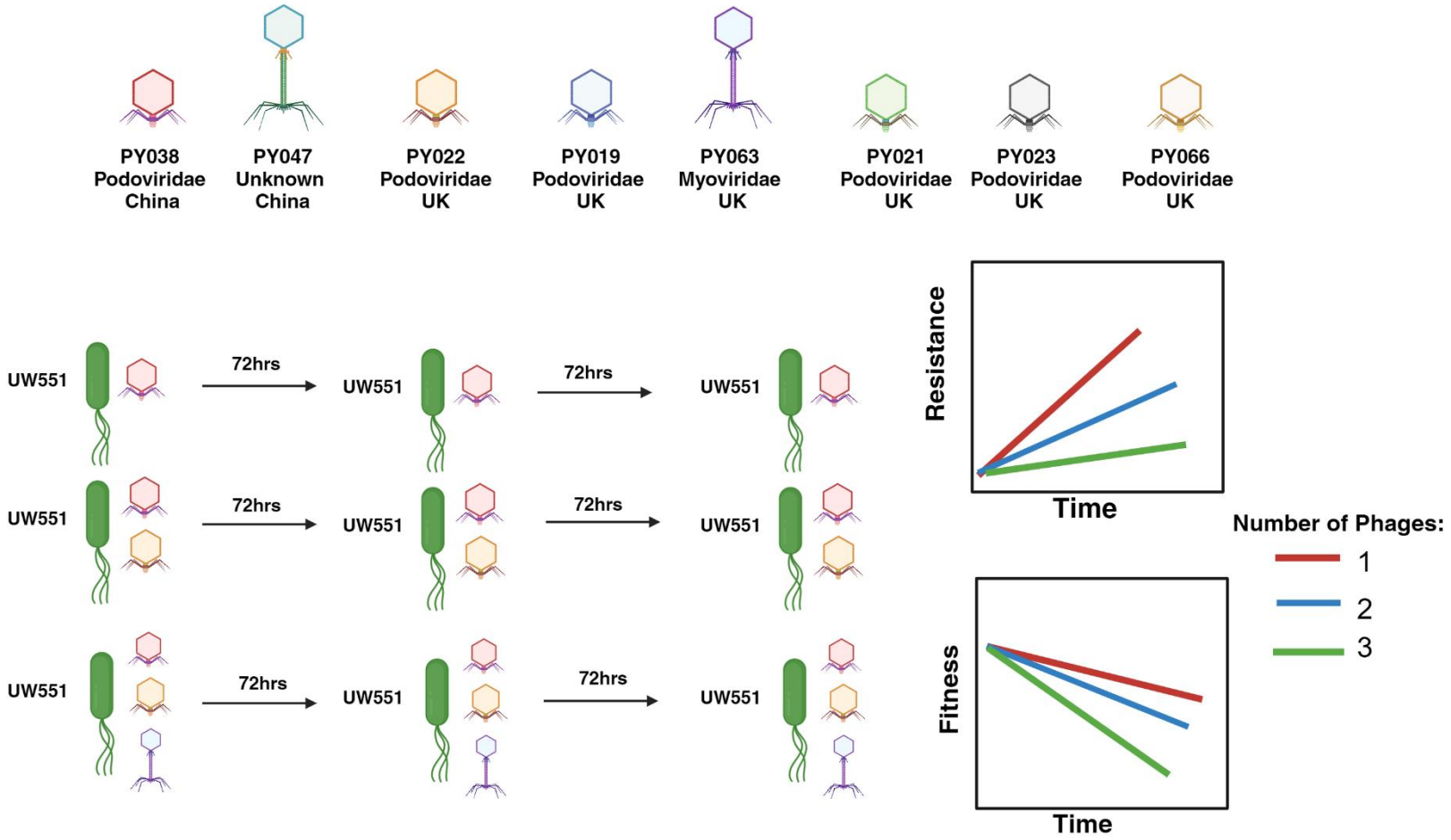
PY038
Podoviridae
China
PY047
Unknown
China
PY022
Podoviridae
UK
PY019
Podoviridae
UK
PY063
Myoviridae
UK
PY021
Podoviridae
UK
PY023
Podoviridae
UK
PY066
Podoviridae
UK
UW551
72hrs
UW551
72hrs
UW551
UW551
72hrs
UW551
72hrs
UW551
UW551
72hrs
UW551
72hrs
UW551
Resistance
Time
Number of Phages:
1
2
3
Fitness
Time

Figure 4.1 – Experimental design of the combination experiment. 8 phages from various sources were incubated in mono- or in combination with *R. solanacearum* UW551 (maximum of 3 phages). We hypothesised that resistance would evolve to higher levels and more readily in monocultures rather than combination cultures. We also hypothesised that resistance within combination cultures would come at a higher cost to fitness with *R. solanacearum*. Note, morphologies of phages within the diagram are not reflective of their true morphologies. Made in Biorender.com.

4.3.4 Isolation of *Ralstonia solanacearum* clones

At the end of the combination experiment we aimed to isolate phage resistance *R. solanacearum* from various combinations. From the final plate, we spotted 2µl of each culture onto a CPG plate (Boekel pin replicator) and left to incubated at +28^{o}C for 48 hours. After the 48 hours, combinations that had colonies were recorded and re-streaked onto circular CPG plates and incubated as described above. A single colony was taken and placed in 25ml of CPG for 72 hours at +28^{o}C (72 hours were used as some genotypes were slow growing). After the 72 hours, clones were cryopreserved (in triplicate) in 20% glycerol (600µl of sample to 400µl of glycerol). We also calculated the CFU/ml at 72 hours for each genotype (see 3.3.5 Quantification of Bacteria Densities .

4.3.5 Microscopy

We decided to use light microscopy to see if any phenotypic changes had occurred. Ancestral UW551 and resistant UW551 was taken from cryo-stocks and placed in 25ml of CPG for 120 hours (allowing *R. solanacearum* to reach the stationary stage). Secure-Seal^{TM} Spacer (ThermoFisher) were used to isolate the samples to the microscope slides. The spacer was firmly placed onto the slide and small amount of agarose (0.7%) into the well and left to set. 5µl of sample was added to the agarose gel and a coverslip was placed on top, sealing the sample inside. The sample was viewed under the microscope at 100x objective with oil emulsion. Photographs of samples were also taken.

4.3.6 Phage Infectivity and Cross-Resistance Assays

We challenged all surviving coevolved *R.* solanacearum UW551 to all 8 phages individually, to test the level of resistance and also test if cross-resistance was observed, see 3.3.9 Phage Infectivity and Cross-Resistance Assays for protocol.

4.3.7 Competitive Fitness (Growth) Assays

To investigate evolutionary trade-offs that might have occurred when phage resistance evolved in UW551, we quantified changes in different indicators of fitness. We used growth assays to determine the competitive fitness of ancestral and coevolved UW551. The protocol from 3.3.10 Fitness Assay was used.

4.3.8 Extracellular polysaccharide (EPS) assays

Extracellular polysaccharide (EPS) is an important virulence factor of *R. solanacearum* and could experience evolutionary trade-offs as phage resistance evolves. We investigated EPS production (measuring N-acetyl galactosamine µg) on the ancestral and phage resistant UW551 to see if any trade-offs had occurred. UW551 was grown in 20ml in CPG at +28^{o}C, shaking 100rpm, for 120 hours. 120 hours was used to exhaust the glucose out of the media before EPS analysis.

EPS was extracted by first filtering the culture through 0.22µm filters into eppendorfs. Then, 0.2ml supernatant was added to 0.004ml 5M NaCl and 0.8ml acetone. The mixture was mixed by briefly vortexing and placed overnight at +4^{o}C. The samples were then centrifuged at 14,000 rpm (maximum speed) for 20 minutes at +4^{o}C. The supernatant was discarded and the eppendorfs were left inverted to drain the pellet (around 15 minutes). To the pellet, 0.2ml deionised water was added. Once the pellet had dissolved, samples were placed in a dry heat bath, heated to +65^{o}C for 10 minutes. Samples were then vortexed and centrifuged at 13,000 rpm at +4^{o}C. The supernatant was collected.

To quantify EPS, we first created standards (Table 4.3). To the standards and the samples (200µl), 150µl of HCl (37%) was added and enough deionised water to make 600µl in total. The samples and standards were mixed by vortexing. They were transferred to a dry bath heater and incubated at +115^{o}C for 30 minutes, covered with aluminium foil. Samples and standards were removed and left to cool to room temperature. The samples and standards were centrifuge to 6000 rpm for 10 seconds. 400µl of 2M Na2CO3 solution was added, carefully. 500µl of freshly made 2% acetyl acetone solution in 1.5M Na2CO3 was added. Samples and standards were vortexed and left with their lids open to remove CO_2. Samples and standards were heated at +100^{o}C for 20 minutes. Samples and standards were left to cool to room temperature, and then centrifuged for 10 seconds at 6000 rpm. Samples and standards were transferred to 15ml falcon tubes, where 1000µl of 99.8% ethanol was added

and mixed well. This was followed by 500µl Erlich's reagent solution and mixed gently. Samples and standards were left to stand for around 30 minutes in the dark (covered in aluminium foil). The optical density (OD 530nm) was taken (BMG-labtech Spectrostar Nano).

Table 4.3 – The standards used to quantify N-acetyl-galactosamine production (durrogate for EPS production). The grey standard values were used as blanks. N-acetyl-galactosamine solution was created by dissolving 50mg in 100ml of water.

N-acetyl-galactosamine (µg)	Volume N-acetyl-galactosamine solution (µl)	Volume deionised water (µl)
0	0	450
5	10	440
10	20	430
20	40	410

4.3.9 Bacterial Genomics

Whole genome sequencing was conducted on ancestral and coevolved UW551, following the protocol 3.3.12 and variant calling analysis was conducted using the pipeline from 2.3.9 Phage Genomics.

4.3.10 Statistical Analysis

Statistical analysis and data visualisation was performed using R statistical software, version 4.2.3 (Team, 2023). Figures were produced using the ggplot2 package (Wickham, 2016). For statistical analysis of phage infectivity assays resistance and cross-resistance of the 12 isolated clones , we used Kruskal-Wallis Tests followed by pairwise Wilcoxon test with Benjamini Hochberg (BH) p value adjustment, using functions from stats R package (Team, 2023). For the phage infectivity assays, we normalised the data against the 0-hour timepoint. For evolutionary trade-offs, Kruskal-Wallis test was conducted on competitive fitness (growth) on bacterial densities at 72 hours followed by post hoc analysis with Dunn's test, using functions from stats R package (ANOVA) and FSA package (Dunn's test). Data was normalised against 0-hour timepoint. For EPS production, we performed statistical analysis with One-way ANOVA using the function from stats R package, followed by post hoc analysis with Duncan's test from the DescTool package (Team, 2023, Signorell, 2022)

4.4 Results

4.4.1 Phages were effective at suppressing the growth of *R. solanacearum* in single and combination treatments, but resistance still evolved and competition between phages emerged.

Overall, phages were highly effective at suppressing the growth of *R. solanacearum* (Figure 4.2). There was pathogen growth suppression from phages in both mono and combination treatments, suggesting that phages had high infectivity (Figure 4.2). However, resistance began to evolve in treatments towards the end of the experiment in terms of increasing bacterial densities (Figure 4.2 and Supplementary Figure 4.2).

Surprisingly, we found that resistance was evolving more often in combination treatments rather than individual phage treatments (Figure 4.2). However, in some cases, this resistance was only evolving in one replicate and not across all replicates with it appearing to be rather spontaneous and resulting in considerable variation among replicates of a treatment (Figure 4.2). We identified five "good" phages (PY038, PY019, PY021, PY023 and PY066), phages that were individually effective at suppressing the growth of *R. solanacearum*. In some cases, the presence of "good" phages in the combination resulted in a highly effective combination, even when "bad" phages were present, for example with combinations "PY047 + PY023" or "PY047 + PY063 + PY023" (Figure 4.2). On the other hand, we had cases where the presence of "good phages" did not result in a high efficacy phage combination, e.g., "PY019 + PY023 + PY066" (Figure 4.2).

To help understand the relationship between phage combinations and phage types, we calculated the expected OD value of combination phage treatments based on the performance (OD values) of single phage treatments from transfer 5. The average OD of each single phage treatment in the combination treatment was added together and the average taken which became the expected OD of the combination. We found that there was no relationship between phage types and combination performance, suggesting that phage identity had little influence over the effectiveness of a phage combinations (Figure 4.3A). Overall, phage combinations performed as expected with many surpassing expectations, only a handful performed worse (Figure 4.3B-C). The combinations performing worse might be a result of competition between phage emerging, reducing the efficiency of the combination. Again, it is difficult to determine whether phage identity was influencing the performance of the combination. There is large variation between replicates in a number of phage combinations, likely as a result of the spontaneous phage resistance evolution in *R. solanacearum* UW551 (Figure 3.4B-

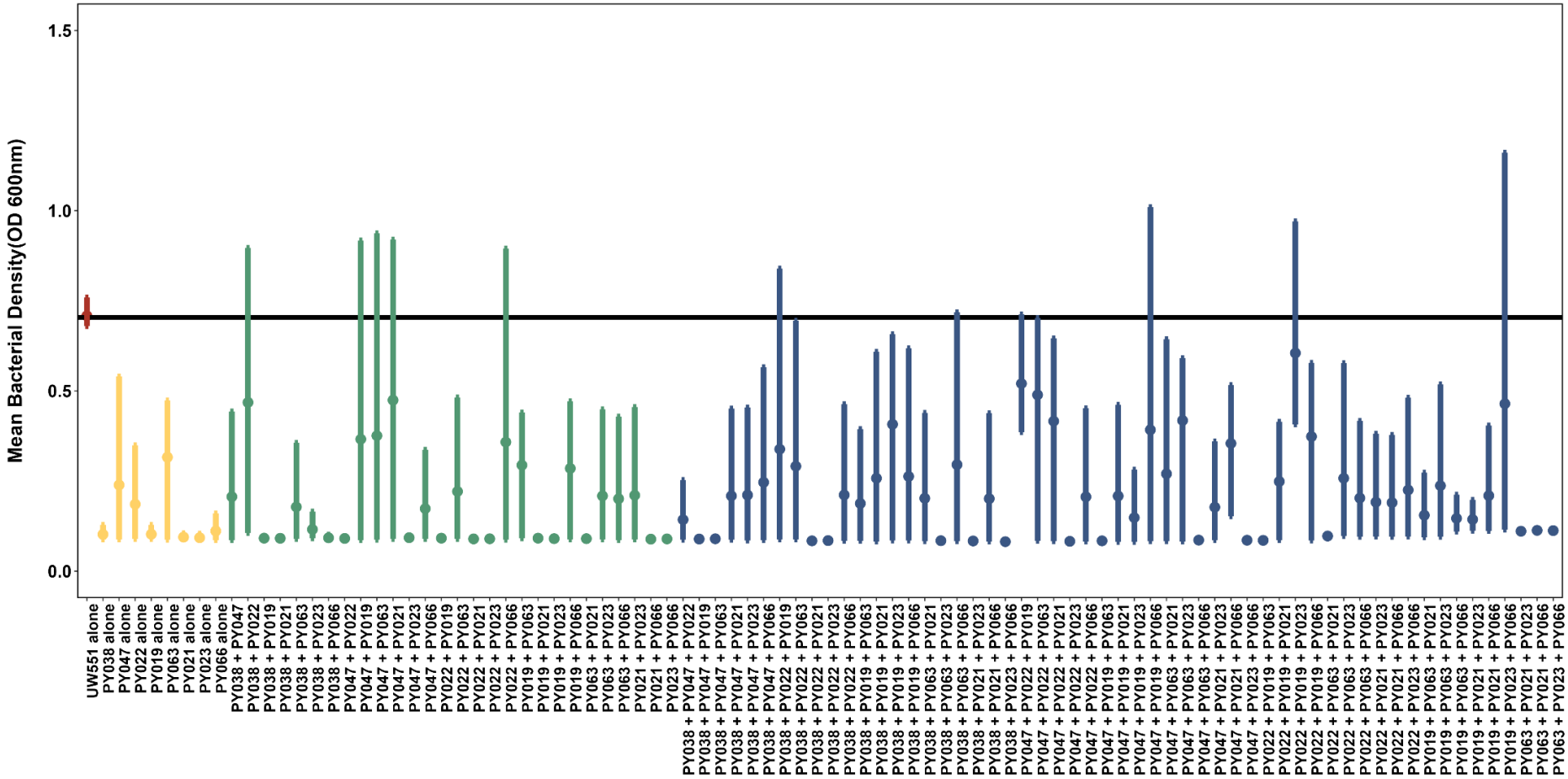
Mean Bacterial Density(OD 600nm)
1.5
1.0
0.5
0.0
UW551 alone
PY038 alone
PY047 alone
PY022 alone
PY019 alone
PY063 alone
PY021 alone
PY023 alone
PY066 alone
PY038 + PY047
PY038 + PY022
PY038 + PY019
PY038 + PY021
PY038 + PY063
PY038 + PY023
PY038 + PY066
PY047 + PY022
PY047 + PY019
PY047 + PY063
PY047 + PY021
PY047 + PY023
PY047 + PY066
PY022 + PY019
PY022 + PY063
PY022 + PY021
PY022 + PY023
PY022 + PY066
PY019 + PY063
PY019 + PY021
PY019 + PY023
PY019 + PY066
PY063 + PY021
PY063 + PY023
PY063 + PY066
PY021 + PY023
PY021 + PY066
PY023 + PY066
PY038 + PY047 + PY022
PY038 + PY047 + PY019
PY038 + PY047 + PY063
PY038 + PY047 + PY021
PY038 + PY047 + PY023
PY038 + PY047 + PY066
PY038 + PY022 + PY019
PY038 + PY022 + PY063
PY038 + PY022 + PY021
PY038 + PY022 + PY023
PY038 + PY022 + PY066
PY038 + PY019 + PY063
PY038 + PY019 + PY021
PY038 + PY019 + PY023
PY038 + PY019 + PY066
PY038 + PY063 + PY021
PY038 + PY063 + PY023
PY038 + PY063 + PY066
PY038 + PY021 + PY023
PY038 + PY021 + PY066
PY038 + PY023 + PY066
PY047 + PY022 + PY019
PY047 + PY022 + PY063
PY047 + PY022 + PY021
PY047 + PY022 + PY023
PY047 + PY022 + PY066
PY047 + PY019 + PY063
PY047 + PY019 + PY021
PY047 + PY019 + PY023
PY047 + PY019 + PY066
PY047 + PY063 + PY021
PY047 + PY063 + PY023
PY047 + PY063 + PY066
PY047 + PY021 + PY023
PY047 + PY021 + PY066
PY047 + PY023 + PY066
PY022 + PY019 + PY063
PY022 + PY019 + PY021
PY022 + PY019 + PY023
PY022 + PY019 + PY066
PY022 + PY063 + PY021
PY022 + PY063 + PY023
PY022 + PY063 + PY066
PY022 + PY021 + PY023
PY022 + PY021 + PY066
PY022 + PY023 + PY066
PY019 + PY063 + PY021
PY019 + PY063 + PY023
PY019 + PY063 + PY066
PY019 + PY021 + PY023
PY019 + PY021 + PY066
PY019 + PY023 + PY066
PY063 + PY021 + PY023
PY063 + PY021 + PY066
PY063 + PY023 + PY066

Figure 4.2 – The final OD (600nm) read taken at transfer 5 to highlight the level of suppression from all phage treatments mono and combination. *R. solanacearum* UW551 was coevolved with 1-3 phages and without phages for 15 days with a transfer into fresh CPG media every three days. The black line is the mean bacterial density of UW551 alone (no phages) at transfer 5, used to highlight the bacterial suppression caused by the phage combination.

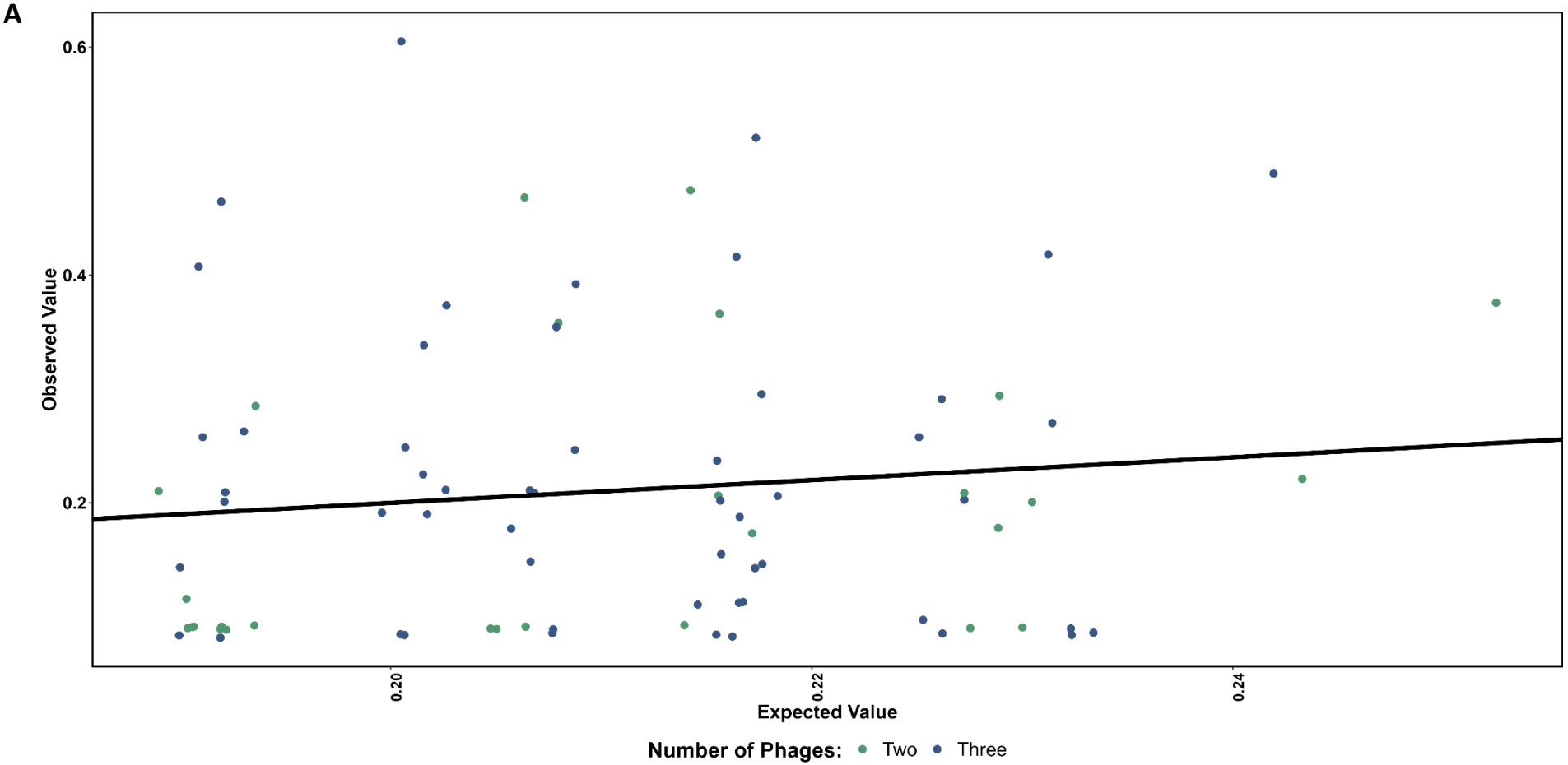
A
0.6
0.4
0.2
Observed Value
0.20
0.22
0.24
Expected Value
Number of Phages:
Two
Three

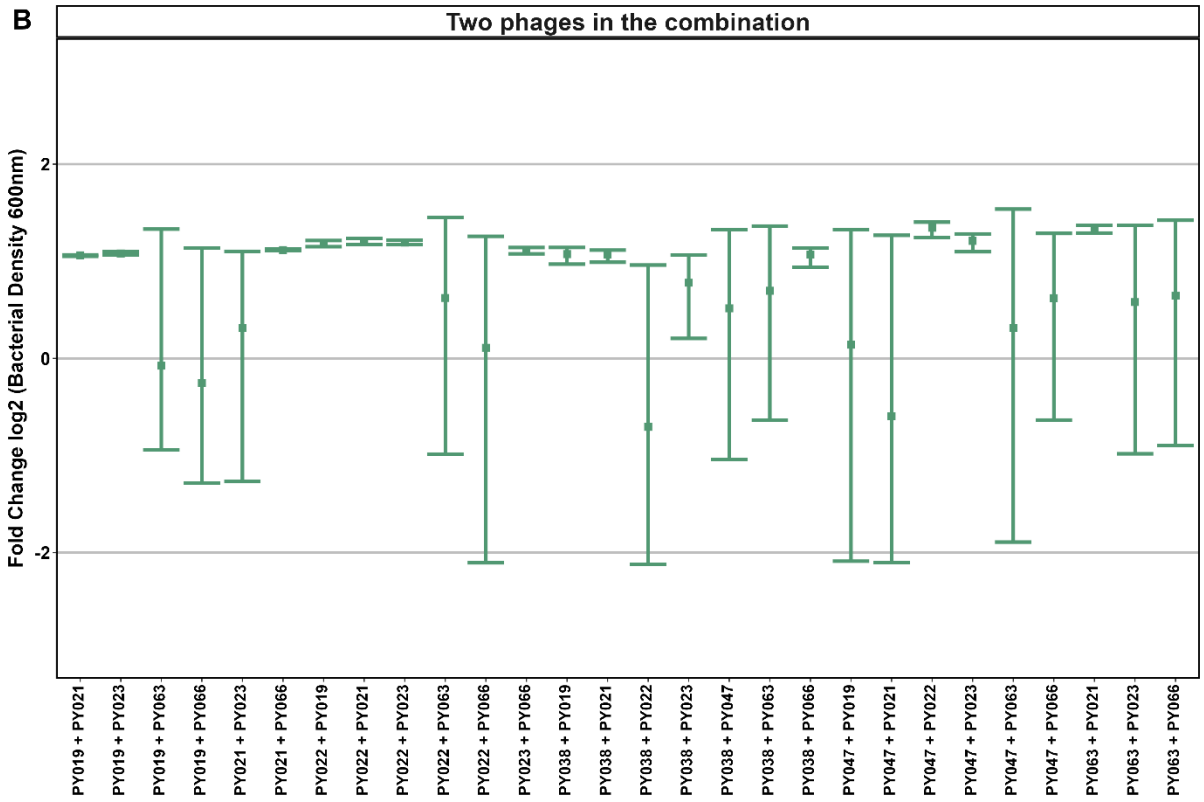
B
Two phages in the combination
Fold Change log2 (Bacterial Density 600nm)
2
0
-2
PY019 + PY021
PY019 + PY023
PY019 + PY063
PY019 + PY066
PY021 + PY023
PY021 + PY066
PY022 + PY019
PY022 + PY021
PY022 + PY023
PY022 + PY063
PY022 + PY066
PY023 + PY066
PY038 + PY019
PY038 + PY021
PY038 + PY022
PY038 + PY023
PY038 + PY047
PY038 + PY063
PY038 + PY066
PY047 + PY019
PY047 + PY021
PY047 + PY022
PY047 + PY023
PY047 + PY063
PY047 + PY066
PY063 + PY021
PY063 + PY023
PY063 + PY066

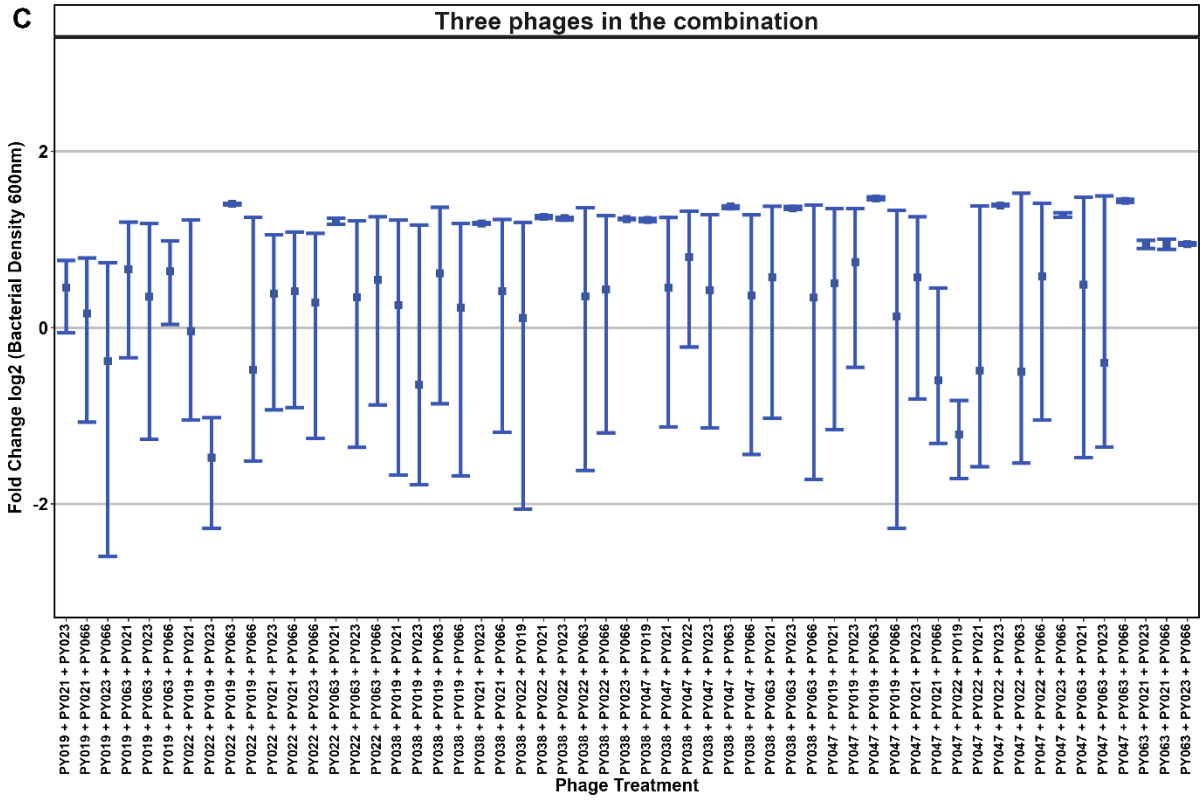
C
Three phages in the combination
Fold Change log2 (Bacterial Density 600nm)
2
0
-2
PY019 + PY021 + PY023
PY019 + PY021 + PY066
PY019 + PY023 + PY066
PY019 + PY063 + PY021
PY019 + PY063 + PY023
PY019 + PY063 + PY066
PY022 + PY019 + PY021
PY022 + PY019 + PY023
PY022 + PY019 + PY063
PY022 + PY019 + PY066
PY022 + PY021 + PY023
PY022 + PY021 + PY066
PY022 + PY023 + PY066
PY022 + PY063 + PY021
PY022 + PY063 + PY023
PY022 + PY063 + PY066
PY038 + PY019 + PY021
PY038 + PY019 + PY023
PY038 + PY019 + PY063
PY038 + PY019 + PY066
PY038 + PY021 + PY023
PY038 + PY021 + PY066
PY038 + PY022 + PY019
PY038 + PY022 + PY021
PY038 + PY022 + PY023
PY038 + PY022 + PY063
PY038 + PY022 + PY066
PY038 + PY023 + PY066
PY038 + PY047 + PY019
PY038 + PY047 + PY021
PY038 + PY047 + PY022
PY038 + PY047 + PY023
PY038 + PY047 + PY063
PY038 + PY047 + PY066
PY038 + PY063 + PY021
PY038 + PY063 + PY023
PY038 + PY063 + PY066
PY047 + PY019 + PY021
PY047 + PY019 + PY023
PY047 + PY019 + PY063
PY047 + PY019 + PY066
PY047 + PY021 + PY023
PY047 + PY021 + PY066
PY047 + PY022 + PY019
PY047 + PY022 + PY021
PY047 + PY022 + PY023
PY047 + PY022 + PY063
PY047 + PY022 + PY066
PY047 + PY023 + PY066
PY047 + PY063 + PY021
PY047 + PY063 + PY023
PY047 + PY063 + PY066
PY063 + PY021 + PY023
PY063 + PY021 + PY066
PY063 + PY023 + PY066
Phage Treatment

Figure 4.3 - The expected versus the observed bacterial densities (OD 600nm) values of combination treatments based on the bacterial density values of single phage treatments, to help understand why some combinations were more effective than others. Expected OD values were calculated from the performance of single phage treatments at transfer 5. The average OD of each single phage treatment in the combination treatment was added together and average taken which became the expected OD of the combination. Observed OD values are the OD readings of the combination treatments taken at Transfer 5. A) The expected vs the mean observed bacterial densities, dots represent a combination of phage treatment (2 or 3), dots closer to the line are working as expected whereas dots further away from the line are working better or worse. B-C) The mean fold change (log2) of the combination treatments, above 0 suggests that the combination was performing better than expected, below 0 suggests that the combination was performing worse than expected. At 0, the combination was performing as expected. B) The mean fold change of two combination phage treatments C) The mean fold change of three combination phage treatments.

4.4.2 No Phenotypic changes of coevolved UW551 were observed.

We were successful in isolating 12 clones of coevolvedUW551 from various phage treatments (Table 4.2). We used light microscopy to observe if any cellular morphology changes had occurred to cells as a result of coevolution with different phage treatments (Figure 4.4). We found no evidence of phenotypic changes in cellular morphology in phage resistant UW551 (Figure 4.4). Coevolved UW551 retained the rod-shaped morphology to the ancestor and control (evolved without the presence of phages, Figure 4.4A-B). Some coevolved UW551 was in considerably lower abundance than the ancestor such as “PY022 + PY066” and “PY021 + PY022” which could suggest an evolutionary trade-off in competitive fitness due to lower growth (Figure 4.4E-F). Other coevolved UW551 maintained a high abundance similar to that of the ancestor and control UW551 such as “PY038 + PY019 + PY066” (Figure 4.4I).

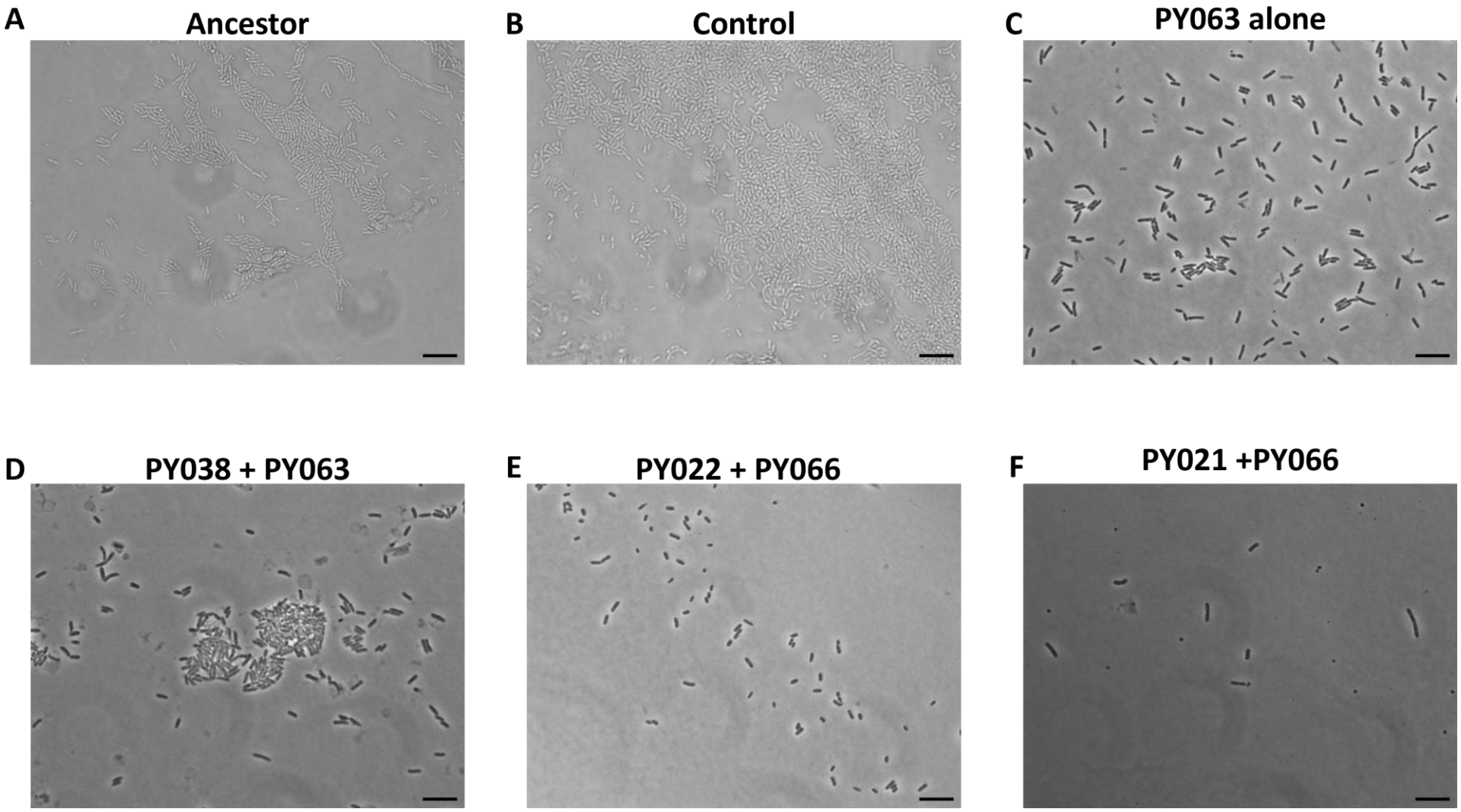
A
Ancestor
B
Control
C
PY063 alone
D
PY038 + PY063
E
PY022 + PY066
F
PY021 +PY066

G PY038 + PY019 + PY023

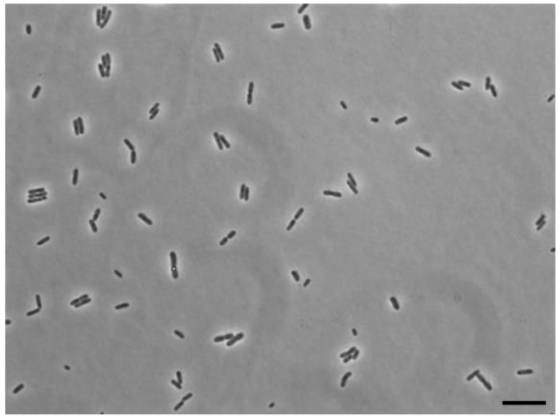

H PY038 + PY022 + PY063

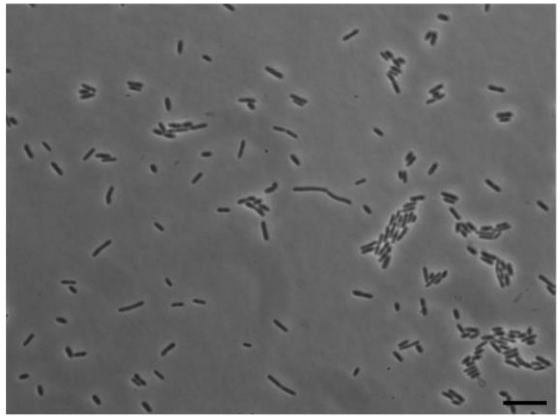

I PY038 + PY019 + PY066

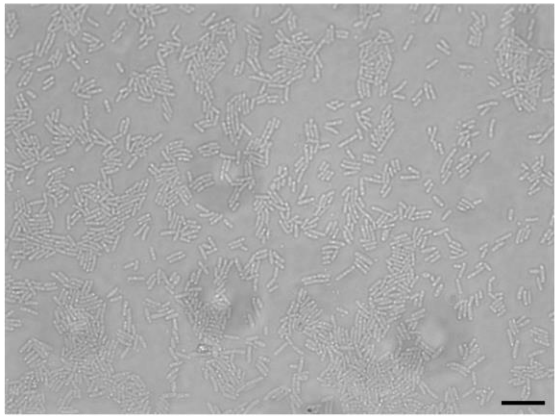

J PY019 + PY063 + PY066

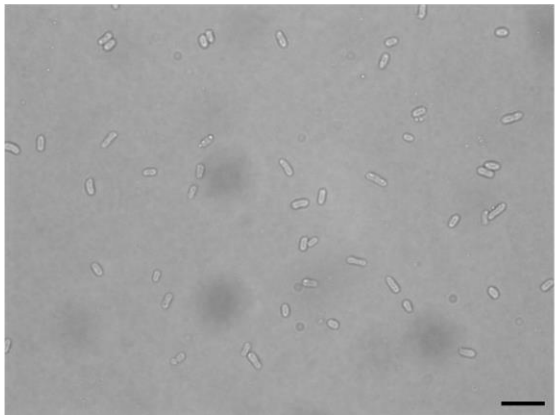

K PY063 + PY021 + PY023

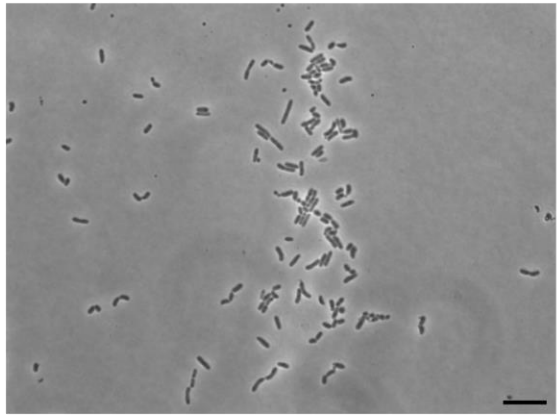

Figure 4.4 – Light microscope photos of *R. solanacearum* UW551, taken at 100x objective to determine if any phenotypic changes to UW551 had occurred as a result of coevolving with different phages and treatments. A) Ancestral UW551, used in the initial start of the combination experiment, not evolved B) The control in the combination experiment, evolved without the presence of phages used to determine if any evolutionary changes that had occurred was a result of phages. C-K) UW551 coevolved in phage combinations, 12 clones were successfully isolated from different phage treatments and used to assess if any coevolutionary changes had occurred. Each photograph is UW551 isolated from different phage treatments, the title above the photo states which phage combination treatment UW551 coevolved in. We were unable to obtain photos of "PY019 + PY066" and "PY019 + PY063 + PY066". Scale bar = 10µm.

4.4.3 High levels of phage resistance and cross-resistance was observed.

To assess the resistance within the 12 coevolved UW551 clones, we challenged all coevolvedUW551 against all phages (ancestral) used in the combination experiment, regardless of whether they coevolved with them or not. We observed that the ancestor remained susceptible to all phage types suggesting that high levels of resistance evolved in UW551 during the combination experiment and cross-resistance was observed (Figure 4.5). We found that five evolved UW551 clones were resistant to all phage types, we found no significant differences between the bacterial densities of each phage type (Figure 4.5 and Table 4.4). For the remaining coevolved UW551 there were significant differences between phages, possibly suggesting that there was no cross-resistance to all eight phages suggesting that evolved UW551 from these phage treatments might remain susceptible to other phages (Figure 4.5 and Table 4.4). However, post hoc analysis (Pairwise Wilcoxon Test) was unable to confirm this ($p > 0.05$). Overall, when resistance evolved, it was quite general providing cross-resistance to other phages.

Table 4.4 - Kruskal-Wallis test for comparisons of phage types on bacterial density on each genotype of UW551l, Mean Rank. The blue denotes a resistant UW551 where cross-resistance was observed, coevolved UW551 from these combination treatments was resistant to all eight (ancestral) phages.

UW551 Genotype	Chi-squared (X^2)	Degrees of freedom	p-value
Ancestor	7.10	8	0.526
PY063 alone	19.865	8	0.012
PY038 + PY063	14.629	8	0.067
PY022 + PY066	10.431	8	0.236
PY019 + PY066	22.053	8	0.005
PY021 + PY066	11.665	8	0.167
PY038 + PY047 + PY066	14.297	8	0.074
PY038 + PY022 + PY063	20.797	8	0.077
PY038 + PY019 + PY066	18.364	8	0.019
PY019 + PY063 + PY066	15.817	8	0.045
PY019 + PY023 + PY066	21.083	8	0.007
PY063 + PY021 + PY023	20.017	8	0.01

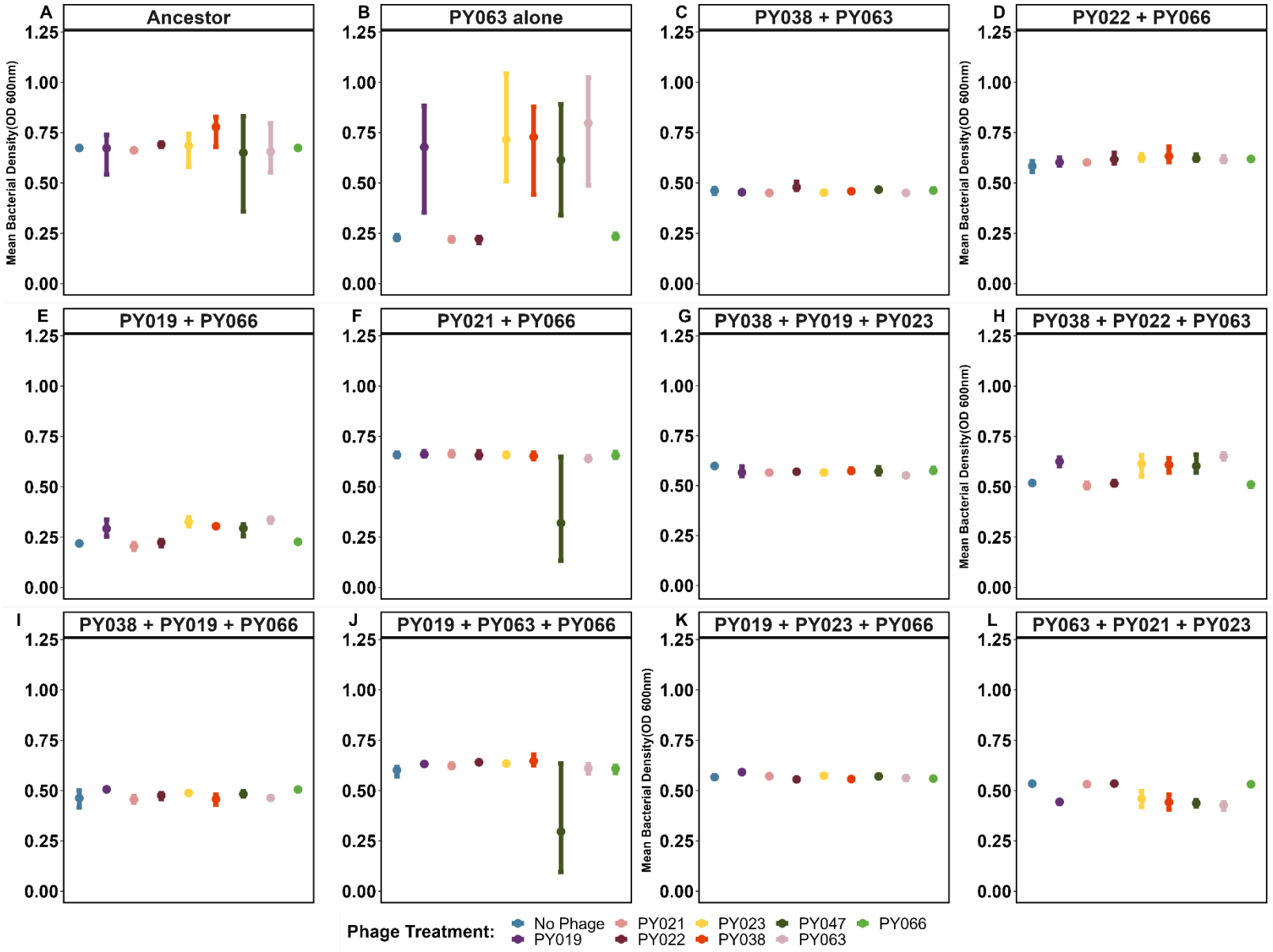
A
Ancestor
B
PY063 alone
C
PY038 + PY063
D
PY022 + PY066
E
PY019 + PY066
F
PY021 + PY066
G
PY038 + PY019 + PY023
H
PY038 + PY022 + PY063
I
PY038 + PY019 + PY066
J
PY019 + PY063 + PY066
K
PY019 + PY023 + PY066
L
PY063 + PY021 + PY023
Mean Bacterial Density(OD 600nm)
0.00
0.25
0.50
0.75
1.00
1.25
Phage Treatment:
No Phage
PY019
PY021
PY022
PY023
PY038
PY047
PY063
PY066

Figure 4.5 – Phage Infectivity assays used to determine if phage resistance was present in *R. solanacearum* UW551. The panels show the bacterial density (OD 600nm) after 72 hours of growth. A) Ancestral UW551, ancestral UW551 was challenged against all ancestral phages used in the combination experiment, to determine if resistance had evolved. B-L) Coevolved UW551 challenged against all ancestral phages used in the combination experiment to determine if phage resistance had evolved and whether cross-resistance was observed. Each panel is a phage combination treatment that UW551 was successfully isolated from at the end of the combination experiment.

4.4.4 Evidence of evolutionary trade-offs with fitness and EPS production

Phage resistance often leads to evolutionary trade-offs with multiple traits often with potential repercussions for the bacteria's fitness and virulence (Burmeister and Turner, 2020). We decided to explore two traits, critical to *R. solanacearum* success as a plant pathogen, competitive fitness (growth) and EPS production.

Competitive fitness is often traded-off with phage resistance. To investigate if a trade-off was observed with this trait, we performed growth assays (Figure 4.6). We observed that five phage resistant genotypes experienced an evolutionary trade-off between competitive fitness and phage resistance (Figure 4.6) Kruskal-Wallis: $X^2_{39.539}$, $p < 0.001$). "PY063 alone", "PY038 + PY063", "PY019 + PY066", and "PY038 + PY019 + PY066" all had significantly reduced growth rates compared to the ancestor (Figure 4.6)). The remaining genotypes did not experience a trade-off between competitive fitness and phage resistance (Figure 4.6). We found no evidence that there was an increase in competitive fitness from any of coevolved UW551.

EPS is an important virulence factor of *R. solanacearum* (Lowe-Power et al., 2018). We investigated whether EPS production (N-acetylgalactosamine µg) experienced evolutionary trade-offs with phage resistance. Overall, we observed evolutionary trade-offs with EPS in only one phage treatment of coevolved UW551 4.7, One-Way ANOVA: $F_{11,23} = 5.635$, $p > 0.001$). We only found two different phage treatment coevolved UW551 that were significantly different from the ancestor, "PY021 + PY066" and "PY022 + PY066" (Duncan's Test, $p = 0.015$ and $p = 0.009$, respectively). With "PY021 + PY066" we observed a decrease in the amount of EPS produced compared to the ancestor. This decrease in EPS by "PY021 + PY066" could indicate a potential evolutionary trade-off (Figure 4.7). Interestingly, for "PY022 + PY066" we observed an increase in the amount of EPS produced compared to the ancestor (Figure 4.7). Perhaps, an indication of an evolutionary trade-up. With the remaining coevolved UW551 we found no significant differences between them and the ancestor (Figure 4.7, Duncan's Test, $p > 0.05$). We did not observe any evolutionary trade-offs or even trade-ups (positive trade-correlations).

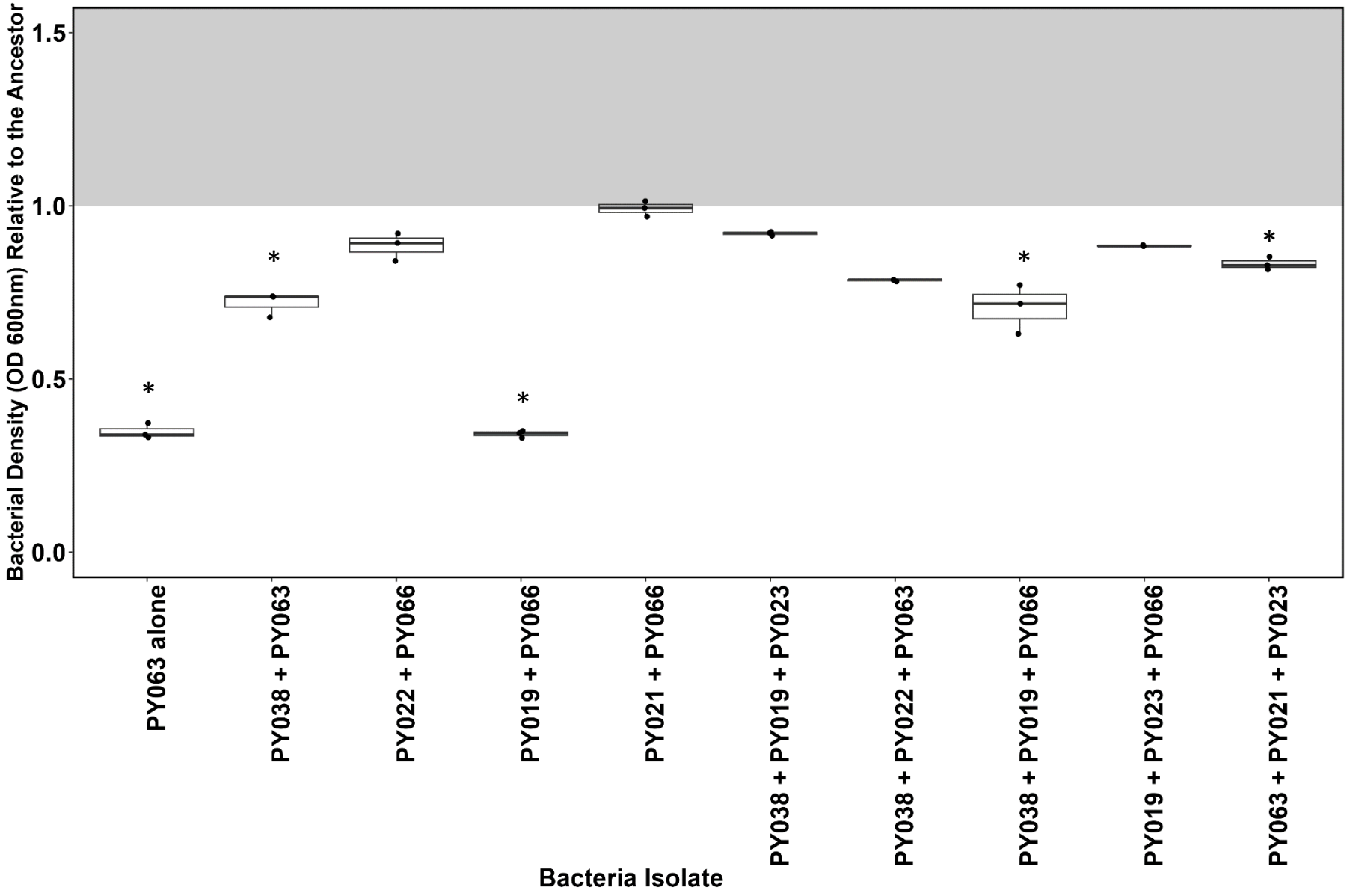
Bacterial Density (OD 600nm) Relative to the Ancestor
1.5
1.0
0.5
0.0
*
*
*
*
*
PY063 alone
PY038 + PY063
PY022 + PY066
PY019 + PY066
PY021 + PY066
PY038 + PY019 + PY023
PY038 + PY022 + PY063
PY038 + PY019 + PY066
PY019 + PY023 + PY066
PY063 + PY021 + PY023
Bacteria Isolate

Figure 4.6 – Growth assays used to determine the competitive fitness of *R. solanacearum* UW551 after coevolving with different phage combinations to determine if any evolutionary trade-offs are present in competitive fitness. The growth of each coevolved UW551 that was successfully isolated from the combination experiment, relative to the growth of ancestral UW551 (no evolutionary change, maximum carrying capacity) after 72 hours at +28^{o}C. The grey area indicates that coevolved UW551 could have a potential increase in competitive fitness if the threshold was reached (above 1.0). Each phage treatment that UW551 coevolved from is stated on the x-axis. The * symbols are significant differences between ancestral UW551 and coevolved UW551 from different phage treatments based on the post hoc test Dunn's test with BH p value adjustment (* $p < 0.05$, ** $p < 0.01$, *** $p < 0.001$).

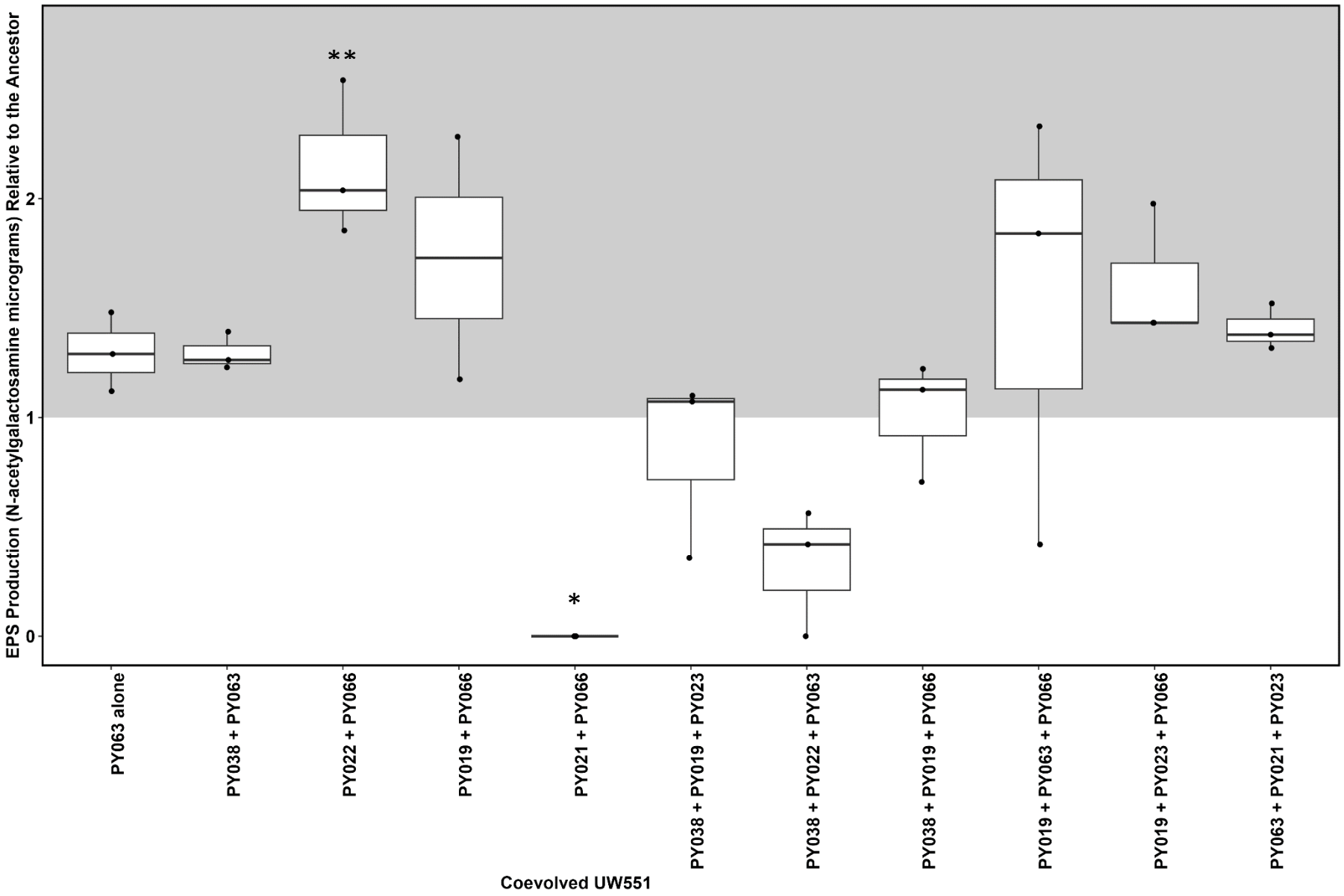
EPS Production (N-acetylgalactosamine micrograms) Relative to the Ancestor
0
1
2
**
*
PY063 alone
PY038 + PY063
PY022 + PY066
PY019 + PY066
PY021 + PY066
PY038 + PY019 + PY023
PY038 + PY022 + PY063
PY038 + PY019 + PY066
PY019 + PY063 + PY066
PY019 + PY023 + PY066
PY063 + PY021 + PY023
Coevolved UW551

181

Figure 4.7 – EPS production (N-acetylgalactosamine µg) of coevolved UW551 relative to the ancestor (no evolutionary change) to determine if any evolutionary trade-offs occurred during coevolution with different phage combinations. EPS is an important virulence factor of *R. solanacearum,* trade-offs here could have significant impacts on *R. solanacearum* success as a pathogen. The grey box indicates that coevolved UW551 could have a potential trade-up, increased EPS production, as the threshold was reached (above 1.0). Each phage treatment that UW551 coevolved from is stated on the x-axis. The * symbols are significant differences between ancestral UW551 and coevolved UW551 from different phage treatments based on the post hoc test Duncan's test (* $p < 0.05$, ** $p < 0.01$, *** $p < 0.001$).

4.4.5 Phage resistance is linked with multiple potential resistance mutations.

We sent all coevolved UW551 for whole-genome sequencing to identify potential mutations that might coincide with the phage resistance as well as help to understand the changes in coevolved UW551 in terms of competitive fitness and EPS production. Overall, we found genetic variation in all 12 coevolved UW551 (Table 4.5). Interestingly, 7 coevolved UW551 identified as hypermutators. Hypermutators are bacteria that experience high frequencies of point mutations where single base nucleotides can be changed, inserted or deleted (Table 4.5). We found that our hypermutators were often associated with lower competitive fitness higher production of EPS and cross-resistance to all 8 phages used.

We also found genetic variation in three coevolved UW551 that were not classed as hypermutators (Table 4.5). Genetic variation was found in three proteins: glucose-1-phosphate thymidylyltransferase, non-ribosomal peptide synthase and TorF family putative porin (identified with BLAST). In all three types of coevolved UW551 genetic variation was found in the non-ribosomal peptide indicating that possible parallel evolution was occurring (Table 4.5). Genetic variation in non-ribosomal peptide was also found in Chapter 3, further strengthening the evidence that parallel evolution in phage resistance is occurring. However, many of the variant types found in non-ribosomal peptide appear to be synonymous and it is unlikely that the amino acid sequence and protein structure changed (Table 4.5). We did find that two SNPs in coevolved “PY021 + PY066” UW551 were nonsynonymous resulting in amino acid changes (Table 4.5). At nucleotide position 779, the nucleotide acid changed from C to T, resulting in amino acid change from alanine to valine at amino acid position 260. At position nucleotide position 817 the nucleotide changes from A to G, changed the amino acid from asparagine to aspartic acid at position 272 (Table 4.5).

A synonymous SNP was identified with coevolved “PY063 alone” UW551 within glucose-1-phosphate thymidylytransferase, it unlikely that the amino acid sequence and protein structure changed.

A single nonsynonymous SNP was identified in TorF family putative porin in coevolved "PY021 + PY066" on the nucleotide position 545, changing the nucleotide sequence from G to A (Table 4.5 and Figure 4.8). The amino acid sequence changed at position 182, changing the amino acid from arginine to glutamine (Figure 4.8A). However, the protein model suggests that there was little structural difference between the ancestor and coevolved UW551 (Figure 4.8B-C), suggesting little change to function and activities of this protein (Figure 4.8).

The only coevolved UW551 with nonsynonymous SNPs was phage treatment "PY021 + PY066" which had significantly reduced competitive fitness, EPS production and was cross-resistant. The nonsynonymous SNPs found in the two proteins (TorF family putative porin and non-ribosomal peptide synthase) might be associated with coevolutionary changes that resulted in high phage resistance but were detrimental to competitive fitness and EPS production.

Table 4.5 – Single nucleotide polymorphism (SNPS) or Multiple Nucleotide Polymorphism (MNP) identified in coevolved UW551 and the changes to the amino acid sequence that occurred. Proteins with amino acid changes have also been identified through BLAST, Ancestral UW551 is used as a reference for the variant calling. Nucleotide position is the position of the variant counting from 1. Only 1 replicate from each combination treatment was sent to sequencing. The variant type “complex” means a combination of SNP and MNP has occurred.

Combination Treatment	Nucleotide Position	The Variant Type	Nucleotide Change	Amino Acid Change	Protein of Interest identified with BLAST
PY063 alone	358 642 670 736 747 779 789 817 825 858	SNP (synonymous) SNP (synonymous) SNP (synonymous) SNP (synonymous) SNP (synonymous) SNP (synonymous) SNP (synonymous) SNP (synonymous) Complex (synonymous) SNP (synonymous)	C → T C → G T → C G → A C → T C → T C → G A → G GGCC → CGCT G → A		Glucose-1-phosphate thymidylyltransferase [UW551] Non-ribosomal peptide synthetase [RSSC]
PY038 + PY063		65924 variants			
PY022 + PY066		68236 variants			
PY019 + PY066		294 variants			
PY021 + PY066	545 609 670 736 747 779 789 817 825 858	SNP (nonsynonymous) SNP (synonymous) SNP (synonymous) SNP (synonymous) SNP (synonymous) SNP (nonsynonymous) SNP (synonymous) SNP (nonsynonymous) Complex (synonymous) SNP (synonymous)	G → A T → C C → G T → C G → A C → T C → G A → G GGCC → CGCT G → A	Arginine → Glutamine Alanine → Valine Asparagine → Aspartic acid	TorF family putative porin [*Ralstonia solanacearum*] Non-ribosomal peptide synthetase [RSSC]
PY038 + PY019 + PY023		67986 variants			
PY038 + PY019 + PY066		6361 variants			
PY019 + PY023 + PY066		69040 variants			
PY019 + PY063 + PY066		56932 variants			

PY063 + PY021 + PY023	642 670 693 736 747 765 779 789 817 858	SNP (synonymous) SNP (synonymous) SNP (synonymous) SNP (synonymous) SNP (synonymous) Complex (synonymous) SNP (synonymous) SNP (synonymous) SNP (synonymous) SNP (synonymous)	C → G T → C C → T G → A C → T GCGCG → ACGCA C → G A → G G → A		Non-ribosomal peptide synthetase [RSSC]

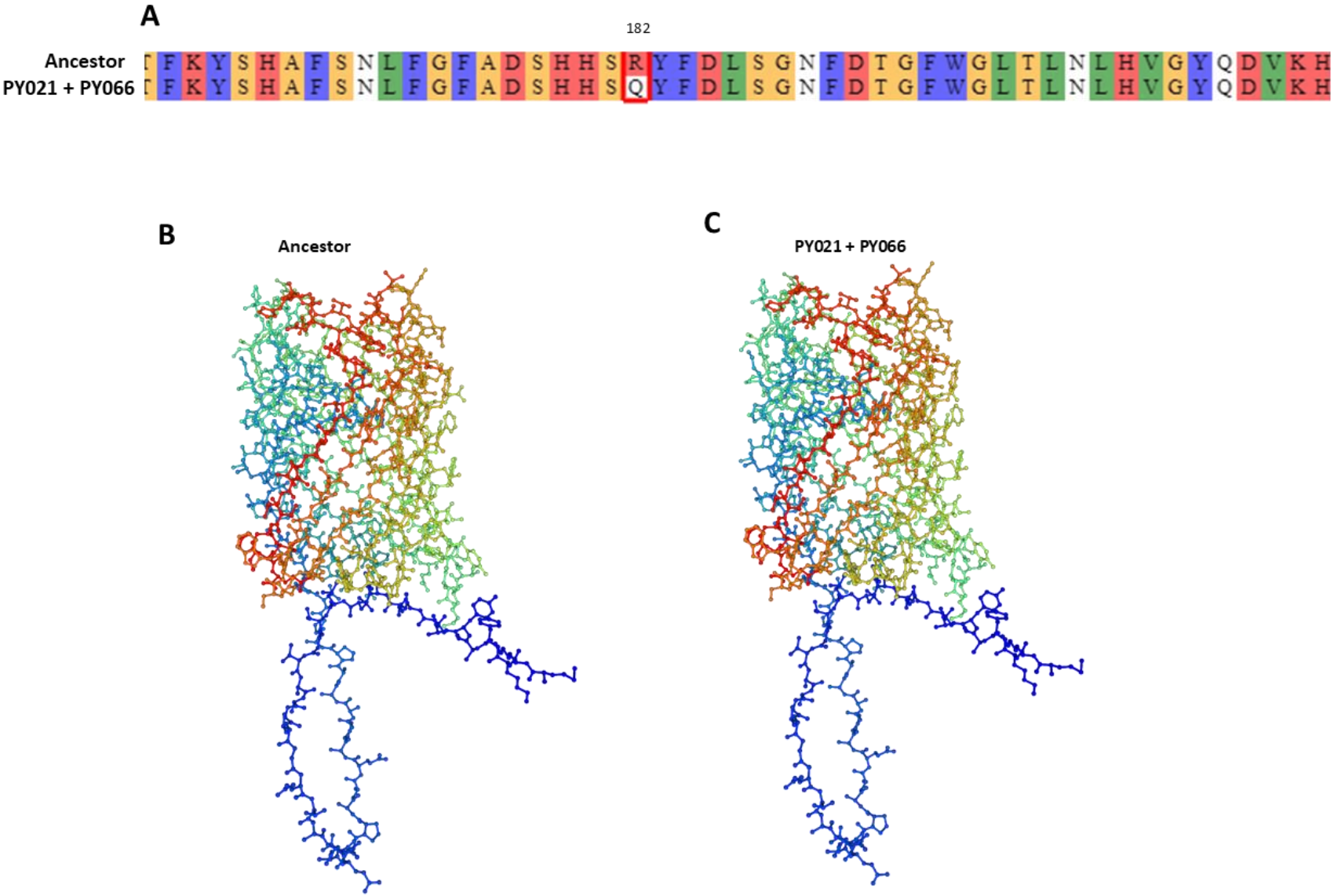
A
182
Ancestor
PY021 + PY066
F K Y S H A F S N L F G F A D S H H S R Y F D L S G N F D T G F W G L T L N L H V G Y Q D V K H
F K Y S H A F S N L F G F A D S H H S Q Y F D L S G N F D T G F W G L T L N L H V G Y Q D V K H
B
Ancestor
C
PY021 + PY066

Figure 4.8 – The partial amino acid sequence and protein structure of a TorF family putative porin, where genetic variation was identified in coevolved *R. solanacearum* UW551 from phage treatment PY021 + PY066. A) The amino acid sequence of TorF family putative porin from both ancestral UW551 and coevolved UW551 aligned in clusteralΩ to highlight the nonsynonymous SNP that resulted in change of an amino acid from arginine to glutamine at amino acid sequence position 182 of the amino acid sequence (highlighted in red). B-C protein models built in the Swiss-model with the aim to understand the structure of the protein, identified as TorF family putative porin of *Ralstonia solanacearum* species complex. B) The ancestral protein, the amino acid sequence of the protein was used from ancestral UW551 to build the model. C) The protein model built from the amino acid sequence of coevolved UW551 with PY021 and PY066 used to identify if any structural changes have occurred as result of the SNP.

4.5 Discussion

Overall, we found that phages can be highly effective at suppressing the growth of *R. solanacearum*. However, in combination we did not observe any significant improvement and occasionally competition emerged. As we observed cross resistance and parallel evolution in phage resistant *R. solanacearum*, this could potentially reduce the efficacy of a phage combination.

Competition between phages could be a possible explanation for the reduced efficacy in phage combinations. A similar situation occurred with *Escherichia coli* cocktails (4 phages, 11 cocktail combinations), cocktails were less effective than phages alone (Niu et al., 2021). Although, competition between lytic phages remains poorly understood, phages compete for hosts and sometimes receptors on their hosts among themselves (Molina et al., 2022). In certain situations, a "winner" could be determined, increasing their progeny but at cost to the other phages within the combination which could overall, reduce the efficacy of phage combination and also make it easier for phage resistance to evolve (Trinh et al., 2017). However, we would require further experiments to understand the effects of competition like population dynamics of phages within combinations. It has been purposed that minimising the number of phages in the combination can minimise competition (Molina et al., 2022). Here, we only used three phages in total and even then, there was evidence of competition suggesting that further understanding of host ranges and receptors in phages is critical to optimising phage combinations, something that could be time-consuming and costly (Gordillo Altamirano and Barr, 2021)

Super exclusion immunity could play a role in reducing the efficacy of combination treatment. Super exclusion immunity is the phages ability to protect and defend itself from other competing phages within a host (Folimonova, 2012). Super exclusion immunity is a common mechanism in temperate phages, especially if they enter the lysogenic cycle (Bondy-Denomy et al., 2016). Prophages can alter receptors preventing phage binding from other phages. The lysogenic phage JBD26 altered the type IV pilus (T4P) receptor binding site in *Pseudomonas aeruginosa* which resulted in strong phage resistance. T4P plays significant roles in biofilm formation where modifications to T4P could have significant impacts on fitness. The modification to T4P by JBD26 had no obvious fitness costs (Bondy-Denomy et al., 2016). If lysogeny is possible with eight phages, one of the phages in the combination could successfully enter the lysogenic cycle and become a prophage. It will likely implement strategies to protect its host and itself from further phage infections, with (Correa et al., 2021) the outcome being that efficacy of combination decreases as the host is now protected due to the presence of a new prophage (Correa et al.,. It could explain how in some phage resistant UW551 we observed little fitness costs (competitive fitness and EPS production), one of the phages could be modifying receptors to prevent binding from other phages but not at a cost to their host (Bondy-Denomy et al., 2016). However, further experiments, especially sequencing of the eight phages would be required to understand if super exclusion immunity plays a role in influencing the efficacy of host combinations. We would need to know if these eight phages can enter the lysogenic cycle and identify the mechanisms involved.

In this chapter, we focused on using phage combinations to mitigate resistance evolution as single phages were ineffective in the previous chapters, even when phages were pre-adapted (Chapter 2) (Doss et al., 2017). However, like the previous chapters, we find *R. solanacearum* quickly evolving resistance to phages. Resistance to phages in this experiment was high and cross-resistance was also observed. Asymmetrical evolution is again possibly playing a critical role (Lenski and Levin, 1985). We are finding that phage resistance is evolving rapidly, and phages cannot overcome it. Cross-resistance to all eight phages could have emerged due to recognition of the same receptor. Although, we aimed to select diverse phages in our collections, if they are targeting the same receptor, cross-resistance can be easily achieved (Markwitz et al., 2022). High levels of cross-resistance could also explain the lack of improved phage efficiency in different phage combinations.

We found evidence of parallel evolution with mutations occurring in non-ribosomal peptide synthase, which is important for lipopeptides synthesis (Matsukawa et al., 2023). This was also found in phage resistant genotypes in Chapter 3. Mutations associated with secondary metabolites can increase production and secondary metabolites can defend bacteria from viruses. For example, doxorubicin and daunorubicin prevent phage replication without affecting bacterial growth with *Streptomyces* (Kronheim et al., 2018). Like *R. solanacearum*, *Streptomyces* is found naturally in the soil and produces secondary metabolites as a trait that helps to compete with other microbes (Kronheim et al., 2018). It is plausible that *R. solanacearum* could employ a similar strategy to protect itself from phage infection. However, further experiments exploring *R. solanacearum* secondary metabolites and their effects on phages would be required. It is important to note that many of the SNPs found in the non-ribosomal peptide were synonymous which results in no change to the amino acid sequence and potentially no change to the protein structure. However, there is increasing evidence that synonymous SNPs have evolutionary importance and could possibly be affecting protein structure and function but understanding remains very limited (Shen et al., 2022)

We identified genetic variants in TorF family putative porin and LysR family transcriptional regulator. These genetic variants could possibly be found in the potential hypermutator backgrounds as well, but more thorough analysis in the future is required. The TorF family putative porin is a possible outer membrane porin (Castillo et al., 2018). Outer membrane porins are composed of lipopolysaccharides (LPS) and other compounds (Henderson et al., 2016). The mutation here could lead to phage receptor modification and phage resistance (Hampton et al., 2020). Outer membrane proteins and polysaccharides are often receptors for phages (Hantke, 2020). Interestingly, we also found genetic variation in the LysR family transcriptional regulator. This regulator plays a key role in regulating virulence, metabolism, quorum sensing and motility (Maddocks and Oyston, 2008). However, we did not find any evidence of evolutionary trade-offs within this genotype "PY019 + PY063 + PY066". However, we only looked at two potential virulence traits, growth and EPS production, and virulence was not tested *in planta*. It would hence be worth exploring the other traits that this regulator regulates to find the impact that genetic change might have on *R. solanacearum*.

Finally, we found genetic variation within Glucose-1-phosphate thymidyltransferase which is involved in the synthesis of lipopolysaccharides, a major component of the outer membrane of gram-negative bacteria, including *R. solanacearum* (Wang et al., 2007). Lipopolysaccharides are known to be phage receptors (Bertozzi Silva et al., 2016). It is possible that mutations in this enzyme would have significant impacts on lipopolysaccharide production, possibly resulting in defects or reduced display on the cell surface, preventing phage infection (Hong et al., 2014). However, further experiments would be required to confirm this, especially considering it was synonymous SNP (Shen et al., 2022).

We classified a number of coevolved UW551 as hypermutators. Hypermutability increases the mutation rates within a population which can be advantageous. It allows advantageous mutations to arise quickly in response to selection pressures, e.g. phage predation (Jayaraman, 2011). *Pseudomonas fluorescens* had increased mutation rates in response to phages with increased phage resistance as a response (Pal et al., 2007). Our hypermutators were the most resistant coevolved UW551, they were resistant to all eight phages used in the combination experiment. The hypermutability of *R. solanacearum* in these treatments allowed resistance and cross-resistance to evolve rapidly. Phase variation (rapid modification of surface molecules) could be responsible for this rapid evolution of resistance (Bayliss, 2009). However, it remains unclear within our hypermutators, further analysis of these genotypes would be required to understand the role of phase variation. Hypermutability often comes at a cost to fitness. Nonadaptive mutations (possibly slightly deleterous) can accumulate and "hitchhike" with the advantageous ones (Couce et al., 2017). We did see fitness costs (growth) in a few of our hypermutators. Nevertheless, hypermutation appears to be an important strategy of *R. solanacearum* to rapidly acquire resistance and cross-resistance.

We found evidence of trade-offs in competitive fitness and EPS, which are two traits critical for success of *R. solanacearum* as a plant pathogen (Hikichi et al., 2017). Competitive fitness is a common trade-off with phage resistance (Scanlan et al., 2015, Gómez and Buckling, 2011). We observed fitness trade-offs in a number of our phage resistant genotypes. Decrease in fitness could have potential repercussions for *R. solanacearum* (Wang et al., 2017). Phage resistant *R. solanacearum* was susceptible to antibiotics produced by its competitor *Bacillus amyloliquefaciens* (Wang et al., 2017). However, we did not see substantial fitness costs in growth rates in some genotypes (Wang et al., 2017). *Pseudomonas syringae* (plant pathogen) did not show fitness costs in media, rather the fitness costs became apparent when grown with their tomato hosts (Meaden et al., 2015). This could be true of our phage resistant genotypes. Further experiments *in planta* could determine if fitness costs are present.

EPS is a major virulence factor of *R. solanacearum*, responsible for the wilting symptoms within plants (Denny and Baek, 1991). During infection cycles of *R. solanacearum,* EPS is produced in large quantities resulting in rapid colonisation of plants and blockages in the xylem, resulting in wilting symptoms and plant death (Lowe-Power et al., 2018, Genin and Denny, 2012). Virulence is often traded-off with phage resistance (Burmeister and Turner, 2020). Considering the importance of EPS as a virulence factor to *R. solanacearum* we decided to explore if any evolutionary trade-offs were present. We only found one genotype that had a significant decrease in EPS. *R. solanacearum* that does produce EPS tend to be less virulent (Yang et al., 2021).

Biofilm formation and EPS production are closely intertwined, in some cases, biofilm cannot be eradicated unless EPS is completely removed as well (Greer et al., 2021). We saw that one genotype increased its EPS production. This could also increase biofilm formation. Biofilm also provide protection against phages. If biofilm production is increased as a result of phage predation, the efficacy of phages could be significantly reduced (Hosseinidoust et al., 2013). However, phages are known to have the ability to degrade biofilms (Ferriol-González and Domingo-Calap, 2020). The potential role of biofilm in *R. solanacearum* phage resistance requires more research in the future.

Conclusion

In conclusion, we find that phages can work effectively as individuals but place them in combination and the efficacy can reduce. We found no relationship between phage type and how effective the combination will be. It is possible that competition and super exclusion immunity might play a significant role in efficacy of a combination. We also found rapid evolution of resistance in *R. solanacearum*, a similar situation occurring in Chapter 2 and 3. The presence of potential hypermutators suggests that *R. solanacearum* can rapidly evolve resistance. Phage resistance is a challenge for developing biocontrols, but evolutionary trade-offs can mitigate some of the concerns. We did find evidence of evolutionary trade-offs in two traits, fitness and EPS. However, we also found some genotypes did not confer evolutionary trade-offs. Nevertheless, phages still remain a promising approach to developing control measures against *R. solanacearum*. However, further characterisation of individual phages should be considered before combining them.

Supplementary Figures

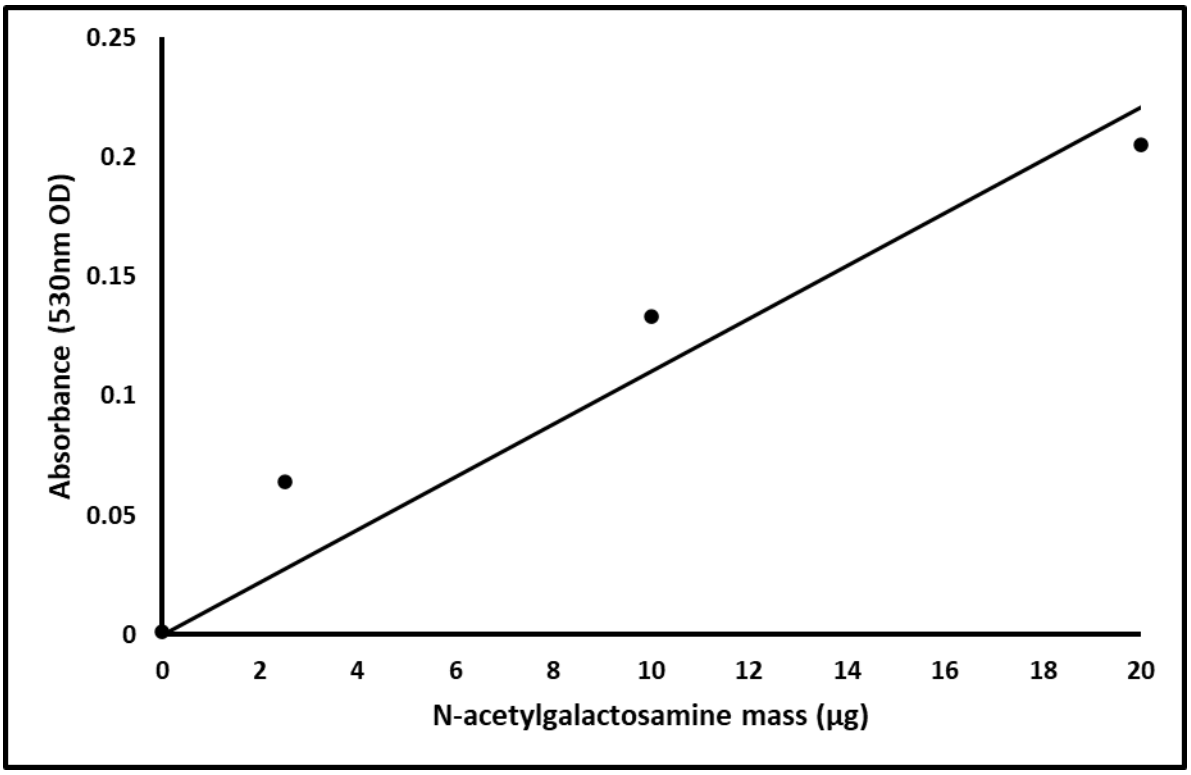

Supplementary Figure 4.1 – The standard curve used to calculate the N-acetylgalactosamine mass (µg)

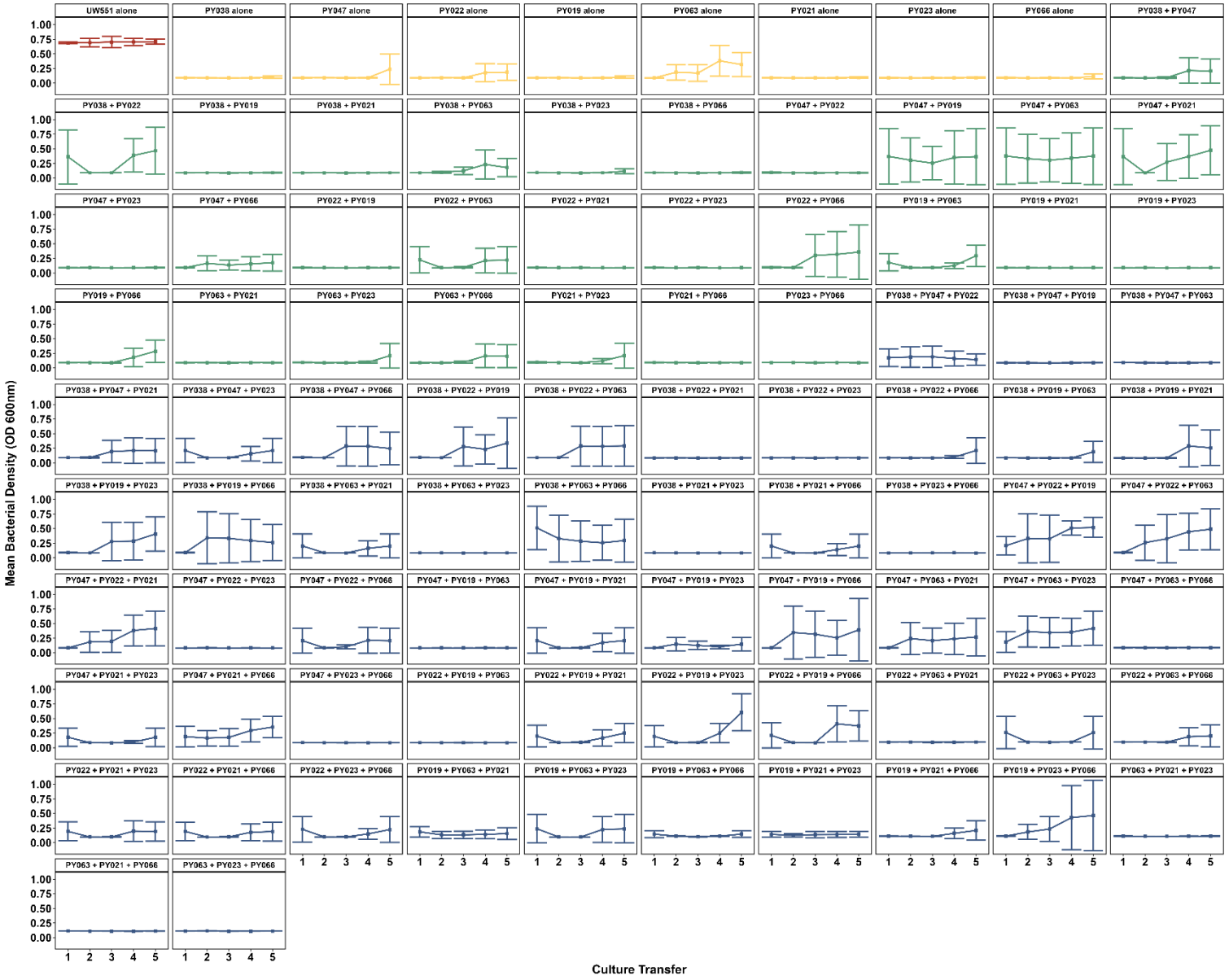
UW551 alone
PY038 alone
PY047 alone
PY022 alone
PY019 alone
PY063 alone
PY021 alone
PY023 alone
PY066 alone
PY038 + PY047
PY038 + PY022
PY038 + PY019
PY038 + PY021
PY038 + PY063
PY038 + PY023
PY038 + PY066
PY047 + PY022
PY047 + PY019
PY047 + PY063
PY047 + PY021
PY047 + PY023
PY047 + PY066
PY022 + PY019
PY022 + PY063
PY022 + PY021
PY022 + PY023
PY022 + PY066
PY019 + PY063
PY019 + PY021
PY019 + PY023
PY019 + PY066
PY063 + PY021
PY063 + PY023
PY063 + PY066
PY021 + PY023
PY021 + PY066
PY023 + PY066
PY038 + PY047 + PY022
PY038 + PY047 + PY019
PY038 + PY047 + PY063
PY038 + PY047 + PY021
PY038 + PY047 + PY023
PY038 + PY047 + PY066
PY038 + PY022 + PY019
PY038 + PY022 + PY063
PY038 + PY022 + PY021
PY038 + PY022 + PY023
PY038 + PY022 + PY066
PY038 + PY019 + PY063
PY038 + PY019 + PY021
PY038 + PY019 + PY023
PY038 + PY019 + PY066
PY038 + PY063 + PY021
PY038 + PY063 + PY023
PY038 + PY063 + PY066
PY038 + PY021 + PY023
PY038 + PY021 + PY066
PY038 + PY023 + PY066
PY047 + PY022 + PY019
PY047 + PY022 + PY063
PY047 + PY022 + PY021
PY047 + PY022 + PY023
PY047 + PY022 + PY066
PY047 + PY019 + PY063
PY047 + PY019 + PY021
PY047 + PY019 + PY023
PY047 + PY019 + PY066
PY047 + PY063 + PY021
PY047 + PY063 + PY023
PY047 + PY063 + PY066
PY047 + PY021 + PY023
PY047 + PY021 + PY066
PY047 + PY023 + PY066
PY022 + PY019 + PY063
PY022 + PY019 + PY021
PY022 + PY019 + PY023
PY022 + PY019 + PY066
PY022 + PY063 + PY021
PY022 + PY063 + PY023
PY022 + PY063 + PY066
PY022 + PY021 + PY023
PY022 + PY021 + PY066
PY022 + PY023 + PY066
PY019 + PY063 + PY021
PY019 + PY063 + PY023
PY019 + PY063 + PY066
PY019 + PY021 + PY023
PY019 + PY021 + PY066
PY019 + PY023 + PY066
PY063 + PY021 + PY023
PY063 + PY021 + PY066
PY063 + PY023 + PY066
Mean Bacterial Density (OD 600nm)
1.00
0.75
0.50
0.25
0.00
1 2 3 4 5
Culture Transfer

Supplementary Figure 4.2 – The mean bacterial density (OD 600nm) of each individual treatment throughout the combination experiment.

Chapter 5

General Discussion

Over the course of this thesis, we have aimed to develop effective phages against *R. solanacearum* through exploitation of their coevolutionary trajectories. First, through one-sided evolution or training (Chapter 2) and then coevolution (Chapter 3). We discovered that asymmetrical evolution was having significant consequences on phages, often making them ineffective (Chapter 2), sometimes driving them to extinction (Chapter 3). Finally, with the aim to reduce resistance evolution in *R. solanacearum*, we tried multiple phages in combination (Chapter 4) but ultimately failed as phage resistance and cross-resistance was evident. Although, our aims were not achieved, we did gain important understanding and insights in asymmetrical evolution and its potential consequences for phage biocontrol against RSSC and other plant pathogenic bacteria. Throughout this thesis there are two recurring observations, 1) phage resistance evolved and often rapidly in *R. solanacearum* and 2) The coevolutionary dynamics were highly asymmetrical. All three methods, training (Chapter 1), coevolution (Chapter 2) and combination (Chapter 3) failed to suppress or slow phage resistance evolution in RSSC (Gordillo Altamirano and Barr, 2021). Due to coevolutionary dynamics, phages are able to adapt and overcome resistance but we failed to see this, instead we saw an asymmetrical coevolutionary dynamic (Lenski and Levin, 1985, Buckling and Rainey, 2002). As a result, we saw a in loss phage infectivity and even phage extinctions. Phage extinction and asymmetrical coevolutionary dynamics have been observed in other bacterial-phage systems (Wright et al., 2016, Turkington et al., 2019). However, our research brings into a wider context plant pathogens and in particular RSSC, if plant pathogens can rapidly evolve resistance to phages and phages fail to keep up, this may raise concern for developing phages as biocontrols for plant pathogens.

Critics of phage biocontrols often cite phage resistance as a limitation (Azam and Tanji, 2019, Garvey, 2022). However, phage resistance does not come without a cost to the bacteria and evolutionary trade-offs between phage resistance and other traits exist (Burmeister and Turner, 2020). Trade-offs can have significant impacts on fitness and virulence (Castledine et al., 2022a). Previous research has shown that evolutionary trade-offs in RSSC can be detrimental to the pathogen, especially around virulence. Trade-offs between VOC-tolerance and virulence in RSSC were observed, resulting in almost complete loss of virulence in their hosts (Wang et al., 2023a).. Our phages failed to completely suppress resistance in *R. solanacearum,* but we observed evolutionary trade-offs in competitive fitness (Chapter 3 and Chapter 4), biofilm (Chapter 3) and extracellular polysaccharide (EPS) production (Chapter 4), likely to be detrimental to the virulence of *R. solanacearum*. In other research, disease incidence in plants was significantly lower in phage resistant RSSC (Wang et al., 2019). If this is the case with our resistant *R. solanacearum,* which is possible because of the lower EPS production (Chapter 4) then it puts forward the argument that we should be changing our approach to phage biocontrol. Shifting focus from complete eradication of their hosts towards exploiting evolutionary trade-offs, reducing virulence or making them vulnerable to other control strategies. However, we would need to do *in planta* experiments on our phage resistant *R. solanacearum* to fully determine if virulence was reduced.

In chapter 4 we found that phage resistance came at little cost to *R. solanacearum* with a possibility of super exclusion immunity playing a significant role. This would be a good avenue to explore, especially considering the wider implications of phage combinations. If super exclusion immunity is causing phage resistance with little costs to the host, the efficacy of phages could be reduced, making it redundant for biocontrol applications (Bondy-Denomy et al., 2016). It is clear that the mechanisms in super exclusion immunity needed to be explored in RSSC, focusing receptor modification caused by temperate phages and its impacts on the hosts, especially around virulence.

All research here was conducted *in vitro*. Although *in vitro* can give us insights into phage and bacteria interactions and outcomes, it might not necessarily reflect natural settings (Hernandez and Koskella, 2019). We used rich media, allowing *R. solanacearum* to adapt quickly and rapidly and possibly responsible for the asymmetrical coevolution dynamic seen. In rich media, the only selection pressure is the phages themselves which could result in rapid adaptation and phage resistance in *R. solanacearum* (Hernandez and Koskella, 2019). But would the results here be reflective in a more natural setting like an agricultural field? Numerous studies have shown resistance to evolve slower and evolutionary outcomes to be different to that of *in vitro* (Hernandez and Koskella, 2019, Gómez and Buckling, 2011). If we used plant systems, even soil microcosm, the outcomes of this resistance and the coevolutionary dynamics might change. The coevolutionary dynamics of *Pseudomonas fluorescens* SBW25 and SBW25ϕ2 changes from ARD in rich media to FSD in soil (Gómez and Buckling, 2011). If a similar experiment with *R. solanacearum* and phages was conducted would asymmetrical coevolutionary be present and would this give phages the opportunity to adapt.Nevertheless, our work *in vitro* did provide important insights and predications into how *R. solanacearum* might evolve against phage selection.

From the phage perspective, we do not know how effective our phages (trained, coevolved or combination) would be in more complicated settings, would our phages cope in different pH soils or a stable for long periods of time? It would be interesting to explore using a plant-based system for phage training rather than rich media, is it possible to train the phages to their environment focusing on other important traits like stability and pH tolerance. In Chapter 2, ancestor PY015 was a highly virulent phage so it might be worth focusing the training onto other traits rather than infectivity.

We saw evidence of competition between phages in combination between chapter 4 with research often suggesting that phages using the same receptor can increase competition and reduce efficacy of the phage combination (Molina et al., 2022). If we identified phage receptors in RSSC phages, would it be possible to reduce competition between phages and create highly effective phage combinations? Also, as rapid phage resistance evolution in RSSC has been a recurring observation in this thesis, it is important to focus on mitigating this. Phage combination with phages that utilise different receptors can slow down resistance evolution and impose higher evolutionary trade-offs (North and Brown, 2021). However, receptor identification is seldom used in phage biocontrols but the work here puts forward the argument that it should be used when developing phage combinations (Gordillo Altamirano and Barr, 2021). It is worth further exploring the role and significance of receptor identification in developing phage combinations against *R. solanacearum*.

Genomic analysis across this thesis highlighted interesting genetic variations as a result of the coevolution between phages and *R. solanacearum*. In particular, the non-ribosomal peptide synthase which saw evidence of parallel evolution to phage resistance across chapters (3-4). The understanding between non-ribosomal peptide synthases and phage resistance in bacteria remains limited so this is definitely an exciting avenue to explore. Non-ribosomal peptide synthases are involved in the production of secondary metabolites, including antimicrobials (Duban et al., 2022). It is possible that this non-ribosomal peptide synthase may play a significant role in the production of chemical protection against phages. Chemical protection has been documented as a strategy to protect bacteria from phages, for example doxorubicin and daunorubicin prevent phage replication (Kronheim et al., 2018). To date, chemical protection from phages has not been reported in RSSC and it is definitely something worth exploring, especially the types of chemicals that this non-ribosomal peptide synthase synthesises and how they protect RSSC from phages. It should be noted that many of the SNPs identified here were synonymous, the amino acid sequence did not change and therefore it is unlikely that the protein structure did. Nevertheless, there is increasing evidence that synonymous SNPs are having an evolutionary effect on proteins and therefore should not be discounted and further exploration is needed (Shen et al., 2022).

The research carried out in this thesis was solely conducted on strains of *Ralstonia solanacearum,* only one of the three species of RSSC. Although, *R. solanacearum* is highly relevant to the UK and Europe, this is beginning to change, in recent years, *Ralstonia pseudosolanacearum* has been isolated in the Netherlands and will spread across Europe (Vogelaar et al., 2023, Bragard et al., 2019). This has increased the urgency for biocontrols that could provide protection to crops against both species. It would be highly useful and relevant to the UK and Europe to conduct similar research on *R. pseudosolanacearum*.

In conclusion, this thesis presents a cautionary tale about the uses of phages in biocontrols. Asymmetrical evolution seems to play a critical role in phage and *R. solanacearum* coevolutionary dynamics. Resistance was high, evolved quickly and was often cross-resistant. However, this does not mean that phages should be a complete write-off. There is still potential, we did successfully manage to identify high virulence phages in our collection (Chapter 4) and in some cases, increase the infectivity with training (Chapter 1). In some cases, resistance does come at a cost to *R. solanacearum*, something that we could also exploit. We have also highlighted some interesting genetic variation associated with phage resistance in *R. solanacearum* that is definitely worth exploring. With further characterisation of phages, more complicated systems could further help to understand the coevolutionary dynamics of phages and *R. solanacearum* as well as exploring the proteins of interest highlighted in this thesis. Nevertheless, this thesis provides important insights and predications into coevolution evolution and phage resistance in RSSC.

References

ABDELSATTAR, A. S., DAWOOUD, A., REZK, N., MAKKY, S., SAFWAT, A., RICHARDS, P. J. & EL-SHIBINY, A. 2021. How to Train Your Phage: The Recent Efforts in Phage Training. *Biologics,* 1**,** 70-88.

ABDURAHMAN, A., PARKER, M. L., KREUZE, J., ELPHINSTONE, J. G., STRUIK, P. C., KIGUNDU, A., ARENGO, E. & SHARMA, K. 2019. Molecular epidemiology of Ralstonia solanacearum species complex strains causing bacterial wilt of potato in Uganda. *Phytopathology,* 109**,** 1922-1931.

ÁCS, N., GAMBINO, M. & BRØNDSTED, L. 2020. Bacteriophage enumeration and detection methods. *Frontiers in Microbiology***,** 2662.

ADDY, H. S., ASKORA, A., KAWASAKI, T., FUJIE, M. & YAMADA, T. 2012a. The filamentous phage ϕRSS1 enhances virulence of phytopathogenic Ralstonia solanacearum on tomato. *Phytopathology,* 102**,** 244-251.

ADDY, H. S., ASKORA, A., KAWASAKI, T., FUJIE, M. & YAMADA, T. 2012b. Loss of virulence of the phytopathogen Ralstonia solanacearum through infection by ϕRSM filamentous phages. *Phytopathology,* 102**,** 469-477.

AHMED, W., YANG, J., TAN, Y., MUNIR, S., LIU, Q., ZHANG, J., JI, G. & ZHAO, Z. 2022. Ralstonia solanacearum, a deadly pathogen: Revisiting the bacterial wilt biocontrol practices in tobacco and other Solanaceae. *Rhizosphere***,** 100479.

AILLOUD, F., LOWE, T., CELLIER, G., ROCHE, D., ALLEN, C. & PRIOR, P. 2015. Comparative genomic analysis of Ralstonia solanacearum reveals candidate genes for host specificity. *Bmc Genomics,* 16**,** 1-11.

ALAWIYE, T. T. & BABALOLA, O. O. 2019. Bacterial diversity and community structure in typical plant rhizosphere. *Diversity,* 11**,** 179.

ALTSCHUL, S. F., MADDEN, T. L., SCHÄFFER, A. A., ZHANG, J., ZHANG, Z., MILLER, W. & LIPMAN, D. J. 1997. Gapped BLAST and PSI-BLAST: a new generation of protein database search programs. *Nucleic acids research,* 25**,** 3389-3402.

ÁLVAREZ, B., BIOSCA, E. G. & LÓPEZ, M. M. 2010. On the life of Ralstonia solanacearum, a destructive bacterial plant pathogen. *Current research, technology and education topics in applied microbiology and microbial biotechnology,* 1**,** 267-279.

ÁLVAREZ, B., LÓPEZ, M. M. & BIOSCA, E. G. 2019. Biocontrol of the major plant pathogen Ralstonia solanacearum in irrigation water and host plants by novel waterborne lytic bacteriophages. *Frontiers in Microbiology,* 10**,** 2813.

ÁLVAREZ, B., LÓPEZ, M. M. & BIOSCA, E. G. 2022. Ralstonia solanacearum facing spread-determining climatic temperatures, sustained starvation, and naturally induced resuscitation of viable but non-culturable cells in environmental water. *Microorganisms,* 10**,** 2503.

AMER, A. O. & VALVANO, M. A. 2001. Conserved amino acid residues found in a predicted cytosolic domain of the lipopolysaccharide biosynthetic protein WecA are implicated in the recognition of UDP-N-acetylglucosamine. *Microbiology (Reading),* 147**,** 3015-25.

ANDREWS, S. 2010. FastQC A Quality Control tool for High Throughput Sequence Data [Online].

ANDRIIANOV, A., TRIGÜIS, S., DROBIAZKO, A., SIERRO, N., IVANOV, N. V., SELMER, M., SEVERINOV, K. & ISAEV, A. 2023. Phage T3 overcomes the BREX defense through SAM cleavage and inhibition of SAM synthesis by SAM lyase. *Cell Reports,* 42.

AOUN, N., GEORGOULIS, S. J., AVALOS, J. K., GRULLA, K. J., MIQUEO, K., TOM, C. & LOWE-POWER, T. M. 2023. A pangenomic atlas reveals that eco-evolutionary dynamics shape plant pathogen type VI secretion systems. Cold Spring Harbor Laboratory.

ASKORA, A., KAWASAKI, T., USAMI, S., FUJIE, M. & YAMADA, T. 2009. Host recognition and integration of filamentous phage ϕRSM in the phytopathogen, Ralstonia solanacearum. *Virology,* 384**,** 69-76.

AVRANI, S., SCHWARTZ, D. A. & LINDELL, D. 2012. Virus-host swinging party in the oceans. *Mobile Genetic Elements,* 2**,** 88-95.

AZAM, A. H. & TANJI, Y. 2019. Bacteriophage-host arm race: an update on the mechanism of phage resistance in bacteria and revenge of the phage with the perspective for phage therapy. *Appl Microbiol Biotechnol,* 103**,** 2121-2131.

AZEREDO, J., GARCÍA, P. & DRULIS-KAWA, Z. 2021. Targeting biofilms using phages and their enzymes. *Current Opinion in Biotechnology,* 68**,** 251-261.

BAE, J. Y., WU, J., LEE, H. J., JO, E. J., MURUGAIYAN, S., CHUNG, E. & LEE, S.-W. 2012. Biocontrol potential of a lytic bacteriophage PE204 against bacterial wilt of tomato. *J. Microbiol. Biotechnol,* 22**,** 1613-1620.

BALIYAN, N., DHIMAN, S., DHEEMAN, S., VISHNOI, V. K., KUMAR, S. & MAHESHWARI, D. K. 2022. Bacteriophage cocktails as antibacterial agents in crop protection. *Environmental Sustainability,* 5**,** 305-311.

BANK, W. 2021. Uganda Economic Update, December 2021: Putting Women at the Center of Uganda's Economic Revival.

BARBOSA, C., VENAIL, P., HOLGUIN, A. V. & VIVES, M. J. 2013. Co-evolutionary dynamics of the bacteria Vibrio sp. CV1 and phages V1G, V1P1, and V1P2: implications for phage therapy. *Microbial ecology,* 66**,** 897-905.

BARRANGOU, R. 2015. The roles of CRISPR–Cas systems in adaptive immunity and beyond. *Current Opinion in Immunology,* 32**,** 36-41.

BARRANGOU, R., FREMAUX, C., DEVEAU, H., RICHARDS, M., BOYAVAL, P., MOINEAU, S., ROMERO, D. A. & HORVATH, P. 2007. CRISPR Provides Acquired Resistance Against Viruses in Prokaryotes. *Science,* 315**,** 1709-1712.

BARRANGOU, R. & VAN DER OOST, J. 2018. Mining for novel bacterial defence systems. *Nature microbiology,* 3**,** 535-536.

BAYLISS, C. D. 2009. Determinants of phase variation rate and the fitness implications of differing rates for bacterial pathogens and commensals. *FEMS Microbiology Reviews,* 33**,** 504-520.

BELL, G. 2010. Fluctuating selection: the perpetual renewal of adaptation in variable environments. *Philos Trans R Soc Lond B Biol Sci,* 365**,** 87-97.

BENNETT, A. F. & LENSKI, R. E. 2007. An experimental test of evolutionary trade-offs during temperature adaptation. *Proceedings of the National Academy of Sciences,* 104**,** 8649-8654.

BERNHEIM, A. & SOREK, R. 2020. The pan-immune system of bacteria: antiviral defence as a community resource. *Nature Reviews Microbiology,* 18**,** 113-119.

BERTONI, M., KIEFER, F., BIASINI, M., BORDOLI, L. & SCHWEDE, T. 2017. Modeling protein quaternary structure of homo-and hetero-oligomers beyond binary interactions by homology. *Scientific reports,* 7**,** 10480.

BERTOZZI SILVA, J., STORMS, Z. & SAUVAGEAU, D. 2016. Host receptors for bacteriophage adsorption. *FEMS microbiology letters,* 363**,** fnw002.

BIENERT, S., WATERHOUSE, A., DE BEER, T. A., TAURIELLO, G., STUDER, G., BORDOLI, L. & SCHWEDE, T. 2017. The SWISS-MODEL Repository—new features and functionality. *Nucleic acids research,* 45**,** D313-D319.

BONDY-DENOMY, J., GARCIA, B., STRUM, S., DU, M., ROLLINS, M. F., HIDALGO-REYES, Y., WIEDENHEFT, B., MAXWELL, K. L. & DAVIDSON, A. R. 2015. Multiple mechanisms for CRISPR–Cas inhibition by anti-CRISPR proteins. *Nature,* 526**,** 136-139.

BONDY-DENOMY, J., QIAN, J., WESTRA, E. R., BUCKLING, A., GUTTMAN, D. S., DAVIDSON, A. R. & MAXWELL, K. L. 2016. Prophages mediate defense against phage infection through diverse mechanisms. *Isme j,* 10**,** 2854-2866.

BORGES, A. L. 2021. How to train your bacteriophage. *Proceedings of the National Academy of Sciences,* 118.

BORGES, A. L., DAVIDSON, A. R. & BONDY-DENOMY, J. 2017. The Discovery, Mechanisms, and Evolutionary Impact of Anti-CRISPRs. *Annual Review of Virology,* 4**,** 37-59.

BORIN, J. M., AVRANI, S., BARRICK, J. E., PETRIE, K. L. & MEYER, J. R. 2021. Coevolutionary phage training leads to greater bacterial suppression and delays the evolution of phage resistance. *Proceedings of the National Academy of Sciences,* 118.

BORN, Y., FIESELER, L., KLUMPP, J., EUGSTER, M. R., ZURFLUH, K., DUFFY, B. & LOESSNER, M. J. 2014. The tail-associated depolymerase of E rwinia amylovora phage L1 mediates host cell adsorption and enzymatic capsule removal, which can enhance infection by other phage. *Environmental microbiology,* 16**,** 2168-2180.

BRAGA, L. P., SOUCY, S. M., AMGARTEN, D. E., DA SILVA, A. M. & SETUBAL, J. C. 2018. Bacterial diversification in the light of the interactions with phages: the genetic symbionts and their role in ecological speciation. *Frontiers in Ecology and Evolution,* 6**,** 6.

BRAGARD, C., DEHNEN-SCHMUTZ, K., DI SERIO, F., GONTHIER, P., JAQUES MIRET, J. A., JUSTESEN, A. F., MACLEOD, A., MAGNUSSON, C. S., MILONAS, P., NAVAS-CORTES, J. A., PARNELL, S., POTTING, R., REIGNAULT, P. L., THULKE, H. H., VAN DER WERF, W., VICENT CIVERA, A., YUEN, J., ZAPPALÀ, L., VAN DER WOLF, J., KALUSKI, T., PAUTASSO, M. & JACQUES, M. A. 2019. Pest categorisation of the Ralstonia solanacearum species complex. *EFSA Journal,* 17.

BROCKHURST, M. A., BUCKLING, A. & RAINEY, P. B. 2005. The effect of a bacteriophage on diversification of the opportunistic bacterial pathogen, Pseudomonas aeruginosa. *Proceedings of the Royal Society B: Biological Sciences,* 272**,** 1385-1391.

BROCKHURST, M. A. & KOSKELLA, B. 2013. Experimental coevolution of species interactions. *Trends in ecology & evolution,* 28**,** 367-375.

BROCKHURST, M. A., MORGAN, A. D., FENTON, A. & BUCKLING, A. 2007. Experimental coevolution with bacteria and phage: the Pseudomonas fluorescens—Φ2 model system. *Infection, Genetics and Evolution,* 7**,** 547-552.

BROWN, S., SANTA MARIA, J. P., JR. & WALKER, S. 2013. Wall teichoic acids of gram-positive bacteria. *Annu Rev Microbiol,* 67**,** 313-36.

BUCKLING, A. & RAINEY, P. B. 2002. Antagonistic coevolution between a bacterium and a bacteriophage. *Proceedings of the Royal Society of London. Series B: Biological Sciences,* 269**,** 931-936.

BURDON, J. J., THRALL, P. H. & ERICSON, L. 2013. Genes, communities & invasive species: understanding the ecological and evolutionary dynamics of host–pathogen interactions. *Current Opinion in Plant Biology,* 16**,** 400-405.

BURMEISTER, A. R., FORTIER, A., ROUSH, C., LESSING, A. J., BENDER, R. G., BARAHMAN, R., GRANT, R., CHAN, B. K. & TURNER, P. E. 2020. Pleiotropy complicates a trade-off between phage resistance and antibiotic resistance. *Proceedings of the National Academy of Sciences,* 117**,** 11207-11216.

BURMEISTER, A. R., LENSKI, R. E. & MEYER, J. R. 2016. Host coevolution alters the adaptive landscape of a virus. *Proc Biol Sci,* 283.

BURMEISTER, A. R., SULLIVAN, R. M., GALLIE, J. & LENSKI, R. E. 2021. Sustained coevolution of phage Lambda and Escherichia coli involves inner-as well as outer-membrane defences and counter-defences. *Microbiology,* 167.

BURMEISTER, A. R. & TURNER, P. E. 2020. Trading-off and trading-up in the world of bacteria-phage evolution. *Curr Biol,* 30**,** R1120-r1124.

BURMEISTER, A. R., TZINTZUN-TAPIA, E., ROUSH, C., MANGAL, I., BARAHMAN, R., BJORNSON, R. D. & TURNER, P. E. 2023. Experimental Evolution of the TolC-Receptor Phage U136B Functionally Identifies a Tail Fiber Protein Involved in Adsorption through Strong Parallel Adaptation. *Applied and Environmental Microbiology***,** e00079-23.

BUTTIMER, C., MCAULIFFE, O., ROSS, R. P., HILL, C., O'MAHONY, J. & COFFEY, A. 2017. Bacteriophages and bacterial plant diseases. *Frontiers in microbiology,* 8**,** 34.

CAHILL, J. & YOUNG, R. 2019. Chapter Two - Phage Lysis: Multiple Genes for Multiple Barriers. *In:* KIELIAN, M., METTENLEITER, T. C. & ROOSSINCK, M. J. (eds.) *Advances in Virus Research.* Academic Press.

CALDWELL, D., KIM, B.-S. & IYER-PASCUZZI, A. S. 2017. Ralstonia solanacearum differentially colonizes roots of resistant and susceptible tomato plants. *Phytopathology,* 107**,** 528-536.

CARTE, J., CHRISTOPHER, R. T., SMITH, J. T., OLSON, S., BARRANGOU, R., MOINEAU, S., GLOVER III, C. V. C., GRAVELEY, B. R., TERNS, R. M. & TERNS, M. P. 2014. The three major types of CRISPR-Cas systems function independently in CRISPR RNA biogenesis in S treptococcus thermophilus. *Molecular microbiology,* 93**,** 98-112.

CARUSO, P., PALOMO, J. L., BERTOLINI, E., ÁLVAREZ, B., LÓPEZ, M. M. & BIOSCA, E. G. 2005. Seasonal variation of Ralstonia solanacearum biovar 2 populations in a Spanish river: recovery of stressed cells at low temperatures. *Applied and Environmental Microbiology,* 71**,** 140-148.

CASTILLO, H., LI, X., SCHILKEY, F. & SMITH, G. B. 2018. Transcriptome analysis reveals a stress response of Shewanella oneidensis deprived of background levels of ionizing radiation. *PLoS One,* 13**,** e0196472.

CASTILLO, J. A. & GREENBERG, J. T. 2007. Evolutionary dynamics of Ralstonia solanacearum. *Applied and Environmental Microbiology,* 73**,** 1225-1238.

CASTILLO, J. A., SECAIRA-MOROCHO, H., MALDONADO, S. & SARMIENTO, K. N. 2020. Diversity and evolutionary dynamics of antiphage defense systems in Ralstonia solanacearum species complex. *Frontiers in Microbiology,* 11**,** 961.

CASTLEDINE, M., PADFIELD, D., SIEROCINSKI, P., SORIA PASCUAL, J., HUGHES, A., MÄKINEN, L., FRIMAN, V.-P., PIRNAY, J.-P., MERABISHVILI, M., DE VOS, D. & BUCKLING, A. 2022a. Parallel evolution of Pseudomonas aeruginosa phage resistance and virulence loss in response to phage treatment in vivo and in vitro. *eLife,* 11**,** e73679.

CASTLEDINE, M., SIEROCINSKI, P., INGLIS, M., KAY, S., HAYWARD, A., BUCKLING, A. & PADFIELD, D. 2022b. Greater Phage Genotypic Diversity Constrains Arms-Race Coevolution. *Front Cell Infect Microbiol,* 12**,** 834406.

CATALÃO, M. J., GIL, F., MONIZ-PEREIRA, J., SÃO-JOSÉ, C. & PIMENTEL, M. 2013. Diversity in bacterial lysis systems: bacteriophages show the way. *FEMS Microbiology Reviews,* 37**,** 554-571.

CELLIER, G., REMENANT, B., CHIROLEU, F., LEFEUVRE, P. & PRIOR, P. 2012. Phylogeny and population structure of brown rot-and Moko disease-causing strains of Ralstonia solanacearum phylotype II. *Applied and environmental microbiology,* 78**,** 2367-2375.

CHALONER, T. M., GURR, S. J. & BEBBER, D. P. 2021. Plant pathogen infection risk tracks global crop yields under climate change. *Nature Climate Change,* 11**,** 710-715.

CHAN, B. K., ABEDON, S. T. & LOC-CARRILLO, C. 2013. Phage cocktails and the future of phage therapy. *Future microbiology,* 8**,** 769-783.

CHAN, B. K., SISTROM, M., WERTZ, J. E., KORTRIGHT, K. E., NARAYAN, D. & TURNER, P. E. 2016. Phage selection restores antibiotic sensitivity in MDR Pseudomonas aeruginosa. *Scientific Reports,* 6**,** 26717.

CHEN, M., ZHANG, L., ABDELGADER, S. A., YU, L., XU, J., YAO, H., LU, C. & ZHANG, W. 2017. Alterations in gp37 Expand the Host Range of a T4-Like Phage. *Applied and Environmental Microbiology,* 83.

CHEN, Y., ZHANG, W.-Z., LIU, X., MA, Z.-H., LI, B., ALLEN, C. & GUO, J.-H. 2010. A real-time PCR assay for the quantitative detection of Ralstonia solanacearum in the horticultural soil and plant tissues. *J. Microbiol. Biotechnol,* 20**,** 193-201.

CHEVALLEREAU, A., PONS, B. J., VAN HOUTE, S. & WESTRA, E. R. 2022. Interactions between bacterial and phage communities in natural environments. *Nat Rev Microbiol,* 20**,** 49-62.

CHOUDHARY, D. K., NABI, S. U., DAR, M. S. & KHAN, K. A. 2018. Ralstonia solanacearum: A wide spread and global bacterial plant wilt pathogen. *Journal of Pharmacognosy and Phytochemistry,* 7**,** 85-90.

CLOUGH, S. E., JOUSSET, A., ELPHINSTONE, J. G. & FRIMAN, V. P. 2022. Combining in vitro and in vivo screening to identify efficient Pseudomonas biocontrol strains against the phytopathogenic bacterium Ralstonia solanacearum. *Microbiologyopen,* 11**,** e1283.

COHEN, D., MELAMED, S., MILLMAN, A., SHULMAN, G., OPPENHEIMER-SHAANAN, Y., KACEN, A., DORON, S., AMITAI, G. & SOREK, R. 2019. Cyclic GMP–AMP signalling protects bacteria against viral infection. *Nature,* 574**,** 691-695.

COLL, N. S. & VALLS, M. 2013. Current knowledge on the R alstonia solanacearum type III secretion system. *Microbial biotechnology,* 6**,** 614-620.

COMMON, J., MORLEY, D., WESTRA, E. R. & VAN HOUTE, S. 2019. CRISPR-Cas immunity leads to a coevolutionary arms race between Streptococcus thermophilus and lytic phage. *Philosophical Transactions of the Royal Society B: Biological Sciences,* 374**,** 20180098.

COMMUNITY, T. G. 2022. The Galaxy platform for accessible, reproducible and collaborative biomedical analyses: 2022 update. *Nucleic Acids Research,* 50**,** W345-W351.

CORNELISSEN, A., CEYSSENS, P.-J., T'SYEN, J., VAN PRAET, H., NOBEN, J.-P., SHABUROVA, O. V., KRYLOV, V. N., VOLCKAERT, G. & LAVIGNE, R. 2011. The T7-related Pseudomonas putida phage ϕ15 displays virion-associated biofilm degradation properties. *PloS one,* 6**,** e18597.

CORRAL, J., SEBASTIÀ, P., COLL, N. S., BARBÉ, J., ARANDA, J. & VALLS, M. 2020. Twitching and swimming motility play a role in Ralstonia solanacearum pathogenicity. *Msphere,* 5**,** 10.1128/msphere. 00740-19.

CORREA, A. M. S., HOWARD-VARONA, C., COY, S. R., BUCHAN, A., SULLIVAN, M. B. & WEITZ, J. S. 2021. Revisiting the rules of life for viruses of microorganisms. *Nature Reviews Microbiology,* 19**,** 501-513.

COSTA, O. Y. A., RAAIJMAKERS, J. M. & KURAMAE, E. E. 2018. Microbial Extracellular Polymeric Substances: Ecological Function and Impact on Soil Aggregation. *Front Microbiol,* 9**,** 1636.

COSTA, P., PEREIRA, C., GOMES, A. T. & ALMEIDA, A. 2019. Efficiency of single phage suspensions and phage cocktail in the inactivation of Escherichia coli and Salmonella Typhimurium: An in vitro preliminary study. *Microorganisms,* 7**,** 94.

COUCE, A., CAUDWELL, L. V., FEINAUER, C., HINDRÉ, T., FEUGEAS, J.-P., WEIGT, M., LENSKI, R. E., SCHNEIDER, D. & TENAILLON, O. 2017. Mutator genomes decay, despite sustained fitness gains, in a long-term experiment with bacteria. *Proceedings of the National Academy of Sciences,* 114**,** E9026-E9035.

CRUMMETT, L. T., PUXTY, R. J., WEIHE, C., MARSTON, M. F. & MARTINY, J. B. H. 2016. The genomic content and context of auxiliary metabolic genes in marine cyanomyoviruses. *Virology,* 499**,** 219-229.

CULOT, A., GROSSET, N. & GAUTIER, M. 2019. Overcoming the challenges of phage therapy for industrial aquaculture: A review. *Aquaculture,* 513**,** 734423.

CZAJKOWSKI, R., OZYMKO, Z. & LOJKOWSKA, E. 2014. Isolation and characterization of novel soilborne lytic bacteriophages infecting Dickeya spp. biovar 3 ('D. solani'). *Plant Pathology,* 63**,** 758-772.

DA SILVA XAVIER, A., DE ALMEIDA, J. C. F., DE MELO, A. G., ROUSSEAU, G. M., TREMBLAY, D. M., DE REZENDE, R. R., MOINEAU, S. & ALFENAS-ZERBINI, P. 2019. Characterization of CRISPR-Cas systems in the Ralstonia solanacearum species complex. *Molecular plant pathology,* 20**,** 223-239.

DE JONGE, P. A., NOBREGA, F. L., BROUNS, S. J. & DUTILH, B. E. 2019. Molecular and evolutionary determinants of bacteriophage host range. *Trends in microbiology,* 27**,** 51-63.

DE PAEPE, M. & TADDEI, F. 2006. Viruses' Life History: Towards a Mechanistic Basis of a Trade-Off between Survival and Reproduction among Phages. *PLoS Biology,* 4**,** e193.

DELGADO-BAQUERIZO, M., GUERRA, C. A., CANO-DÍAZ, C., EGIDI, E., WANG, J.-T., EISENHAUER, N., SINGH, B. K. & MAESTRE, F. T. 2020. The proportion of soil-borne pathogens increases with warming at the global scale. *Nature Climate Change,* 10**,** 550-554.

DENAMUR, E. & MATIC, I. 2006. Evolution of mutation rates in bacteria. *Molecular microbiology,* 60**,** 820-827.

DENNY, T. P. & BAEK, S.-R. 1991. Genetic Evidence that Extracellular Polysaccharide ls a Virulence Factor. *Molecular Plant-Microbe Interactions,* 4**,** 198-206.

DESSAU, M., GOLDHILL, D., MCBRIDE, R. L., TURNER, P. E. & MODIS, Y. 2012. Selective Pressure Causes an RNA Virus to Trade Reproductive Fitness for Increased Structural and Thermal Stability of a Viral Enzyme. *PLoS Genetics,* 8**,** e1003102.

DEVEAU, H., BARRANGOU, R., GARNEAU, J. E., LABONTÉ, J., FREMAUX, C., BOYAVAL, P., ROMERO, D. A., HORVATH, P. & MOINEAU, S. 2008. Phage Response to CRISPR-Encoded Resistance in Streptococcus thermophilus. *Journal of Bacteriology,* 190**,** 1390-1400.

DEWALD-WANG, E. A., PARR, N., TILEY, K., LEE, A. & KOSKELLA, B. 2022. Multiyear Time-Shift Study of Bacteria and Phage Dynamics in the Phyllosphere. *The American Naturalist,* 199**,** 126-140.

DI MARTINO, P. 2018. Extracellular polymeric substances, a key element in understanding biofilm phenotype. *AIMS Microbiol,* 4**,** 274-288.

DION, M. B., OECHSLIN, F. & MOINEAU, S. 2020. Phage diversity, genomics and phylogeny. *Nature Reviews Microbiology,* 18**,** 125-138.

DORON, S., MELAMED, S., OFIR, G., LEAVITT, A., LOPATINA, A., KEREN, M., AMITAI, G. & SOREK, R. 2018. Systematic discovery of antiphage defense systems in the microbial pangenome. *Science,* 359**,** eaar4120.

DOSS, J., CULBERTSON, K., HAHN, D., CAMACHO, J. & BAREKZI, N. 2017. A Review of Phage Therapy against Bacterial Pathogens of Aquatic and Terrestrial Organisms. *Viruses,* 9**,** 50.

DOWAH, A. S. A. & CLOKIE, M. R. J. 2018. Review of the nature, diversity and structure of bacteriophage receptor binding proteins that target Gram-positive bacteria. *Biophysical Reviews,* 10**,** 535-542.

DUBAN, M., COCIANCICH, S. & LECLÈRE, V. 2022. Nonribosomal Peptide Synthesis Definitely Working Out of the Rules. *Microorganisms,* 10**,** 577.

DUNCAN-LOWEY, B. & KRANZUSCH, P. J. 2022. CBASS phage defense and evolution of antiviral nucleotide signaling. *Current Opinion in Immunology,* 74**,** 156-163.

DUPUIS, M.-È., VILLION, M., MAGADÁN, A. H. & MOINEAU, S. 2013. CRISPR-Cas and restriction–modification systems are compatible and increase phage resistance. *Nature Communications,* 4**,** 2087.

EBERT, D. & FIELDS, P. D. 2020. Host–parasite co-evolution and its genomic signature. *Nature Reviews Genetics***,** 1-15.

ELHALAG, K., NASR-ELDIN, M., HUSSIEN, A. & AHMAD, A. 2018. Potential use of soilborne lytic Podoviridae phage as a biocontrol agent against Ralstonia solanacearum. *Journal of basic microbiology,* 58**,** 658-669.

ELPHINSTONE, J., HENNESSY, J., WILSON, J. & STEAD, D. 1996a. Sensitivity of different methods for the detection of Ralstonia solanacearum in potato tuber extracts. *Eppo Bulletin,* 26**,** 663-678.

ELPHINSTONE, J. G., HENNESSY, J., WILSON, J. K. & STEAD, D. E. 1996b. Sensitivity of different methods for the detection of Ralstonia solanacearum in potato tuber extracts. *EPPO Bulletin,* 26**,** 663-678.

FARNHAM, E. M. 2022. *Exploring the phenotypic and genetic diversity of a bacterial plant pathogen, the Ralstonia solanacearum species complex (RSSC).* University of York.

FAVOR, A. H., LLANOS, C. D., YOUNGBLUT, M. D. & BARDALES, J. A. 2020. Optimizing bacteriophage engineering through an accelerated evolution platform. *Scientific reports,* 10**,** 1-10.

FEGAN, M. & PRIOR, P. 2005. How complex is the Ralstonia solanacearum species complex. *Bacterial wilt disease and the Ralstonia solanacearum species complex,* 1**,** 449-461.
FERENCI, T. 2016. Trade-off Mechanisms Shaping the Diversity of Bacteria. *Trends in Microbiology,* 24**,** 209-223.
FERRIOL-GONZÁLEZ, C. & DOMINGO-CALAP, P. 2020. Phages for biofilm removal. *Antibiotics,* 9**,** 268.
FILIPPOV, A. A., SERGUEEV, K. V., HE, Y., HUANG, X.-Z., GNADE, B. T., MUELLER, A. J., FERNANDEZ-PRADA, C. M. & NIKOLICH, M. P. 2011. Bacteriophage-resistant mutants in Yersinia pestis: identification of phage receptors and attenuation for mice. *PloS one,* 6**,** e25486.
FLEMMING, H.-C. 2016. EPS—then and now. *Microorganisms,* 4**,** 41.
FLEMMING, H.-C., NEU, T. R. & WOZNIAK, D. J. 2007. The EPS Matrix: The "House of Biofilm Cells". *Journal of Bacteriology,* 189**,** 7945-7947.
FLEMMING, H.-C., WINGENDER, J., SZEWZYK, U., STEINBERG, P., RICE, S. A. & KJELLEBERG, S. 2016. Biofilms: an emergent form of bacterial life. *Nature Reviews Microbiology,* 14**,** 563-575.
FOLIMONOVA, S. Y. 2012. Superinfection exclusion is an active virus-controlled function that requires a specific viral protein. *J Virol,* 86**,** 5554-61.
FORD, S. A., WILLIAMS, D., PATERSON, S. & KING, K. C. 2017. Co-evolutionary dynamics between a defensive microbe and a pathogen driven by fluctuating selection. *Molecular ecology,* 26**,** 1778-1789.
FORTIER, L. C. & SEKULOVIC, O. 2013. Importance of prophages to evolution and virulence of bacterial pathogens. *Virulence,* 4**,** 354-65.
FORTUNA, M. A., BARBOUR, M. A., ZAMAN, L., HALL, A. R., BUCKLING, A. & BASCOMPTE, J. 2019. Coevolutionary dynamics shape the structure of bacteria-phage infection networks. *Evolution,* 73**,** 1001-1011.
FRIMAN, V. P., SOANES-BROWN, D., SIEROCINSKI, P., MOLIN, S., JOHANSEN, H. K., MERABISHVILI, M., PIRNAY, J. P., DE VOS, D. & BUCKLING, A. 2016. Pre-adapting parasitic phages to a pathogen leads to increased pathogen clearance and lowered resistance evolution with Pseudomonas aeruginosa cystic fibrosis bacterial isolates. *J Evol Biol,* 29**,** 188-98.
FUJIWARA, A., FUJISAWA, M., HAMASAKI, R., KAWASAKI, T., FUJIE, M. & YAMADA, T. 2011. Biocontrol of Ralstonia solanacearum by treatment with lytic bacteriophages. *Appl Environ Microbiol,* 77**,** 4155-62.
FUJIWARA, A., KAWASAKI, T., USAMI, S., FUJIE, M. & YAMADA, T. 2008. Genomic characterization of Ralstonia solanacearum phage ϕRSA1 and its related prophage (ϕRSX) in strain GMI1000. *Journal of bacteriology,* 190**,** 143-156.
GAO, Z. & FENG, Y. 2023. Bacteriophage strategies for overcoming host antiviral immunity. *Frontiers in Microbiology,* 14**,** 1211793.
GARBE, J., BUNK, B., ROHDE, M. & SCHOBERT, M. 2011. Sequencing and characterization of Pseudomonas aeruginosa phage JG004. *BMC microbiology,* 11**,** 1-12.
GARVEY, M. 2022. Bacteriophages and Food Production: Biocontrol and Bio-Preservation Options for Food Safety. *Antibiotics (Basel),* 11.
GENG, R., CHENG, L., CAO, C., LIU, Z., LIU, D., XIAO, Z., WU, X., HUANG, Z., FENG, Q., LUO, C., CHEN, Z., ZHANG, Z., JIANG, C., REN, M. & YANG, A. 2022. Comprehensive Analysis

Reveals the Genetic and Pathogenic Diversity of Ralstonia solanacearum Species Complex and Benefits Its Taxonomic Classification. *Front Microbiol,* 13**,** 854792.
GENIN, S. 2010. Molecular traits controlling host range and adaptation to plants in Ralstonia solanacearum. *New Phytologist,* 187**,** 920-928.
GENIN, S. & BOUCHER, C. 2002. Ralstonia solanacearum: secrets of a major pathogen unveiled by analysis of its genome. *Molecular plant pathology,* 3**,** 111-118.
GENIN, S. & DENNY, T. P. 2012. Pathogenomics of the Ralstonia solanacearum species complex. *Annual review of phytopathology,* 50**,** 67-89.
GEORJON, H. & BERNHEIM, A. 2023. The highly diverse antiphage defence systems of bacteria. *Nature Reviews Microbiology,* 21**,** 686-700.
GOLDFARB, T., SBERRO, H., WEINSTOCK, E., COHEN, O., DORON, S., CHARPAK-AMIKAM, Y., AFIK, S., OFIR, G. & SOREK, R. 2015. BREX is a novel phage resistance system widespread in microbial genomes. *Embo j,* 34**,** 169-83.
GOLDHILL, D. H. & TURNER, P. E. 2014. The evolution of life history trade-offs in viruses. *Current Opinion in Virology,* 8**,** 79-84.
GÓMEZ, P. & BUCKLING, A. 2011. Bacteria-phage antagonistic coevolution in soil. *Science,* 332**,** 106-109.
GONÇALVES, O. S., SOUZA, F. D. O., BRUCKNER, F. P., SANTANA, M. F. & ALFENAS-ZERBINI, P. 2021. Widespread distribution of prophages signaling the potential for adaptability and pathogenicity evolution of Ralstonia solanacearum species complex. *Genomics,* 113**,** 992-1000.
GONZALEZ, F., HELM, R. F., BROADWAY, K. M. & SCHARF, B. E. 2018. More than Rotating Flagella: Lipopolysaccharide as a Secondary Receptor for Flagellotropic Phage 7-7-1. *Journal of Bacteriology,* 200.
GORDEEVA, J., MOROZOVA, N., SIERRO, N., ISAEV, A., SINKUNAS, T., TSVETKOVA, K., MATLASHOV, M., TRUNCAITĖ, L., MORGAN, R. D., IVANOV, N. V., SIKSNYS, V., ZENG, L. & SEVERINOV, K. 2018. BREX system of Escherichia coli distinguishes self from non-self by methylation of a specific DNA site. *Nucleic Acids Research,* 47**,** 253-265.
GORDILLO ALTAMIRANO, F. L. & BARR, J. J. 2021. Unlocking the next generation of phage therapy: the key is in the receptors. *Current Opinion in Biotechnology,* 68**,** 115-123.
GRANATO, E. T., MEILLER-LEGRAND, T. A. & FOSTER, K. R. 2019. The evolution and ecology of bacterial warfare. *Current biology,* 29**,** R521-R537.
GREENFIELD, J., SHANG, X., LUO, H., ZHOU, Y., LINDEN, S. B., HESELPOTH, R. D., LEIMAN, P. G., NELSON, D. C. & HERZBERG, O. 2020. Structure and function of bacteriophage CBA120 ORF211 (TSP2), the determinant of phage specificity towards E. coli O157:H7. *Scientific Reports,* 10**,** 15402.
GREENROD, S. T. E., STOYCHEVA, M., ELPHINSTONE, J. & FRIMAN, V.-P. 2022. Global diversity and distribution of prophages are lineage-specific within the Ralstonia solanacearum species complex. *BMC Genomics,* 23**,** 689.
GREER, H. M., OVERTON, K., FERGUSON, M. A., SPAIN, E. M., DARLING, L. E. O., NÚÑEZ, M. E. & VOLLE, C. B. 2021. Extracellular Polymeric Substance Protects Some Cells in an Escherichia coli Biofilm from the Biomechanical Consequences of Treatment with Magainin 2. *Microorganisms,* 9.
GROUP, W. B. 2016. *Ethiopia: Priorities for Ending Extreme Poverty and Promoting Shared Prosperity*, World Bank.

GUEX, N., PEITSCH, M. C. & SCHWEDE, T. 2009. Automated comparative protein structure modeling with SWISS-MODEL and Swiss-PdbViewer: A historical perspective. *Electrophoresis,* 30**,** S162-S173.
HALL, A. R., ASHBY, B., BASCOMPTE, J. & KING, K. C. 2020. Measuring coevolutionary dynamics in species-rich communities. *Trends in Ecology & Evolution*.
HALL, A. R., SCANLAN, P. D., MORGAN, A. D. & BUCKLING, A. 2011. Host-parasite coevolutionary arms races give way to fluctuating selection. *Ecol Lett,* 14**,** 635-42.
HALL, J. P. J., HARRISON, E. & BROCKHURST, M. A. 2013. Viral host-adaptation: insights from evolution experiments with phages. *Current Opinion in Virology,* 3**,** 572-577.
HAMMOND-KOSACK, K. E. & PARKER, J. E. 2003. Deciphering plant–pathogen communication: fresh perspectives for molecular resistance breeding. *Current opinion in biotechnology,* 14**,** 177-193.
HAMPTON, H. G., WATSON, B. N. & FINERAN, P. C. 2020. The arms race between bacteria and their phage foes. *Nature,* 577**,** 327-336.
HANTKE, K. 2020. Compilation of Escherichia coli K-12 outer membrane phage receptors – their function and some historical remarks. *FEMS Microbiology Letters,* 367.
HAY, I. D. & LITHGOW, T. 2019. Filamentous phages: masters of a microbial sharing economy. *EMBO reports,* 20**,** e47427.
HEINEMAN, R. H. & BROWN, S. P. 2012. Experimental Evolution of a Bacteriophage Virus Reveals the Trajectory of Adaptation across a Fecundity/Longevity Trade-Off. *PLoS ONE,* 7**,** e46322.
HEMBRY, D. H., YODER, J. B. & GOODMAN, K. R. 2014. Coevolution and the diversification of life. *The American Naturalist,* 184**,** 425-438.
HENDERSON, J. C., ZIMMERMAN, S. M., CROFTS, A. A., BOLL, J. M., KUHNS, L. G., HERRERA, C. M. & TRENT, M. S. 2016. The Power of Asymmetry: Architecture and Assembly of the Gram-Negative Outer Membrane Lipid Bilayer. *Annual Review of Microbiology,* 70**,** 255-278.
HERNANDEZ, C. A. & KOSKELLA, B. 2019. Phage resistance evolution in vitro is not reflective of in vivo outcome in a plant-bacteria-phage system. *Evolution*.
HESSE, E. & BUCKLING, A. 2016. Host population bottlenecks drive parasite extinction during antagonistic coevolution. *Evolution,* 70**,** 235-240.
HIKICHI, Y., MORI, Y., ISHIKAWA, S., HAYASHI, K., OHNISHI, K., KIBA, A. & KAI, K. 2017. Regulation involved in colonization of intercellular spaces of host plants in Ralstonia solanacearum. *Frontiers in plant science,* 8**,** 967.
HOBBS, S. J., WEIN, T., LU, A., MOREHOUSE, B. R., SCHNABEL, J., LEAVITT, A., YIRMIYA, E., SOREK, R. & KRANZUSCH, P. J. 2022. Phage anti-CBASS and anti-Pycsar nucleases subvert bacterial immunity. *Nature,* 605**,** 522-526.
HOLGUÍN, A. V., CÁRDENAS, P., PRADA-PEÑARANDA, C., RABELO LEITE, L., BUITRAGO, C., CLAVIJO, V., OLIVEIRA, G., LEEKITCHAROENPHON, P., MØLLER AARESTRUP, F. & VIVES, M. J. 2019. Host resistance, genomics and population dynamics in a Salmonella Enteritidis and phage system. *Viruses,* 11**,** 188.
HOLTAPPELS, D., FORTUNA, K., LAVIGNE, R. & WAGEMANS, J. 2021. The future of phage biocontrol in integrated plant protection for sustainable crop production. *Current Opinion in Biotechnology,* 68**,** 60-71.
HONG, Y.-H., HUANG, C., WANG, K.-C., CHU, T.-H., LI, C.-H., CHU, Y.-J. & CHENG, C.-P. 2014. Mutations in Ralstonia solanacearum loci involved in lipopolysaccharide biogenesis,

phospholipid trafficking and peptidoglycan recycling render bacteriophage infection. *Archives of Microbiology,* 196**,** 667-674.
HOSSEINIDOUST, Z., TUFENKJI, N. & VAN DE VEN, T. G. 2013. Formation of biofilms under phage predation: considerations concerning a biofilm increase. *Biofouling,* 29**,** 457-468.
HOWARD-VARONA, C., HARGREAVES, K. R., SOLONENKO, N. E., MARKILLIE, L. M., WHITE, R. A., BREWER, H. M., ANSONG, C., ORR, G., ADKINS, J. N. & SULLIVAN, M. B. 2018. Multiple mechanisms drive phage infection efficiency in nearly identical hosts. *The ISME journal,* 12**,** 1605-1618.
HUANG, Q., YAN, X. & WANG, J.-F. 2012. Improved biovar test for Ralstonia solanacearum. *Journal of Microbiological Methods,* 88**,** 271-274.
HUET, G. 2014. Breeding for resistances to Ralstonia solanacearum. *Frontiers in plant science,* 5**,** 715.
HUSS, C. P., HOLMES, K. D. & BLUBAUGH, C. K. 2022. Benefits and Risks of Intercropping for Crop Resilience and Pest Management. *Journal of Economic Entomology,* 115**,** 1350-1362.
HYMAN, P. 2019. Phages for phage therapy: isolation, characterization, and host range breadth. *Pharmaceuticals,* 12**,** 35.
HYMAN, P. & ABEDON, S. T. 2010. Chapter 7 - Bacteriophage Host Range and Bacterial Resistance. *Advances in Applied Microbiology.* Academic Press.
JAMES, S. L., RABIEY, M., NEUMAN, B. W., PERCIVAL, G. & JACKSON, R. W. 2020. Isolation, characterisation and experimental evolution of phage that infect the horse chestnut tree pathogen, Pseudomonas syringae pv. aesculi. *Current microbiology,* 77**,** 1438.
JAYARAMAN, R. 2011. Hypermutation and stress adaptation in bacteria. *Journal of Genetics,* 90**,** 383-391.
JURADO, A., FERNÁNDEZ, L., RODRÍGUEZ, A. & GARCÍA, P. 2022. Understanding the mechanisms that drive phage resistance in staphylococci to prevent phage therapy failure. *Viruses,* 14**,** 1061.
KASHIWAGI, A. & YOMO, T. 2011. Ongoing phenotypic and genomic changes in experimental coevolution of RNA bacteriophage Qβ and Escherichia coli. *PLoS Genet,* 7**,** e1002188.
KELMAN, A. 1954. The relationship of pathogenicity of Pseudomonas solanacearum to colony appearance in a tetrazolium medium. *Phytopathology,* 44.
KIM, J., PARK, H., RYU, S. & JEON, B. 2021. Inhibition of antimicrobial-resistant Escherichia coli using a broad host range phage cocktail targeting various bacterial phylogenetic groups. *Frontiers in Microbiology,* 12**,** 699630.
KINTZ, E., DAVIES, M. R., HAMMARLÖF, D. L., CANALS, R., HINTON, J. C. & VAN DER WOUDE, M. W. 2015. A BTP 1 prophage gene present in invasive non-typhoidal S almonella determines composition and length of the O-antigen of the lipopolysaccharide. *Molecular microbiology,* 96**,** 263-275.
KLEINKAUF, H. & VON DOHREN, H. 1990. Nonribosomal biosynthesis of peptide antibiotics. *European Journal of Biochemistry,* 192**,** 1-15.
KOONIN, E. V., MAKAROVA, K. S. & ZHANG, F. 2017. Diversity, classification and evolution of CRISPR-Cas systems. *Current Opinion in Microbiology,* 37**,** 67-78.
KOROTKOV, K. V., SANDKVIST, M. & HOL, W. G. J. 2012. The type II secretion system: biogenesis, molecular architecture and mechanism. *Nature Reviews Microbiology,* 10**,** 336-351.

KORTRIGHT, K. E., CHAN, B. K., EVANS, B. R. & TURNER, P. E. 2022a. Arms race and fluctuating selection dynamics in Pseudomonas aeruginosa bacteria coevolving with phage OMKO1. *Journal of Evolutionary Biology,* 35**,** 1475-1487.

KORTRIGHT, K. E., DONE, R. E., CHAN, B. K., SOUZA, V. & TURNER, P. E. 2022b. Selection for phage resistance reduces virulence of Shigella flexneri. *Applied and Environmental Microbiology,* 88**,** e01514-21.

KOSKELLA, B. 2014. Bacteria-phage interactions across time and space: merging local adaptation and time-shift experiments to understand phage evolution. *The American Naturalist,* 184**,** S9-S21.

KOSKELLA, B. & BROCKHURST, M. A. 2014. Bacteria–phage coevolution as a driver of ecological and evolutionary processes in microbial communities. *FEMS microbiology reviews,* 38**,** 916-931.

KOSKELLA, B., HERNANDEZ, C. A. & WHEATLEY, R. M. 2022. Understanding the Impacts of Bacteriophage Viruses: From Laboratory Evolution to Natural Ecosystems. *Annual Review of Virology,* 9**,** 57-78.

KOSKELLA, B. & TAYLOR, T. B. 2018. Multifaceted impacts of bacteriophages in the plant microbiome. *Annual review of phytopathology*.

KRONHEIM, S., DANIEL-IVAD, M., DUAN, Z., HWANG, S., WONG, A. I., MANTEL, I., NODWELL, J. R. & MAXWELL, K. L. 2018. A chemical defence against phage infection. *Nature,* 564**,** 283-286.

KUTSCHERA, A. & RANF, S. 2019. The multifaceted functions of lipopolysaccharide in plant-bacteria interactions. *Biochimie,* 159**,** 93-98.

LAANTO, E., HOIKKALA, V., RAVANTTI, J. & SUNDBERG, L.-R. 2017. Long-term genomic coevolution of host-parasite interaction in the natural environment. *Nature communications,* 8**,** 1-8.

LABRIE, S. J., SAMSON, J. E. & MOINEAU, S. 2010. Bacteriophage resistance mechanisms. *Nature Reviews Microbiology,* 8**,** 317-327.

LAHLALI, R., EZRARI, S., RADOUANE, N., KENFAOUI, J., ESMAEEL, Q., EL HAMSS, H., BELABESS, Z. & BARKA, E. A. 2022. Biological control of plant pathogens: A global perspective. *Microorganisms,* 10**,** 596.

LAI, R., YOU, M., JIANG, L., LAI, B., CHEN, S., ZENG, W. & JIANG, D. 2011. Evaluation of garlic intercropping for enhancing the biological control of Ralstonia solanacearum in flue-cured tobacco fields. *Biocontrol science and technology,* 21**,** 755-764.

LAURE, N. N. & AHN, J. 2022. Phage resistance-mediated trade-offs with antibiotic resistance in Salmonella Typhimurium. *Microbial Pathogenesis,* 171**,** 105732.

LEBEAU, A., DAUNAY, M.-C., FRARY, A., PALLOIX, A., WANG, J.-F., DINTINGER, J., CHIROLEU, F., WICKER, E. & PRIOR, P. 2011. Bacterial wilt resistance in tomato, pepper, and eggplant: genetic resources respond to diverse strains in the Ralstonia solanacearum species complex. *Phytopathology,* 101**,** 154-165.

LEE, I. M., TU, I. F., YANG, F.-L., KO, T.-P., LIAO, J.-H., LIN, N.-T., WU, C.-Y., REN, C.-T., WANG, A. H. J., CHANG, C.-M., HUANG, K.-F. & WU, S.-H. 2017. Structural basis for fragmenting the exopolysaccharide of Acinetobacter baumannii by bacteriophage ΦAB6 tailspike protein. *Scientific Reports,* 7**,** 42711.

LEGGETT, H. C., BUCKLING, A., LONG, G. H. & BOOTS, M. 2013. Generalism and the evolution of parasite virulence. *Trends in ecology & evolution,* 28**,** 592-596.

LENSKI, R. E. 1988. EXPERIMENTAL STUDIES OF PLEIOTROPY AND EPISTASIS IN ESCHERICHIA COLI. I. VARIATION IN COMPETITIVE FITNESS AMONG MUTANTS RESISTANT TO VIRUS T4. *Evolution,* 42**,** 425-432.

LENSKI, R. E. & LEVIN, B. R. 1985. Constraints on the coevolution of bacteria and virulent phage: a model, some experiments, and predictions for natural communities. *The American Naturalist,* 125**,** 585-602.

LEPRINCE, A. & MAHILLON, J. 2023. Phage Adsorption to Gram-Positive Bacteria. *Viruses,* 15**,** 196.

LEWIS IVEY, M. L., JIMENEZ MADRID, A. M., DAUNAY, M.-C. & SHAH, D. A. 2021. Evaluation of tomato, eggplant and pepper accessions for resistance to Ralstonia solanacearum species complex (RSSC) strains from Louisiana. *European Journal of Plant Pathology,* 159**,** 279-293.

LI, C.-H., WANG, K.-C., HONG, Y.-H., CHU, T.-H., CHU, Y.-J., CHOU, I.-C., LU, D.-K., CHEN, C.-Y., YANG, W.-C. & LIN, Y.-M. 2014a. Roles of different forms of lipopolysaccharides in Ralstonia solanacearum pathogenesis. *Molecular Plant-Microbe Interactions,* 27**,** 471-478.

LI, C., SHI, T., SUN, Y. & ZHANG, Y. 2022. A Novel Method to Create Efficient Phage Cocktails via Use of Phage-Resistant Bacteria. *Applied and Environmental Microbiology,* 88**,** e02323-21.

LI, H., HANDSAKER, B., WYSOKER, A., FENNELL, T., RUAN, J., HOMER, N., MARTH, G., ABECASIS, G., DURBIN, R. & SUBGROUP, G. P. D. P. 2009. The Sequence Alignment/Map format and SAMtools. *Bioinformatics,* 25**,** 2078-2079.

LI, Y., CHI, L., MAO, L., YAN, D., WU, Z., MA, T., GUO, M., WANG, Q., OUYANG, C. & CAO, A. 2014b. Control of soilborne pathogens of zingiber officinale by methyl iodide and chloropicrin in China. *Plant disease,* 98**,** 384-388.

LI, Y., FENG, J., ZHENG, L., HUANG, J., YANG, Y. & LI, X. 2020. Intercropping with marigold promotes soil health and microbial structure to assist in mitigating tobacco bacterial wilt. *Journal of Plant Pathology,* 102**,** 731-742.

LINDELL, D., JAFFE, J. D., JOHNSON, Z. I., CHURCH, G. M. & CHISHOLM, S. W. 2005. Photosynthesis genes in marine viruses yield proteins during host infection. *Nature,* 438**,** 86-89.

LING, L., HAN, X., LI, X., ZHANG, X., WANG, H., ZHANG, L., CAO, P., WU, Y., WANG, X. & ZHAO, J. 2020. A Streptomyces sp. NEAU-HV9: isolation, identification, and potential as a biocontrol agent against Ralstonia solanacearum of tomato plants. *Microorganisms,* 8**,** 351.

LIU, L., SUN, C., LIU, X., HE, X., LIU, M., WU, H., TANG, C., JIN, C. & ZHANG, Y. 2016. Effect of calcium cyanamide, ammonium bicarbonate and lime mixture and ammonia water on survival of Ralstonia solanacearum and microbial community. *Scientific Reports,* 6**,** 19037.

LIU, N., LEWIS, C., ZHENG, W. & FU, Z. Q. 2020. Phage cocktail therapy: Multiple ways to suppress pathogenicity. *Trends in plant science,* 25**,** 315-317.

LOC-CARRILLO, C. & ABEDON, S. T. 2011. Pros and cons of phage therapy. *Bacteriophage,* 1**,** 111-114.

LOH, B., KUHN, A. & LEPTIHN, S. 2019. The fascinating biology behind phage display: filamentous phage assembly. *Molecular Microbiology,* 111**,** 1132-1138.

LOPATINA, A., TAL, N. & SOREK, R. 2020. Abortive infection: bacterial suicide as an antiviral immune strategy. *Annual review of virology,* 7**,** 371-384.
LÓPEZ, D., VLAMAKIS, H. & KOLTER, R. 2010. Biofilms. *Cold Spring Harbor perspectives in biology,* 2**,** a000398.
LOSSOUARN, J., BRIET, A., MONCAUT, E., FURLAN, S., BOUTEAU, A., SON, O., LEROY, M., DUBOW, M. S., LECOINTE, F. & SERROR, P. 2019. Enterococcus faecalis countermeasures defeat a virulent Picovirinae bacteriophage. *Viruses,* 11**,** 48.
LOWE-POWER, T. M., KHOKHANI, D. & ALLEN, C. 2018. How Ralstonia solanacearum exploits and thrives in the flowing plant xylem environment. *Trends in microbiology,* 26**,** 929-942.
MACHO, A. P., GUIDOT, A., BARBERIS, P., BEUZÓN, C. R. & GENIN, S. 2010. A competitive index assay identifies several Ralstonia solanacearum type III effector mutant strains with reduced fitness in host plants. *Molecular plant-microbe interactions,* 23**,** 1197-1205.
MADDOCKS, S. E. & OYSTON, P. C. F. 2008. Structure and function of the LysR-type transcriptional regulator (LTTR) family proteins. *Microbiology (Reading),* 154**,** 3609-3623.
MAHBOU SOMO TOUKAM, G., CELLIER, G., WICKER, E., GUILBAUD, C., KAHANE, R., ALLEN, C. & PRIOR, P. 2009. Broad diversity of Ralstonia solanacearum strains in Cameroon. *Plant disease,* 93**,** 1123-1130.
MALIK, D. J., SOKOLOV, I. J., VINNER, G. K., MANCUSO, F., CINQUERRUI, S., VLADISAVLJEVIC, G. T., CLOKIE, M. R. J., GARTON, N. J., STAPLEY, A. G. F. & KIRPICHNIKOVA, A. 2017. Formulation, stabilisation and encapsulation of bacteriophage for phage therapy. *Advances in Colloid and Interface Science,* 249**,** 100-133.
MANGIAFICO, S. 2022. rcompanion: Functions to Support Extension Education Program Evaluation.
MANSFIELD, J., GENIN, S., MAGORI, S., CITOVSKY, V., SRIARIYANUM, M., RONALD, P., DOW, M., VERDIER, V., BEER, S. V. & MACHADO, M. A. 2012. Top 10 plant pathogenic bacteria in molecular plant pathology. *Molecular plant pathology,* 13**,** 614-629.
MARKWITZ, P., LOOD, C., OLSZAK, T., VAN NOORT, V., LAVIGNE, R. & DRULIS-KAWA, Z. 2022. Genome-driven elucidation of phage-host interplay and impact of phage resistance evolution on bacterial fitness. *The ISME Journal,* 16**,** 533-542.
MARSTON, M. F., PIERCIEY, F. J., SHEPARD, A., GEARIN, G., QI, J., YANDAVA, C., SCHUSTER, S. C., HENN, M. R. & MARTINY, J. B. H. 2012. Rapid diversification of coevolving marine Synechococcus and a virus. *Proceedings of the National Academy of Sciences,* 109**,** 4544-4549.
MARTIN, F. N. 2003. Development of alternative strategies for management of soilborne pathogens currently controlled with methyl bromide. *Annu Rev Phytopathol,* 41**,** 325-50.
MARTINEAU, F., PICARD, F. J., KE, D., PARADIS, S., ROY, P. H., OUELLETTE, M. & BERGERON, M. G. 2001. Development of a PCR assay for identification of staphylococci at genus and species levels. *J Clin Microbiol,* 39**,** 2541-7.
MATEUS, L., COSTA, L., SILVA, Y. J., PEREIRA, C., CUNHA, A. & ALMEIDA, A. 2014. Efficiency of phage cocktails in the inactivation of Vibrio in aquaculture. *Aquaculture,* 424-425**,** 167-173.

MATSUKAWA, N., TSUMORI, C., OHNISHI, K. & KAI, K. 2023. Discovery of Cyclic Lipopeptides Ralstopeptins A and B from Ralstonia solanacearum Species Complex and Analysis of Biosynthetic Gene Evolution. *ACS Chemical Biology,* 18**,** 572-582.

MAURO, A. A. & GHALAMBOR, C. K. 2020. Trade-offs, Pleiotropy, and Shared Molecular Pathways: A Unified View of Constraints on Adaptation. *Integrative and Comparative Biology,* 60**,** 332-347.

MCGARVEY, J., DENNY, T. & SCHELL, M. 1999. Spatial-temporal and quantitative analysis of growth and EPS I production by Ralstonia solanacearum in resistant and susceptible tomato cultivars. *Phytopathology,* 89**,** 1233-1239.

MEADEN, S., PASZKIEWICZ, K. & KOSKELLA, B. 2015. The cost of phage resistance in a plant pathogenic bacterium is context-dependent. *Evolution,* 69**,** 1321-1328.

MEDINA, M., BAKER, D. M., BALTRUS, D. A., BENNETT, G. M., CARDINI, U., CORREA, A., DEGNAN, S. M., CHRISTA, G., KIM, E. & LI, J. 2022. Grand challenges in coevolution. *Frontiers in Ecology and Evolution,* 9**,** 916.

MEESKE, A. J., JIA, N., CASSEL, A. K., KOZLOVA, A., LIAO, J., WIEDMANN, M., PATEL, D. J. & MARRAFFINI, L. A. 2020. A phage-encoded anti-CRISPR enables complete evasion of type VI-A CRISPR-Cas immunity. *Science,* 369**,** 54-59.

MILLING, A., BABUJEE, L. & ALLEN, C. 2011. Ralstonia solanacearum Extracellular Polysaccharide Is a Specific Elicitor of Defense Responses in Wilt-Resistant Tomato Plants. *PLoS ONE,* 6**,** e15853.

MILLMAN, A., BERNHEIM, A., STOKAR-AVIHAIL, A., FEDORENKO, T., VOICHEK, M., LEAVITT, A., OPPENHEIMER-SHAANAN, Y. & SOREK, R. 2020a. Bacterial retrons function in anti-phage defense. *Cell,* 183**,** 1551-1561. e12.

MILLMAN, A., MELAMED, S., AMITAI, G. & SOREK, R. 2020b. Diversity and classification of cyclic-oligonucleotide-based anti-phage signalling systems. *Nature microbiology,* 5**,** 1608-1615.

MINA, I., JARA, N., CRIOLLO, J. & CASTILLO, J. 2019. The critical role of biofilms in bacterial vascular plant pathogenesis. *Plant Pathology,* 68**,** 1439-1447.

MINH TRAN, T., MACINTYRE, A., KHOKHANI, D., HAWES, M. & ALLEN, C. 2016. Extracellular DNases of Ralstonia solanacearum modulate biofilms and facilitate bacterial wilt virulence. *Environmental microbiology,* 18**,** 4103-4117.

MOLINA, F., MENOR-FLORES, M., FERNÁNDEZ, L., VEGA-RODRÍGUEZ, M. A. & GARCÍA, P. 2022. Systematic analysis of putative phage-phage interactions on minimum-sized phage cocktails. *Scientific Reports,* 12**,** 2458.

MORI, Y., INOUE, K., IKEDA, K., NAKAYASHIKI, H., HIGASHIMOTO, C., OHNISHI, K., KIBA, A. & HIKICHI, Y. 2016. The vascular plant-pathogenic bacterium Ralstonia solanacearum produces biofilms required for its virulence on the surfaces of tomato cells adjacent to intercellular spaces. *Mol Plant Pathol,* 17**,** 890-902.

MORRIS, C. E. & MOURY, B. 2019. Revisiting the Concept of Host Range of Plant Pathogens. *Annual Review of Phytopathology,* 57**,** 63-90.

MOULTON-BROWN, C. E. & FRIMAN, V. P. 2018. Rapid evolution of generalized resistance mechanisms can constrain the efficacy of phage–antibiotic treatments. *Evolutionary applications,* 11**,** 1630-1641.

MUKHTAR, S., MEHNAZ, S. & MALIK, K. A. 2019. Microbial diversity in the rhizosphere of plants growing under extreme environments and its impact on crop improvement. *Environmental Sustainability,* 2**,** 329-338.

NAKAMURA, S. & MINAMINO, T. 2019. Flagella-Driven Motility of Bacteria. *Biomolecules,* 9.
NARULITA, E., ADDY, H. S., KAWASAKI, T., FUJIE, M. & YAMADA, T. 2016. The involvement of the PilQ secretin of type IV pili in phage infection in Ralstonia solanacearum. *Biochemical and Biophysical Research Communications,* 469**,** 868-872.
NION, Y. A. & TOYOTA, K. 2015. Recent trends in control methods for bacterial wilt diseases caused by Ralstonia solanacearum. *Microbes and environments,* 30**,** 1-11.
NIU, Y. D., LIU, H., DU, H., MENG, R., SAYED MAHMOUD, E., WANG, G., MCALLISTER, T. A. & STANFORD, K. 2021. Efficacy of individual bacteriophages does not predict efficacy of bacteriophage cocktails for control of Escherichia coli O157. *Frontiers in Microbiology,* 12**,** 616712.
NORTH, O. I. & BROWN, E. D. 2021. Phage–antibiotic combinations: a promising approach to constrain resistance evolution in bacteria. *Annals of the New York Academy of Sciences,* 1496**,** 23-34.
NUNES-ALVES, C. 2015. Putting the 'BREX' on phage replication. *Nature Reviews Microbiology,* 13**,** 129-129.
OECHSLIN, F. 2018. Resistance development to bacteriophages occurring during bacteriophage therapy. *Viruses,* 10**,** 351.
OFIR, G., MELAMED, S., SBERRO, H., MUKAMEL, Z., SILVERMAN, S., YAAKOV, G., DORON, S. & SOREK, R. 2018. DISARM is a widespread bacterial defence system with broad anti-phage activities. *Nature microbiology,* 3**,** 90-98.
OWEN, S. V., WENNER, N., DULBERGER, C. L., RODWELL, E. V., BOWERS-BARNARD, A., QUINONES-OLVERA, N., RIGDEN, D. J., RUBIN, E. J., GARNER, E. C., BAYM, M. & HINTON, J. C. D. 2021. Prophages encode phage-defense systems with cognate self-immunity. *Cell Host Microbe,* 29**,** 1620-1633.e8.
PAL, C., MACIÁ, M. D., OLIVER, A., SCHACHAR, I. & BUCKLING, A. 2007. Coevolution with viruses drives the evolution of bacterial mutation rates. *Nature,* 450**,** 1079-1081.
PATERSON, S., VOGWILL, T., BUCKLING, A., BENMAYOR, R., SPIERS, A. J., THOMSON, N. R., QUAIL, M., SMITH, F., WALKER, D. & LIBBERTON, B. 2010. Antagonistic coevolution accelerates molecular evolution. *Nature,* 464**,** 275-278.
PAWLUK, A., DAVIDSON, A. R. & MAXWELL, K. L. 2018. Anti-CRISPR: discovery, mechanism and function. *Nature Reviews Microbiology,* 16**,** 12-17.
PAWLUK, A., STAALS, R. H. J., TAYLOR, C., WATSON, B. N. J., SAHA, S., FINERAN, P. C., MAXWELL, K. L. & DAVIDSON, A. R. 2016. Inactivation of CRISPR-Cas systems by anti-CRISPR proteins in diverse bacterial species. *Nature Microbiology,* 1**,** 16085.
PAYNE, L. J., MEADEN, S., MESTRE, M. R., PALMER, C., TORO, N., FINERAN, P. C. & JACKSON, S. A. 2022. PADLOC: a web server for the identification of antiviral defence systems in microbial genomes. *Nucleic acids research,* 50**,** W541-W550.
PEREIRA, C., MOREIRINHA, C., LEWICKA, M., ALMEIDA, P., CLEMENTE, C., CUNHA, Â., DELGADILLO, I., ROMALDE, J. L., NUNES, M. L. & ALMEIDA, A. 2016. Bacteriophages with potential to inactivate Salmonella Typhimurium: Use of single phage suspensions and phage cocktails. *Virus research,* 220**,** 179-192.
PEYRAUD, R., COTTRET, L., MARMIESSE, L., GOUZY, J. & GENIN, S. 2016. A Resource Allocation Trade-Off between Virulence and Proliferation Drives Metabolic Versatility in the Plant Pathogen Ralstonia solanacearum. *PLOS Pathogens,* 12**,** e1005939.
PIEL, D., BRUTO, M., LABREUCHE, Y., BLANQUART, F., GOUDENÈGE, D., BARCIA-CRUZ, R., CHENIVESSE, S., LE PANSE, S., JAMES, A., DUBERT, J., PETTON, B., LIEBERMAN, E.,

WEGNER, K. M., HUSSAIN, F. A., KAUFFMAN, K. M., POLZ, M. F., BIKARD, D., GANDON, S., ROCHA, E. P. C. & LE ROUX, F. 2022. Phage–host coevolution in natural populations. *Nature Microbiology,* 7**,** 1075-1086.

PINHEIRO J, B. D., R CORE TEAM (2023) 2023. nlme: Linear and Nonlinear Mixed Effect Models_. R package verison 3.1-162.

POUEYMIRO, M. & GENIN, S. 2009. Secreted proteins from Ralstonia solanacearum: a hundred tricks to kill a plant. *Current opinion in microbiology,* 12**,** 44-52.

POULLAIN, V., GANDON, S., BROCKHURST, M. A., BUCKLING, A. & HOCHBERG, M. E. 2008. THE EVOLUTION OF SPECIFICITY IN EVOLVING AND COEVOLVING ANTAGONISTIC INTERACTIONS BETWEEN A BACTERIA AND ITS PHAGE. *Evolution,* 62**,** 1-11.

PRJIBELSKI, A., ANTIPOV, D., MELESHKO, D., LAPIDUS, A. & KOROBEYNIKOV, A. 2020. Using SPAdes de novo assembler. *Current protocols in bioinformatics,* 70**,** e102.

RAMÍREZ, M., NEUMAN, B. & RAMÍREZ, C. A. 2020. Bacteriophages as promising agents for the biological control of moko disease (Ralstonia solanacearum) of banana. *Biological Control***,** 104238.

REMENANT, B., COUPAT-GOUTALAND, B., GUIDOT, A., CELLIER, G., WICKER, E., ALLEN, C., FEGAN, M., PRUVOST, O., ELBAZ, M. & CALTEAU, A. 2010. Genomes of three tomato pathogens within the Ralstonia solanacearum species complex reveal significant evolutionary divergence. *BMC genomics,* 11**,** 1-16.

REMENANT, B., DE CAMBIAIRE, J.-C., CELLIER, G., JACOBS, J. M., MANGENOT, S., BARBE, V., LAJUS, A., VALLENET, D., MEDIGUE, C., FEGAN, M., ALLEN, C. & PRIOR, P. 2011. Ralstonia syzygii, the Blood Disease Bacterium and Some Asian R. solanacearum Strains Form a Single Genomic Species Despite Divergent Lifestyles. *PLoS ONE,* 6**,** e24356.

RIPLEY, W. N. V. A. B. D. 2002. Modern Applied Statistics with S. Springer.

ROHDE, C., RESCH, G., PIRNAY, J.-P., BLASDEL, B. G., DEBARBIEUX, L., GELMAN, D., GÓRSKI, A., HAZAN, R., HUYS, I., KAKABADZE, E., ŁOBOCKA, M., MAESTRI, A., ALMEIDA, G. M. D. F., MAKALATIA, K., MALIK, D. J., MAŠLAŇOVÁ, I., MERABISHVILI, M., PANTUCEK, R., ROSE, T., ŠTVERÁKOVÁ, D., VAN RAEMDONCK, H., VERBEKEN, G. & CHANISHVILI, N. 2018. Expert Opinion on Three Phage Therapy Related Topics: Bacterial Phage Resistance, Phage Training and Prophages in Bacterial Production Strains. *Viruses,* 10**,** 178.

ROSS, A., WARD, S. & HYMAN, P. 2016. More Is Better: Selecting for Broad Host Range Bacteriophages. *Frontiers in Microbiology,* 7.

SAFNI, I., CLEENWERCK, I., DE VOS, P., FEGAN, M., SLY, L. & KAPPLER, U. 2014. Polyphasic taxonomic revision of the Ralstonia solanacearum species complex: proposal to emend the descriptions of Ralstonia solanacearum and Ralstonia syzygii and reclassify current R. syzygii strains as Ralstonia syzygii subsp. syzygii subsp. nov., R. solanacearum phylotype IV strains as Ralstonia syzygii subsp. indonesiensis subsp. nov., banana blood disease bacterium strains as Ralstonia syzygii subsp. celebesensis subsp. nov. and R. solanacearum phylotype I and III strains as Ralstoniapseudosolanacearum sp. nov. *International journal of systematic and evolutionary microbiology,* 64**,** 3087-3103.

SAILE, E., MCGARVEY, J. A., SCHELL, M. A. & DENNY, T. P. 1997. Role of extracellular polysaccharide and endoglucanase in root invasion and colonization of tomato plants by Ralstonia solanacearum. *Phytopathology,* 87**,** 1264-1271.

SALMOND, G. P. C. & FINERAN, P. C. 2015. A century of the phage: past, present and future. *Nature Reviews Microbiology,* 13**,** 777.
SAMSON, J. E., MAGADÁN, A. H., SABRI, M. & MOINEAU, S. 2013. Revenge of the phages: defeating bacterial defences. *Nature Reviews Microbiology,* 11**,** 675-687.
SANT, D. G., WOODS, L. C., BARR, J. J. & MCDONALD, M. J. 2021. Host diversity slows bacteriophage adaptation by selecting generalists over specialists. *Nature Ecology & Evolution,* 5**,** 350-359.
SANTIAGO, T., LOPES, C., CAETANO-ANOLLÉS, G. & MIZUBUTI, E. 2017. Phylotype and sequevar variability of Ralstonia solanacearum in Brazil, an ancient centre of diversity of the pathogen. *Plant Pathology,* 66**,** 383-392.
SANTOS, B. M., GILREATH, J. P., MOTIS, T. N., NOLING, J. W., JONES, J. P. & NORTON, J. A. 2006. Comparing methyl bromide alternatives for soilborne disease, nematode and weed management in fresh market tomato. *Crop protection,* 25**,** 690-695.
SCANLAN, J. G., HALL, A. R. & SCANLAN, P. D. 2019. Impact of bile salts on coevolutionary dynamics between the gut bacterium Escherichia coli and its lytic phage PP01. *Infection, Genetics and Evolution,* 73**,** 425-432.
SCANLAN, P. D., BUCKLING, A. & HALL, A. R. 2015. Experimental evolution and bacterial resistance:(co) evolutionary costs and trade-offs as opportunities in phage therapy research. *Bacteriophage,* 5**,** e1050153.
SCANLAN, P. D., HALL, A. R., LOPEZ-PASCUA, L. D. & BUCKLING, A. 2011. Genetic basis of infectivity evolution in a bacteriophage. *Molecular Ecology,* 20**,** 981-989.
SCHWARTZ, D. A. & LINDELL, D. 2017. Genetic hurdles limit the arms race between Prochlorococcus and the T7-like podoviruses infecting them. *The ISME Journal,* 11**,** 1836-1851.
SEED, K. D., YEN, M., SHAPIRO, B. J., HILAIRE, I. J., CHARLES, R. C., TENG, J. E., IVERS, L. C., BONCY, J., HARRIS, J. B. & CAMILLI, A. 2014. Evolutionary consequences of intra-patient phage predation on microbial populations. *Elife,* 3**,** e03497.
SEEMANN, T. 2014. Prokka: rapid prokaryotic genome annotation. *Bioinformatics,* 30**,** 2068-2069.
SHARMA, P., JOHNSON, M. A., MAZLOOM, R., ALLEN, C., HEATH, L. S., LOWE-POWER, T. M. & VINATZER, B. A. 2022. Meta-analysis of the Ralstonia solanacearum species complex (RSSC) based on comparative evolutionary genomics and reverse ecology. *Microb Genom,* 8.
SHEN, X., SONG, S., LI, C. & ZHANG, J. 2022. Synonymous mutations in representative yeast genes are mostly strongly non-neutral. *Nature,* 606**,** 725-731.
SHIN, H., LEE, J.-H., KIM, H., CHOI, Y., HEU, S. & RYU, S. 2012. Receptor diversity and host interaction of bacteriophages infecting Salmonella enterica serovar Typhimurium.
SIEIRO, C., AREAL-HERMIDA, L., PICHARDO-GALLARDO, Á., ALMUIÑA-GONZÁLEZ, R., DE MIGUEL, T., SÁNCHEZ, S., SÁNCHEZ-PÉREZ, Á. & VILLA, T. G. 2020. A hundred years of bacteriophages: Can phages replace antibiotics in agriculture and aquaculture? *Antibiotics,* 9**,** 493.
SIEVERS, F., WILM, A., DINEEN, D., GIBSON, T. J., KARPLUS, K., LI, W., LOPEZ, R., MCWILLIAM, H., REMMERT, M. & SÖDING, J. 2011. Fast, scalable generation of high-quality protein multiple sequence alignments using Clustal Omega. *Molecular systems biology,* 7**,** 539.
SIGNORELL, A. 2022. DescTools: Tools for descriptive statistics. 0.99.45 ed.

SIMPSON, D. J., SACHER, J. C. & SZYMANSKI, C. M. 2015. Exploring the interactions between bacteriophage-encoded glycan binding proteins and carbohydrates. *Current Opinion in Structural Biology,* 34**,** 69-77.
SINGH, B. K., DELGADO-BAQUERIZO, M., EGIDI, E., GUIRADO, E., LEACH, J. E., LIU, H. & TRIVEDI, P. 2023. Climate change impacts on plant pathogens, food security and paths forward. *Nature Reviews Microbiology,* 21**,** 640-656.
SIRI, M. I., SANABRIA, A. & PIANZZOLA, M. J. 2011. Genetic diversity and aggressiveness of Ralstonia solanacearum strains causing bacterial wilt of potato in Uruguay. *Plant disease,* 95**,** 1292-1301.
SOTO, S. M. 2013. Role of efflux pumps in the antibiotic resistance of bacteria embedded in a biofilm. *Virulence,* 4**,** 223-9.
SPROUFFSKE, K. 2020. growthcurver: Simple Metrics to Summarize Growth Curves. 0.3.1 ed.
STONE, E., CAMPBELL, K., GRANT, I. & MCAULIFFE, O. 2019. Understanding and exploiting phage–host interactions. *Viruses,* 11**,** 567.
STOYCHEVA, M. 2022. *Comparative genomic analysis of Ralstonia solanacearum species complex.* University of York.
STUDER, G., REMPFER, C., WATERHOUSE, A. M., GUMIENNY, R., HAAS, J. & SCHWEDE, T. 2020. QMEANDisCo—distance constraints applied on model quality estimation. *Bioinformatics,* 36**,** 1765-1771.
SUNDIN, G. W., CASTIBLANCO, L. F., YUAN, X., ZENG, Q. & YANG, C. H. 2016. Bacterial disease management: challenges, experience, innovation and future prospects: challenges in bacterial molecular plant pathology. *Molecular plant pathology,* 17**,** 1506-1518.
TAN, G., NORDIN, M., NAPSIAH, A. & ROSNAH, H. 2009. Lysis activity of bacteriophages isolated from sewage against Ralstonia solanacearum and Erwinia chrysanthemi. *J. Trop. Agric. and Fd. Sc,* 37**,** 203-209.
TASLEM MOUROSI, J., AWE, A., GUO, W., BATRA, H., GANESH, H., WU, X. & ZHU, J. 2022. Understanding Bacteriophage Tail Fiber Interaction with Host Surface Receptor: The Key "Blueprint" for Reprogramming Phage Host Range. *Int J Mol Sci,* 23.
TEAM, R. C. 2023. R: A Language and Environment for Statistical Computing. 4.2.3 ed.
TESSON, F., HERVÉ, A., MORDRET, E., TOUCHON, M., D'HUMIÈRES, C., CURY, J. & BERNHEIM, A. 2022. Systematic and quantitative view of the antiviral arsenal of prokaryotes. *Nature communications,* 13**,** 2561.
TRINH, J. T., SZÉKELY, T., SHAO, Q., BALÁZSI, G. & ZENG, L. 2017. Cell fate decisions emerge as phages cooperate or compete inside their host. *Nature Communications,* 8**,** 14341.
TROTEREAU, A., BOYER, C., BORNARD, I., PÉCHEUR, M. J. B., SCHOULER, C. & TORRES-BARCELÓ, C. 2021. High genomic diversity of novel phages infecting the plant pathogen Ralstonia solanacearum, isolated in Mauritius and Reunion islands. *Scientific reports,* 11**,** 1-10.
TURKINGTON, C. J., MOROZOV, A., CLOKIE, M. R. & BAYLISS, C. D. 2019. Phage-resistant phase-variant sub-populations mediate herd immunity against bacteriophage invasion of bacterial meta-populations. *Frontiers in Microbiology,* 10**,** 1473.
URUSOVA, D. V., KINSELLA, R. L., SALINAS, N. D., HAURAT, M. F., FELDMAN, M. F. & TOLIA, N. H. 2019. The structure of Acinetobacter-secreted protease CpaA complexed with its chaperone CpaB reveals a novel mode of a T2SS chaperone–substrate interaction. *Journal of Biological Chemistry,* 294**,** 13344-13354.

VAILLEAU, F. & GENIN, S. 2023. Ralstonia solanacearum: An Arsenal of Virulence Strategies and Prospects for Resistance. *Annual Review of Phytopathology,* 61**,** 25-47.
VAN ELSAS, J. D., KASTELEIN, P., VAN BEKKUM, P., VAN DER WOLF, J. M., DE VRIES, P. M. & VAN OVERBEEK, L. S. 2000. Survival of Ralstonia solanacearum biovar 2, the causative agent of potato brown rot, in field and microcosm soils in temperate climates. *Phytopathology,* 90**,** 1358-1366.
VASU, K. & NAGARAJA, V. 2013. Diverse functions of restriction-modification systems in addition to cellular defense. *Microbiology and molecular biology reviews,* 77**,** 53-72.
VELDERS, G. J., ANDERSEN, S. O., DANIEL, J. S., FAHEY, D. W. & MCFARLAND, M. 2007. The importance of the Montreal Protocol in protecting climate. *Proceedings of the National Academy of Sciences,* 104**,** 4814-4819.
VIKRAM, A., WOOLSTON, J. & SULAKVELIDZE, A. 2021. Phage biocontrol applications in food production and processing. *Current issues in molecular biology,* 40**,** 267-302.
VOGELAAR, M., VAN DE BILT, J., BLOM, N., PEL, M., VAN DOORN, B., LANDMAN, N., GORKINK-SMITS, P., RAAYMAKERS, T., VREEBURG, R. & BERGSMA-VLAMI, M. 2023. Presence of Ralstonia pseudosolanacearum (Phylotype I) in Aquatic Environments in the Netherlands. *Plant Disease***,** PDIS-11-22-2628-SC.
WANG, G., KONG, J., CUI, D., ZHAO, H., ZHAO, P., FENG, S., ZHAO, Y. & WANG, W. 2018. Comparative proteomic analysis of two Ralstonia solanacearum isolates differing in aggressiveness. *International journal of molecular sciences,* 19**,** 2444.
WANG, J., RAZA, W., JIANG, G., YI, Z., FIELDS, B., GREENROD, S., FRIMAN, V.-P., JOUSSET, A., SHEN, Q. & WEI, Z. 2023a. Bacterial volatile organic compounds attenuate pathogen virulence via evolutionary trade-offs. *The ISME Journal,* 17**,** 443-452.
WANG, J., WANG, X., YANG, K., LU, C., FIELDS, B., XU, Y., SHEN, Q., WEI, Z. & FRIMAN, V.-P. 2023b. Phage selection drives resistance–virulence trade-offs in Ralstonia solanacearum plant-pathogenic bacterium irrespective of the growth temperature. *Evolution Letters,* 8**,** 253-266.
WANG, X., WEI, Z., LI, M., WANG, X., SHAN, A., MEI, X., JOUSSET, A., SHEN, Q., XU, Y. & FRIMAN, V.-P. 2017. Parasites and competitors suppress bacterial pathogen synergistically due to evolutionary trade-offs. *Evolution,* 71**,** 733-746.
WANG, X., WEI, Z., YANG, K., WANG, J., JOUSSET, A., XU, Y., SHEN, Q. & FRIMAN, V.-P. 2019. Phage combination therapies for bacterial wilt disease in tomato. *Nature Biotechnology,* 37**,** 1513-1520.
WANG, Y., XU, Y., PEREPELOV, A. V., QI, Y., KNIREL, Y. A., WANG, L. & FENG, L. 2007. Biochemical characterization of dTDP-D-Qui4N and dTDP-D-Qui4NAc biosynthetic pathways in Shigella dysenteriae type 7 and Escherichia coli O7. *Journal of bacteriology,* 189**,** 8626-8635.
WANG, Z., LUO, W., CHENG, S., ZHANG, H., ZONG, J. & ZHANG, Z. 2023c. Ralstonia solanacearum–a soil borne hidden enemy of plants: research development in management strategies, their action mechanism and challenges. *Frontiers in Plant Science,* 14**,** 1141902.
WANNASRICHAN, W., HTOO, H. H., SUWANSAENG, R., POGLIANO, J., NONEJUIE, P. & CHAIKEERATISAK, V. 2022. Phage-resistant Pseudomonas aeruginosa against a novel lytic phage JJ01 exhibits hypersensitivity to colistin and reduces biofilm production. *Frontiers in Microbiology,* 13**,** 1004733.

WARWICK-DUGDALE, J., BUCHHOLZ, H. H., ALLEN, M. J. & TEMPERTON, B. 2019. Host-hijacking and planktonic piracy: how phages command the microbial high seas. *Virology Journal,* 16**,** 15.

WATERHOUSE, A., BERTONI, M., BIENERT, S., STUDER, G., TAURIELLO, G., GUMIENNY, R., HEER, F. T., DE BEER, T. A. P., REMPFER, C. & BORDOLI, L. 2018. SWISS-MODEL: homology modelling of protein structures and complexes. *Nucleic acids research,* 46**,** W296-W303.

WEI, Y., OCAMPO, P. & LEVIN, B. R. 2010. An experimental study of the population and evolutionary dynamics of Vibrio cholerae O1 and the bacteriophage JSF4. *Proceedings of the Royal Society B: Biological Sciences,* 277**,** 3247-3254.

WEISBERG, J. F. A. S. 2019. An {R} Companion to Applied Regression. Sage.

WENDLINGER, G., LOESSNER, M. J. & SCHERER, S. 1996. Bacteriophage receptors on Listeria monocytogenes cells are the N-acetylglucosamine and rhamnose substituents of teichoic acids or the peptidoglycan itself. *Microbiology,* 142**,** 985-992.

WICKHAM, H. 2016. ggplot2: Elegant Graphics for Data Analysis. Springer-Verlag New York.

WILLIAMSON, K. E., FUHRMANN, J. J., WOMMACK, K. E. & RADOSEVICH, M. 2017. Viruses in soil ecosystems: an unknown quantity within an unexplored territory. *Annual Review of Virology,* 4**,** 201-219.

WRIGHT, R. C. T., BROCKHURST, M. A. & HARRISON, E. 2016. Ecological conditions determine extinction risk in co-evolving bacteria-phage populations. *BMC Evolutionary Biology,* 16**,** 227.

WU, B., WANG, X., YANG, L., YANG, H., ZENG, H., QIU, Y., WANG, C., YU, J., LI, J., XU, D., HE, Z. & CHEN, S. 2016. Effects of Bacillus amyloliquefaciens ZM9 on bacterial wilt and rhizosphere microbial communities of tobacco. *Applied Soil Ecology,* 103**,** 1-12.

XAVIER, A. D. S., MELO, A. G. D., HENDRICH, C. G., TREMBLAY, D. M., ROUSSEAU, G. M., PLANTE, P.-L., FOREST, K. T., ALFENAS-ZERBINI, P., ALLEN, C. & MOINEAU, S. 2022. In through the Out Door: A Functional Virulence Factor Secretion System Is Necessary for Phage Infection in Ralstonia solanacearum. *mBio,* 13**,** e01475-22.

XIA, G., CORRIGAN, R. M., WINSTEL, V., GOERKE, C., GRÜNDLING, A. & PESCHEL, A. 2011. Wall Teichoic Acid-Dependent Adsorption of Staphylococcal Siphovirus and Myovirus. *Journal of Bacteriology,* 193**,** 4006-4009.

XUE, H., LOZANO-DURÁN, R. & MACHO, A. P. 2020. Insights into the root invasion by the plant pathogenic bacterium Ralstonia solanacearum. *Plants,* 9**,** 516.

YAMADA, T. 2012. Bacteriophages of Ralstonia solanacearum: their diversity and utilization as biocontrol agents in agriculture. *Bacteriophages***,** 113-138.

YANG, K., WANG, X., HOU, R., LU, C., FAN, Z., LI, J., WANG, S., XU, Y., SHEN, Q., FRIMAN, V.-P. & WEI, Z. 2023. Rhizosphere phage communities drive soil suppressiveness to bacterial wilt disease. *Microbiome,* 11**,** 16.

YANG, L., DING, W., XU, Y., WU, D., LI, S., CHEN, J. & GUO, B. 2016. New insights into the antibacterial activity of hydroxycoumarins against Ralstonia solanacearum. *Molecules,* 21**,** 468.

YANG, L., WEI, Z., LI, S., XIAO, R., XU, Q., RAN, Y. & DING, W. 2021. Plant secondary metabolite, daphnetin reduces extracellular polysaccharides production and virulence factors of Ralstonia solanacearum. *Pesticide Biochemistry and Physiology,* 179**,** 104948.

YANG, W.-C., LIN, Y.-M., CHENG, Y.-S. & CHENG, C.-P. 2013. Ralstonia solanacearum RSc0411 (lptC) is a determinant for full virulence and has a strain-specific novel function in the T3SS activity. *Microbiology,* 159**,** 1136-1148.

YANG, Y., SHEN, W., ZHONG, Q., CHEN, Q., HE, X., BAKER, J. L., XIONG, K., JIN, X., WANG, J. & HU, F. 2020. Development of a bacteriophage cocktail to constrain the emergence of phage-resistant Pseudomonas aeruginosa. *Frontiers in microbiology,* 11**,** 327.

YUAN, Y., PENG, Q., ZHANG, S., LIU, T., YANG, S., YU, Q., WU, Y. & GAO, M. 2019. Phage reduce stability for regaining infectivity during antagonistic coevolution with host bacterium. *Viruses,* 11**,** 118.

YUN, Y.-B., HAN, J.-H. & KIM, Y.-K. 2018. Characterization of phage-resistant strains derived from Pseudomonas tolaasii 6264, which causes brown blotch disease. *Journal of microbiology and biotechnology,* 28**,** 2064-2070.

ZHANG, M., QIAN, J., XU, X., AHMED, T., YANG, Y., YAN, C., ELSHARKAWY, M. M., HASSAN, M. M., ALORABI, J. A. & CHEN, J. 2022. Resistance of Xanthomonas oryzae pv. oryzae to lytic phage X2 by spontaneous mutation of lipopolysaccharide synthesis-related glycosyltransferase. *Viruses,* 14**,** 1088.

ZHANG, Q. G., CHU, X. L. & BUCKLING, A. 2021. Overcoming the growth–infectivity trade-off in a bacteriophage slows bacterial resistance evolution. *Evolutionary Applications,* 14**,** 2055-2063.

ZHAO, Y., SHU, M., ZHANG, L., ZHONG, C., LIAO, N. & WU, G. 2024. Phage-driven coevolution reveals trade-off between antibiotic and phage resistance in Salmonella anatum. *ISME Communications,* 4.